Copyright

by

Justin Patrick Shofner

2008

The Dissertation Committee for Justin Patrick Shofner certifies that this is the approved version of the following dissertation:

Oral Delivery of Protein-Transporter Bioconjugates Using Intelligent Complexation Hydrogels

Committee:

_____
Nicholas A. Peppas, Supervisor

_____
Jennifer S. Brodbelt, Co-Supervisor

_____
Donald R. Paul

_____
Jennifer Maynard

_____
Christopher J. Ellison

Oral Delivery of Protein-Transporter Bioconjugates Using Intelligent Complexation Hydrogels

by

Justin Patrick Shofner, B.S.

Dissertation

Presented to the Faculty of the Graduate School of

The University of Texas at Austin

In Partial Fulfillment

Of the Requirements

For the Degree of

Doctor of Philosophy

The University of Texas at Austin

December 2008

To my wife, Chelsy, and to my family for their constant support…

ACKNOWLEDGEMENTS

I would like to express my deepest thanks and gratitude for everyone who has helped me along the way to achieving this goal. First and foremost, the members of my family have been my support system and guidance throughout my entire academic career. Without their caring and understanding, I could not have made it to this point. Also, my wife Chelsy has been extraordinary at keeping me focused, on track, but still grounded and mindful that life is about the journey, not just the destination. The culmination of my academic career with a doctoral degree reflects just as much on Chelsy and my family as it does on me.

I would also like to recognize the amazing contribution of Nicholas Peppas to my development and career as a scientist. Nicholas has always been able to perceive both my accomplishments and my failures in a positive manner, helping me to learn from my mistakes and move forward as a researcher. His constant support and reassurance have helped me get through the tougher parts of research and have gotten me to the end of my academic career.

I would like to thank the other members of my Ph.D. committee: Professors Jennifer Brodbelt of Chemistry and Professors Don Paul, Jennifer Maynard, Christopher Ellison of Chemical Engineering. This body of work would not have been possible if not for some of my collaborators. I would like to thank Professor Miyako Morishita and Khafagy El-Sayed for their help with the animal studies. I would also like to thank Maggie Phillips for her assistance with the cellular studies.

I am also very grateful for the assistance of the two undergraduate researchers who helped me complete many of the studies. Adrianne Rosales was very helpful in

completing many of the preliminary loading and release studies and Michael Sinclair contributed greatly to the *in vitro* analyses of the calcitonin-transferrin conjugate.

Lastly, I would like to give special thanks to all of the Peppamers who made my graduate school career more enjoyable and rewarding: Adam, Amber, Bill, Brandon, Brock, Carolyn, Daniel, David, Diana, Don, Hunter, Kristy, Maggie, Marty, Melissa, Michael, Omar, Ruben, Shahana, Steve, Tania, and Terry. I would have never gotten this far without the assistance and great friendships of all of my labmates.

Oral Delivery of Protein-Transporter Bioconjugates

Using Intelligent Complexation Hydrogels

Publication No. _____

Justin Patrick Shofner, Ph.D.

The University of Texas at Austin, 2008

Supervisor: Nicholas A. Peppas

Co-Supervisor: Jennifer S. Brodbelt

Several polymer systems including P(MAA-g-EG) and P(MAA-co-NVP) with crosslinking agents TEGDMA and PEGDMA1000, monomer-to-solvent ratios of 67:33, 60:40, and 50:50, and particle sizes of <75 microns, 90-150 microns, and 150-212 microns were synthesized for use with protein-transporter conjugates. All synthesized systems were characterized by SEM which demonstrated the visual size, surface features, and surface textures of the polymer microparticles.

Insulin-transferrin and calcitonin-transferrin conjugates were successfully synthesized using the protein crosslinker SPDP, binding the two proteins with a disulfide bond. The multi-step conjugation reactions used to create the conjugates were analyzed by the use of UV spectroscopy and HPLC to ensure the quality of the final products. In both conjugation reactions, the final product yield was found to be over 70%.

The *in vitro* loading and release characteristics for insulin-transferrin and calcitonin-transferrin were separately investigated. By testing loading and release using a number of different polymer systems with different synthesis parameters, it was

possible to optimize the hydrogel carriers for use with each of the conjugates independently. Upon optimization, the ideal system for use with insulin-transferrin and calcitonin-transferrin was found to be P(MAA-g-EG) microparticles of <75 microns formed using a PEGDMA1000 crosslinker and a 50:50 monomer-to-solvent ratio for both conjugates through separate optimization processes. This optimized polymer carrier was found to release upwards of 50% of loaded insulin-transferrin conjugate and near 90% of loaded calcitonin-transferrin conjugate.

The insulin-transferrin conjugate was further evaluated through the use of cellular and animal models. Using cellular models, the insulin-transferrin conjugate was shown to increase transport relative to insulin by a factor of 7, achieving an apparent permeability of 37 x 10^9 cm/s. Also, in the presence of polymer microparticles, the insulin-transferrin conjugate increased transport by a factor of 14 times relative to insulin, achieve an apparent permeability of 72.8 x 10^9 cm/s. The presence of the microparticles near the cells was found to improve conjugate transport by nearly 100%. The preliminary animal studies verified the successful synthesis of the insulin-transferrin conjugate as well as demonstrated the bioactivity of the insulin portion of the molecule by achieving a drop in blood glucose level upon subcutaneous injection.

TABLE OF CONTENTS

Chapter 1: Introduction 1

References 5

Chapter 2: Background 7

2.1 Diabetes Mellitus 8

2.2 Insulin and Insulin Therapies 12

2.3 Osteoporosis and Paget's Disease 15

2.4 Calcitonin Therapy 17

2.5 Alternative Routes for Protein Delivery 19

2.5.1 Pulmonary Delivery 20

2.5.2 Transdermal Delivery 21

2.5.3 Nasal Delivery 23

2.5.4 Buccal Delivery 25

2.5.5 Other Routes for Protein Delivery 27

2.6 Oral Protein Delivery 27

2.6.1 Physiology of the GI Tract 29

2.6.1.1 Anatomy and Physiology of the Stomach 30

2.6.1.2 Physiology of the Small Intestine 31

2.6.1.3 Epithelial Cell Layer and Transport Pathways 33

2.6.2 Strategies for Enhancing Oral Delivery 35

2.6.2.1 Hydrogels and Carriers 35

2.6.2.2 Drug Modification 38

2.7 Conclusions 40

References 48

Chapter 3: Objectives 60

Chapter 4: Synthesis and Characterization of Methacrylic Acid Based Hydrogels as Carriers for Novel Protein-Transporter Bioconjugates 63

4.1 Introduction 63

4.2 Materials and Methods 72

4.2.1 Polymer Microparticle Formation by UV Polymerization 72

4.2.2 Polymer Microparticle Characterization by Scanning Electron Microscopy .. 74

4.3 Results and Discussion 74

4.3.1 Polymer Microparticle Formation by UV Polymerization 74

4.3.2 Polymer Microparticle Characterization by Scanning Electron Microscopy .. 77

4.4 Conclusions 81

References 101

Chapter 5: Synthesis and Characterization of Protein-Transporter Conjugates for Oral Delivery Using Complexation Hydrogels 103

5.1 Introduction 103

5.2 Materials and Methods 109
5.2.1 Synthesis of Insulin-Transferrin Conjugates 109
5.2.2 Synthesis of Calcitonin-Transferrin Conjugates 112
5.2.3 Analysis of Protein-Transporter Conjugates 115
5.3 Results and Discussion 118
5.3.1 Synthesis of Insulin-Transferrin Conjugates 118
5.3.2 Synthesis of Calcitonin-Transferrin Conjugates 121
5.3.3 Analysis of Protein Transporter Conjugates 123
5.4 Conclusions 126
References 141

Chapter 6: Loading and Release Characteristics of Insulin-Transferrin Conjugates from Complexation Hydrogels 144
6.1 Introduction 144
6.2 Materials and Methods 148
6.2.1 Polymer Microparticle Formation by UV Polymerization 148
6.2.2 Loading Time Determination for Large Molecules (Transferrin) 150
6.2.3 Loading of Transferrin into Polymer Microparticles 151
6.2.4 Transferrin Release Studies 152
6.2.5 Loading of Insulin-Transferrin Conjugates into Polymer Microparticles 153
6.2.6 Insulin-Transferrin Conjugate Release Studies 155

6.2.7 Protein Sample Concentration Analysis by HPLC 156
6.3 Results and Discussion 157
6.3.1 Polymer Microparticle Formation by UV Polymerization 157
6.3.2 Loading Time Determination for Large Molecules (Transferrin) 158
6.3.3 Loading of Transferrin into Polymer Microparticles 159
6.3.4 Transferrin Release Studies 161
6.3.5 Loading of Insulin-Transferrin Conjugates into Polymer Microparticles 163
6.3.6 Insulin-Transferrin Conjugate Release Studies 169
6.3.7 Protein Sample Concentration Analysis by HPLC 175
6.4 Conclusions 176
References 194

Chapter 7: Evaluation of Calcitonin-Transferrin Conjugates by Investigation into Loading and Release Properties from Complexation Hydrogels 196
7.1 Introduction 196
7.2 Materials and Methods 201
7.2.1 Polymer Microparticle Formation by UV Polymerization 201
7.2.2 Loading of Calcitonin-Transferrin Conjugates into Polymer Microparticles 203
7.2.3 Calcitonin-Transferrin Conjugate Release Studies 204
7.2.4 Protein Sample Concentration Analysis by HPLC 206
7.3 Results and Discussion 207

7.3.1 Polymer Microparticle Formation by UV Polymerization 207

7.3.2 Loading of Insulin-Transferrin Conjugates into Polymer Microparticles 207

7.3.3 Calcitonin-Transferrin Conjugate Release Studies 214

7.3.4 Protein Sample Concentration Analysis by HPLC 221

7.4 Conclusions 222

References 235

Chapter 8: Evaluation of Insulin-Transferrin Conjugates by Investigation Using Cellular Models and *In Vivo* Animal Models 237

8.1 Introduction 237

8.2 Materials and Methods 242

8.2.1 Development of Caco-2/HT29-MTX Monolayers 242

8.2.2 Protein Transport Across the Cell Monolayer 243

8.2.3 Protein Transport Across the Cell Monolayer in the Presence of P(MAA-g-EG) Microparticles 244

8.2.4 Apical Sample Protein Concentration Analysis by HPLC 245

8.2.5 Measurement of Transported Insulin and Insulin-Transferrin Conjugate Using ELISA Assay Kits 246

8.2.6 *In Vivo* Animal Studies 247

8.3 Results and Discussion 249

8.3.1 Development of Caco-2/HT29-MTX Monolayers 249

8.3.2 Protein Transport Across the Cell Monolayer 250

8.3.3 Protein Transport Across the Cell Monolayer in the Presence of P(MAA-g-EG) Microparticles 254

8.3.4 Apical Sample Protein Concentration Analysis by HPLC 257

8.3.5 Measurement of Transported Insulin and Insulin-Transferrin Conjugate Using ELISA Assay Kits 258

8.3.6 *In Vivo* Animal Studies 258

8.4 Conclusions 260

References 274

Chapter 9: Conclusions 276

References 281

Bibliography 282

Vita…… 300

LIST OF TABLES

Table 4.1: Synthesis parameters used in successfully prepared polymer films 83

Table 8.1: Apparent permeability values for each of the transport studies calculated using Equation 8.3 261

LIST OF FIGURES

Figure 2.1: Basic structure of insulin 41

Figure 2.2: Basic structure of calcitonin 42

Figure 2.3: Schematic of the human digestive system 43

Figure 2.4: Diagram of the human stomach 44

Figure 2.5: Cellular mechanisms of absorption in the small intestine 45

Figure 2.6: Schematic showing interpolymer hydrogen bonding and electrostatic repulsion which cause swelling/deswelling response of polymer 46

Figure 2.7: Structures of components comprising P(MAA-g-EG) systems 47

Figure 4.1: Structures of components comprising P(MAA-g-EG) systems 84

Figure 4.2: Structures of components comprising P(MAA-co-NVP) systems 85

Figure 4.3: Schematic showing interpolymer hydrogen bonding and electrostatic repulsion which cause swelling/deswelling response of P(MAA-g-EG) 86

Figure 4.4: Schematic showing interpolymer hydrogen bonding and electrostatic repulsion which cause swelling/deswelling response of P(MAA-co-NVP) .. 87

Figure 4.5: Illustration showing mucosa interactions of polymer formulations 88

Figure 4.6: Illustration of permeation enhancement ability of anionic hydrogels through calcium binding 89

Figure 4.7: Schematic showing effect of crosslinker length on mesh size of the polymer network 90

Figure 4.8: Schematic showing magnitude of diffusion path length based on particle size 91

Figure 4.9: Method of UV polymerization for thin film polymers 92

Figure 4.10: SEM micrograph of P(MAA-g-EG) with a size <75 microns 93

Figure 4.11: SEM micrograph of P(MAA-g-EG) with a size of 90-150 microns 94

Figure 4.12: SEM micrograph of P(MAA-g-EG) with a size 150-212 microns 95

Figure 4.13: SEM micrograph of P(MAA-g-EG) with 67:33 monomer-to-solvent ratio... 96

Figure 4.14: SEM micrograph of P(MAA-co-NVP) 97

Figure 4.15: SEM micrograph comparison of P(MAA-g-EG) with particle sizes of (a) less than 75 microns, (b) 90-150 microns, and (c) 150-212 microns 98

Figure 4.16: SEM micrograph comparison of P(MAA-g-EG) with (a) PEGDMA1000 crosslinker and 50:50 monomer-to-solvent ration and (b) TEGDMA crosslinker and 67:33 monomer-to-solvent ratio 99

Figure 4.17: SEM micrograph comparison of (a) P(MAA-g-EG) and (b) P(MAA-co-NVP) 100

Figure 5.1: Structure and reactive sites of succinimidyl 3-(2-pyridyldithio) propionate (SPDP)..... 128

Figure 5.2: Step I of insulin-transferrin conjugation reaction..... 129

Figure 5.3: Step II of insulin-transferrin conjugation reaction 130

Figure 5.4: Step III of insulin-transferrin conjugation reaction 131

Figure 5.5: Step IV of insulin-transferrin conjugation reaction 132

Figure 5.6: Step I of calcitonin-transferrin conjugation reaction 133

Figure 5.7: Step II of calcitonin-transferrin conjugation reaction 134

Figure 5.8: Step III of calcitonin-transferrin conjugation reaction 135

Figure 5.9: Step IV of calcitonin-transferrin conjugation reaction 136

Figure 5.10: Structure and conjugation reactivity of insulin. 137

Figure 5.11: HPLC chromatogram showing elution times for insulin, transferrin, and the insulin-transferrin conjugate 138

Figure 5.12: HPLC chromatogram showing elution times for calcitonin, transferrin, and the calcitonin-transferrin conjugate 139

Figure 5.13: Average reaction yields for both the insulin-transferrin conjugation reaction and the calcitonin-transferrin conjugation reaction 140

Figure 6.1: Loading profiles versus time for transferrin loading in P(MAA-g-EG) in PBS buffer (pH 7.4). 177

Figure 6.2: Release profiles for transferrin-loaded microparticles from an extended loading experiment incorporating transferrin in P(MAA-g-EG) for over 29 hours 178

Figure 6.3: Loading efficiencies of transferrin in P(MAA-g-EG) before and after particle collapse and surface washing 179

Figure 6.4: Polymer weight fractions of transferrin in loaded P(MAA-g-EG) microparticles 180

Figure 6.5: Release profiles of transferrin loaded in P(MAA-g-EG) microparticles and placed in PBS buffer (pH 7.4) 181

Figure 6.6: Loading efficiencies of insulin-transferrin conjugates in P(MAA-g-EG) microparticles of differing crosslinker lengths before and after particle collapse and surface washing 182

Figure 6.7: Polymer weight fractions of insulin-transferrin conjugates in P(MAA-g-EG) formulations of differing crosslinker lengths 183

Figure 6.8: Loading efficiencies of insulin-transferrin conjugates in P(MAA-g-EG) formulations of differing monomer-to-solvent ratios before and after particle collapse and surface washing 184

Figure 6.9: Polymer weight fractions of insulin-transferrin conjugates in P(MAA-g-EG) formulations synthesized using different monomer-to-solvent ratios 185

Figure 6.10: Loading efficiencies of insulin-transferrin conjugates in P(MAA-g-EG) formulations of differing particle sizes before and after particle collapse and surface washing. 186

Figure 6.11: Polymer weight fractions of insulin-transferrin conjugates in P(MAA-g-EG) formulations of different particle size ranges 187

Figure 6.12: Loading efficiencies of insulin-transferrin conjugates in P(MAA-g-EG) and P(MAA-co-NVP) polymer formulations before and after particle collapse and surface washing 188

Figure 6.13: Polymer weight fractions of insulin-transferrin conjugates in P(MAA-g-EG) and P(MAA-co-NVP) polymer formulations 189

Figure 6.14: Release profiles of insulin-transferrin conjugates loaded in P(MAA-g-EG) microparticles of differing crosslinker lengths and placed in PBS buffer (pH 7.4) 190

Figure 6.15: Release profiles of insulin-transferrin conjugates loaded in P(MAA-g-EG) microparticles of differing monomer-to-solvent ratios and placed in PBS buffer (pH 7.4) 191

Figure 6.16: Release profiles of insulin-transferrin conjugates loaded in P(MAA-g-EG) microparticles of differing particle sizes and placed in PBS buffer (pH 7.4) 192

Figure 6.17: Release profiles of insulin-transferrin conjugates loaded in P(MAA-g-EG) and P(MAA-co-NVP) microparticles and placed in either PBS buffer (pH 7.4) or PBS buffer (pH 3.2) 193

Figure 7.1: Loading efficiencies of calcitonin-transferrin conjugates in P(MAA-g-EG) microparticles of differing crosslinker lengths before and after particle collapse and surface washing 223

Figure 7.2: Polymer weight fractions of calcitonin-transferrin in loaded P(MAA-g-EG) formulations of differing crosslinker lengths. 224

Figure 7.3: Loading efficiencies of calcitonin-transferrin conjugates in P(MAA-g-EG) formulations of differing monomer-to-solvent ratios before and after particle collapse and surface washing 225

Figure 7.4: Polymer weight fractions of calcitonin-transferrin conjugates in P(MAA-g-EG) formulations synthesized using different monomer-to-solvent ratios 226

Figure 7.5: Loading efficiencies of calcitonin-transferrin conjugates in P(MAA-g-EG) formulations of differing particle sizes before and after particle collapse and surface washing 227

Figure 7.6: Polymer weight fractions of calcitonin-transferrin conjugates in P(MAA-g-EG) formulations of different particle size ranges..... 228

Figure 7.7: Loading efficiencies of calcitonin-transferrin conjugates in P(MAA-g-EG) and P(MAA-co-NVP) polymer formulations before and after particle collapse and surface washing 229

Figure 7.8: Polymer weight fractions of calcitonin-transferrin conjugates in P(MAA-g-EG) and P(MAA-co-NVP) polymer formulations..... 230

Figure 7.9: Release profiles of calcitonin-transferrin conjugates loaded in P(MAA-g-EG) microparticles of differing crosslinker lengths and placed in PBS buffer (pH 7.4) 231

Figure 7.10: Release profiles of calcitonin-transferrin conjugates loaded in P(MAA-g-EG) microparticles of differing monomer-to-solvent ratios and placed in PBS buffer (pH 7.4) 232

Figure 7.11: Release profiles of calcitonin-transferrin conjugates loaded in P(MAA-g-EG) microparticles of differing particle sizes and placed in PBS buffer (pH 7.4) 233

Figure 7.12: Release profiles of calcitonin-transferrin conjugates loaded in P(MAA-g-EG) and P(MAA-co-NVP) microparticles and placed in either PBS buffer (pH 7.4) or PBS buffer (pH 3.2) 234

Figure 8.1: Cellular mechanisms of absorption in the small intestine 262

Figure 8.2: Experimental setup for transport studies using Caco-2/HT29-MTX co-culture cell models..... 263

Figure 8.3: Average transepithelial electrical resistance (TEER) of cell monolayers for one hour after exposure to warm HBSS solution 264

Figure 8.4: Cellular transport profile showing the cumulative amount of insulin transported across the monolayer of Caco-2/HT29-MTX cells over time. 265

Figure 8.5: Cellular transport profile showing the cumulative amount of insulin-transferrin conjugates transported across the monolayer of Caco-2/HT29-MTX cells over time 266

Figure 8.6: Cellular transport profile showing the cumulative amount of insulin-transferrin conjugates transported across the monolayer of Caco-2/HT29-MTX cells while in the presence of excess unmodified transferrin..... 267

Figure 8.7: Average transepithelial electrical resistance (TEER) values throughout the duration of transport studies involving protein solutions consisting of either insulin, insulin-transferrin conjugates, or insulin-transferrin conjugates with excess unmodified transferrin 268

Figure 8.8: Cellular transport profile showing the cumulative amount of insulin transported across the monolayer of Caco-2/HT29-MTX cells while in the presence of P(MAA-g-EG) microparticles 269

Figure 8.9: Cellular transport profile showing the cumulative amount of insulin-transferrin conjugate transported across the monolayer of Caco-2/HT29-MTX cells while in the presence of P(MAA-g-EG) microparticles..... 270

Figure 8.10: Average transepithelial electrical resistance (TEER) values throughout the duration of transport studies of insulin or insulin-transferrin conjugates in the presence of P(MAA-g-EG) microparticles..... 271

Figure 8.11: Calibration curve consisting of known concentrations of insulin in solution. Calibration curve used to determine insulin concentrations of unknown samples..... 272

Figure 8.12: Blood glucose level of male Sprague-Dawley rats after injection of different dosages of insulin-transferrin conjugate or recombinant human insulin (control). Reduction below 100% blood glucose level indicates insulin activity..... 273

CHAPTER 1

INTRODUCTION

Due to the recent growth in the fields of biomedical and pharmaceutical research, an increasing portion of current therapeutic agents is comprised of macromolecules such as proteins. Because of the low solubility and low permeability of most therapeutic proteins, it has been exceedingly difficult to formulate successful oral dosage forms for administering protein drugs. While the oral route remains the preferred route of therapeutic administration, the nature of most protein drugs requires administration through injection to ensure high bioavailability and high efficacy. Insulin, which is used to treat diabetes, is an example of a therapeutic protein which has traditionally been injected. Many patients consider insulin injections to be painful, generally leading to a decrease in patient compliance [1].

Lack of patient compliance in treating diabetes can lead to many serious complications such as blindness, kidney failure, amputations, cardiovascular disease, and even death [2]. Similar consequences also can occur from noncompliance issues with other illnesses treated by protein drugs. In an effort to decrease injections and increase patient compliance, there has been a strong emphasis in recent years on the development of alternative formulations for the delivery of therapeutic proteins [3-5].

Each route of administration for therapeutic agents has its inherent advantages and disadvantages [3]. For therapeutic proteins, the possibility of pulmonary delivery, or delivery through the lungs, has been investigated [6]. While pulmonary delivery allows for rapid drug absorption through the very thin (0.1-0.5 μm) alveolar epithelium with a large surface area (~75 m^2) for absorption in the lung, it also has barriers to effective delivery such as delivery device inefficiency and rapid clearance of the drug from the lungs through enzymatic degradation, mucocilliary clearance, and phagocytosis [7].

Another alternative route for protein delivery is through the skin, or transdermal delivery. Transdermal delivery systems are simple to administer and are relatively painless, but such systems typically suffer from low bioavailability and protein size limitations [8]. It has been shown that iontophoresis, a common enhancement technology for transdermal delivery, can effectively transport a 12.4 kDa protein across the skin [9]. Other enhancement technologies for transdermal delivery are being investigated in an attempt to increase the size limitation of this type of delivery.

Rectal delivery and ocular delivery of proteins have also been considered, but the patient acceptability and discomfort associated with rectal delivery and the effective defense mechanisms of the eye leading to low bioavailability for ocular delivery exclude either from becoming a viable mainstream option [10]. Intravaginal delivery has also received some consideration [4], but the patient discomfort and obvious gender limitations prevent the possibility of its widespread use. The oral route of administration for therapeutic proteins remains the most attractive route of drug delivery for investigation, despite several inherent challenges [11]. This body of work will focus on the development of an effective oral delivery system which utilizes natural transport pathways in an effort to increase bioavailability of the therapeutic protein being delivered.

Oral delivery of proteins is beneficial due to the increased patient compliance, low cost, ease of administration, and the overall increased quality of life for the patient in comparison to injection therapy. To achieve an effective oral delivery system, several physiological barriers must be overcome. For the protein to reach the absorption site of the small intestine, it must first resist proteolytic degradation and the low pH environment of the stomach.

Due to their sensitive nature, most proteins will be degraded or denatured by the enzymes in the stomach [12]. The protein-enzyme interaction can be minimized with the introduction of a protective carrier for the therapeutic protein. By encapsulating the protein in a pH-sensitive hydrogel carrier, it can be protected in the

harsh environment of the stomach and then released in the small intestine based on the physical pH change [13]. As the hydrogel carrier reaches the small intestine, it needs an appropriate residence time at the site of absorption to effectively release the loaded protein. In an effort to increase residence time, tethers consisting of polymer chains can be grafted onto the hydrogel to promote adhesion to the mucosa lining the small intestine [14]. The addition of polymer tethers mitigates the effect of intestinal motility, allowing additional time for the protein to be released.

The primary biological barrier investigated in this work exists as the site of absorption. Due to the large molecular weight of most proteins, transport across the intestinal epithelium into the bloodstream is often extremely difficult. Increased protein transport through the paracellular route can be achieved by a reversible opening of the tight junctions in the presence of polymer hydrogels [15]. The transcellular route of protein transport through the epithelium by conjugation to a transporter ligand has also been investigated [16]. Transcellular protein transport is advantageous for use in a drug delivery system because of less viral risk due to the tight junctions not being opened and the selective targeting of the transporter ligand to its specific receptor on the cell.

This thesis focuses on utilizing the transcellular mechanism of absorption in an attempt to increase overall protein transport across the epithelium. Multiple protein-transporter conjugates were synthesized and characterized for incorporation into polymer hydrogel carriers developed in this lab as drug delivery systems [17]. The hydrogel systems were also optimized for maximum efficiency in the loading and release of each conjugate synthesized. Cellular and animal studies were performed to determine the effect of the conjugate systems on overall protein transport and bioactivity.

Within this body of work, the completed thesis is split into several chapters. Chapter 2 gives in-depth background information on diabetes, insulin, osteoporosis, calcitonin, alternative routes for protein delivery, physiology of the GI tract, and oral

delivery design strategies. Chapter 3 outlines the objectives of this work. The synthesis and modification of the different polymer hydrogel systems is covered in Chapter 4. The synthesis and characterization of multiple protein-transporter conjugates is discussed in Chapter 5. Chapter 6 details the encapsulation and release procedures for *in vitro* analysis of insulin-transferrin conjugates. Loading and release studies performed on calcitonin-transferrin conjugates is discussed in Chapter 7. Chapter 8 contains cellular evaluations of the potential of some of the synthesized conjugate formulations as well as preliminary animal studies conducted using the conjugate. The thesis ends with Chapter 9 which will be comprised of several conclusions about the work performed as a whole.

REFERENCES

1. Zambanini, A., Newson, R.B., Maisey, M., and Feher, M.D., *Injection related anxiety in insulin-treated diabetes.* Diabetes Res. Clin. Pr., 1999. **46**(3): p. 239-246.

2. Helme, D.W., and Harrington, N.G., *Patient accounts for noncompliance with diabetes self-care regimens and physician compliance-gaining response.* Patient Educ. Couns., 2004. **55**(2): p. 281-292.

3. Berlin, C.M., et al., *Alternative Routes of Drug Administration---Advantages and Disadvantages (Subject Review).* Pediatrics, 1997. **100**(1): p. 143-152.

4. Owens, D.R., Zinman, B., and Bolli, G., *Alternative routes of insulin delivery.* Diabetic Med., 2003. **20**(11): p. 886-898.

5. Langer, R., and Peppas, N.A., *Advances in biomaterials, drug delivery, and bionanotechnology.* AIChE J., 2003. **49**(12): p. 2990-3006.

6. Agu, R.U., Ugwoke, M.I., Armand, M., Kinget, R., and Verbeke, N., *The lung as a route for systemic delivery of therapeutic proteins and peptides.* Resp. Res., 2001. **2**(4): p. 198-209.

7. Edwards, D.A., Ben-Jebria, A., and Langer, R., *Recent advances in pulmonary drug delivery using large, porous inhaled particles.* J. Appl. Physiol., 1998. **85**(2): p. 379-385.

8. Banga, Ajay, *Theme Section: Transdermal Delivery of Proteins.* Pharm. Res., 2007. **24**(7): p. 1357-1359.

9. Cázares-Delgadillo, J., Naik, A., Ganem-Rondero, A., Quintanar-Guerrero, D., and Kalia, Y., *Transdermal Delivery of Cytochrome C—A 12.4 kDa Protein—Across Intact Skin by Constant–Current Iontophoresis.* Pharm. Res., 2007. **24**(7): p. 1360-1368.

10. Peppas, N.A., Bures, P., Leobandung, W., and Ichikawa, H., *Hydrogels in pharmaceutical formulations.* Eur. J. Pharm. Biopharm., 2000. **50**(1): p. 27-46.

11. Morishita, M., and Peppas, N.A., *Is the oral route possible for peptide and protein drug delivery?* Drug Discov. Today, 2006. **11**(19-20): p. 905-910.

12. Langguth, P., Bohner, V., Heizmann, J., Merkle, H.P., Wolffram, S., Amidon, G.L., and Yamashita, S., *The challenge of proteolytic enzymes in intestinal peptide delivery.* J. Control. Release, 1997. **46**(1-2): p. 39-57.

13. Yamagata, T., Morishita, M., Kavimandan, N.J., Nakamura, K., Fukuoka, Y., Takayama, K., and Peppas, N.A., *Characterization of insulin protection properties of complexation hydrogels in gastric and intestinal enzyme fluids.* J. Control. Release, 2006. **112**(3): p. 343-349.

14. Serra, L., Domenech, J., and Peppas, N.A., *Design of poly(ethylene glycol)-tethered copolymers as novel mucoadhesive drug delivery systems.* Eur. J. Pharm. Biopharm., 2006. **63**(1): p. 11-18.

15. Ichikawa, H., and Peppas, N.A. , *Novel complexation hydrogels for oral peptide delivery: In vitro evaluation of their cytocompatibility and insulin-transport enhancing effects using Caco-2 cell monolayers.* J. Biomed. Mater. Res. Part A, 2003. **67A**(2): p. 609-617.

16. Kavimandan, N.J., Losi, E., and Peppas, N.A., *Novel delivery system based on complexation hydrogels as delivery vehicles for insulin-transferrin conjugates.* Biomaterials, 2006. **27**(20): p. 3846-3854.

17. Lowman, A.M., Morishita, M., Kajita, M., Nagai, T., and Peppas, N.A., *Oral delivery of insulin using pH-responsive complexation gels.* J. Pharm. Sci., 1999. **88**(9): p. 933-937.

CHAPTER 2

BACKGROUND

Recent advances in the field of biotechnology have led to increased usage of pharmaceutical formulations involving therapeutic proteins. There is a wide variety of therapeutic proteins that are used to treat a wide variety of illnesses. One of the most prevalent therapeutic proteins based on medical need is insulin, which is used to treat diabetes. Another prevalent therapeutic protein is calcitonin, which is administered to treat Paget's disease, bone metastases, hypercalcemia, and postmenopausal osteoporosis.

Due to the sensitive nature of these proteins, they are typically administered through injection as to ensure high bioavailability and biological activity. However, injection therapy often causes patient discomfort, leading to a lack of patient compliance and the complications which can occur as a result. Because of the nature of injection therapy, an alternative route of administration for the therapeutic proteins is highly desired to increase patient compliance and improve overall quality of life. Among the alternative routes of administration, oral delivery of therapeutic proteins is typically considered the most desired route due to its ease of administration, low cost, and high patient compliance. However, designing an effective oral protein delivery formulation is difficult due to protein degradation by digestive enzymes in the stomach, a narrow absorption window in the small intestine, and the epithelial cell barrier lining the villi of the small intestine.

This chapter covers diseases such as diabetes, Paget's disease, hypercalcemia, and others as well as the therapeutic proteins used to treat these illnesses. Also, several alternatives routes of administration for the delivery of proteins will be explored such as transdermal delivery and pulmonary delivery among several others. Then, oral protein delivery is investigated by first discussing the physiological conditions of the

gastrointestinal tract and then discussing strategies to circumvent the natural biological barriers to effective oral protein delivery that are present in the body. The chapter will conclude with a summary of why it is important to understand the target diseases and the proteins which treat them as well as the physiological conditions of the GI tract when designing an effective oral protein delivery system.

2.1 Diabetes Mellitus

Diabetes is an illness in which the body cannot produce or properly use insulin. Specifically, diabetes mellitus refers to a group of diseases which are characterized by chronic hypoglycemia and abnormal metabolism due to a deficiency in the overall effect of insulin in the body [1]. Over 16 million people in the United States are estimated to have diabetes mellitus [2], many of whom are unaware they have the disease. Diabetes affects people of many races and ethnicities, and even appears to have a more profound presence in certain ethnic groups [3]. In fact, diabetes is over 50% more common in African-Americans than in Americans of white or European heritage [4].

Globally, diabetes mellitus is estimated to affect over 150 million people [5] and is prevalent on virtually every continent including Europe [6], Africa [7], and Asia [8]. Moreover, the number of diabetics is predicted to double to over 300 million worldwide in the next 30 years [9]. The most alarming fact is that diabetes is already the 4^{th}-5^{th} leading cause of death in developed countries and is quickly rising in developing countries [10]. The combination of the death toll from diabetes and the expected increase of diabetics to over 300 million by 2030 suggest that diabetes will become a worldwide epidemic in the upcoming decades.

There are several types of diabetes mellitus. Type I diabetes is a disease characterized by the loss of insulin-secreting β cells, leading to insulin deficiency. Type I diabetics generally account for 5-10% of all diabetics worldwide [11]. Type II diabetes is a disease referred to as “adult-onset diabetes” because it often occurs later in life as the body builds up a resistance to insulin. Since the early 1990s, the number of cases of

type II diabetes has increased by over 60% and is still rising due to increasingly sedentary lifestyles [12].

Another condition, called pre-diabetes, is related to type II diabetes in that it is characterized by people with higher blood glucose levels that are at risk for type II diabetes but are technically not in that classification. The number of cases of pre-diabetes is also rising, increasing from an estimated 12 million in 1994 [13] to an estimated 41 million in 2006 [14]. There is another subset of diabetes mellitus which affects pregnant women and their children which consists of two diseases: pregestational diabetes mellitus (PDM) and gestational diabetes mellitus (GDM). PDM and GDM occur in 0.3-0.6% and 2-9% of all pregnancies and typically have adverse effects on the mother and newborn child [15].

Type I diabetes is often referred to as autoimmune diabetes mellitus because of the autoimmune attack of insulin-secreting β cells, leading to insulin deficiency. The autoimmune attack is mediated by T-cells and occurs in the β cells in the pancreatic islets of Langerhans. Generally, no preventative measures can be taken against type I diabetes. However, some options for preservation of β cells are being investigated. One option is to regenerate the β cells through β cell growth factors and stem cell technologies [16]. Another approach is to replace the β cells with either healthy β cells, transplanted islets, artificial insulin-secreting cells, or an artificial pancreas [17]. The protection of β cells through modulation of cytokine signaling, anti-oxidative stress, and the increase of intracellular levels of NAD have also been investigated [18]. Apart from possible technologies resulting from recent research, type I diabetics are generally dependent on insulin therapy to maintain proper blood glucose levels. Regular and controlled insulin dosage is required for the survival of type I diabetics. Improper insulin dosage can result in extremely high blood glucose levels and ketoacidosis, a condition in which the body undergoes abnormal metabolism and releases dangerous amounts of ketone bodies into the bloodstream [19]. If ketoacidosis is not recognized and treated immediately, it can result in a coma or even death of the patient.

Type II diabetes is the most common form of diabetes mellitus and generally develops as a result of the combination effect of an increased insulin resistance as well as a decrease in insulin secretion. The exact cause of type II diabetes is unknown, but obesity, high carbohydrate intake, and lack of physical activity have been shown to increase insulin resistance in the body [20]. Many patients at risk for developing type II diabetes, or those with pre-diabetes, have the possibility of preventing or at least delaying the onset of type II diabetes by adopting healthy eating habits, being regularly active, and maintaining a healthy body weight [21]. Once a patient has developed type II diabetics, the level of insulin dependence can vary over a wide range. Diabetics in the early stages of type II diabetes often do not require therapeutic insulin, but the transition into insulin therapy is typically inevitable due to the progressive nature of the disease [22]. Type II diabetics often have difficulty in determining when they should begin their insulin therapy. Noncompliance of insulin-dependent diabetics, either by skipping needed injections or by miscalculating the amount of insulin, is a point of emphasis in diabetes education and can lead to serious complications if repeated over prolonged periods [23].

Pregestational diabetes mellitus (PDM) and gestational diabetes mellitus (GDM) are two of the less common forms of diabetes and only affect a small percentage of all pregnancies. Gestational diabetes is typically characterized by an elevated blood glucose level in the later months of the pregnancy due to an inadequate adjustment to the glucose metabolism required during pregnancy [24]. Similar to type II diabetes, the risk factors for PDM and GDM include obesity and lack of activity [25]. In some cases, PDM or GDM results from patients which are unaware that they have type II diabetes until they enter a pregnancy. As with type II diabetes, the risk of PDM and GDM can be minimized by maintaining healthy eating habits and an active lifestyle before becoming pregnant. At the onset of gestational diabetes, very precise blood glucose levels must be maintained to prevent diabetic symptoms in the newborn. Blood glucose levels can be controlled primarily through diet; if diet fails, then precise amounts of insulin therapy

are needed [26]. If gestational diabetes in pregnant females is not detected or is not properly treated, childbirth complications such as hydramnios, fetal anomalies, and preterm births can occur [27].

Patients who feel they are at risk for diabetes may get tested in one of two ways. Health care providers will typically either perform a oral glucose tolerance test (OGTT) or a fasting plasma glucose (FPG) test [28]. These tests can be performed to determine if the patient is normal, pre-diabetic, or diabetic. Patients with pre-diabetic blood glucose levels are said to have either impaired glucose tolerance (IGT), or impaired fasting glycemia (IFG) [29]. The American Diabetes Association recommends the use of only FPG to diagnose diabetes, while the World Health Organization recommends the use of OGTT for subjects with IFG [30].

Fasting plasma glucose tests are performed by requiring the patient to perform an overnight fast, then analyzing the blood glucose level the following morning [31]. According to the ADA, normal blood glucose level is indicated by an FPG level of less than 5.6 mmol/L. Patients with FPG levels between 5.6 mmol/L and 7 mmol/L are said to have pre-diabetes, while those with FPG levels over 126 mg/dL are diagnosed with diabetes [32].

Oral glucose tolerance tests are performed similar to FPG tests, but the patient is required to drink a glucose-rich beverage at the end of the overnight fast, and the blood glucose level is measured 2 hours after beverage consumption (2H-PG value). In an OGTT, a normal blood glucose level is represented by a 2H-PG value less than 7.8 mmol/L. If the patient has a 2H-PG value between 7.8 mmol/L and 11.1 mmol/L, he or she is considered pre-diabetic while a 2H-PG value over 11.1 mmol/L classifies the patient as diabetic [33]. FPG tests are becoming the accepted standard for diagnosing diabetes because they are cheaper and faster to perform. In fact, a complete FPG test is performed within the protocol for an OGTT analysis, making FPG tests simpler and quicker to perform.

The most important factor for patients who have developed diabetes is glycemic control. Researchers have investigated and modified insulin for use in insulin therapy for diabetics. Some of the developments in insulin therapy to further diabetes treatment and maintain better glycemic control are discussed in the next section.

2.2 Insulin and Insulin Therapies

The ongoing discovery of the role of insulin in diabetes has had several notable benchmarks over the past 125 years. In 1889, two European physicians, von Mering and Minkowski, removed the pancreas from a healthy dog to determine its effect on biological processes. The scientists discovered that removal of the pancreas caused the dog to develop diabetes. Through further study, they concluded that the pancreas secreted a substance which is used for metabolism of sugar [34]. Attempts to extract this substance now known as insulin were mostly met with frustration due to degradation by digestive enzymes until 1921, when Frederick Banting was able to successfully isolate insulin for use in diabetic subjects [35]. The insulin extraction technique Banting discovered was used to extract insulin for diabetics for several decades without a complete understanding of the structure and function of insulin. In 1959, Joseph Sanger discovered the primary structure of insulin, allowing for greater understanding of its activity and function [36].

Insulin is a hormone protein which is synthesized in the β cells of the pancreas. Insulin is initially produced as a large preprohormone (~11.5 kDa) and later cleaved into proinsulin (~9 kDa). Proinsulin splits into two pieces, one of which is common insulin. Insulin (~5.8 kDa) is comprised of 51 amino acids and has a hydrodynamic radius of 20 Å [37]. The structure of insulin consists of an A chain with 21 amino acids and a B chain with 30 amino acids connected by two disulfide bonds. The structure of insulin is shown in Figure 2.1.

In healthy individuals, the blood glucose level is maintained within a narrow range from 3.5-7.0 mmol/L despite a wide range of fluctuations induced by exercise or

food intake [38]. The maintenance of blood glucose levels is achieved by the regulatory action of the pancreas, which controls the release of insulin and glucagon. While insulin is secreted during periods of high blood glucose, glucagon is just the opposite and is released during periods of low blood glucose. Glucagon is a 29 amino acid polypeptide (~3.5 kDa) which helps increase blood glucose level by binding to glucagon receptors on hepatocytes, causing the liver to release glucose into the bloodstream [39].

The mechanism of insulin release in response to high blood glucose levels begins in the pancreas. After food intake or variable glucose change, glucose enters the β cells in the pancreas via the glucose transporter GLUT2. The glucose in the β cells cause ATP molecules to be formed which can cause the potassium channels to close. Closing of the potassium channels depolarizes the cell, which leads to the intake of calcium through calcium channels. An increased concentration of calcium within the cell allows previously stored insulin to be released from the β cell.

After insulin has been released it will reach the bloodstream via the liver. Freely circulating insulin will interact with several types of cells, the majority of which are fat and muscle cells. Insulin then binds with the insulin receptors on the cell surface. The insulin receptor consists of two extracellular α-subuntis and two transmembrane β-subunits joined by disulfide bonds. Upon insulin binding, the receptor undergoes a rapid conformational change, resulting in activation of the tyrosine kinase domain [40]. Activation of this domain is referred to as receptor autophosphorylation. After phosphorylation of the β-subunits, the insulin receptor activates key enzymes which undergo a complex series of signaling using several signaling pathways which ultimately increase the cell permeability to glucose [41]. The increased permeability in the affected cells allow for increased glucose uptake, providing needed energy for the normal function of the cells. Overall, improper insulin levels affect the body's ability to regulate blood-glucose level, which can lead to serious complications [42].

Insulin therapy is essential to maintaining an average quality of life for millions of insulin-dependent diabetics. Generally, diabetics undergo several injections a day to

maintain their blood glucose levels. Within their daily dosing regimen, diabetics require several different types of insulin. Rapid-acting insulin yields the quickest therapeutic response, beginning to work 5 minutes after injection, peaking at 1 hour, and continuing to work for 2 to 4 hours. Rapid-acting insulin is most often use to immediately reduce post-prandial blood glucose levels [43].

Insulin analogues which take longer to take effect are known as regular insulin, which takes effect 30 minutes after injection, peaks at 2 to 3 hours, and lasts for 3 to 6 hours, and intermediate-acting insulin, which gives a response 2 to 4 hours after injection, peaks at 4 to 12 hours, and lasts 12 to 18 hours. These intermediate insulin analogues are typically injected to maintain a constant blood glucose level through the day, or even in the evening before the patient sleeps [44]. The slowest therapeutic response but also longest lasting effect is produced by long-acting insulin, or basal insulin, which takes effect 6 to 10 hours after injection and usually lasts for 20 to 24 hours. Basal insulin is mostly injected to achieve a minimum basal level of insulin in the bloodstream that is intended to last for 24 hours [45].

Apart from injections performed by the patient several times a day, there are also alternative delivery devices to inject the required insulin. Gaining prominence in the past decade is the use of the insulin pump. The insulin pump eliminates the need for individual injections by supplying regular, accurate amounts of insulin for both basal dosages and bolus dosages after meals. However, insulin pumps are often expensive and have several disadvantages such as an associated weight gain, importance of somewhat complex training, and a possibility of induced ketoacidosis if disconnected from pump [46]. To help alleviate some of the pain and complications which arise from traditional vial and syringe injections, insulin pens were developed. Insulin pens increase therapeutic utility and make injections easier for diabetic patients [47]. However, there is still an associated level of complexity from using the device as well as an associated pain.

Insulin therapy in its most basic form consists of patients injecting themselves multiple times per day. Because of this painful inconvenience that is required of all diabetics to maintain a high quality of life, alternative routes of administration for therapeutic insulin need to be investigated. Several attempts at designing alternative routes of administration for insulin will be explored and discussed later in this section.

2.3 Osteoporosis and Paget's Disease

Protein therapy is used to treat a variety of other illnesses as well. Specifically, calcitonin is used in the treatment of osteoporosis and Paget's disease, as well as hypercalcemia and bone metastases [48]. Osteoporosis is a disease in which bone structure deteriorates and there is a resultant low bone mass. Osteoporosis affects 10 million Americans, and it is especially common in postmenopausal Caucasian women [49]. Paget's disease of bone refers to the condition marked by excessive and abnormal remodeling of bone into a disorganized bone formation. Paget's disease affects only 3% of the population over 40 years old, but approximately 10% of the population over 85 years old [50].

Osteoporosis is marked by a biological imbalance of osteoclast activity, which removes bone tissue, and osteoblast activity, which helps to reform bone tissue. Specifically, osteoporosis occurs in the presence of excessive osteoclast activity, or increased bone resorption, resulting in reduced bone mass and increased chance of fracture [51]. Osteoporosis generally has a greater presence in the postmenopausal female generation, but it can affect men as well [52]. Risk factors for the development of osteoporosis include but are not limited to age, Asian or Caucasian ethnicity, excessive alcohol or smoking, family history of osteoporosis, lack of weight-bearing exercise, sedentary lifestyle, and small body frame [53]. If a patient determines they are at risk for osteoporosis, suggested prevention techniques include physical activity, increased calcium and vitamin D intake, as well as everyday fall prevention [54]. The diagnosis of osteoporosis is most commonly determined by the measurement of bone

mineral density (BMD) using dual energy X-ray absorptiometry (DXA) on the hip or lumbar spine region [55]. The diagnostic criteria for osteoporosis are determined based on the patient's T-score, or number of standard deviations of his or her BMD from the standard set by the World Health Organization. A patient is said to have normal bone mass if his or her T-score is greater than -1. Someone with low bone mass and at risk for osteoporosis would have a T-score between -1 and -2.5. A patient is diagnosed with osteoporosis if he or she has a T-score less than -2.5 [56].

Currently, there are no known cures for osteoporosis but the disease is typically treated with salmon calcitonin, a calcitonin analog that is usually more potent than human calcitonin [57]. Calcitonin acts as an inhibitor to the development of osteoclasts, or bone cells which remove bone tissue [58]. By controlling the amount of osteoclasts, calcitonin mitigates the rate of bone degradation in patients, thus lowering the chance of a fracture. If a patient were noncompliant with his or her required calcitonin dosage, possibly due to the nature of injection therapy, the development of osteoclasts would continue unabated, resulting in bone density loss, elevated calcium levels, and a high chance for bone fracture [59].

Paget's disease of bone is an illness in which there is an excessive amount of bone deterioration and subsequent reformation. The reformation of the affected bone tissue often results in an overall weaker bone structure, thus increasing the chances for pain, arthritis, and bone fractures. Specifically, the cause of the illness comes from abnormal number, size and activity of osteoclasts at the affected bone site. However, Paget's disease largely differs from osteoporosis in that the abnormal activity of the osteoclasts is also mirrored by an abnormal amount of activity in the osteoblasts as well, or cells that create bone tissue [60]. The resultant rapid resorption and reformation of bone tissue is the most recognizable feature of Paget's disease. The exact cause of Paget's disease, however, is somewhat more uncertain. Several have suggested that the abnormal osteoclast function stems from the presence of paramyxoviruses present in the nuclei of the affected osteoclasts, while others suggest the presence of the viruses

are merely a reflection of the abnormal activity rather than a cause [61]. There appear to be no risk factors for Paget's disease related to one's lifestyle, but family history of the disease has been stated as a factor for increased risk of developing the disease [62]. If a patient is at risk for Paget's disease, there is no known method for prevention of development of the disease, but regular physical activity for strengthening bone structure could alleviate some of the future symptoms. There are no known cures for Paget's disease, but it can typically be treated with salmon calcitonin and biphosphonates [63]. Calcitonin and biphosphonates inhibit osteoclast activity and significantly decrease the rate of bone resorption and reformation that is characteristic of Paget's disease, thus decreasing pain felt by the patient and increasing overall quality of life [64]. Due to the nature of calcitonin injection therapy, many patients have to choose to live with the pain associated with Paget's disease or to live with the pain and inconvenience inherent to daily injection therapy.

Calcitonin is a major therapeutic protein for the treatment of diseases related to bone structure. Calcitonin acts as an osteoclast inhibitor, thus reducing bone resorption and strengthening bone structure. While effective in treating osteoporosis and Paget's disease of bone, calcitonin is also used to treat other afflictions resulting from increased bone resorption such as hypercalcemia or bone metastases. The next section will discuss calcitonin therapy in greater detail, including the structure and biological function of calcitonin within the body.

2.4 Calcitonin Therapy

The discovery and development of calcitonin as a therapeutic protein has occurred much more recently than some other therapeutic proteins, such as insulin, but still has undergone many changes in the past 40 years for treating bone diseases. Calcitonin was largely discovered in the early 1960s, when Copp noted that a hormone from the parathyroids regulated the "tone" of calcium in body fluids. He named the protein calcitonin [65]. The ability of calcitonin to lower the calcium levels in the body

were quickly determined to be due to osteoclast inhibition. Knowing that osteoporosis occurred because of increased osteoclast activity, calcitonin was researched as a therapeutic for osteoporosis by the late 1970s. After many years of FDA testing, the first injectable calcitonin, called Calcimar, was approved for treatment of osteoporosis [65].

Calcitonin is a hormone polypeptide which is produced in the thyroid cells of humans. The final form of calcitonin is achieved after the proteolytic cleavage of a large α calcitonin gene. If the α calcitonin gene is cleaved at the 4^{th} exon of 6, the protein calcitonin will result [66]. Calcitonin (~3.4 kDa) is comprised of 32 amino acids with a cyclical end connected by a disulfide linkage. The structure of calcitonin can be seen in Figure 2.2.

Calcitonin formation generally occurs in the thyroidal C cells through alternatively splicing of the α calcitonin gene. The resulting product of the alternative gene splice is α-calcitonin gene-related peptide (α-CGRP). The α-CGRP is mainly a neuropeptide, but it has been found outside of the nervous system [67]. Calcitonin is generally formed in the body in response to a hypercalcemic stimulus [68]. After its formation, the primary function of calcitonin is to decrease calcium levels in the body, mostly through osteoclast inhibition. In addition to its primary function, calcitonin also provides some secondary functions as well. Calcitonin has been shown to have analgesic effects, inhibit postprandial calcium intake, and reduce gastric acid secretion as well as intestinal motility. Many of these effects are thought to occur through calcitonin interaction with receptors in the central nervous system [69].

The mechanism of osteoclast inhibition by calcitonin is initiated by a ligand-receptor interaction. The calcitonin receptor belongs to the class II family of the 7-trans-membrane G-protein-coupled receptors and is expressed on osteoclasts [70]. Moreover, the calcitonin receptor is the primary characteristic used to differentiate osteoclasts from other cell types such as macrophages and phagocytic cells [71]. Upon calcitonin binding to the calcitonin receptor, the osteoclasts undergo a conformational

change, reducing their activity and bone resorption ability. Reduced bone resorption leads to lower serum calcium levels and stronger bone structure in patients with osteoporosis.

Calcitonin therapy in treating osteoporosis and Paget's disease typically consists of patients injecting themselves daily with salmon calcitonin. Human and salmon calcitonin only share 16 of 32 amino acids, but the only sequence required for activity is an 8 amino acid sequence near the N-terminal disulfide bridge. Salmon calcitonin is up to forty times more potent than human calcitonin due to a highly flexible α-helical peptide structure which allows for optimal binding with the calcitonin receptor [72].

Many patients have improved their quality of life by undergoing treatment with salmon calcitonin injections. However, these injections are still painful and may eventually lead to noncompliance with chronic use. Noncompliance in calcitonin therapy may very often lead to an increased risk of fracture and weaker bone structure. Because of the nature of injection therapy, alternative routes of administration for calcitonin need to be investigated. The next section will cover attempts at alternatives to injection therapy for therapeutic proteins such as insulin and calcitonin.

2.5 Alternative Routes for Protein Delivery

Currently, diabetic patients must inject themselves several times a day with insulin to maintain their blood glucose levels. Daily injection therapy often leads to noncompliance, thus lowering the overall efficacy of the treatment. Alternative routes of administration for insulin which are non-invasive and convenient are being investigated. The development of such a system would mean an increase if efficacy and quality of life for diabetic patients worldwide. In this section, several alternative systems will be discussed. The systems will be categorized by their route of delivery and will include pulmonary, transdermal, nasal, buccal, ocular, rectal, and vaginal delivery systems.

2.5.1 Pulmonary Delivery

Recently, there have been many attempts to use pulmonary delivery, or delivery through the lungs, to administer therapeutic proteins [73]. Delivery through the lungs offers many advantages such as a very thin (0.1-0.5 μm) alveolar epithelium and a large surface area (~75 m^2) for absorption. Also, pulmonary delivery allows for avoidance of first pass hepatic metabolism [74]. However, within pulmonary delivery also exists many barriers to effective absorption including delivery device inefficiency and rapid clearance of the drug from the lungs through enzymatic degradation, mucociliary clearance, and phagocytosis [75]. Despite these challenges, there have been several moderately successful therapeutic protein pulmonary delivery systems.

Several pulmonary delivery systems have been designed specifically for insulin, many of which have actually made it into FDA testing. Some of these systems include AERx Insulin Diabetes Management System (AERx iDMS) (Aradigm/Novo Nordisk), AIR system (Alkermes/Eli Lilly), Technosphere (MannKind Corporation), and Kos Inhaled Insulin (Kos Pharmaceuticals) [76]. However, probably the furthest progressed and most notable formulation of inhalable insulin to enter the marketplace is Exubera (Nektar/Pfizer/Sanofi-Aventis). The Exubera delivery system consists of rapid-acting dry powder human insulin packaged in blister packaging for stability and delivered through use of an inhaler device which has a holding chamber from which the patient inhales the insulin. Exubera is intended to be used for post-prandial blood glucose maintenance due to its relatively quick peak insulin concentrations occurring after 49 minutes [77]. However, the size and complexity of the Exubera delivery device reduced its convenience. Also, patients were still required to inject themselves with basal insulin everyday as well as undergo periodic lung tests to ensure proper lung function. These disadvantages of Exubera limited the market success and subsequently caused Pfizer to abandon the sale of the device. In a similar situation, Novo Nordisk also abandoned their inhalable insulin device, AERx iDMS [78]. Development of other inhalable insulin products like MannKind's Technosphere continue in an effort to learn from the mistakes

of the market predecessors, but inherent disadvantages to pulmonary insulin delivery such as delivery device inefficiency and unreliable dosing present challenges that must be addressed.

Although less publicized relative to inhalable insulin, researchers are investigating the possibility of pulmonary calcitonin delivery. Patton et al. used intratracheal administration to deliver salmon and human calcitonin to rats and were able to achieve 17% absolute bioavailability in both cases [79]. Also, using a different dry powder salmon calcitonin formulation, Deftos et al. were able to administer inhaled calcitonin with 66% of the bioactivity and 28% relative bioavailability to calcitonin injections [80]. In both cases, the inhalable calcitonin formulations benefited from the inherent advantages of pulmonary delivery (higher bioavailabilities than alternative routes, reduced side effects) but still must overcome complexities of the delivery device and unreliable dosing regimens to become a viable mainstream option.

Pulmonary delivery devices for the administration of therapeutic proteins have probably achieved more success than most of the other types of delivery devices as evident by the push of new inhalable insulin products into the pharmaceutical marketplace. The moderate success can most likely be attributed to the high bioavailability values achievable through pulmonary delivery. However, further research is needed to overcome the existing challenges with pulmonary delivery mentioned in this section.

2.5.2 Transdermal Delivery

In recent years, researchers have also focused on administering therapeutic proteins using transdermal delivery, or delivery through the skin [81]. The major advantages of transdermal delivery are simplicity of design and ease of administration. Most formulations would only require the patient to apply a small patch to his or her skin or to apply a topical cream. Transdermal systems would be extremely non-invasive and painless. However, most transdermal delivery systems suffer from poor transport

into the bloodstream due to the stratum corneum, a protective layer which lines the skin. Effective delivery of large molecules such as therapeutic proteins across the skin requires disruption or a bypass of the stratum corneum. Common methods to circumvent this barrier include iontophoresis, electroporation, ultrasound, and high velocity powder penetration [82]. Iontophoresis involves applying a small electrical current to the skin to allow protein delivery, although the maximum amount delivered is often less than one milligram and the method can suffer from protein size limitations [83]. Electroporation is the method by which brief high energy bursts are used to disrupt the skin and allow for protein transport. Ultrasound has also been used to increase protein transport by disrupting the stratum corneum by cavitation. Another method to increase transport is to use high velocity powders driven by helium at supersonic speeds [82]. Using these methods, several researchers have designed transdermal delivery systems which show promise for future transdermal delivery research.

Many scientists have investigated the possibility of insulin delivery through a transdermal route of administration. Smith et al. used ultrasound-mediated transdermal delivery to deliver insulin across the stratum corneum and were able to achieve a sevenfold increase in insulin transport relative to a passive transmission control [84]. However, a sevenfold increase in transmission of insulin naturally across the skin still results in a low bioavailability and limits the use of the research as a potential delivery device, even though it does promise potential for possible inclusion of the technique in the design of future devices. Also, using electroporation as a transdermal delivery enhancer, Sen et al. [85] showed that lipids, specifically 1,2-dimyristoyl-3-phosphatidylserine (DMPS), present during electroporation can increase insulin transport by a factor of twenty. However, lipid enhanced electroporation generally can only increase transport of molecules up to 10 kDa in size, limiting its application for larger therapeutic proteins. In both transdermal insulin delivery systems,

the devices suffer from low bioavailability due to the effective protection of the stratum corneum.

In addition to transdermal insulin delivery systems, researchers have also investigated the possibility of transdermal salmon calcitonin delivery. Nakamura et al. designed a transdermal delivery system for salmon calcitonin using pulse depolarization-iontophoresis. Iontophoresis generally has a protein size limitation of around 11 kDa, but because salmon calcitonin is relatively small (~3.4 kDa), it is a suitable candidate for delivery through iontophoresis. Nakamura et al. [86] showed an increase in calcitonin for an increase of current up to 0.5 mA and also achieved an absolute bioavailability of ~35% [86]. While transdermal delivery of salmon calcitonin is somewhat effective through iontophoresis, many proteins are excluded from iontophoresis as a transport enhancer due to their large size.

Transdermal delivery systems for the administration of therapeutic proteins have gained increasing interest over the past several years. The increased desire for the appearance of one of these systems in the marketplace most likely results from the high degree of non-invasiveness associated with transdermal delivery systems as well as the ease of administration. However, before suitable transdermal delivery systems can be sold to the general public, researchers must continue to search for ways in which protein transport can be increased across the stratum corneum as well as ways to eliminate the protein size limitations typically inherent to transdermal delivery.

2.5.3 Nasal Delivery

In addition to pulmonary and transdermal delivery, researchers have also investigated administration of therapeutic proteins through the nasal route, or delivery through the nasal cavity [87]. Nasal drug delivery offers many advantages such as a large surface area for absorption, a thin nasal epithelium allowing for increased absorption, and an avoidance of first pass metabolism [88]. Most nasal delivery devices consist of a inhaler to be administered through the nostril of the patient. An effective

nasal delivery device would have the advantages of being non-invasive to the patient and relatively easy to administer. In many ways, nasal delivery devices benefit from the same advantages as pulmonary delivery devices with the major difference being the site of absorption. However, as with pulmonary devices, there are also associated disadvantages for nasal delivery systems. Administration through the nasal route can be affected by barriers to permeability such as enzymes in the nasal cavity or nasal mucosa, mucociliary clearance or ciliary beating. Also, nasal delivery is often limited by molecule size, excluding the majority of proteins from being delivered efficiently [89]. Despite these challenges, several attempts have been made to design an effective nasal delivery system for the administration of therapeutic proteins.

In an effort to decrease the invasiveness of insulin therapy, researchers have begun investigating the possibility of using nasal delivery to administer therapeutic insulin. Dondeti et al. administered an insulin spray formulation to diabetic rabbits to observe its hypoglycemic effect. The insulin spray formulations were combined with bioadhesive polymers and permeation enhancers to increase the overall bioavailability. In the most successful of the formulations (insulin, microcrystal cellulose, and sodium taurocholate), the absolute bioavailability was found to be 8.36% [90]. While a significant increase from insulin administered with no additives, the achieved bioavailability is still considerably lower than bioavailability levels expected to warrant the formation of a marketplace product for insulin. The decrease in bioavailability of insulin administered through the nasal route in this research is most likely due to the barriers to permeability such as enzymes and mucociliary clearance.

In relation to insulin(~5.8 kDa), salmon calcitonin (~3.4 kDa) is significantly smaller in size, making it a more likely candidate for effective delivery through the nasal cavity. In fact, the ability of calcitonin to be delivered nasally was recognized by Sandoz Pharmaceuticals, who introduced Miacalcin in 1995. Miacalcin is a nasal spray formulation for calcitonin which has been shown to reduce postmenopausal bone loss as well as reduce the incidence of vertebral fracture by 60% [91]. However, the

bioavailability was shown to vary greatly among patients, fluctuating from 0.3% to 30.6% with an average bioavailability of 3% relative to injections. The significant variability most likely increases the difficulty of calculating proper dosages, leading to inefficient clinical use and wasted therapeutic calcitonin. Despite these drawbacks, nasal delivery of calcitonin shows promise for alleviating the inconvenience of daily injections for patients with bone disorders.

Nasal delivery systems for the administration of therapeutic proteins have gained considerable attention over the past decade and will continue to grow in interest. The potential benefits of a non-invasive, simple administration nasal delivery device have led researchers to try and overcome some of the barriers of nasal delivery such as barriers to permeation and drug size limitations. Because of the size limitation, many therapeutic proteins may not make suitable candidates for nasal delivery. However, the smaller proteins such as calcitonin represent the subcategory of therapeutic proteins most suitable for nasal delivery and should be investigated further.

2.5.4 Buccal Delivery

Recently, there has also been increased emphasis on administering therapeutic proteins using buccal delivery, or delivery through the mucosa of the mouth [92]. Some of the associated benefits of buccal delivery are direct access to systemic circulation allowing a bypass of first pass metabolism, low enzymatic activity, ease of administration, and an ability to easily include permeation enhancers or enzyme inhibitors in the formulation [93]. However, buccal delivery also presents many challenges or barriers which must be overcome. The buccal membrane typically offers a smaller area for absorption (170 cm^2) as well as having a low associated permeability. Also, the continuous secretion of saliva also presents challenges such as dilution of the drug, loss of drug or dosage form through swallowing, and even a danger of choking on the delivery system [94]. Several researchers have attempted to overcome these challenges and to design an effective buccal delivery system for therapeutic proteins.

Because of its prevalence in patients worldwide, insulin has become a target for the design of an effective buccal delivery system. Portero et al. [95] designed a novel system to attempt to overcome many of the challenges of buccal delivery of insulin. The system consists of a mucoadhesive chitosan layer containing insulin and an impermeable protective layer composed of ethylcellulose. This device design allows for unidirectional insulin release, preventing significant loss of the drug due to saliva scavenging. While this design helps to alleviate the problems arising from saliva production, it still does not address the challenge of small area for absorption or low permeability. Alternative research has suggested the use of permeation enhancers and enzyme inhibitors to increase insulin absorption in the oral cavity [96]. A successful and effective buccal insulin delivery system would most likely require a combinatorial approach, utilizing the concept of mucoadhesiveness and unidirectional drug flow as well as increase permeability and stability.

Buccal delivery of calcitonin has not been investigating nearly to the extent that many other proteins have been investigated. Buccal calcitonin delivery systems still must overcome the same challenges of low absorption area, low permeability, and saliva production. However, the size of calcitonin is considerably less than that of insulin and many other proteins, most likely increasing its ability to diffuse through the mucosa lining the oral cavity. While not receiving widespread attention in the research field, the possibility of buccal calcitonin delivery has been investigated [97]. Further investigation is needed to determine if calcitonin administration using buccal delivery is a viable alternative to injection therapy.

Buccal delivery systems for the delivery of therapeutic proteins have been gaining increasing attention from the scientific community. While not as publicized as other alternative routes such as transdermal delivery or pulmonary delivery, buccal delivery offers many unique advantages for protein delivery including avoidance of first pass metabolism, low enzymatic activity, simple administration, and an ability to easily introduce permeation enhancers or enzyme inhibitors into the formulation. However,

researchers must formulate approaches which can overcome natural barriers to protein absorption such as low permeability and saliva production.

2.5.5 Other Routes for Protein Delivery

Apart from the aforementioned alternative routes for delivery, there are also several less publicized routes of delivery also being investigated. One alternative route which is being investigated is ocular delivery, or delivery through the eye [98]. However, due to the effective defensive mechanism in the eye, transport into the bloodstream and bioavailability are typically low for ocular delivery. Intravaginal delivery has also received some consideration [99], but the patient discomfort and obvious gender limitations prevent the possibility of its widespread use. Rectal delivery has also been investigated [100], but reduced surface area for absorption and wide variability in patient acceptability limits the potential for rectal delivery of proteins. One final alternative route for protein delivery is oral delivery. The oral route of administration for therapeutic proteins remains the most attractive route of drug delivery for investigation, despite several inherent challenges [101]. Since oral protein delivery is the focus of this thesis, the benefits and challenges as well as possible strategies to overcome those barriers will be discussed in greater detail in the following section.

2.6 Oral Protein Delivery

Among the routes of administration as alternatives to injection therapy, oral delivery remains the preferred route of administration by most patients. Oral delivery of proteins is beneficial due to its low cost, ease of administration, and high patient compliance. Therapeutic proteins administered in a pill or capsule form would greatly improve the quality of life of patients who require the medicine if the oral delivery form could either partially or completely remove their injection therapy regimen. However, designing an effective oral protein delivery system requires overcoming several barriers inherent to the oral route of administration.

Due to the sensitive nature of most therapeutic proteins, they are typically degraded in the stomach after being administered orally, allowing only a minute fraction to reach the site of absorption in the small intestine. The degradation occurs due to the harsh environment of the gastric environment, including low pH and an abundance of digestive enzymes which are intended to break down proteins for food and energy. Also, intestinal motility presents a challenge in that it shortens the absorption window for the protein to absorb in the small intestine. The reduced residence time of any intact protein in the small intestine further reduces the chance for protein absorption into the bloodstream. Finally, the epithelial cell layer lining the microvilli in the small intestine also presents a final barrier to protein absorption. Epithelial cells form a tight monolayer which is designed to prevent introduction of toxins and foreign bodies into the bloodstream. Absorption of a large therapeutic protein would require a disruption of the cell monolayer or enhanced transport of the protein. Researchers have designed many different systems to overcome these challenges and to create an effective oral delivery system for therapeutic proteins.

Over the past several years, many methods have been employed to overcome the barriers inherent to oral protein delivery. Approaches to increase bioavailability of the protein include the use of permeation enhancers to increase epithelial transport [102], protease inhibitors to reduce protein degradation [103], enteric coatings for protection in the harsh environment of the stomach [104], encapsulation of the protein in polymer microparticles for protection and increased residence time at the site of absorption [105], and combinatorial approaches as well [106]. Several of these approaches are discussed in greater detail in later sections.

In order to design a more effective oral protein delivery system, it is necessary first to understand the conditions surrounding the oral route of administration including the influence and effect the surrounding environment has on the administered dosage form. Specifically, it is important to understand the physiology of the gastrointestinal (GI) tract for oral delivery systems. The physiology of the GI tract, including the

physiology of the stomach, small intestine, and epithelial cell layer, are discussed in detail in the following section.

2.6.1 Physiology of the GI Tract

The gastrointestinal (GI) tract, or alimentary canal, is the system of organs which comprise the digestive system in animals. The primary functions of the digestive system are digestion of food to extract energy and essential nutrients and excretion of the remaining waste. When medication is administered orally, the medicine is subjected to the same processes the digestive system uses to break down food. It is important when designing oral drug delivery formulations to consider the physiological barriers and challenges that will arise throughout the transit of the GI tract.

The GI tract consists of many different organs which perform several individual functions. Within the GI tract, the stomach and small intestine are the primary organs affecting the design of an oral protein delivery system. A schematic of the GI tract is shown in Figure 2.3. Most therapeutic proteins are dangerously susceptible to degradation by proteolytic enzymes in the GI tract, especially in the stomach. After the protein passes the stomach, it enters the small intestine. There is still a risk of proteolytic degradation in the small intestine, albeit reduced in comparison to the stomach.

The most formidable barrier in the small intestine is the difficult absorption and transport of the protein into the bloodstream. The high molecular weight of most proteins and the tight junctions of the epithelial cell layer make protein transport across the epithelium nearly impossible. Therapeutic proteins such as insulin which have been administered orally in their native form have been shown to have a bioavailability, or portion of the total drug which reaches the bloodstream, as low as <0.1% [107]. An in-depth understanding of the anatomy and physiology of the stomach and small intestine is essential to circumventing such barriers for an oral delivery system.

2.6.1.1 Anatomy and Physiology of the Stomach

The stomach is divided into four major regions: the cardia, the fundus, the body (or corpus), and the pylorus (or antrum). The cardia is the upper region of the stomach where the contents of the esophagus are emptied into the stomach. The fundus is the region formed by the upper curvature of the stomach. The fundus and the body, the central region of the stomach, harbor the acid-secreting glands within the stomach [108]. The pylorus is located at the bottom of the stomach and facilitates the emptying of the contents of the stomach into the small intestine. A schematic of the stomach is shown in Figure 2.4. In order for the required nutrients to be absorbed into the bloodstream, the stomach must first break down the large proteins into peptides that can be further digested in the small intestine.

Proteins in the stomach are typically broken down by digestive enzymes called proteases. Pepsinogen, an abundant protease in the stomach, is secreted by the gastric chief cells lining the stomach lumen. Pepsinogen is an inactive enzyme, but it is readily converted to the active protease pepsin in the presence of the hydrochloric acid found in the stomach [109]. Pepsin and other digestive enzymes such as trypsin are largely responsible for the major degradation that proteins endure within the stomach.

The stomach presents a major challenge to oral protein delivery in the preservation of the activity of the ingested protein. Efforts to overcome this challenge have included the introduction of protease inhibitors and protective encapsulation of the protein. Upon administration of the protease inhibitor aprotinin with the therapeutic protein insulin (in bile acid), insulin absorption was amplified approximately 30 times relative to the administration of insulin alone [110]. However, the resultant bioavailability of the formulation was still somewhat low (~0.75%).

Researchers have also been focusing on the idea of protective encapsulation for the protein. The protective matrices are designed to prevent the diffusion of external digestive enzymes into the system, thus protecting the protein on its transit through the stomach. The inherent difficulty in designing a protective encapsulation for protein

delivery is that it must limit diffusion in the stomach but it must also promote diffusion in the small intestine. In an attempt to achieve the required dual function of the delivery system, degradable microspheres have been proposed as protein carriers [111]. An alternate design strategy is to utilize a physiological difference between the stomach and the small intestine as an external trigger for the switch between the protection and release functions. A significant physiological difference exists between the pH of the stomach (pH~2) and the small intestine (pH~7), prompting the need for a pH-sensitive carrier system. The introduction of intelligent, pH-responsive hydrogels as protein carriers has shown tremendous possibility for the systems and the research remains one of the most promising prospects for oral protein delivery [112].

2.6.1.2 Physiology of the Small Intestine

The small intestine is divided into three sections: the duodenum, the jejunum, and the ileum. Ingested food empties from the stomach into the duodenum, the upper region of the small intestine. The duodenum is approximately 0.26 m in length and is responsible for the majority of the digestion that occurs in the small intestine. The duodenum empties its contents into the jejunum, the middle portion of the small intestine. The jejunum is approximately 2.5 m long and empties into the ileum, the lower part of the small intestine. The ileum is approximately 3.5 m long and serves to absorb any products of digestion that were note absorbed by the jejunum. In order to increase absorption of necessary nutrients, the small intestine contains many surface features to maximize the possible surface area for nutrient uptake. The small intestine contains circular folds throughout called valvulae conniventes that increase the surface area by a factor of 3.

Lining the intestinal wall are finger-like projections called villi, which effectively increase the surface area of the small intestine by a factor of 10. The intestinal villi have additional finger-like projections called microvilli, which increase the surface area by a factor of 20. The valvulae conniventes, villi, and microvilli effectively increase the

overall surface area by a factor of 600 compared to that of a hollow cylinder of the same dimensions [113]. The large surface area of the small intestine, comparable to the area of a tennis court, provides an ideal environment for absorption.

The physiology of the small intestine presents multiple unique challenges for oral protein delivery. Digestive enzymes are still present in the small intestine but are mostly contained in the duodenum. Another challenge in oral protein delivery is intestinal motility. Intestinal motility refers to flow through the lumen of the small intestine and the muscles and motions of the wall which regulate the flow. Proteins administered free of any encapsulation or protective coating are generally affected by intestinal motility significantly less due to the possibility immediate absorption of the protein. However, proteins administered without a protective encapsulation are much less likely to survive the transit to the small intestine [105].

Encapsulated proteins have an associated diffusion time for release from the carrier system. The protein diffusion time combined with the narrow absorption window of low solubility, low permeability proteins form a major challenge for effective oral protein delivery. Increasing the residence time of the protective carriers in the small intestine is essential for allowing time for the protein to diffuse and maximizing the protein absorption window [114]. Mucoadhesive materials are often used in designing polymeric carriers in an attempt to increase residence time by contact with the intestinal mucosa [115]. Mucoadhesive drug delivery systems also allow for site specific targeting within the brush border region of the small intestine. Further work has shown that the addition of polymeric tethers to the pH-sensitive carrier systems can further promote mucoadhesion and enhance the complexation/decomplexation effect of the carrier [116]. The combination of the protection abilities of carrier systems with the system modifications to increase residence time is proving to be substantial progress towards the goal of designing an effective oral protein delivery system.

2.6.1.3 Epithelial Cell Layer and Transport Pathways

When nutrients are absorbed during the process of digestion, they must pass through the epithelial cell layer lining the small intestine in order to reach the bloodstream. The same barrier exists for therapeutics intended for absorption into the bloodstream. An administered therapeutic can be absorbed either through the paracellular or transcellular transport pathways. *Paracellular* refers to transport of the molecule between the cells, while *transcellular* refers to transport through the cell itself. A diagram demonstrating the different mechanisms of absorption is shown in Figure 2.5. Paracellular transport of large molecules is typically limited by the tight junctions between the epithelial cells. Under normal conditions, the tight junctions will only permit the transport of molecules with radii <11 Å [117]. However, research is being performed to formulate strategies by which the normal paracellular transport can be enhanced to allow absorption of large therapeutic proteins [118].

A common strategy for enhancing paracellular transport is the use of permeation enhancers. Ethylenediamine-tetraacetic acid (EDTA) can act as a permeation enhancer by binding to extracellular Ca^{2+}, thus lowering the intracellular Ca^{2+}, an important molecule in regulating the tight junctions [119]. Though permeation enhancers increase overall absorption of large proteins, they achieve the increase in permeability by disrupting the cell monolayer in a manner non-specific to the protein, thus allowing possible toxins and biological pathogens to enter the bloodstream [120]. Paracellular transport remains a viable option for the transport of large molecules such as proteins. However, the feasibility of an oral delivery system which utilizes paracellular transport hinges on a design in which the tight junctions are opened reversibly and without permanent damage as well as in a manner specific to the therapeutic protein.

There are four types of transcellular transport: passive diffusion, carrier-mediated transcytosis, receptor-mediated transcytosis, and efflux transport. Utilizing transcellular transport in a design strategy for oral protein delivery has the inherent advantage that the tight junctions will not be opened, greatly decreasing the risk of

viruses or toxins entering the bloodstream. However, transport of a large protein across the cell is very difficult under normal conditions.

The simplest type of transcellular transport, passive diffusion, is simple diffusion of a molecule from one side of the cell monolayer to the other side and is typically only possible for small molecules such as carbon dioxide and oxygen [121].

Another type of transcellular transport, efflux transport, typically does not result in transcytosis of the molecule, rendering it useless for most oral delivery applications.

Carrier-mediated transcytosis and receptor-mediated transcytosis involve the molecule interacting with the lipid bilayer and reversibly binding to either a carrier molecule or a specific receptor. The complex is then transported to the inside of the cell. In carrier-mediated transport, the molecule-carrier complex dissociates after transporting the molecule inside the cell, allowing the molecule to drift to the other side and engage in a similar carrier-mediated process to exit the cell [121]. However, in receptor-mediated transcytosis, a specific molecule binds to a specific receptor on the cell surface due to its high affinity for the receptor. The molecule-receptor complex is then transported into the cell and remains intact until it dissociates on the opposite side of the cell.

Receptor-mediated transport is a naturally occurring process typically used to transport essential nutrients into the body but recently has gained interest as a design strategy for oral drug delivery [122]. Strategies include conjugating the drug of choice to a targeting ligand which is recognized by a specific receptor and transported across the cell. Receptor-mediated protein delivery systems benefit from specificity achieved due to the high affinity of the receptor molecule for only the ligand molecule, ensuring no toxins enter the bloodstream. The specific uptake of therapeutic proteins could also lead to a significant increase in bioavailability. Having a thorough understanding of the physiology of the stomach, small intestine, and epithelial cell layer allows for employment of several specific strategies in design of an oral delivery system. The

following section details the background knowledge necessary to understand the specific approaches taken within this research to design oral protein delivery systems.

2.6.2 Strategies for Enhancing Oral Delivery

The strategies employed in this work to enhance oral delivery of proteins can be classified into two categories. The first category of strategies explored consists of carrier entities. This strategy does not modify the protein itself, but instead incorporates it into a system which can protect it in the stomach, target the site of absorption, and facilitate release of the therapeutic protein for subsequent absorption. In contrast, the second category of strategies consists of drug modification. Fundamentally different from carrier strategies, drug modification strategies consist of modifying the therapeutic protein itself to change its mechanics and properties. Specifically, these strategies typically consist of covalent conjugation of another molecule to the protein of interest in such a way as to preserve medicinal activity but also enhancing transport properties. In this work, drug modification is used to increase transport across the epithelial cell layer in the small intestine. The following sections detail necessary background information concerning incorporation of carriers and drug modification for improved oral protein delivery.

2.6.2.1 Hydrogels and Carriers

The sensitivity and delicate nature of most therapeutic proteins have led many researchers to investigate the possibility of encapsulating proteins to be delivered orally [123]. These novel carrier systems are designed to protect the protein within the environment of the stomach, and also to release the protein to be absorbed within the small intestine. One of the more promising options for protein carrier systems are hydrogel carriers [98, 124, 125]. A hydrogel carrier is comprised of a three-dimensional hydrophilic polymer network which will typically swell and imbibe water under certain specific conditions. The swelling is considered an “intelligent” response to the stimulus

generated by the specific conditions. Hydrogel systems can be designed such that in the swollen state, large molecules such as proteins are free to diffuse in and out of the system. However, these same systems can be forced to collapse using a specific stimulus, thus entrapping any proteins present within the polymer network. Entrapped proteins will remain within the polymer network as long as the carrier is collapsed, preventing any diffusion inward of enzymes or other substances which could degrade the protein. Hydrogels possess tremendous potential for oral protein delivery in that a protein can be protected in the stomach while in the collapsed state and then subsequently released for absorption in the small intestine by the swelling response of the system.

Hydrogels are crosslinked, water-insoluble polymeric carriers capable of exhibiting a stimuli-sensitive swelling response. Swelling behavior can be triggered in response to changes in factors such as temperature, pH, electric field, light, and even the presence of specific molecules [126]. For oral delivery applications, swelling of the hydrogel carrier is desired near the site of absorption in the small intestine. One of the most notable differences between the stomach (pH ~ 2) and the small intestine (pH ~ 7) is the pH of surrounding environment. For this reason, many oral protein delivery systems are designed around the use of pH-sensitive hydrogels [105].

Hydrogels are generally divided into four categories: neutral, ampholytic, anionic, and cationic [127]. Most pH-sensitive hydrogels are typically either classified as anionic or cationic hydrogels depending on the nature of their ionizable pendant groups. Cationic hydrogels contain pendant groups which become protonated at a pH *below* the pKa of the ionizable groups. The protonation results in local positive charges throughout the network, causing the system to swell as a result of electrostatic repulsion. At a pH *above* the pKa of the ionizable groups, cationic hydrogels will remain collapsed due to interpolymer hydrogen bonding. Anionic hydrogels exhibit an opposite response to environmental pH compared with cationic hydrogels. Anionic hydrogels contain pendant groups which become deprotonated at a pH *above* the pKa of the

ionizable groups. The deprotonated pendant groups results in local negative charges throughout the polymer system, causing an overall swelling response. At a pH *below* the pKa of the ionizable groups, anionic hydrogels will remain collapsed due to interpolymer hydrogen bonding. For oral protein delivery applications, the hydrogel carrier needs to protect the protein in the stomach (remain collapsed) and release the protein for absorption in the small intestine (become swollen). Based on the design requirements, the pH-sensitive hydrogels investigated in this thesis will be anionic.

The primary hydrogel system under investigation in this thesis is comprised of a poly(methacrylic acid) polymer backbone grafted with poly(ethylene glycol) tethers (P(MAA-g-EG)). However, other hydrogel systems such as poly(methacrylic acid) polymerized with the copolymer N-vinyl pyrrolidone (P(MAA-co-NVP)) will also be investigated. The primary materials used in synthesizing P(MAA-g-EG) are methacrylic acid (MAA) and poly(ethylene glycol) monomethyl ether monomethacrylate (PEGMA). In acidic conditions, MAA and PEG form interpolymer complexes due to hydrogen bonding, forming physical crosslinks within the system and forcing the polymer into a collapsed state. A schematic showing the interaction of the MAA and PEG polymer chains in the collapsed and swollen states is presented in Figure 2.6. The P(MAA-g-EG) hydrogels are crosslinked by poly(ethylene glycol) dimethacrylate (PEGDMA), which can have an effect on the mesh size and release characteristics of the system by altering the length of the crosslinker and the crosslinking ratio. The polymer hydrogels are synthesized by UV initiated free radical polymerization using the UV initiator Irgacure 184^{TM}. The structures of the materials used in the synthesis of P(MAA-g-EG) hydrogels can be seen in Figure 2.7.

P(MAA-g-EG) microparticles have been shown to possess desirable characteristics for oral delivery such as the ability to protect proteins such as insulin within the stomach and also the ability to increase residence time through mucoadhesion within the small intestine. Encapsulation of insulin within P(MAA-g-EG) microparticles has been shown to preserve over 80% of the loaded insulin after being

treated for one hour in gastric fluid. In contrast, only 20% of free insulin remained intact after the same treatment with gastric fluid [128]. The addition of PEG tethers to a poly(acrylic acid) (PAA) system design was shown to increase the mucoadhesive capacity of the microparticles, generating a work of adhesion of approximately 130 x 10^{-3} mJ, or five times that of a pure PAA system. P(MAA-g-EG) microparticles have proven to be a viable means for delivering insulin to the bloodstream, achieving a 12.8% bioavailability relative to subcutaneous injection [129]. The implementation of P(MAA-g-EG) hydrogel microparticles as an oral delivery system for proteins has shown significant promise through scientific results and the system remains a viable option for further research and optimization. However, the system design needs to be modified to address such concerns as the intestinal transport of the protein in an effort to increase overall bioavailability, thus leading to a more economical and viable alternative to injections of therapeutic proteins.

2.6.2.2 Drug Modification

One of the major challenges of oral protein delivery is transport across the epithelium of the small intestine. To increase intestinal transport, researchers have investigated the possibility of drug modification by conjugation to a transporter molecule, often proteins or polypeptides, which can utilize specific membrane transport mechanisms [130]. One transporter protein being investigated for its possible use in oral delivery systems is transferrin, a glycoprotein used by the body for iron transport into the bloodstream. Transferrin (~80 kDa) is a single chain protein naturally occurring in the human body which has the ability to bind to two iron ions per transferrin molecule. Transferrin bound with two iron ions (holo-transferrin) has a greater affinity for the transferrin-receptor than transferrin bound with one iron ion (mono-transferrin) or no iron ions (apo-transferrin) [131]. Transferrin-receptors are expressed on many types of cells in the human body, including intestinal epithelial cells. The transferrin-receptor is a homodimer comprised of two identical subunit monomers of

approximately 90 kDa each [122]. When iron bound transferrin binds to the transferrin-receptor on the apical side of the cell layer, the complex can undergo either endocytosis, which is transport into the cell, or transcytosis, which is transport to the basolateral side of the cell layer [132]. Due to its ability to serve as a transporter targeting ligand for specific cellular uptake as well as its ability to resist trypsin and chymotrypsinogen degradation [121], transferrin remains an attractive option for circumventing the limited transport of the epithelium for drug delivery applications.

Aside from transferrin, another receptor-mediated transport system being considered for its potential applications to oral protein delivery is the vitamin B_{12} system [133]. Researchers have investigated the use of the vitamin B_{12} transport mechanism for oral delivery of insulin using dextran nanoparticles [134] and for uptake of erythropoietin in cellular models [135]. Vitamin B_{12} (~1.36 kDa) is used by the body primarily for the formation of red blood cells and regulation of the nervous system.

The vitamin B_{12} transport mechanism involves a number of transport proteins. Vitamin B_{12} is initially released when food substances are digested in the stomach. The vitamin B_{12} binds to the transport protein haptocorrin, a binding protein secreted in saliva. The vitamin B_{12}-haptocorrin complex travels through the stomach and into the duodenum, where the haptocorrin is degraded by trypsin and chymotrypsin. Vitamin B_{12} then binds to the transport protein intrinsic factor, which is produced in the parietal cells of the stomach. The vitamin B_{12}-intrinsic factor complex travels into the small intestine until it reaches the ileum, where the complex will bind to specific intrinsic factor receptors on the intestinal epithelium. The receptor-transporter-vitamin complex undergoes receptor-mediated endocytosis and enters the cell. Within the cell, the vitamin B_{12} is released from intrinsic factor and binds to another transport protein, transcobalamin II. The transcobalamin II-vitamin B_{12} complex completes the transcytosis and is released into blood circulation [136].

Due to the involvement of multiple transport proteins in the vitamin B_{12} transport mechanism, strategies for drug delivery using vitamin B_{12} would most likely

require drug conjugation to the vitamin itself and not the transport protein. Within this thesis, there will be no attempt to synthesize an actual protein-B_{12} conjugate due to prohibitive cost of the transport protein intrinsic factor. However, the possibility of forming B_{12} conjugates is explored. The ability of intrinsic factor to act as a targeting ligand for the uptake of vitamin B_{12}-protein conjugates combined with the ability of the conjugate complexes to be effectively transcytosed merits the investigation of the vitamin B_{12} transport mechanism as a viable solution to increase epithelial protein transport.

2.7 Conclusions

Due to the nature of injection therapy, doctors, patients, and the medical community have been waiting for a suitable alternative for the administration of therapeutic proteins. Scientists have attempted to design systems using many alternative routes of administration such as pulmonary, transdermal, nasal, buccal, and oral delivery. Because of its high patient acceptability and ease of administration, many researchers have investigated the possibility of designing effective oral protein delivery systems. To address challenges inherent to oral delivery such as protein degradation and poor transport, oral protein formulations include the use of strategies such as permeation enhancers, protease inhibitors, protein encapsulation, and drug modification. While several of these strategies have been met with moderate success, the optimal approach to maximize bioavailability of administered proteins most likely consists of a combination of design strategies as well as an optimization of the systems employed within the formulation.

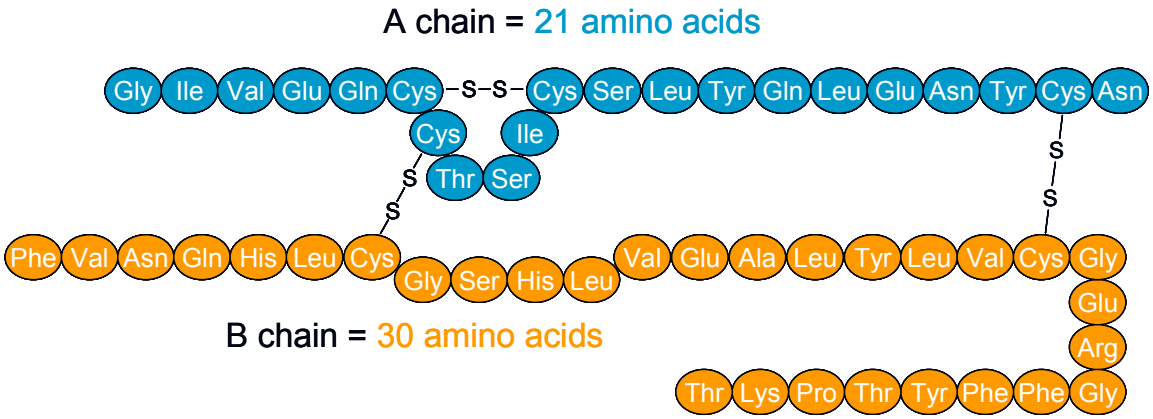

Figure 2.1 Basic structure of insulin.

Insulin contains a total of 51 amino acids comprised of two separate chains connected by disulfide linkages. The A-chain contains 21 amino acids while the B-chain contains 30 amino acids. The molecular weight of insulin is approximately 5,728 Da.

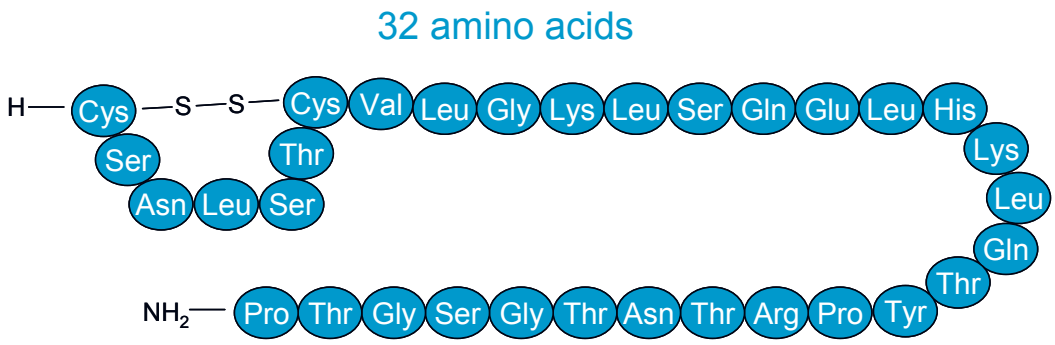

Figure 2.2 Basic structure of calcitonin.

Calcitonin contains a total of 32 amino acids in a single long chain. The molecular weight of insulin is approximately 3,418 Da.

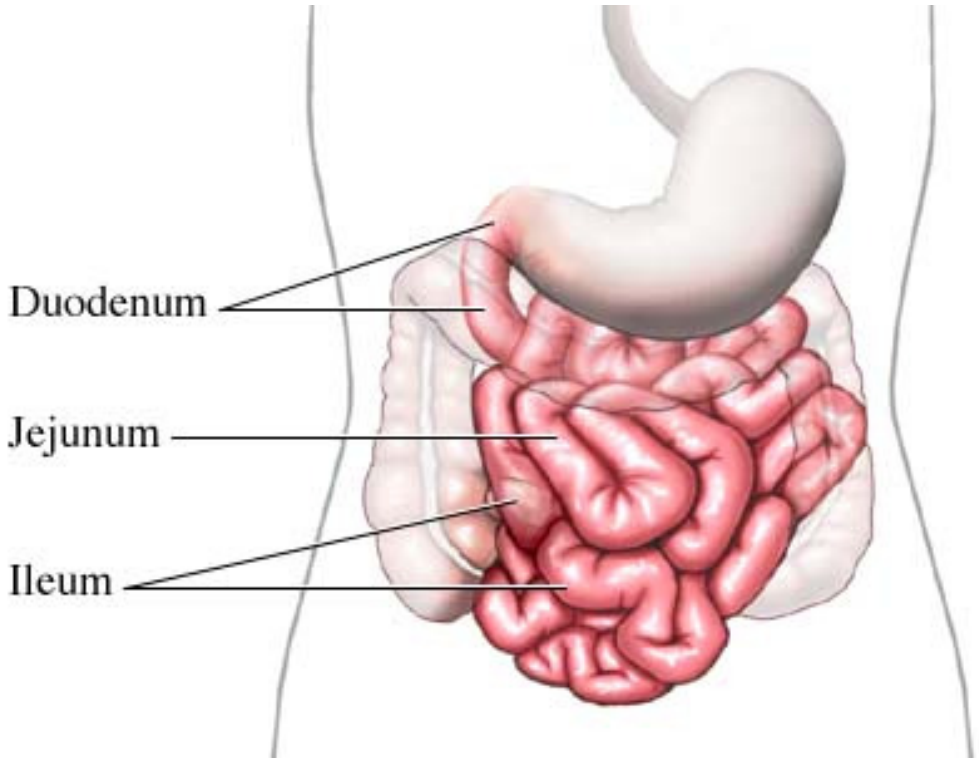

Figure 2.3 Schematic of the human digestive system.

Image shows the stomach as well as the three sections of the small intestine: the duodenum, the jejunum, and the ileum.

(Illustration copyright 2001 by Nucleus Communications, Inc. Adapted from original image)

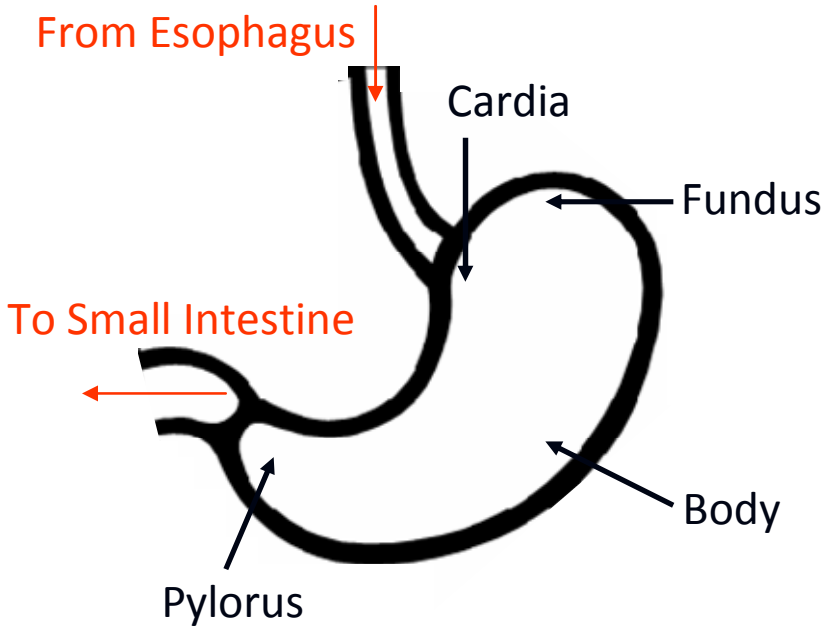

Figure 2.4 Diagram of the human stomach.

Images shows the location within the stomach of its 4 major regions: the cardia, fundus, body, and the pylorus.

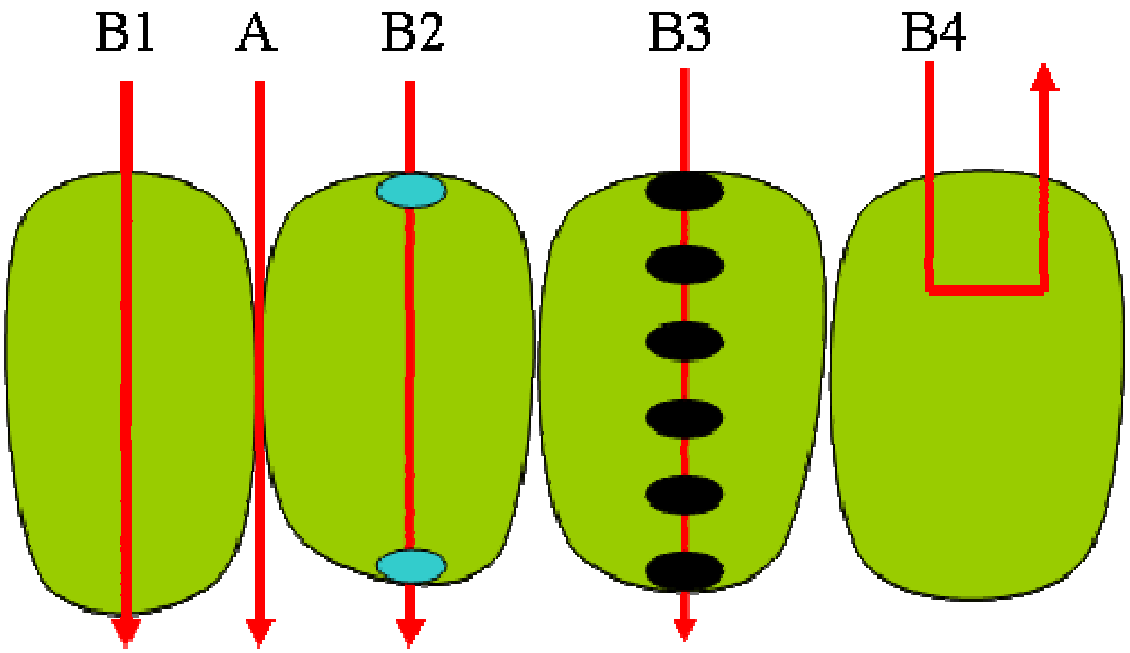

Figure 2.5 Cellular mechanisms of absorption in the small intestine.

Schematic of (A) paracellular transport and (B) transcellular transport. Specific types of transcellular transport include (B1) passive diffusion, (B2) carrier-mediated transcytosis, (B3) receptor-mediated transcytosis, and (B4) efflux transport.

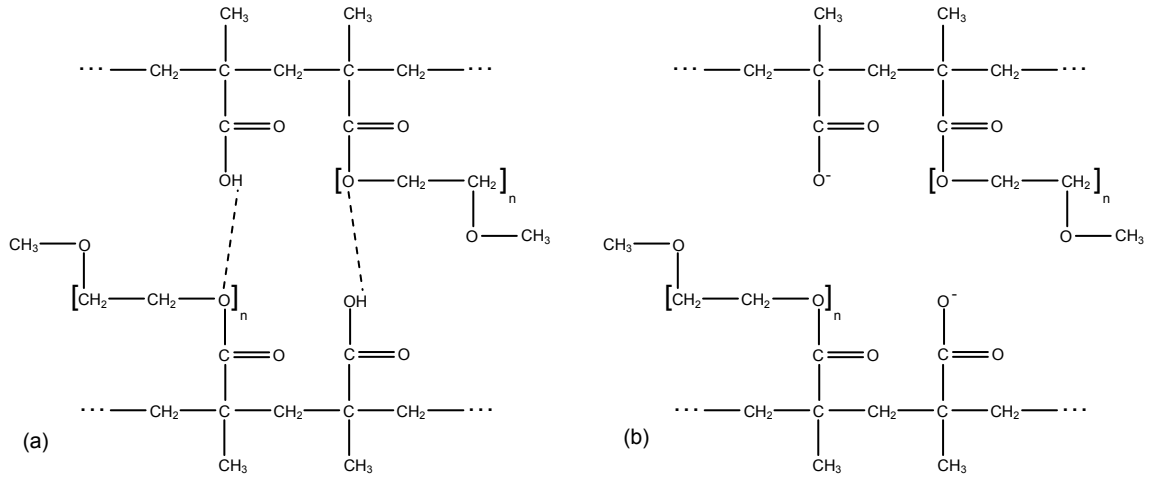

Figure 2.6 Schematic showing interpolymer hydrogen bonding and electrostatic repulsion which cause swelling/deswelling response of polymer.

Chains of P(MAA-g-EG) exhibiting (a) hydrogen bonding at a low pH, allowing for a collapsed, complexed system, and (b) electrostatic repulsion from local negative charges, forcing the system to swell.

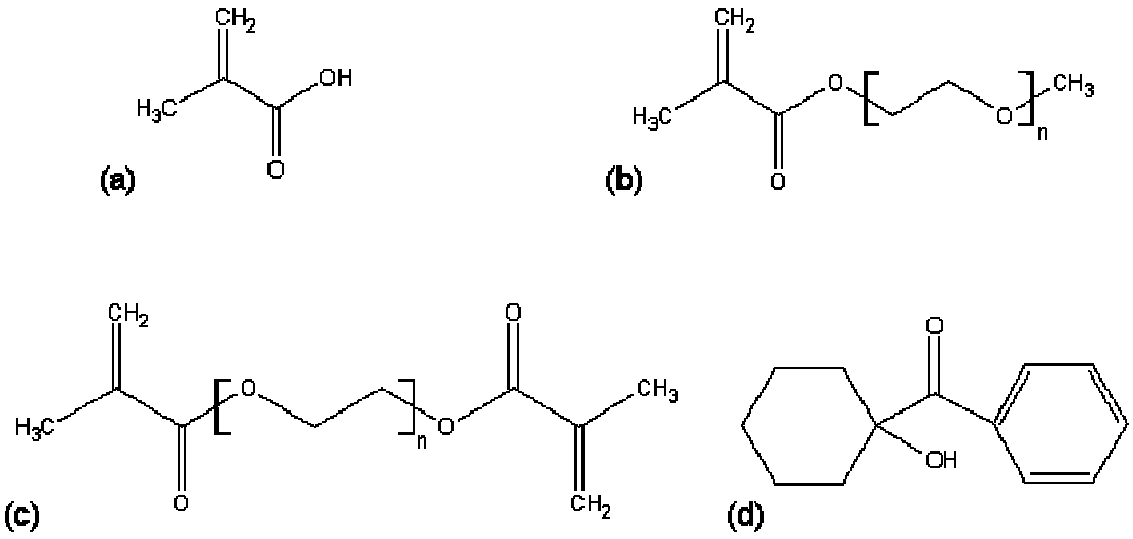

Figure 2.7 Structures of components comprising P(MAA-g-EG) systems.

P(MAA-g-EG) polymer systems are comprised of (a) methacrylic acid (MAA), which forms the polymer backbone, (b) poly(ethylene glycol) monomethyl ether monomethacrylate (PEGMA), which grafts a PEG polymer of chosen molecular weight as a tether, (c) poly(ethylene glycol) dimethacrylate (PEGDMA), which serves as a crosslinker to form a polymer network, and (d) Irgacure 184^{TM}, a UV initiator used to start the polymerization reaction.

REFERENCES

1. Kuzuya, T., Nakagawa, S., Satoh, J., Kanazawa, Y., Iwamoto, Y., Kobayashi, M., Nanjo, K., Sasaki, A., Seino, Y., Ito, C., Shima, K., Nonaka, K., and Kadowaki, T., *Report of the committee on the classification and diagnostic criteria of diabetes mellitus.* Diabetes Res. Clin. Pr., 2002. **55**(1): p. 65-85.

2. McKinlay, J., and Marceau, L., *US public health and the 21st century: diabetes mellitus.* Lancet, 2000. **356**(9231): p. 757-761.

3. Chalew, S.A., Gomez, R., Butler, A., Hempe, J., Compton, T., Mercante, D., Rao, J., and Vargas, A., *Predictors of glycemic control in children with Type 1 diabetes: The importance of race.* J. Diabetes Complicat., 2000. **14**(2): p. 71-77.

4. Brancati, F.L., Whelton, P.K., Kuller, L.H., and Klag, M.J., *Diabetes mellitus, race, and socioeconomic status a population-based study.* Ann. Epidemiol., 1996. **6**(1): p. 67-73.

5. Larkin, Marilynn, *Diabetes on the rise worldwide and website.* Lancet, 2001. **357**(9258): p. 815-815.

6. Group, EURODIAB ACE Study, *Variation and trends in incidence of childhood diabetes in Europe.* Lancet, 2000. **355**(9207): p. 873-876.

7. Papoz, L., Delcourt, C., Ponton-Sanchez, A., Lokrou, A., Darrack, R., Touré, I.A., and Cuisinier-Raynal, J.C., *Clinical classification of diabetes in tropical West Africa.* Diabetes Res. Clin. Pr., 1998. **39**(3): p. 219-227.

8. Craig, M.E., Jones, T.W., Silink, M., Ping, Y.J., *Diabetes care, glycemic control, and complications in children with type 1 diabetes from Asia and the Western Pacific Region.* J. Diabetes Complicat., 2007. **21**(5): p. 280-287.

9. Chaturvedi, N., *The burden of diabetes and its complications: Trends and implications for intervention.* Diabetes Res. Clin. Pr., 2007. **76**(3, Supp. 1): p. S3-S12.

10. Park, K.S., *Prevention of type 2 diabetes mellitus from the viewpoint of genetics.* Diabetes Res. Clin. Pr., 2004. **66**(Supplement 1): p. S33-S35.

11. Daneman, D., *Type 1 diabetes.* Lancet. **367**(9513): p. 847-858.

12. Caballero, A.E., *Long-term benefits of insulin therapy and glycemic control in overweight and obese adults with type 2 diabetes.* J. Diabetes Complicat., 2007. **In Press**.

13. Norris, S.L., Zhang, X., Avenell, A., Gregg, E., Bowman, B., Schmid, C.H., and Lau, J., *Long-term effectiveness of weight-loss interventions in adults with pre-diabetes: A review.* Am. J. Prev. Med., 2005. **28**(1): p. 126-139.

14. Bonometti, E.C., *Medical nutrition therapy (MNT) for pre-diabetes can prevent or delay type 2 diabetes.* J. Am. Diet. Assoc., 2006. **106**(8, Supp. 1): p. A30-A30.

15. Bell, J.C., Ford, J.B., Cameron, C.A., and Roberts, C.L., *The accuracy of population health data for monitoring trends and outcomes among women with diabetes in pregnancy.* Diabetes Res. Clin. Pr., 2006. **In Press**.

16. Yamaoka, T., *Regeneration therapy of pancreatic [beta] cells: towards a cure for diabetes?* Biochem. Bioph. Res. Co., 2002. **296**(5): p. 1039-1043.

17. Efrat, S., *Beta-cell replacement for insulin-dependent diabetes mellitus.* Adv. Drug Deliver. Rev., 2008. **60**(2): p. 114-123.

18. Kawasaki, E., Abiru, N., and Eguchi, K., *Prevention of type 1 diabetes: from the view point of [beta] cell damage.* Diabetes Res. Clin. Pr., 2004. **66**(Supp. 1): p. S27-S32.

19. Nattrass, M., *Diabetic Ketoacidosis.* Medicine, 2002. **30**(2): p. 51-53.

20. Yurgin, N., Secnik, K., and Lage, M.J., *Obesity and the use of insulin: a study of patients with type 2 diabetes in the UK.* J. Diabetes Complicat., 2006. **In Press**.

21. Feuerstein, B.L., and Weinstock, R.S., *Diet and exercise in type 2 diabetes mellitus.* Nutrition, 1997. **13**(2): p. 95-99.

22. Eldor, R., Stern, E., Milicevic, Z., and Raz, I., *Early use of insulin in type 2 diabetes.* Diabetes Res. Clin. Pr., 2005. **68**(Supp. 1): p. S30-S35.

23. Bezie, Y., Molina, M., Hernandez, N., Batista, R., Niang, S., and Huet, D., *Therapeutic compliance: a prospective analysis of various factors involved in the adherence rate in type 2 diabetes.* Diabetes Metab., 2006. **32**(6): p. 611-616.

24. Hernando, M.E., Gómez, E.J., Corcoy, R., and del Pozo, F., *Evaluation of DIABNET, a decision support system for therapy planning in gestational diabetes.* Comput. Meth. Prog. Bio., 2000. **62**(3): p. 235-248.

25. Bottalico, J.N., *Recurrent gestational diabetes: risk factors, diagnosis, management, and implications.* Semin. Perinatol., 2007. **31**(3): p. 176-184.

26. Kestilä, K.K., Ekblad, U.U., and Rönnemaa, T., *Continuous glucose monitoring versus self-monitoring of blood glucose in the treatment of gestational diabetes mellitus.* Diabetes Res. Clin. Pr., 2007. **77**(2): p. 174-179.

27. Bartha, J.L., Martinez-Del-Fresno, P., and Comino-Delgado, R., *Early diagnosis of gestational diabetes mellitus and prevention of diabetes-related complications.* Eur. J. Obstet. Gyn. R. B., 2003. **109**(1): p. 41-44.

28. Nakagami, T., Qiao, Q., Tuomilehto, J., Balkau, B., Carstensen, B., Tajima, N., and Iwamoto, Y., *The fasting plasma glucose cut-point predicting a diabetic 2-h OGTT glucose level depends on the phenotype.* Diabetes Res. Clin. Pr., 2002. **55**(1): p. 35-43.

29. Rasmussen, S.S., Glümer, C., Sandbaek, A., Lauritzen, T., Carstensen, B., and Borch-Johnsen, K., *Short-term reproducibility of impaired fasting glycaemia, impaired glucose tolerance and diabetes: The ADDITION study, DK.* Diabetes Res. Clin. Pr., 2008. **80**(1): p. 146-152.

30. Puavilai, G., Chanprasertyotin, S., and Sriphrapradaeng, A., *Diagnostic criteria for diabetes mellitus and other categories of glucose intolerance: 1997 criteria by the Expert Committee on the Diagnosis and Classification of Diabetes Mellitus (ADA), 1998 WHO Consultation criteria, and 1985 WHO criteria.* Diabetes Res. Clin. Pr., 1999. **44**(1): p. 21-26.

31. Inoue, K., Matsumoto, M., and Kobayashi, Y., *The combination of fasting plasma glucose and glycosylated hemoglobin predicts type 2 diabetes in Japanese workers.* Diabetes Res. Clin. Pr., 2007. **77**(3): p. 451-458.

32. Jiamjarasrangsi, W., Lohsoonthorn, V., Lertmaharit, S., and Sangwatanaroj, S., *Incidence and predictors of abnormal fasting plasma glucose among the university hospital employees in Thailand.* Diabetes Res. Clin. Pr., 2008. **79**(2): p. 343-349.

33. Nitiyanant, W., Ploybutr, S., Sriussadaporn, S., Yamwong, P., and Vannasaeng, S., *Evaluation of the new fasting plasma glucose cutpoint of 7.0 mmol/l in detection of diabetes mellitus in the Thai population.* Diabetes Res. Clin. Pr., 1998. **41**(3): p. 171-176.

34. Patlak, M., *New weapons to combat an ancient disease: treating diabetes.* FASEB J., 2002. **16**(14): p. 1853e-.

35. Banting, F.G., Best, C.H., Collip, J.B., Campbell, W.R., and Fletcher, A.A., *Pancreatic extracts in the treatment of diabetes mellitus: preliminary report. 1922.* Can. Med. Assoc. J., 1991. **145**(10): p. 1281-1286.

36. Sanger, F., *Chemistry of insulin: determination of the structure of insulin opens the way to greater understanding of life processes.* Science, 1959. **129**(3359): p. 1340-1344.

37. Oliva, A., Farina, J., and Llabres, M., *Development of two high-performance liquid chromatographic methods for the analysis and characterization of insulin and its degradation products in pharmaceutical preparations.* J. Chromatogr. B, 2000. **749**(1): p. 25-34.

38. Owens, D.R., Zinman, B., and Bolli, G., *Insulins today and beyond.* Lancet, 2001. **358**(9283): p. 739-746.

39. Fanelli, C.G., Porcellati, F., Rossetti, P., and Bolli, G.B., *Glucagon: The effects of its excess and deficiency on insulin action.* Nutr. Metab. Cardiovas., 2006. **16**(Supplement 1): p. S28-S34.

40. Nystrom, F.H., and Quon, M.J., *Insulin Signalling: Metabolic Pathways and Mechanisms for Specificity.* Cell. Sig., 1999. **11**(8): p. 563-574.

41. Hill, R.A., Strat, A.L., Hughes, N.J., Kokta, T.J., Dodson, M.V., and Gertler, A., *Early insulin signaling cascade in a model of oxidative skeletal muscle: mouse Sol8 cell line.* BBA-Mol. Cell Res., 2004. **1693**(3): p. 205-211.

42. Helme, D.W., and Harrington, N.G., *Patient accounts for noncompliance with diabetes self-care regimens and physician compliance-gaining response.* Patient Educ. Couns., 2004. **55**(2): p. 281-292.

43. Gallagher, A., Butler, T.J., and Home, P.D., *The effect of the optimal use of rapid-acting insulin analogues on insulin secretion in Type 2 diabetes.* Diabetes Res. Clin. Pr., 2007. **76**(3): p. 327-334.

44. Halbron, M., Jacqueminet, S., Sachon, C., Bosquet, F., Hartemann-Heurtier, A., and Grimaldi, A., *Insulin therapy for type 2 diabetes: premixed or basal-prandial?* Diabetes Metab., 2007. **33**(4): p. 316-320.

45. Monnier, L., and Colette, C., *Addition of rapid-acting insulin to basal insulin therapy in type 2 diabetes: indications and modalities.* Diabetes Metab., 2006. **32**(1): p. 7-13.

46. Renard, E., *Implantable closed-loop glucose-sensing and insulin delivery: the future for insulin pump therapy.* Curr. Opin. Pharmacol., 2002. **2**(6): p. 708-716.

47. Niskanen, L., Jensen, L.E., Råstam, J., Nygaard-Pedersen, L., Erichsen, K., and Vora, J.P., *Randomized, multinational, open-label, 2-period, crossover comparison of biphasic insulin aspart 30 and biphasic insulin lispro 25 and pen devices in adult patients with type 2 diabetes mellitus.* Clin. Ther., 2004. **26**(4): p. 531-540.

48. Body, J. J., *Calcitonin for the long-term prevention and treatment of postmenopausal osteoporosis.* Bone, 2002. **30**(5, Supplement 1): p. 75-79.

49. Davidson, M.R., *Pharmacotherapeutics for osteoporosis prevention and treatment.* J. Midwifery Wom. Heal., 2003. **48**(1): p. 39-52.

50. Whitten, C.R., and Saifuddin, A., *MRI of Paget's disease of bone.* Clin. Radiol., 2003. **58**(10): p. 763-769.

51. Väänänen, K., *Mechanism of osteoclast mediated bone resorption--rationale for the design of new therapeutics.* Adv. Drug Deliver. Rev., 2005. **57**(7): p. 959-971.

52. Boonen, S., Kaufman, J., Goemaere, S., Bouillon, R., and Vanderschueren, D., *The diagnosis and treatment of male osteoporosis: Defining, assessing, and preventing skeletal fragility in men.* Eur. J. Int. Med., 2007. **18**(1): p. 6-17.

53. Moyad, M.A., *Osteoporosis: a rapid review of risk factors and screening methods.* Urol. Oncol.-Semin. O. I., 2003. **21**(5): p. 375-379.

54. Gass, M., and Dawson-Hughes, B., *Preventing osteoporosis-related fractures: an overview.* Am. J. Med., 2006. **119**(4, Supplement 1): p. S3-S11.

55. Reginster, J., and Burlet, N., *Osteoporosis: A still increasing prevalence.* Bone, 2006. **38**(2, Supplement 1): p. 4-9.

56. Kanis, J.A., McCloskey, E.V., Johansson, H., Oden, A., Melton Iii, L.J., and Khaltaev, N., *A reference standard for the description of osteoporosis.* Bone, 2008. **42**(3): p. 467-475.

57. Avioli, L.V., *Salmon calcitonin in the prevention and treatment of osteoporosis.* Trends Endocrin. Met., 1997. **8**(3): p. 89-92.

58. Cornish, J., Callon, K.E., Bava, U., Kamona, S.A., Cooper, G.J.S., and Reid, I.R., *Effects of calcitonin, amylin, and calcitonin gene-related peptide on osteoclast development.* Bone, 2001. **29**(2): p. 162-168.

59. Brookhart, M.A., Avorn, J., Katz, J.N., Finkelstein, J.S., Arnold, M., Polinski, J.M., Patrick, A.R., Mogun, H., and Solmon, D.H., *Gaps in treatment among users of osteoporosis medications: The dynamics of noncompliance.* Am. J. Med., 2007. **120**(3): p. 251-256.

60. Rousière, M., Michou, L., Cornélis, F., and Orcel, P., *Paget's disease of bone.* Best Pract. Res. Cl. Rh., 2003. **17**(6): p. 1019-1041.

61. Anderson, D.C., *Paget's Disease; evidence for a viral cause.* Bone, 1995. **17**(1): p. 97-97.

62. Siris, E.S., *Epidemiological aspects of Paget's disease: Family history and relationship to other medical conditions.* Semin. Arthritis Rheu., 1994. **23**(4): p. 222-225.

63. Reginster, J.Y.L., and Lecart, M.P., *Efficacy and safety of drugs for Paget's disease of bone.* Bone, 1995. **17**(5, Supp. 1): p. S485-S488.

64. Smith, R., *Paget's disease of bone: past and present.* Bone, 1999. **24**(5, Supplement 1): p. 1S-2S.

65. Colman, E., Hedin, R., Swann, J., and Orloff, D., *A brief history of calcitonin.* Lancet, 2002. **359**(9309): p. 885-886.

66. Zaidi, M., Inzerillo, A.M., Moonga, B.S., Bevis, P.J.R., and Huang, C.L.H., *Forty years of calcitonin--where are we now? A tribute to the work of Iain Macintyre, FRS.* Bone, 2002. **30**(5): p. 655-663.

67. Huebner, A.K., Keller, J., Catala-Lehnen, P., Perkovic, S., Streichert, T., Emeson, R.B., Amling, M., and Schinke, T., *The role of calcitonin and [alpha]-calcitonin gene-related peptide in bone formation.* Arch. Biochem. Biophys., 2008. **473**(2): p. 210-217.

68. Notoya, M., Arai, R., Katafuchi, T., Minamino, N., and Hagiwara, H., *A novel member of the calcitonin gene-related peptide family, calcitonin receptor-stimulating peptide, inhibits the formation and activity of osteoclasts.* Eur. J. Pharmacol., 2007. **560**(2-3): p. 234-239.

69. Fischer, J.A., and Born, W., *Novel peptides from the calcitonin gene: Expression, receptors and biological function.* Peptides, 1985. **6**(Supp. 3): p. 265-271.

70. Quinn, J.M.W., Morfis, M., Lam, M.H.C., Elliott, J., Kartsogiannis, V., Williams, E.D., Gillespie, M.T., Martin, T.J., and Sexton, P.M., *Calcitonin receptor antibodies in the identification of osteoclasts.* Bone, 1999. **25**(1): p. 1-8.

71. Galvin, R.J.S., Bryan, P., Venugopalan, M., Smith, D.P., and Thomas, J.E., *Calcitonin responsiveness and receptor expression in porcine and murine osteoclasts: a comparative study.* Bone, 1998. **23**(3): p. 233-240.

72. Visser, E.J., *A review of calcitonin and its use in the treatment of acute pain.* Acute Pain, 2005. **7**(4): p. 185-189.

73. Agu, R.U., Ugwoke, M.I., Armand, M., Kinget, R., and Verbeke, N., *The lung as a route for systemic delivery of therapeutic proteins and peptides.* Resp. Res., 2001. **2**(4): p. 198-209.

74. Shoyele, S.A., and Slowey, A., *Prospects of formulating proteins/peptides as aerosols for pulmonary drug delivery.* Int. J. Pharm., 2006. **314**(1): p. 1-8.

75. Edwards, D.A., Ben-Jebria, A., and Langer, R., *Recent advances in pulmonary drug delivery using large, porous inhaled particles.* J. Appl. Physiol., 1998. **85**(2): p. 379-385.

76. Mastrandrea, L.D., and Quattrin, T., *Clinical evaluation of inhaled insulin.* Adv. Drug Deliver. Rev., 2006. **58**(9-10): p. 1061-1075.

77. Davis, S.N., *The role of inhaled insulin in the treatment of type 2 diabetes.* J. Diabetes Complicat. **In Press, Corrected Proof**.

78. Opar, A., *Another blow for inhaled protein therapeutics.* Nat. Rev. Drug. Discov., 2008. **7**(3): p. 189-190.

79. Patton, J.S., Trinchero, P., and Platz, R.M., *Bioavailability of pulmonary delivered peptides and proteins: [alpha]-interferon, calcitonins and parathyroid hormones.* J. Control. Release, 1994. **28**(1-3): p. 79-85.

80. Deftos, L.J., Nolan, J.J., Seely, B.L., Clopton, P.L., Cote, G.J., Whitham, C.L., Florek, L.J., Christensen, T.A., and Hill, M.R., *Intrapulmonary drug delivery of salmon calcitonin.* Calcified Tissue Int., 1997. **61**(4): p. 345-347.

81. Thomas, B.J., and Finnin, B.C., *The transdermal revolution.* Drug Discov. Today, 2004. **9**(16): p. 697-703.

82. Cleland, J.L., Daugherty, A., Mrsny, R., *Emerging protein delivery methods.* Curr. Opin. Biotech., 2001. **12**(2): p. 212-219.

83. Banga, Ajay, *Theme Section: Transdermal Delivery of Proteins.* Pharm. Res., 2007. **24**(7): p. 1357-1359.

84. Smith, N.B., Lee, S., Maione, E., Roy, R.B., McElligott, S., and Shung, K.K., *Ultrasound-mediated transdermal transport of insulin in vitro through human skin using novel transducer designs.* Ultrasound Med. Biol., 2003. **29**(2): p. 311-317.

85. Sen, A., Daly, M.E., and Hui, S.W., *Transdermal insulin delivery using lipid enhanced electroporation.* BBA-Biomembranes, 2002. **1564**(1): p. 5-8.

86. Nakamura, K., Katagai, K., Mori, K., Higo, N., Sato, S., and Yamamoto, K., *Transdermal administration of salmon calcitonin by pulse depolarization-iontophoresis in rats.* Int. J. Pharm., 2001. **218**(1-2): p. 93-102.

87. Davis, S.S., *Further developments in nasal drug delivery.* Pharm. Sci. Technol. To., 1999. **2**(7): p. 265-266.

88. Ugwoke, M.I., Agu, R.U., Verbeke, N., andKinget, R., *Nasal mucoadhesive drug delivery: Background, applications, trends and future perspectives.* Adv. Drug Deliver. Rev., 2005. **57**(11): p. 1640-1665.

89. Arora, P., Sharma, S., and Garg, S., *Permeability issues in nasal drug delivery.* Drug Discov. Today, 2002. **7**(18): p. 967-975.

90. Dondeti, P., Zia, H., and Needham, T.E., *In vivo evaluation of spray formulations of human insulin for nasal delivery.* Int. J. Pharm., 1995. **122**(1-2): p. 91-105.

91. Patton, J.S., *Pulmonary delivery of drugs for bone disorders.* Adv. Drug Deliver. Rev., 2000. **42**(3): p. 239-248.

92. Junginger, H.E., Hoogstraate, J.A., and Verhoef, J.C., *Recent advances in buccal drug delivery and absorption -- in vitro and in vivo studies.* J. Control. Release, 1999. **62**(1-2): p. 149-159.

93. Sudhakar, Y., Kuotsu, K., and Bandyopadhyay, A.K., *Buccal bioadhesive drug delivery -- A promising option for orally less efficient drugs.* J. Control. Release, 2006. **114**(1): p. 15-40.

94. Salamat-Miller, N., Chittchang, M., and Johnston, T.P., *The use of mucoadhesive polymers in buccal drug delivery.* Adv. Drug Deliver. Rev., 2005. **57**(11): p. 1666-1691.

95. Portero, A., Teijeiro-Osorio, D., Alonso, M.J., and Remuñán-López, C., *Development of chitosan sponges for buccal administration of insulin.* Carbohyd. Polym., 2007. **68**(4): p. 617-625.

96. Veuillez, F., Kalia, Y.N., Jacques, Y., Deshusses, J., and Buri, P., *Factors and strategies for improving buccal absorption of peptides.* Eur. J. Pharm. Biopharm., 2001. **51**(2): p. 93-109.

97. Heiber, S.J., Ebert, C.D., Dave, S.C., Smith, K., Kim, S.W., and Mix, D., *In-vivo buccal delivery of calcitonin.* J. Control. Release, 1994. **28**(1-3): p. 269-271.

98. Peppas, N.A., Bures, P., Leobandung, W., and Ichikawa, H., *Hydrogels in pharmaceutical formulations.* Eur. J. Pharm. Biopharm., 2000. **50**(1): p. 27-46.

99. Owens, D.R., Zinman, B., and Bolli, G., *Alternative routes of insulin delivery.* Diabetic Med., 2003. **20**(11): p. 886-898.

100. Mackay, M., Phillips, J., and Hastewell, J., *Peptide drug delivery: Colonic and rectal absorption.* Adv. Drug Deliver. Rev., 1997. **28**(2): p. 253-273.

101. Morishita, M., and Peppas, N.A., *Is the oral route possible for peptide and protein drug delivery?* Drug Discov. Today, 2006. **11**(19-20): p. 905-910.

102. Whitehead, K., Karr, N., and Mitragotri, S., *Discovery of synergistic permeation enhancers for oral drug delivery.* J. Control. Release, 2008. **128**(2): p. 128-133.

103. Carino, G.P., and Mathiowitz, E., *Oral insulin delivery.* Adv. Drug Deliver. Rev., 1999. **35**(2-3): p. 249-257.

104. Delgado, A., Lavelle, E.C., Hartshorne, M., and Davis, S.S., *PLG microparticles stabilised using enteric coating polymers as oral vaccine delivery systems.* Vaccine, 1999. **17**(22): p. 2927-2938.

105. Lowman, A.M., Morishita, M., Kajita, M., Nagai, T., and Peppas, N.A., *Oral delivery of insulin using pH-responsive complexation gels.* J. Pharm. Sci., 1999. **88**(9): p. 933-937.

106. Hosny, E.A., Al-Shora, H.I., and Elmazar, M.M.A., *Oral delivery of insulin from enteric-coated capsules containing sodium salicylate: effect on relative hypoglycemia of diabetic beagle dogs.* Int. J. Pharm., 2002. **237**(1-2): p. 71-76.

107. Foss, A.C., Goto, T., Morishita, M., and Peppas, N.A., *Development of acrylic-based copolymers for oral insulin delivery.* Eur. J. Pharm. Biopharm., 2004. **57**(2): p. 163-169.

108. Soybel, D.I., *Anatomy and Physiology of the Stomach.* Surg. Clin. N. Am., 2005. **85**(5): p. 875-894.

109. Gritti, I., Banfi, G., and Roi, G.S., *Pepsinogens: physiology, pharmacology, pathophysiology, and exercise.* Pharm. Res., 2000. **41**(3): p. 265-281.

110. Ziv, E., Lior, O., and Kidron, M., *Absorption of protein via the intestinal wall : A quantitative model.* Biochem. Pharmacol., 1987. **36**(7): p. 1035-1039.

111. Franssen, O., Stenekes, R.J.H., and Hennink, W.E., *Controlled release of a model protein from enzymatically degrading dextran microspheres.* J. Control. Release, 1999. **59**(2): p. 219-228.

112. Madsen, F., and Peppas, N.A., *Complexation graft copolymer networks: swelling properties, calcium binding and proteolytic enzyme inhibition.* Biomaterials, 1999. **20**(18): p. 1701-1708.

113. Peppas, N.A., and Kavimandan, N.J., *Nanoscale analysis of protein and peptide absorption: Insulin absorption using complexation and pH-sensitive hydrogels as delivery vehicles.* Eur. J. Pharm. Sci., 2006. **29**(3-4): p. 183-197.

114. Ponchel, G., and Irache, J., *Specific and non-specific bioadhesive particulate systems for oral delivery to the gastrointestinal tract.* Adv. Drug Deliver. Rev., 1998. **34**(2-3): p. 191-219.

115. Peppas, N.A., and Sahlin, J.J., *Hydrogels as mucoadhesive and bioadhesive materials: a review.* Biomaterials, 1996. **17**(16): p. 1553-1561.

116. Serra, L., Domenech, J., and Peppas, N.A., *Design of poly(ethylene glycol)-tethered copolymers as novel mucoadhesive drug delivery systems.* Eur. J. Pharm. Biopharm., 2006. **63**(1): p. 11-18.

117. Fasano, A., *Novel approaches for oral delivery of macromolecules.* J. Pharm. Sci., 1998. **87**(11): p. 1351-1356.

118. Salamat-Miller, N., and Johnston, T.P., *Current strategies used to enhance the paracellular transport of therapeutic polypeptides across the intestinal epithelium.* Int. J. Pharm., 2005. **294**(1-2): p. 201-216.

119. Kan, K.S., and Coleman, R., *The calcium ionophore A23187 increases the tight-junctional permeability in rat liver.* Biochem. J., 1988. **256**(3): p. 1039-1041.

120. Bernkop-Schnurch, A., Kast, C.E., and Guggi, D., *Permeation enhancing polymers in oral delivery of hydrophilic macromolecules: thiomer/GSH systems.* J. Control. Release, 2003. **93**(2): p. 95-103.

121. Blanchette, J., Kavimandan, N.J., and Peppas, N.A., *Principles of transmucosal delivery of therapeutic agents.* Biomed. Pharmacother., 2004. **58**(3): p. 142-151.

122. Widera, A., Norouziyan, F., and Shen, W.C., *Mechanisms of TfR-mediated transcytosis and sorting in epithelial cells and applications toward drug delivery.* Adv. Drug Deliver. Rev., 2003. **55**(11): p. 1439-1466.

123. Lee, K.Y., and Yuk, S.H., *Polymeric protein delivery systems.* Prog. Polym. Sci., 2007. **32**(7): p. 669-697.

124. Hoffman, A.S., *Hydrogels for biomedical applications.* Adv. Drug Deliver. Rev., 2002. **54**(1): p. 3-12.

125. Gupta, P., Vermani, K., and Garg, S., *Hydrogels: from controlled release to pH-responsive drug delivery.* Drug Discov. Today, 2002. **7**(10): p. 569-579.

126. Qiu, Y., and Park, K., *Environment-sensitive hydrogels for drug delivery.* Adv. Drug Deliver. Rev., 2001. **53**(3): p. 321-339.

127. Peppas, N.A., *Hydrogels*. Biomaterials Science, ed. B.D. Ratner, Hoffman, A., Schoen, F., and Lemons, J. 2004, San Diego, CA: Elsevier Academic Press. pp. 100-106.

128. Yamagata, T., Morishita, M., Kavimandan, N.J., Nakamura, K., Fukuoka, Y., Takayama, K., and Peppas, N.A., *Characterization of insulin protection properties of complexation hydrogels in gastric and intestinal enzyme fluids.* J. Control. Release, 2006. **112**(3): p. 343-349.

129. Morishita, M., Goto, T., Peppas, N.A., Joseph, J.I., Torjman, M.C., Munsick, C., Nakamura, K., Yamagata, T., Takayama, K., and Lowman, A.M., *Mucosal insulin delivery systems based on complexation polymer hydrogels: effect of particle size on insulin enteral absorption.* J. Control. Release, 2004. **97**(1): p. 115-124.

130. Tamai, I., and Tsuji, A., *Carrier-mediated approaches for oral drug delivery.* Adv. Drug Deliver. Rev., 1996. **20**(1): p. 5-32.

131. Huebers, H.A., Csiba, E., Huebers, E., and Finch, C.A., *Competitive advantage of diferric transferrin in delivering iron to reticulocytes.* P. Natl. Acad. Sci.-Biol., 1983. **80**(1): p. 300-304.

132. Jones, A.T., Gumbleton, M., and Duncan, R., *Understanding endocytic pathways and intracellular trafficking: a prerequisite for effective design of advanced drug delivery systems.* Adv. Drug Deliver. Rev., 2003. **55**(11): p. 1353-1357.

133. Russell-Jones, G.J., *The potential use of receptor-mediated endocytosis for oral drug delivery.* Adv. Drug Deliver. Rev., 2001. **46**(1-3): p. 59-73.

134. Chalasani, K.B., Russell-Jones, G.J., Yandrapu, S.K., Diwan, P.V., and Jain, S.K., *A novel vitamin B12-nanosphere conjugate carrier system for peroral delivery of insulin.* J. Control. Release, 2007. **117**(3): p. 421-429.

135. Habberfield, A., Jensen-Pippo, K., Ralph, L., Westwood, S.W., and Russell-Jones, G.J., *Vitamin B12-mediated uptake of erythropoietin and granulocyte colony stimulating factor in vitro and in vivo.* Int. J. Pharm., 1996. **145**(1-2): p. 1-8.

136. Russell-Jones, G.J., *Oral delivery of therapeutic proteins and peptides by the vitamin B_{12} uptake system*. Peptide-Based Drug Design: Controlling Transport and Metabolism, ed. M.D. Taylor, and Amidon, G.L. 1995, Washington, DC: ACS. pp. 181-198.

CHAPTER 3

OBJECTIVES

The advantages of oral delivery for administration of therapeutic proteins are well known to the pharmaceutical industry. Advantages such as the low cost, ease of administration, and increased patient compliance of oral protein delivery make the development of a successful oral protein delivery formulation a highly sought after goal for the industry. Orally delivered proteins could greatly increase the efficacy of treatment regimens for patients worldwide, significantly improving overall health. However, oral protein delivery presents many challenges which, until recently, were though to be insurmountable. Over recent years, scientists have made significant advances in overcoming natural barriers to oral protein delivery such as protein degradation, narrow absorption window, and low epithelial transport.

One strategy to overcome some of the barriers of oral protein delivery has been investigated in this laboratory and involves incorporation of the protein in complexation hydrogel carriers. Hydrogel carriers used as delivery systems benefit from their ability to protect the protein in the harsh environment of the stomach as well as increase residence time at the site of absorption by using mucoadhesive materials and polymer tethers. Another strategy to increase overall efficacy of oral protein delivery formulations is the modification of the therapeutic protein itself by conjugation to a transporter ligand which can utilize the natural transcellular transport pathways. As mentioned in Chapter 2, a combinatorial approach utilizing hydrogel carriers and drug modification may result in significantly increased bioavailability relative to other oral formulations.

The overall goal of this research was to synthesize protein-transporter bioconjugates to be incorporated into complexation hydrogels and to optimize the

hydrogel carriers as to achieve the greatest potential for high bioavailability in the bloodstream. The specific aims of this research are as follows:

(1) Optimization of synthesis parameters of the poly(methacrylic acid)-based microparticles with specific emphasis on crosslinker, monomer to solvent ratio, particle size and incorporated comonomer for maximal protection and release of bioconjugates.

(2) Formulation and characterization of conjugation reactions of therapeutic proteins to transporter molecules using heterobifunctional crosslinkers.

(3) Investigation into the *in vitro* properties of the insulin-transferrin conjugate, specifically its ability to be loaded and released from several hydrogel formulations.

(4) Evaluation of the interactions between synthesized calcitonin-transferrin conjugate with the hydrogel polymer carrier formulations including loading and release characteristics.

(5) Evaluation of the effect of synthesized conjugates and polymer carriers on bioavailability and bioactivity using *in vitro* cell culture models and *in vivo* animal models.

Within this body of work, each specific aim was covered in separate chapters. Specific Aim #1 was addressed and investigated in Chapter 4. The conjugation reactions described by Specific Aim #2 were covered in Chapter 5. As described in Specific Aim #3, the synthesized insulin-transferrin conjugate was investigated as a potential entity to be loaded and released in Chapter 6. Chapter 7 contains the studies mentioned in Specific

Aim #4, which are investigations into the polymer-conjugate interactions existing between the calcitonin-transferrin conjugate and the polymer carrier via loading and release studies. Finally, Specific Aim #5 was addressed in Chapter 8 by investigation into cellular studies and animal studies using synthesized conjugates. With each specific aim addressed in previous chapters, Chapter 9 provides general conclusions encompassing the entire body of research.

CHAPTER 4

SYNTHESIS AND CHARACTERIZATION OF METHACRYLIC ACID BASED HYDROGELS AS CARRIERS FOR NOVEL PROTEIN-TRANSPORTER BIOCONJUGATES

4.1 Introduction

Generally, bioavailability of orally administered therapeutic proteins is significantly lowered due to degradation in the stomach. Any protein administered orally must endure the low pH environment as well as the multitude of digestive enzymes present in the stomach. The average pH of the stomach is approximately 2.0, creating an environment which can readily damage or denature therapeutic proteins and render them inactive [1]. Also, digestive enzymes such as pepsin and trypsin will attack administered proteins and cleave them into smaller peptide fragments to facilitate uptake for energy within the small intestine. Bioavailability of orally delivered proteins can also be reduced by lack of residence time at the site of absorption and poor epithelial transport. Any design strategy intended to increase bioavailability of orally administered proteins must include ways to protect from degradation, increase residence time at the site of absorption, and increase epithelial transport.

Many researchers have designed methods to overcome these barriers to oral protein delivery. Much research has focused on the inclusion of protease inhibitors into the oral dosage formulation. Protease inhibitors would effectively inhibit the activity of proteolytic enzymes, preventing them from attacking administered therapeutic proteins, thereby preserving the bioactivity of the dosage form. For example, Ziv et al. [2] demonstrated that upon administration of the protease inhibitor aprotinin with the therapeutic protein insulin (in bile acid), insulin absorption was amplified approximately 30 times relative to the administration of insulin alone. However, the resultant bioavailability of the formulation was still very low (~0.75%).

An alternative strategy to increase bioavailability of administered proteins is the use of permeation enhancers, which focus on increasing epithelial transport across the cell monolayer. Permeation enhancers are administered with the dosage form to disrupt or in some way modify the cell monolayer, specifically the tight junctions of the monolayer.

The tight junctions between the cells are composed of the transmembrane proteins occludin and claudin, and cytoplasmic plaque proteins zonula occludens (ZO)-1, ZO-2, ZO-3, cingulin, and 7H6 [3]. These proteins are of a dynamic nature, responding and altering their function based on changes in the extracellular environment. Most permeation enhancers operate by altering the extracellular environment in such as way as it forces the transmembrane proteins to relax or loosen the tight junctions between the cells. For example, ethylenediamine-tetraacetic acid (EDTA) can act as a permeation enhancer by binding to extracellular Ca^{2+}, thus lowering the extracellular Ca^{2+} concentration and consequently lowering the intracellular Ca^{2+} concentration due to passive diffusion. Because of the importance of calcium to the transmembrane proteins' regulating of the tight junctions, the tight junctions are loosened in the presence of EDTA and transport across them is increased [4].

While protease inhibitors and permeation enhancers each present a possible solution to different individual barriers of oral protein delivery, design strategies utilizing methods to address all the oral protein delivery barriers are more desirable and represent greater potential to achieve high bioavailability of the protein in the bloodstream.

One method which at least partially addresses all of the oral protein delivery barriers is the incorporation of the protein into hydrogel carriers. A hydrogel carrier is a three-dimensional hydrophilic polymer network which will typically swell and imbibe water under certain specific conditions. The swelling is considered an "intelligent" response to the stimulus generated by the specific conditions. Swelling behavior can be triggered in response to changes in factors such as temperature, pH, electric field, light,

and even the presence of specific molecules [5]. Also, hydrogel systems can be tailored such that in the swollen state, large molecules such as proteins are free to diffuse in and out of the system. However, these same systems can be forced to collapse using a specific stimulus, thus entrapping any proteins present within the polymer network. Entrapped proteins will remain within the polymer network as long as the carrier is collapsed, preventing any diffusion inward of enzymes or other substances which could degrade the protein. Because of the ability of hydrogel carriers to protect encapsulated proteins in the harsh environment of the stomach, they effectively address the protein degradation barrier to oral protein delivery.

For oral delivery applications, swelling of the hydrogel carrier is desired near the site of absorption in the small intestine. One of the most notable differences between the stomach (pH ~ 2) and the small intestine (pH ~ 7) is the pH of the surrounding environment. For this reason, many oral protein delivery systems are based on pH-sensitive hydrogels [6].

Hydrogels are generally divided into four categories: neutral, anionic, cationic, and ampholytic [7]. Most pH-sensitive hydrogels are typically either classified as anionic or cationic hydrogels depending on the nature of their ionizable pendant groups. Cationic hydrogels contain pendant groups which become protonated at a pH *below* the pKa of the ionizable groups. The protonation results in local positive charges throughout the network, causing the system to swell as a result of electrostatic repulsion. At a pH *above* the pKa of the ionizable groups, cationic hydrogels will remain collapsed due to interpolymer hydrogen bonding. Anionic hydrogels exhibit an opposite response to environmental pH compared with cationic hydrogels. Anionic hydrogels contain pendant groups which become deprotonated at a pH *above* the pKa of the ionizable groups. The deprotonated pendant groups results in local negative charges throughout the polymer system, causing an overall swelling response. At a pH *below* the pKa of the ionizable groups, anionic hydrogels will remain collapsed due to interpolymer hydrogen bonding. For oral protein delivery applications, the hydrogel

carrier needs to protect the protein in the stomach (remain collapsed) and release the protein for absorption in the small intestine (become swollen). Based on the design requirements, the pH-sensitive hydrogels investigated in this thesis will be anionic.

In addition to their ability to protect proteins, hydrogels can be constructed using mucoadhesive materials which can bind to the mucosa lining the small intestine. This binding increases residence time next to the wall of the small intestine, allowing more time for diffusion of the protein out of the system as well as time for increased absorption. The addition of polymer tethers which can penetrate the mucosa and act as anchors to mucoadhesive polymers combine for an even further increased residence time and increased chance for absorption. In addition to increased residence time, certain hydrogels can also somewhat increase epithelial transport due to their ability to bind to extracellular calcium. Similar to permeation enhancers, the depleted levels of extracellular calcium cause a relaxation of the tight junctions, increasing paracellular transport. However, calcium binding will only occur with anionic hydrogel carriers due to the negative charges spread throughout the system. Ca^{2+} ions have a positive charge, causing attraction to the negatively charged hydrogel carrier. Hydrogels possess tremendous potential for oral protein delivery in that protein degradation is minimized due to the collapsing of the system, residence time at the site of absorption is increased from the use of mucoadhesive polymers and polymer tethers, and epithelial transport is increased due to the calcium binding of the system in the swollen state.

Over the past few decades, scientists have become increasingly aware of the potential of hydrogels as carriers for the oral delivery of therapeutic proteins [8-10]. The major interest in hydrogels began as early as 1960 with the work of Wichterle and Lim [11] on crosslinked HEMA hydrogels. The work of Wichterle and Lim showed the biocompatibility of hydrogels as well as their hydrophilic nature, gaining the interest of biomaterials researchers worldwide. Later, in 1980, Lim and Sun [12] created a system for cell encapsulation using calcium alginate microcapsules. A few years later, Yannas et al. [13] utilized collagen and shark cartilage in a hydrogel network to use as artificial

burn dressings. In the late 1980's to early 1990's, hydrogels were beginning to be considered for the delivery of therapeutic proteins [14]. However, it was not until recently that a system designed using hydrogels was able to achieve a significant increase in bioavailability relative to subcutaneous injection [15].

Within our laboratory, significant research has been performed to further the understanding of hydrogels for use in oral protein delivery. In 1991, Brannon-Peppas and Peppas [16] investigated the kinetics of the response of ionic hydrogels to changes in environmental pH and ionic strength. Also, Khare et al. [17] determined the degree of swelling of the hydrogel that occurs due to changes in pH and ionic strength. An understanding of the kinetics and degree of the swelling reaction of specific ionic hydrogels to changes in environmental pH and ionic strength is essential to advancement towards designing an effective oral protein delivery system. In 1995, am Ende et al. [18] detailed the factors which affect protein release from ionic hydrogels. Also, Bell and Peppas [19] described diffusion characteristics of water, solute, and proteins within the hydrogel network. After understanding the swelling characteristics of the ionic hydrogels, it is necessary to investigate the diffusion of entities within the network as well as factors affecting protein release to fully understand the characteristics of a hydrogel system for therapeutic proteins.

After performing fundamental research related to the kinetics and factors of swelling, diffusion modeling, and factors affecting protein release, research in our laboratory focused on obtaining *in vitro* results to determine the effectiveness of the delivery system as well as system optimization to provide the highest potential for increased bioavailability. In recent years, our hydrogel systems have exhibited properties which show strong potential for overcoming many of the known barriers for oral protein delivery. For example, Yamagata et al. [20] demonstrated the potential of the hydrogel carriers to protect proteins by encapsulating insulin within P(MAA-g-EG) microparticles and achieving preservation of over 80% of the loaded insulin after being treated for one hour in gastric fluid. In contrast, only 20% of free insulin remained

intact after the same treatment with gastric fluid. Also, increased residence time at the site of absorption has been achieved by the addition of polymers which are known to be mucoadhesive [21] and through the implementation of polymer tethers. Serra et al. [22] showed that the addition of PEG tethers to a poly(acrylic acid) (PAA) hydrogel system increased the mucoadhesive capacity of the microparticles, generating a work of adhesion of approximately 130 x 10^{-3} mJ, or five times that of a pure PAA system. Finally, Morishita et al. [15] demonstrated the overall effectiveness and potential of the hydrogel system by performing *in vivo* studies in which insulin was administered in P(MAA-g-EG) carriers to diabetic rats, resulting in a bioavailability of 12.8%, a significant increase over insulin administered alone. Currently, our research continues to search for novel ways to improve efficacy and bioavailability of proteins administered in hydrogel carriers. Currently researched design strategies include drug conjugation, particle conjugation, inclusion of sensors, and improved materials.

The hydrogels synthesized and investigated in this thesis are based on a poly(methacrylic acid) (P(MAA)) backbone. The primary polymer hydrogel being investigated is a polymer comprised of poly(methacrylic acid) with grafted poly(ethylene glycol) (PEG) tethers (henceforth denoted as P(MAA-g-EG)). The components which comprise P(MAA-g-EG) are shown in Figure 4.1.

Another polymer formulation being investigated as well is a comonomer comprised of poly(methacrylic acid) and N-vinyl pyrrolidone (NVP) (henceforth denoted as P(MAA-co-NVP)). The components which comprise P(MAA-co-NVP) are shown in Figure 4.2.

P(MAA-g-EG) and P(MAA-co-NVP) are anionic hydrogels which means that the system will be complexed at a lower pH and swollen at a higher pH. The MAA groups have a pKa of around 4.9, allowing for complexation at a significantly lower pH than 4.9 and swelling at a significantly higher pH than 4.9. As P(MAA-g-EG) enters the stomach (pH ~ 2), hydrogen bonding is occurring between hydrogens in the MAA groups and etheric oxygens in the PEG crosslinkers or grafted tethers. For P(MAA-co-NVP), the

hydrogen bonding exists between the hydrogen in the MAA group and the oxygen in the NVP pendant group. However, as the formulations pass into the small intestine (pH ~ 7), the MAA pendant groups become deprotonated and gain a local negative charges. The negatives charges accumulate throughout the system and cause static repulsion, swelling the hydrogel. A schematic showing P(MAA-g-EG) at the molecular level in both low and neutral pH is shown in Figure 4.3. A schematic showing molecular interactions for P(MAA-co-NVP) at low and neutral pH is shown in Figure 4.4.

In addition to their abilities to swell, P(MAA-g-EG) and P(MAA-co-NVP) are both constructed with a methacrylic acid, a mucoadhesive polymer. The mucoadhesive capacity of MAA allows for a binding interaction between the polymer carrier and the mucosa lining the small intestine. The binding creates a longer residence time for the carrier at the specific site of absorption, allowing for greater time for diffusion and a higher probability for absorption. In addition to its mucoadhesive capacity, P(MAA-g-EG) also benefits from its design structure of having grafted tethers. The grafted PEG tethers are thought to penetrate within the mucus and generate an "anchor" effect, thus creating a stronger interaction between the hydrogel carrier and the mucosa. The increased binding should further increase residence time and also increase the potential for higher bioavailability. The hypothesized interactions of P(MAA-g-EG) and P(MAA-co-NVP) with the mucosa layer are shown in Figure 4.5.

Anionic hydrogels such as P(MAA-g-EG) and P(MAA-co-NVP) are also known to act as permeation enhancers for increasing epithelial transport. As mentioned earlier, the MAA groups become deprotonated in the neutral pH of the small intestine, creating local negative charges. Because of these negative charges, the hydrogel carriers are able to bind positively-charged calcium, or Ca^{2+}, from the extracellular domain. Binding extracellular calcium lowers the calcium concentration outside the cell, creating diffusion of intracellular calcium outside the cell. Intracellular calcium has been shown to be important in regulating tight junctions, and a significant decrease in intracellular calcium will loosen the tight junctions and increase transport of large molecules such as

proteins [4]. A diagram demonstrating the calcium binding ability of the hydrogel systems is shown in Figure 4.6.

In addition to the general properties of the hydrogel design, the carriers can be specifically modified to optimize the loading and release of specific therapeutics. Therapeutic proteins or modified protein formulations can vary in size, structure, surface charges, isoelectric point, or a myriad of other properties which can affect its interaction with the hydrogel carrier. Through manipulation of synthesis parameters, one can change the properties of the resultant formulation. In this thesis, the synthesis parameters for P(MAA-g-EG) were altered to obtain optimal loading and release of synthesized bioconjugates. The synthesis parameters investigated include crosslinker length, monomer-to-solvent ratio, particle size, and replacement of the PEG graft comonomer with a NVP comonomer.

Crosslinks in a hydrogel polymer network are small connecting polymer chains which connect the longer polymer backbones. In theory, longer crosslinker chains create more distance between connected polymer backbones. While longer crosslinker chains may not generate distance in the collapsed state because of coiling and compression due to hydrogen bonding. However, in the swollen state, the polymer strands are trying to spread apart due to local negative charges throughout the system. As the polymer backbone increasingly expands, the presence of a longer crosslinker will allow greater separation within the polymer network. The increased expansion of the network will translate to an increased average mesh size for the network. Larger mesh size upon swelling allows for increased and quicker diffusion of the therapeutic out of the system, giving better overall release. A diagram showing the relationship of crosslinker length and mesh size is shown in Figure 4.7.

Another way to increase the effective mesh size of hydrogel carriers is to alter the monomer-to-solvent ratio. The relationship between amounts of monomer and solvent in a polymer formulation is crucial to developing a polymer carrier. If the amount of monomer or solvent is too high relative to the other, it is typically difficult to

synthesize a workable polymer. However, if the monomer-to-solvent ratio is within a certain range, then the polymer can easily be synthesized. Within the workable range, the monomer-to-solvent ratio can be altered to modify the polymer properties. Generally, a lower monomer-to-solvent ratio results in creating a polymer carrier with increased effective mesh size and thus increased diffusion of therapeutic. The inclusion of more solvent in the system introduces more solvent molecules around which the backbones will polymerize, thus creating a more open and porous network. As the network becomes more porous, the therapeutic protein inside will release quicker and to a higher overall degree.

The effect of manipulation of the particle size is different than the effects of modification of crosslinker length or monomer-to-solvent ratio. Rather than increase the mesh size of the polymer, changing the particle size affects the diffusion path length of the therapeutic protein. In theory, creating smaller particles means the therapeutic proteins have a quicker route for release, and therefore should exit the carrier faster. Also, during loading the proteins cannot penetrate as deeply, allowing a greater overall release in a given time for the smaller particle system. In addition to quicker diffusion, smaller particles also have an increased ability to penetrate deeper into the mucosa, thus release their protein closer to the site of absorption. In fact, Morishita et al. showed a significantly quicker release, increased mucoadhesive capacity, and increased absorption into the bloodstream using small particles (<43 μm) relative to larger particles (180-230 μm) [15]. A diagram showing the diffusion path length and mucosa interaction of two differently sized particles is shown in Figure 4.8.

Optimization of P(MAA-g-EG) for the loading and release of synthesized bioconjugates consists of opening up the system and increasing mesh size to effectively release the larger bioconjugates. However, the mesh size cannot be increased too much or the therapeutic protein will diffuse out in the collapsed state in the stomach. If an attempt to modify synthesis parameters such as to generate stronger complexation and greater protection in the stomach, the replacement of PEG tethers with NVP was

investigated. Due to strong intermolecular affinity between the chains, the MAA/NVP interaction is stronger and allows for greater complexation relative to MAA/PEG systems [23]. P(MAA-co-NVP) is thought to protect encapsulated proteins in the stomach better than P(MAA-g-EG) which could lead to have more intact, bioactive protein for release in the small intestine.

The objective of this section of the thesis is to synthesize and characterize several different polymer formulations with the ultimate goal of creating the optimal carrier for ideal loading and release of synthesized bioconjugates. In an effort to create four variables for optimization, synthesis parameters such as crosslinker length, monomer-to-solvent ratio, particle size, and comonomer were modified within the synthesized polymers. The systems were then characterized to observe any differences between the systems other than loading and release characteristics. The synthesis and characterization of all polymer formulations used in this thesis will be covered in this chapter.

4.2 Materials and Methods

4.2.1 Polymer Microparticle Formation by UV Polymerization

P(MAA-g-EG) and P(MAA-co-NVP) were prepared using a free radical UV polymerization in solution. P(MAA-g-EG) was prepared by mixing MAA (Sigma-Aldrich Inc., St. Louis, MO) with poly(ethylene glycol) monomethyl ether monomethacrylate with a approximate molecular weight of 1000 (PEGMA1000, Polysciences Inc., Warrington, PA) in a 1:1 molar ratio of MAA:EG. P(MAA-co-NVP) was prepared by mixing MAA with NVP (Sigma-Aldrich Inc., St. Louis, MO) in a 1:1 molar ratio of MAA:NVP. Crosslinkers were then added into the monomer mixtures consisting of MAA/EG or MAA/NVP. The crosslinkers used within this study were tetraethylene glycol dimethacrylate (TEGDMA, Sigma-Aldrich Inc., St. Louis, MO) and poly(ethylene glycol) dimethacrylate with an approximately molecular weight of 1000 (PEGDMA1000, Polysciences Inc., Warrington, PA). The amount of crosslinker added to each monomer

mixture was equal to 1 mol% of the total amount of monomer (MAA/EG or MAA/NVP). In order to eventually initiate the polymerization, the photoinitiator 1-hydroxycyclohexyl phenyl ketone (Irgacure 184, Sigma-Aldrich Inc., St. Louis, MO) was added to the polymerization mixture in the amount of 1 wt% of the total monomer added (MAA/EG or MAA/NVP). A solvent mixture consisting of 50:50 by weight deionized water (Milli-Q Plus system, Millipore) and ethanol (AAPER Alcohol, Shelbyville, KY) was added to the polymer mixture in the amounts of either 50:50, 60:40, or 67:33 by weight polymer mixture to solvent mixture. The presence of the solvent solution is essential to prevent autopolymerization as well as to produce a workable thin polymer film.

To ensure all components dissolved and went into a homogenous solution, the polymer mixture was sonicated for 15 minutes. After sonication, nitrogen was bubbled through the polymer solution within a nitrogen environment to eliminate oxygen. Oxygen is a free radical scavenger and significant oxygen levels could prematurely end the polymerization process. After removal of oxygen by nitrogen purging, the polymer mixture was poured between two glass slides (153 x 153 x 3 mm) separated by a Teflon spacer (0.7 mm) while still in a nitrogen environment. The glass slide apparatus containing the polymer solution spread into a thin film was then placed under a UV light source while still in a nitrogen environment. The solution was allowed to polymerize under the light source within an intensity range of 16-17 mW/cm^2 for 30 minutes. After the polymerization was completed, the polymer gels were removed from the nitrogen environment, separated from the glass slides, and placed in deionized water. The polymer films were washed in the deionized water for 7 days to remove excess monomer and contaminants. After washing was completed, the polymers were dried in a vacuum oven at approximately 30° C for 2 days.

After completely drying the polymer films, they were removed from the vacuum oven and crushed into microparticles using a mortar and pestle. The crushed microparticles were then sieved into appropriate size ranges of either less than 75

microns, 90-150 microns, or 150-212 microns. The crushed and sieved microparticles were then stored in a vial within a desiccator to prevent moisture entering until further use. A schematic of the polymerization process is shown in Figure 4.9.

4.2.2 Polymer Microparticle Characterization by Scanning Electron Microscopy

Characterization of size, morphology, and surface texture of the polymer formulations was performed using a field emission scanning electron microscope (FE-SEM, LEO 1530, Oberkochen, Germany). The polymer formulations examined included P(MAA-g-EG) and P(MAA-co-NVP), all three particle size ranges (less than 75 microns, 90-150 microns, and 150-212 microns), the two extremes of monomer-to-solvent ratios (50:50 and 67:33 monomer-to-solvent ratio), and the TEGDMA and PEGDMA1000 crosslinked systems. The microparticles were dried in a vacuum oven prior to analysis to reduce any moisture present. The microparticles were applied to conductive carbon tape and mounted on an aluminum SEM stage. The particles were then coated with gold for 20 seconds using a sputter-coater (Model 3, Pelco, Redding, CA) in an argon environment. The gold-coated particles were placed in the SEM, which was operated between 2 kV and 10 kV. All images were taken from magnifications ranging from 50X to 1000X.

4.3 Results and Discussion

4.3.1 Polymer Microparticle Formation by UV Polymerization

Optimization of the hydrogel carriers for encapsulation of synthesized bioconjugates required the synthesis of several polymer formulations. Within these polymer formulations, several synthesis parameters were individually varied to determine their effect on the loading and release characteristics of the system. As a result of the analysis, an optimized hydrogel carrier could be designed. The altered synthesis parameters include crosslinker length, monomer-to-solvent ratio, particle size,

and comonomer used. A table of all successfully synthesized polymer formulations is presented in Table 4.1.

As evident from Table 4.1, two polymer formulations were synthesized while varying crosslinker length. One formulation was crosslinked with TEGDMA (4 ethylene glycol repeat units) and the other with PEGDMA1000 (~23 ethylene glycol repeat units). The length of the crosslinker has a direct effect on mesh size and overall openness of the polymer network. Consequently, polymer formulations containing TEGDMA crosslinker will be tighter and able to protect the conjugate better in the stomach due to a tighter collapsed state. However, polymer formulations containing PEGDMA1000 crosslinker will allow more diffusion of the protein in both the collapsed and swollen state. While minimal diffusion is desired in the collapsed state, an effective hydrogel carrier requires that the swollen state promotes maximal diffusion as to have a quick and total release. The trade-off between these characteristics is investigated in later chapters. The synthesis of a polymer film using the crosslinker poly(ethylene glycol) diacrylate with a molecular weight of 4000 (PEGDA4000) was attempted but was not successful because the longer crosslinker created a polymer which was not rigid enough to undergo thin film washing and drying. This problem may be possible to prevent with a different type of polymerization such as solution polymerization but for the purpose of analyzing the effect of crosslinker length, the two crosslinkers used were sufficient.

Three polymer formulations were synthesized with variation with respect to the monomer-to-solvent ratio. The three monomer-to-solvent ratios used in the polymerizations were 50:50, 60:40, and 67:33 monomer-to-solvent ratios. The monomer-to-solvent ratio is known to have an effect on the porosity of the system, the mesh size, and the relative space within the polymer network. The polymer formulation with a 67:33 monomer-to-solvent ratio forms a tighter network which limits diffusion, making it ideal for protecting the loaded bioconjugate in the stomach. However, while diffusion is limited in the systems with more monomers, diffusion is increased in the systems with relatively more solvent, such as the 50:50 monomer-to-solvent system.

The increased capacity for diffusion would be ideal for obtaining a quicker and greater total release than the other systems. The balance between the two effects of altering monomer-to-solvent ratio is investigated in later chapters. Synthesis of polymer films with 40:60 and 33:67 monomer-to-solvent ratios were attempted but were not successful using the thin film method. Excess solvent separates the monomer and crosslinker molecules to the degree that a complete polymer network cannot be formed, resulting in a loose polymer gel. However, the effect of monomer-to-solvent ratio can clearly be observed by testing the three formulations synthesized in this work.

As seen in Table 4.1, three polymer formulations were synthesized while varying the particle size of the microparticles. Microparticles were synthesized within the size ranges of less than 75 microns, 90-150 microns, and 150-212 microns. The particle size does not have an effect on the general internal characteristics of the polymer network, but instead on the overall dynamics of loading and release. The larger microparticles, such as those in the 150-212 micron size range, have a longer diffusion path length for any object diffusing in or out of the system. This has advantages and drawbacks in that it is more difficult for digestive enzymes and gastric acid to reach the protein, preserving its stability, but it is also more difficult for the protein to diffuse out of the system in the small intestine, leading to slower release and decreased amounts released. Conversely, smaller particles, such as those that are less than 75 microns, have shorter diffusion path lengths which may present a danger in the stomach but will lead to better release in the small intestine as well as a release closer to the site of absorption due their ability to penetrate further into the mucosa. The effect of particle size on loading and release is investigated in later chapters. Particles in a size range above 212 microns were not synthesized due to the diminished probability of larger microparticles being effective protein delivery devices. Particles in a size range significantly less than 75 microns were not synthesized due to the inability to reach such small sizes using a mortar and pestle. Smaller particles could be formed through the use of different polymerization techniques or possibly a different crushing method.

In addition to altering synthesis parameters, the polymer structure was also altered by creating two formulations, P(MAA-g-EG) and P(MAA-co-NVP). The introduction of NVP as a replacement comonomer to PEG is thought to result in a more stable system with a higher capacity to complex and form stronger hydrogen bonds. The stronger interaction would provide better protection for the loaded bioconjugate, thus preserving its activity and increasing the chance for higher efficacy. However, the increased interaction would have minimal effect on the swelling response of the hydrogel. Also, replacing PEG tethers with NVP also results with a loss of the ability of the PEG tethers to penetrate the mucosa, generating an increased residence time at the site of absorption. The effect of P(MAA-g-EG) and P(MAA-co-NVP) on the loading and release of synthesized bioconjugates is explored in later chapters.

An effective oral delivery hydrogel carrier must be able to perform a dual function: protection of the protein in the stomach and release in the small intestine. Because one of these functions depends on limiting diffusion and the other on promoting diffusion, systems must be designed very carefully to utilize both attributes. Because the protection and release characteristics are so inherently different, it is extremely difficult to determine the optimal system for incorporation of a specific protein or conjugate without experimental investigation. Experiments testing the loading and release characteristics of all the specific systems are required to maintain the correct balance between protection and release and are performed in Chapter 6 and Chapter 7.

4.3.2 Polymer Microparticle Characterization by Scanning Electron Microscopy

To analyze and characterize the synthesized polymer formulations, several different formulations of microparticles were examined using a scanning electron microscope (SEM). Analysis of the microparticles by SEM yielded information regarding size, morphology, and surface texture which can be used to better understand the differences between the formulations and their effects on the efficiency of the drug

delivery system. Polymer formulations including TEGDMA and PEGDMA crosslinker polymers, the highest and lowest monomer-to-solvent ratios, all three particle size ranges, and P(MAA-g-EG) and P(MAA-co-NVP) were analyzed through SEM.

The first polymer formulation characterized by SEM was that of P(MAA-g-EG) with a 50:50 monomer-to-solvent ratio, crosslinked by PEGDMA1000, and sized less than 75 microns. The SEM micrograph of this formulation is shown as Figure 4.10. As can be seen in Figure 4.10, the observed sizes of the microparticles generally measure around 75 microns or less. The particles are not spherical or any other regular shape but instead are randomly shaped with long, flat edges. The formation of the edges is most likely a result from shear inherent to crushing by mortar and pestle. This particular formulation shows very little surface features and instead shows a very smooth outer surface. The interesting data from the SEM image for this formulation is the wide variation in particle sizes all the way down to less than 10 microns. Because the particles were crushed with no lower limit on size, smaller particles can develop. Microparticles that are significantly smaller will most likely have different loading and release characteristics, but within this formulation the characteristics are used to describe an average particle size.

Another polymer formulation characterized by SEM was the polymer formulation of P(MAA-g-EG) with a 50:50 monomer-to-solvent ratio, crosslinked by PEGDMA1000, and sized between 90-150 microns. The SEM image of this polymer formulation is shown as Figure 4.11. Within Figure 4.11, it can be observed that the measurable size of the microparticles generally fall within the 90-150 microns size range. Similar to the previous formulation, the shape of the microparticles are not regular but instead random with flat edges. Relative to the previous formulation, the polymer microparticles in Figure 4.11 appear to exhibit different surface features. Specifically, the surface appears to be rougher with more imperfections than the smooth formulation of less than 75 microns. The change in surface texture may be attributed to

sample to sample variation, or possibly variation within the method of crushing by mortar and pestle.

The polymer formulation of P(MAA-g-EG) with a 50:50 monomer-to-solvent ratio, crosslinked by PEGDMA1000, and sized between 150-212 microns was also characterized by SEM. The SEM image of this formulation is shown as Figure 4.12. As seen in Figure 4.12, the visual sizes of the microparticles in the image closely represent the specified range of 150-212 microns. As with all other polymer formulations, the shape is not regular or spherical but instead is random with long, flat edges. The surface features of this polymer formulation are somewhere between the smoothness of the less than 75 microns formulation and the roughness of the 90-150 microns formulation. The variations in surface texture between the three formulations with different particle size ranges are mostly insignificant and can be attributed to variation between samples. Changing only the synthesis parameter of particle size should not have an observed effect in the surface of a microparticle other than artificial effects which arise from the processing (crushing, sieving, etc.) of the microparticles.

To determine the effect of monomer-to-solvent ratio and crosslinker length, a polymer formulation of P(MAA-g-EG) with a 67:33 monomer-to-solvent ratio crosslinked with TEGDMA and size below 75 microns was characterized by SEM. The SEM micrograph of this formulation is shown as Figure 4.13. The sizes of the particles are consistent with their specified size of less than 75 microns. Also, because shape was not controlled in the synthesis, the microparticles are mostly random with flat edges. The surface of this polymer formulation appears very smooth, most likely due to the network being tighter with features that are more difficult to observe at the specified magnification.

The last polymer formulation characterized by SEM consisted of P(MAA-co-NVP) with a 50:50 monomer-to-solvent ratio, crosslinked with PEGDMA1000, and sized below 75 microns. The obtained SEM image is shown as Figure 4.14. The visible sizes of the microparticles in Figure 4.14 appear to accurately represent the size range of less than

75 microns. As with all polymer formulations in this thesis, the shape is mostly random with curved edges. The surface texture of the microparticles has more distinct regions and features than many of the other formulations.

To determine the effect of each synthesis parameter on the characteristics of the microparticle, it is necessary to compare the SEM micrographs of the polymer formulations. The first synthesis parameter investigated through SEM characterization is the particle size range. A composite image showing the three size range formulations is shown as Figure 4.15. In Figure 4.15, one can clearly see the difference in size among the three formulations. Differences in size are very easy to observe but the micrographs also confirm the accuracy of the method of crushing and sieving into a specific particle size range. Apart from particle size, the three formulations appear to have similar shape and similar surface textures, although differences can be observed when comparing individual particles.

After size characterization of the particles, the effect of the tightness of the polymer network on the microparticles was investigated by comparing SEM micrographs. A formulation with a tighter network containing TEGDMA crosslinker and a 67:33 monomer-to-solvent ratio was compared against a looser network containing PEGDMA1000 crosslinker and a 50:50 monomer-to-solvent ratio. The comparison of the SEM images is shown as Figure 4.16. While the sizes and shapes of the microparticles appear to be congruent between the two images, slight differences can be observed between the surface features. The tighter-networked polymer (TEGDMA crosslinked and 67:33 monomer-to-solvent ratio) appears to consists of smoother surfaces with fewer distinguishable surface features than the looser-networked polymer (PEGDMA1000 crosslinked and 50:50 monomer-to-solvent ratio). The increase in surface features in the looser polymer formulation may be a result of the more open network allowing for extrusions and movement of the polymer segments while the tighter network may constrict movement of the polymer during crushing thus limiting surface features. However, it is difficult to definitively declare a difference in the two

surfaces. Significantly further magnification could possibly allow visualization of the differences in network rigidity, but the degree of magnification required to observe the polymer mesh is beyond the capabilities of the scanning electron microscope.

The effect of the replacement of the PEG tether comonomer with the NVP comonomer on the polymer microparticles was also investigated by comparing SEM images of P(MAA-g-EG) and P(MAA-co-NVP). The comparison of the SEM images of the two formulations is presented as Figure 4.17. As specified by their individual synthesis parameters, the size and random shape of the two formulations are mostly consistent. However, upon further analysis it is possible to see differences between the structures and surfaces of P(MAA-g-EG) and P(MAA-co-NVP). The P(MAA-g-EG) formulation differs in its structure in that the particles formed contain flat, smooth faces while the P(MAA-co-NVP) particles are more globular, having very few flat sides or edges. The difference in structure can most likely be attributed to the reaction of each to the shear force applied from crushing using a mortar and pestle. P(MAA-g-EG) microparticles may fracture and create straight breaks throughout the face while P(MAA-co-NVP) reacts more like a powder and simply splits apart randomly without following a specific fracture line. Also, P(MAA-co-NVP) differs in that it has generally more surface roughness and surface features than do the smooth surfaces of the P(MAA-g-EG) microparticles. Characterization of the differences in the surfaces and the overall structures of P(MAA-g-EG) and P(MAA-co-NVP) is vital to understanding the different mechanical properties and particle characteristics which will ultimately affect loading and release properties of the system.

4.4 Conclusions

Several polymer formulations including P(MAA-g-EG) and P(MAA-co-NVP) of different crosslinker lengths, monomer-to-solvent ratios, and particle sizes were successfully synthesized. The majority of the formulations were analyzed and characterized by scanning electron microscopy to elucidate the size variations,

morphology, and surface features of each system. Based on the characterizations, insight can be gained on the visual changes rigidity and tightness of the polymer network can create between systems as well as insight into mechanical properties which will ultimately affect the performance of the polymer carriers. The variations created through polymer synthesis in this chapter and characterized by SEM also in this chapter will provided the basis for selecting an optimal polymer carrier for effective delivery of protein bioconjugates.

Parameter	Successfully Synthesized		
Solvent/monomer ratio	50/50	40/60	33/67
Particle size	<75 microns	90-150 microns	150-212 microns
Crosslinker length	4 repeat units		~23 repeat units
Presence of Copolymer	P(MAA-g-EG)		P(MAA-co-NVP)

Table 4.1 Synthesis parameters used in successfully prepared polymer films.

Synthesized polymers differ in crosslinker lengths, particle sizes, solvent to monomer ratios, and comonomer used.

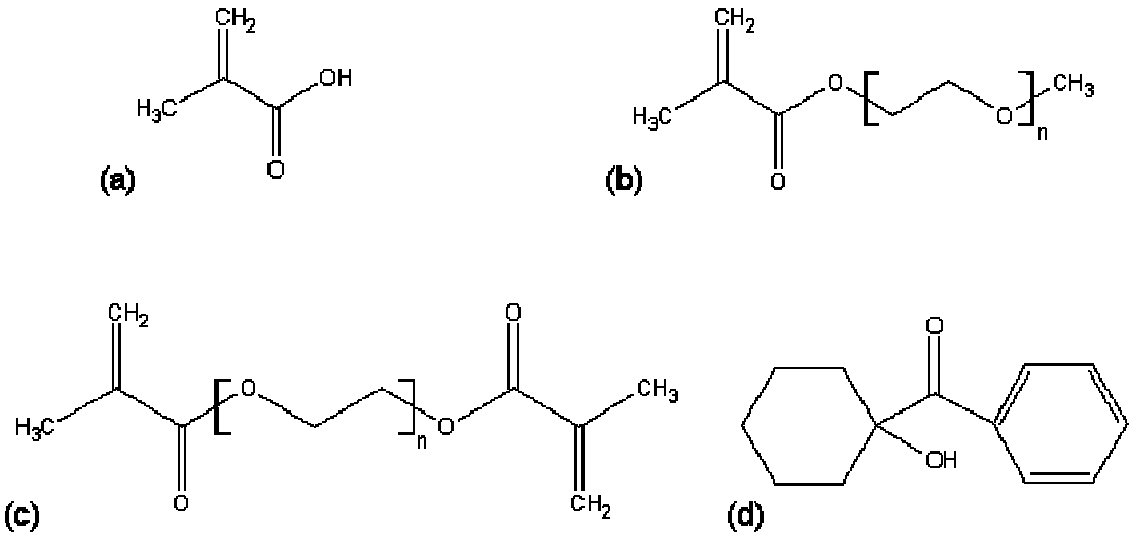

Figure 4.1 Structures of components comprising P(MAA-g-EG) systems.

P(MAA-g-EG) polymer systems are comprised of (a) methacrylic acid (MAA), which forms the polymer backbone, (b) poly(ethylene glycol) monomethyl ether monomethacrylate (PEGMA), which grafts a PEG polymer of chosen molecular weight as a tether, (c) poly(ethylene glycol) dimethacrylate (PEGDMA), which serves as a crosslinker to form a polymer network, and (d) Irgacure 184^{TM}, a UV initiator used to start the polymerization reaction.

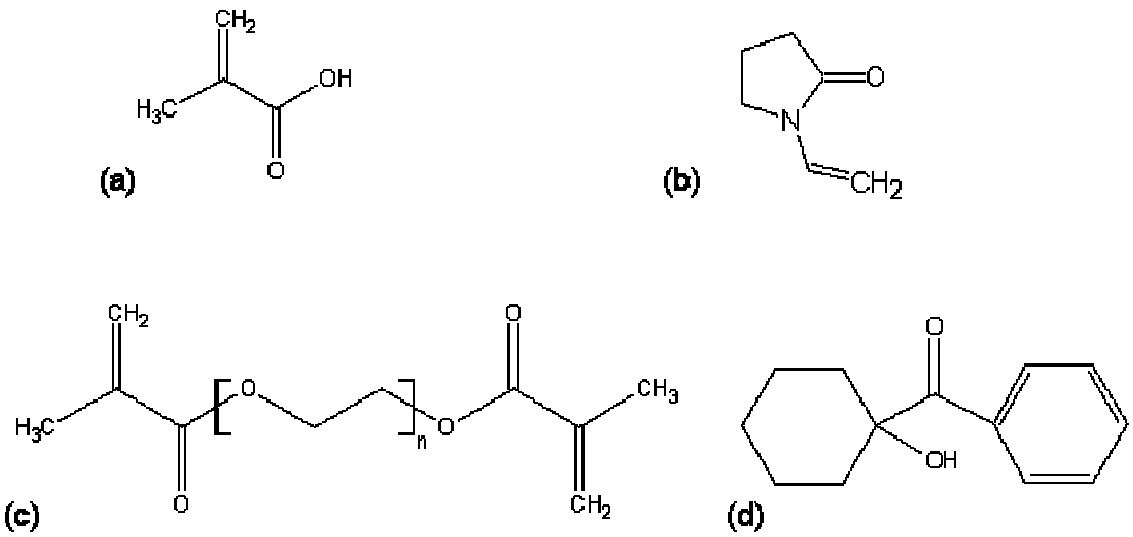

Figure 4.2 Structures of components comprising P(MAA-co-NVP) systems.

P(MAA-co-NVP) polymer systems are comprised of (a) methacrylic acid (MAA), which forms the polymer backbone, (b) n-vinyl pyrrolidone (NVP), a comonomer added to increase interpolymer complexation, (c) poly(ethylene glycol) dimethacrylate (PEGDMA), which serves as a crosslinker to form a polymer network, and (d) Irgacure 184^{TM}, a UV initiator used to start the polymerization reaction.

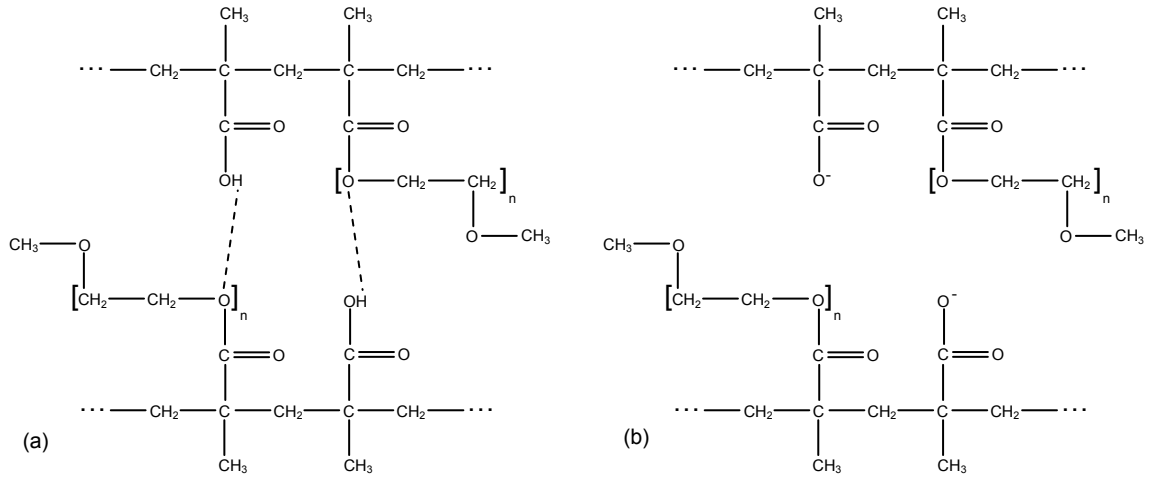

Figure 4.3 Schematic showing interpolymer hydrogen bonding and electrostatic repulsion which cause swelling/deswelling response of P(MAA-g-EG).

Chains of P(MAA-g-EG) exhibiting (a) hydrogen bonding at a low pH, allowing for a collapsed, complexed system, and (b) electrostatic repulsion from local negative charges, forcing the system to swell at neutral pH.

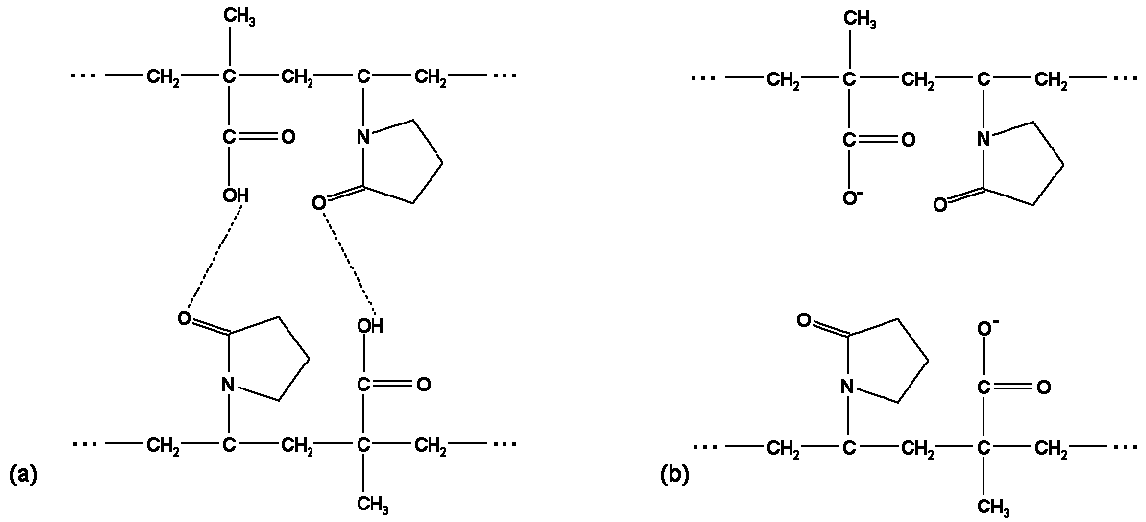

Figure 4.4 Schematic showing interpolymer hydrogen bonding and electrostatic repulsion which cause swelling/deswelling response of P(MAA-co-NVP).

Chains of P(MAA-co-NVP) exhibiting (a) hydrogen bonding at a low pH, allowing for a collapsed, complexed system, and (b) electrostatic repulsion from local negative charges, forcing the system to swell at neutral pH.

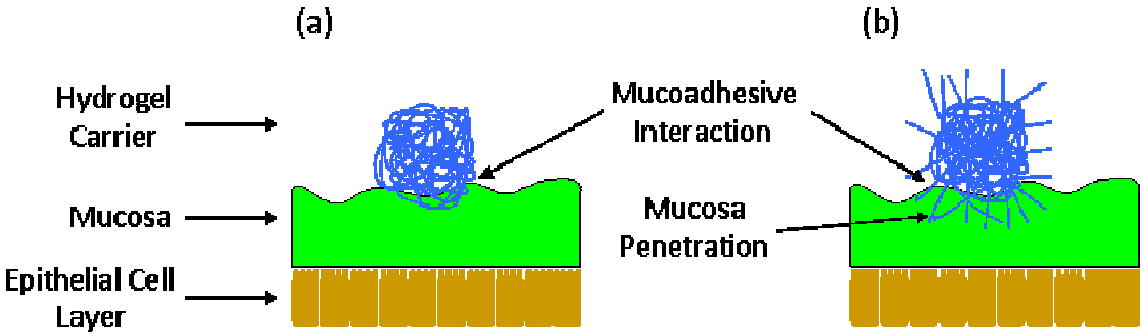

Figure 4.5 Illustration showing mucosa interactions of polymer formulations

Polymer formulation of (a) P(MAA-co-NVP) binds to the mucosa from use of mucoadhesive materials. Polymer formulation of (b) P(MAA-g-EG) binds to the mucosa from the use of mucoadhesive material and also has PEG tethers which penetrate the mucosa, creating a stronger interaction with the mucosa layer.

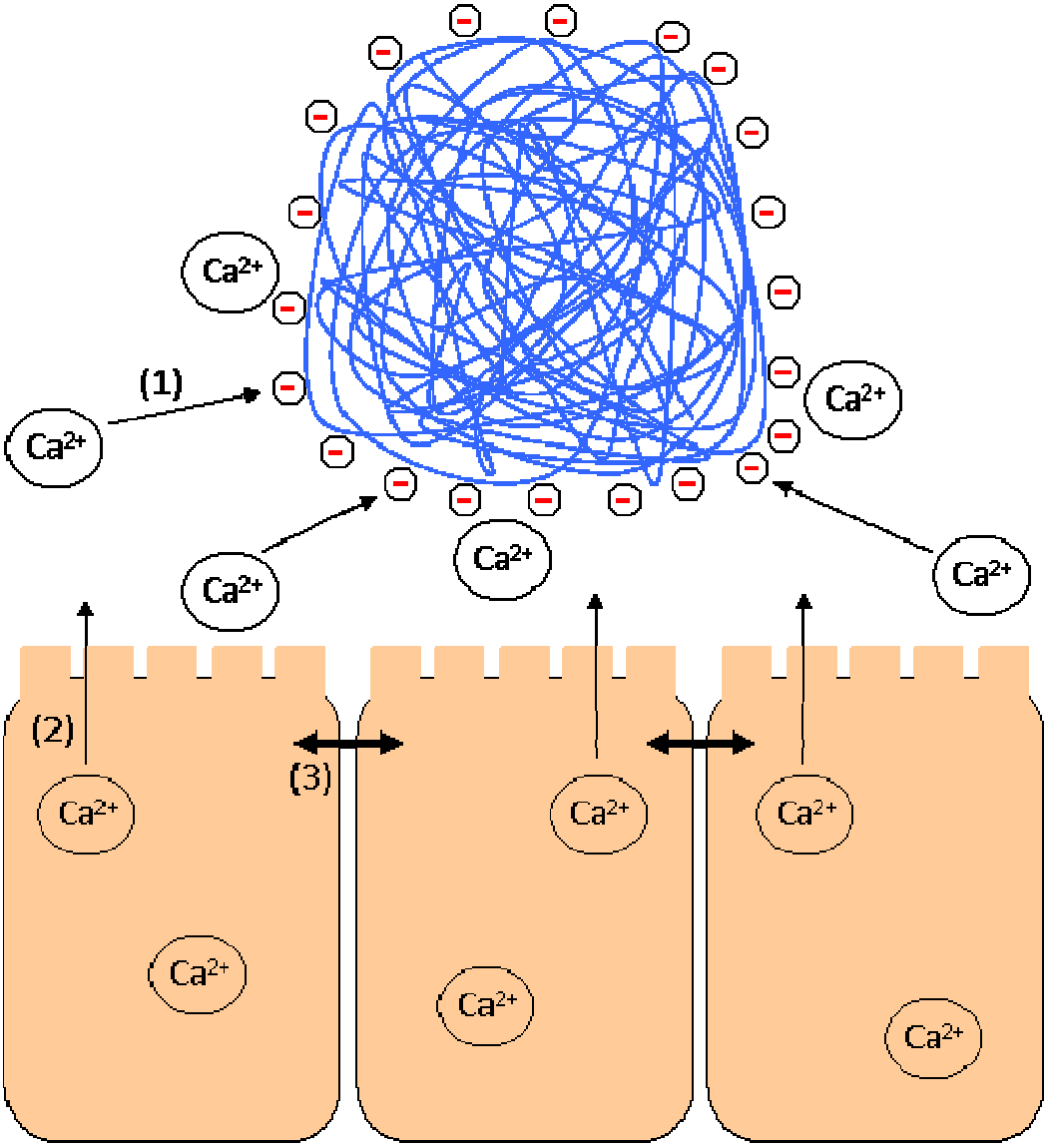

Figure 4.6 Illustration of permeation enhancement ability of anionic hydrogels through calcium binding

Epithelial transport is increased by the presence of the hydrogels in a 3-step manner: (1) Negative charges throughout the network cause positively-charged calcium to bind to the polymer. (2) Depletion of extracellular calcium causes intracellular calcium to diffuse out of epithelial cells. (3) Loss of intracellular calcium results in a loosening of tight junctions, allowing transport of larger molecules across the cell layer.

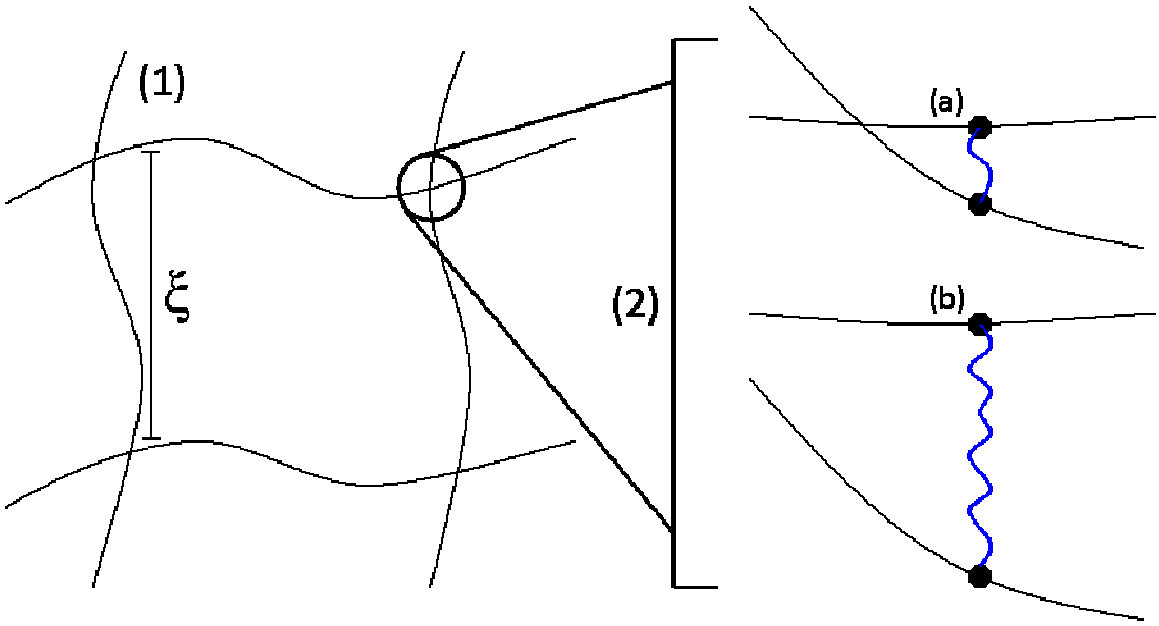

Figure 4.7 Schematic showing effect of crosslinker length on mesh size of the polymer network

Mesh size, ξ, is measured (1) from one crosslink to the next crosslink. If examining a specific crosslink (2), one can see the crosslinker is a small polymer chain that connects the two larger strands. If the polymer chain is short (a), the longer polymer strands are very close to each other and minimal length is added to the mesh size. However, if the polymer chain is longer (b), it further separates the polymer strands and increases the mesh size proportionately.

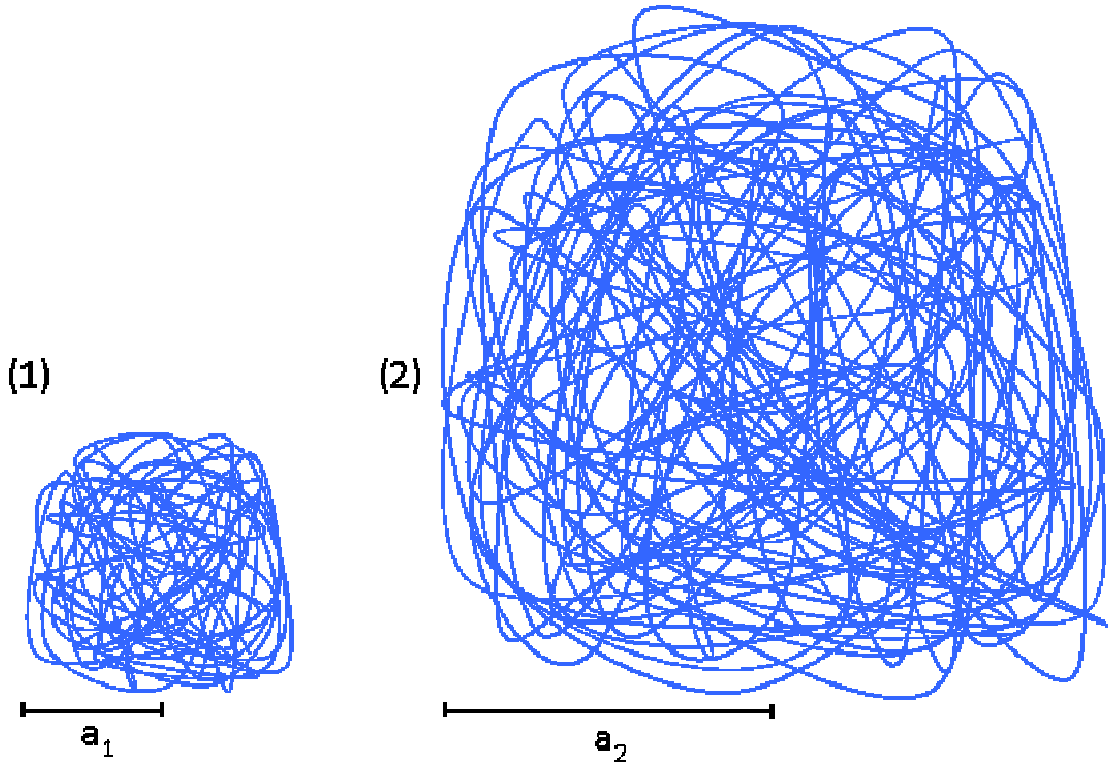

Figure 4.8 Schematic showing magnitude of diffusion path length based on particle size

Diffusion path length, a, is dependent upon particle size. In a smaller particle (1), the diffusion path length (a_1) is short, allowing for quick release. In a larger particle (2), the diffusion path length (a_2) is increased, thus taking longer for an encapsulated protein to diffuse out from the center of the particle.

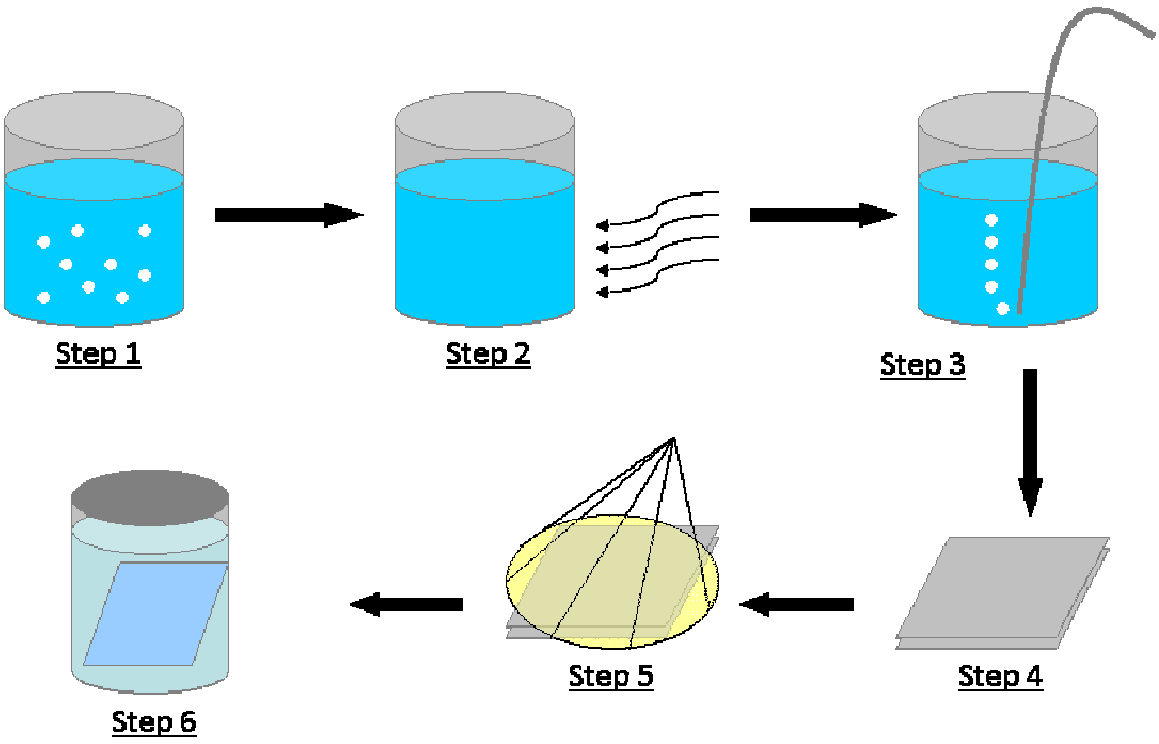

Figure 4.9 Method of UV polymerization for thin film polymers

The UV polymerization process contains several steps: (1) mix components in desired monomer-to-solvent ratio, (2) sonicate solution, (3) purge with nitrogen to remove oxygen, (4) pour between glass slides, (5) UV polymerize for 30 mins, and (6) wash film for 7 days and crush to desired particle size.

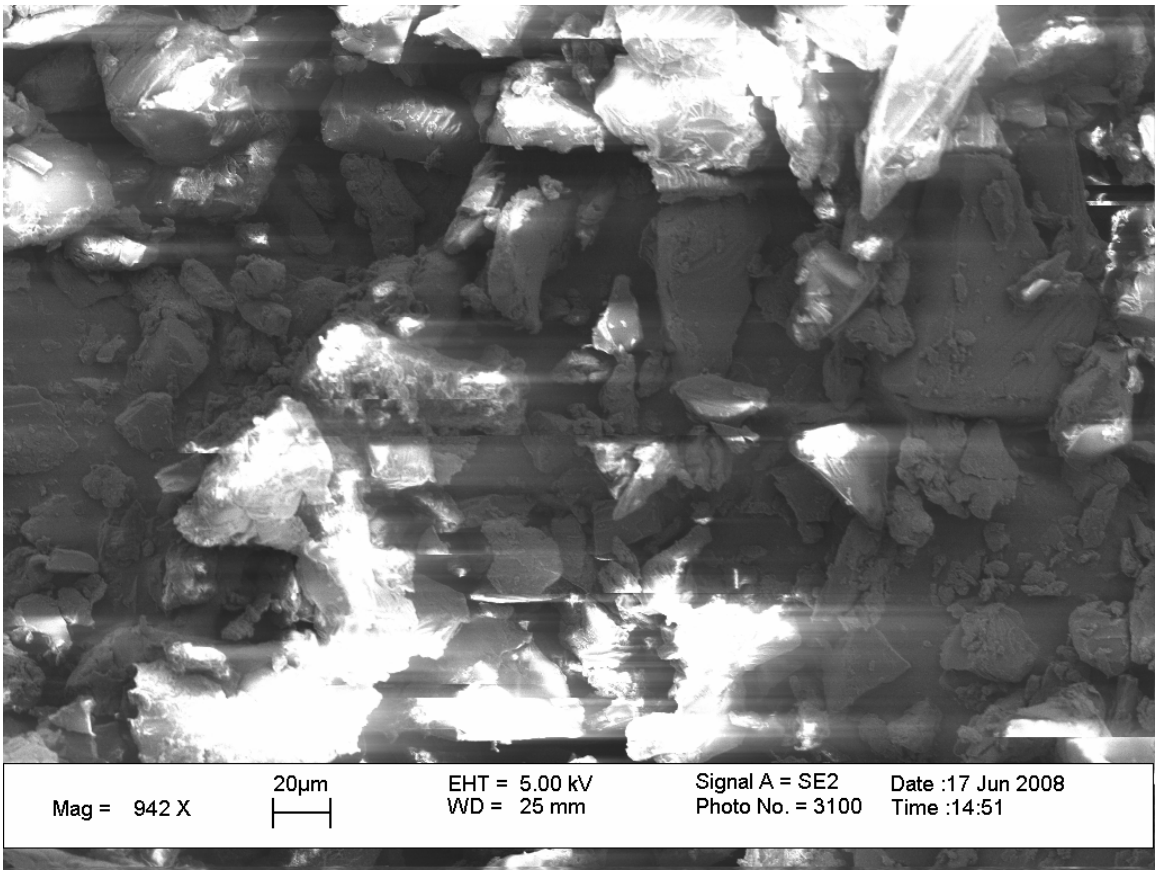

Figure 4.10 SEM micrograph of P(MAA-g-EG) with a size <75 microns

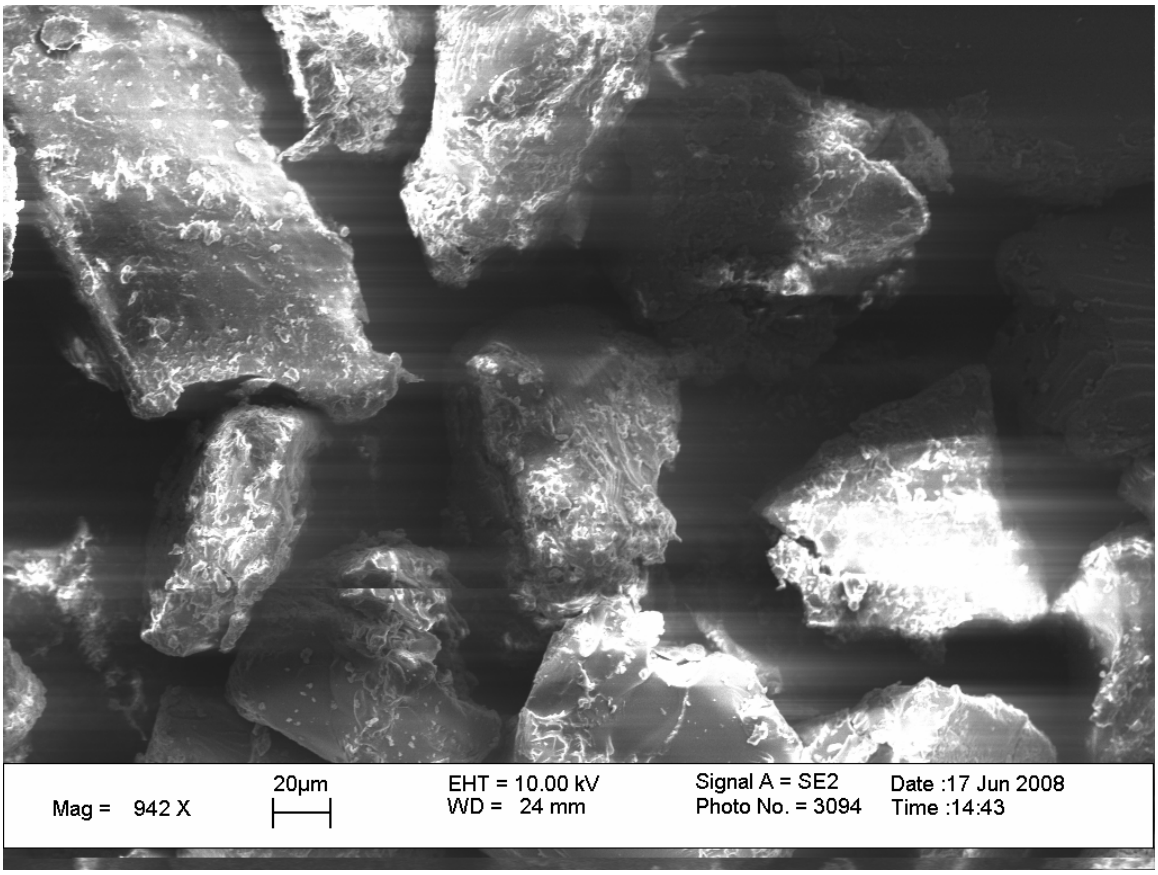

Figure 4.11 SEM micrograph of P(MAA-g-EG) with a size 90-150 microns

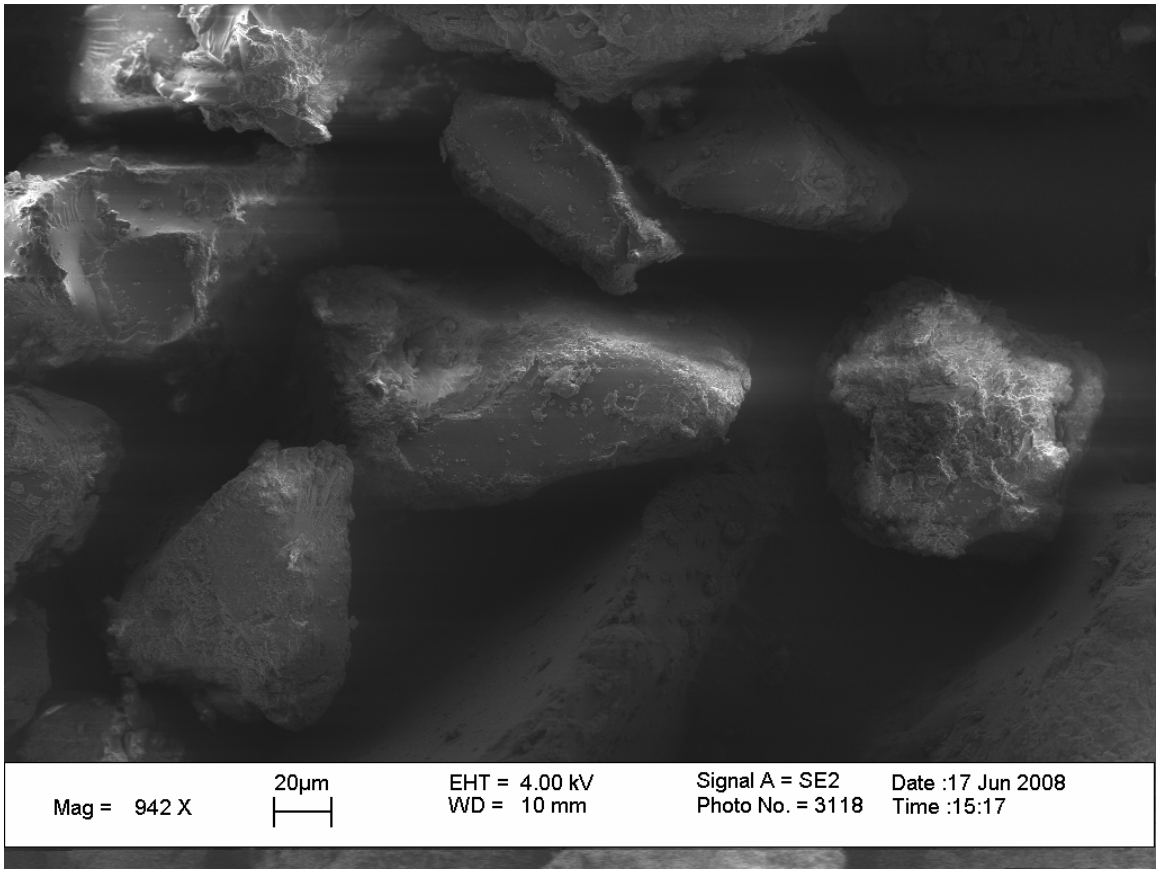

Figure 4.12 SEM micrograph of P(MAA-g-EG) with a size 150-212 microns

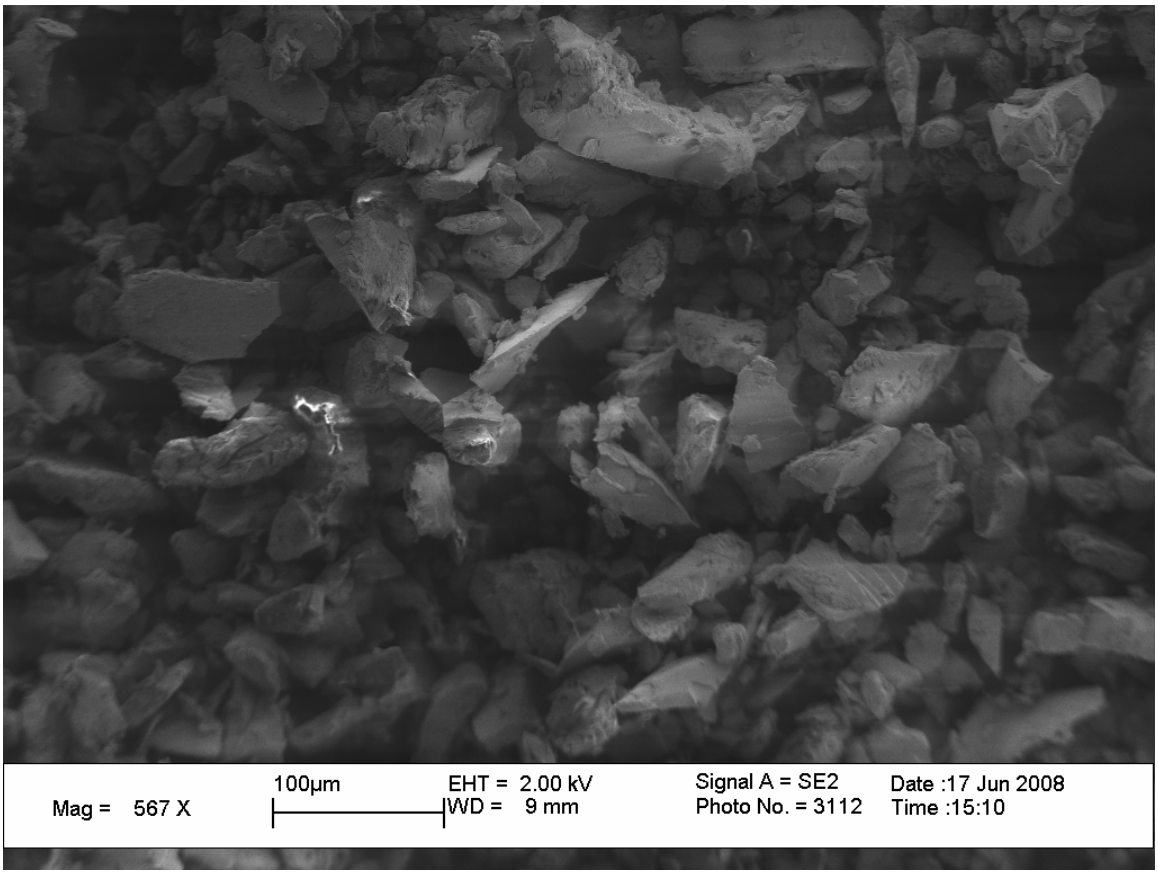

Figure 4.13 SEM micrograph of P(MAA-g-EG) with 67:33 monomer-to-solvent ratio

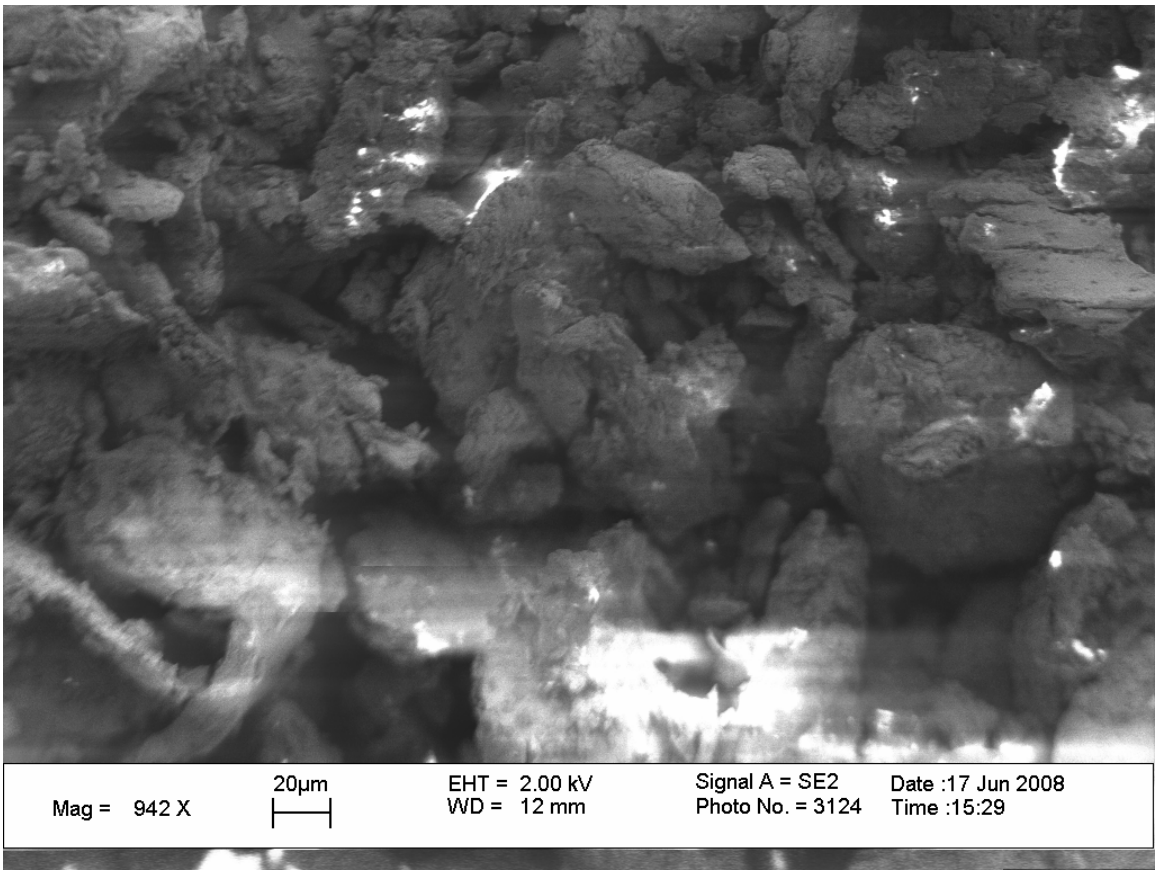

Figure 4.14 SEM micrograph of P(MAA-co-NVP)

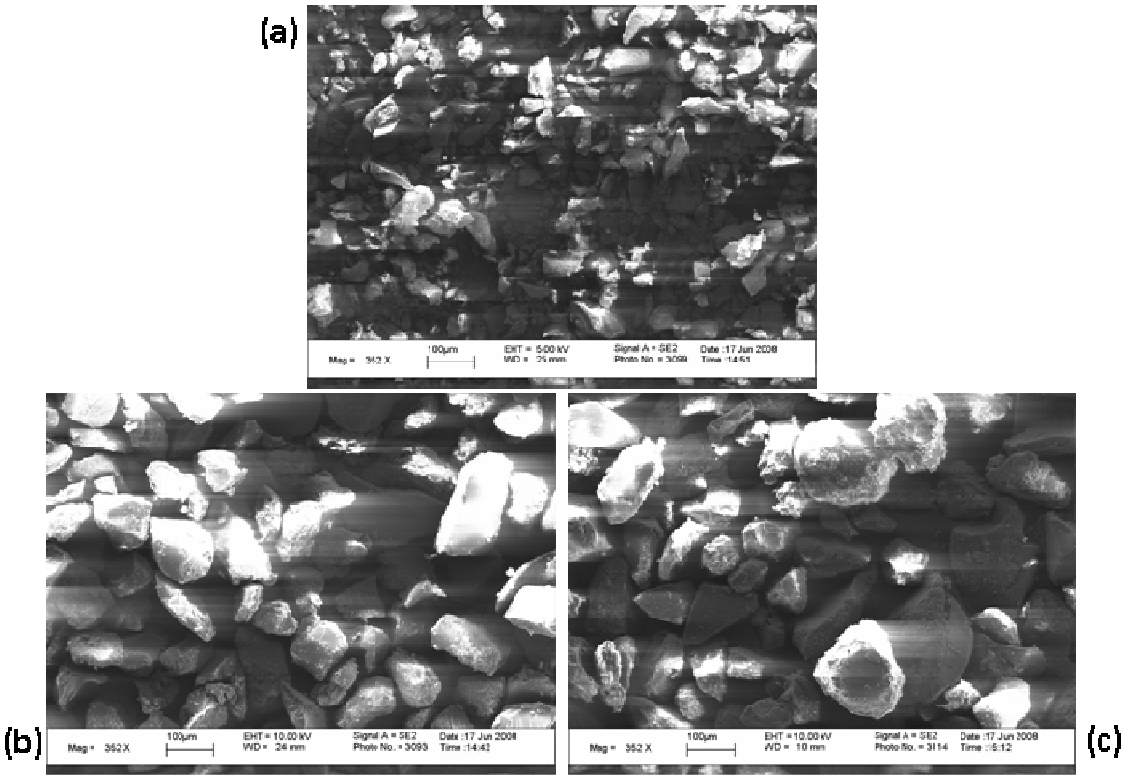

Figure 4.15 SEM micrograph comparison of P(MAA-g-EG) with particle sizes of (a) less than 75 microns, (b) 90-150 microns, and (c) 150-212 microns

Comparison of three particle size ranges demonstrates differences in visual size of the average P(MAA-g-EG) microparticles.

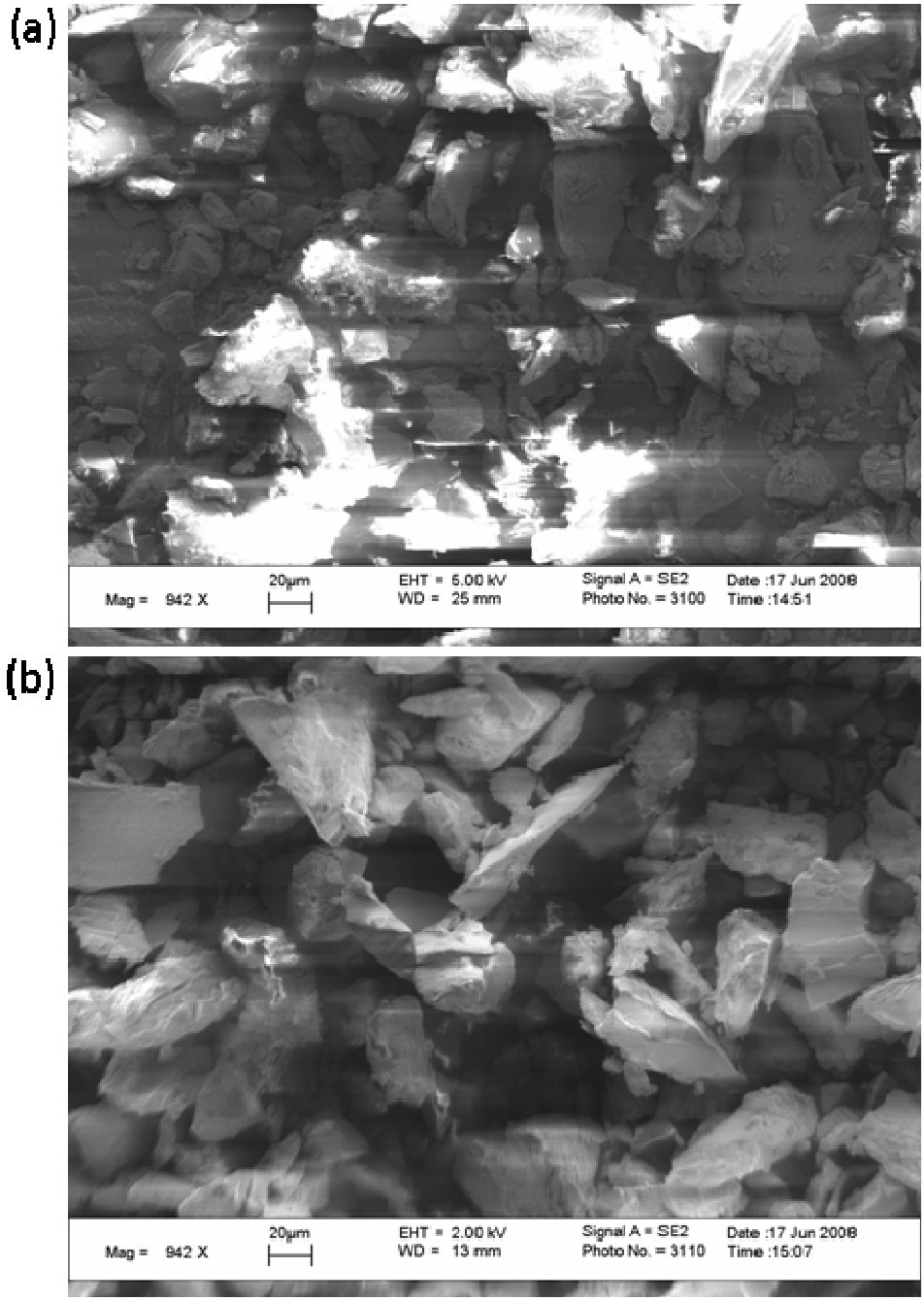

Figure 4.16 SEM micrograph comparison of P(MAA-g-EG) with (a) PEGDMA1000 crosslinker and 50:50 monomer-to-solvent ration and (b) TEGDMA crosslinker and 67:33 monomer-to-solvent ratio

Comparison shows the effect of crosslinker length and monomer-to-solvent ratio on surface texture and surface features.

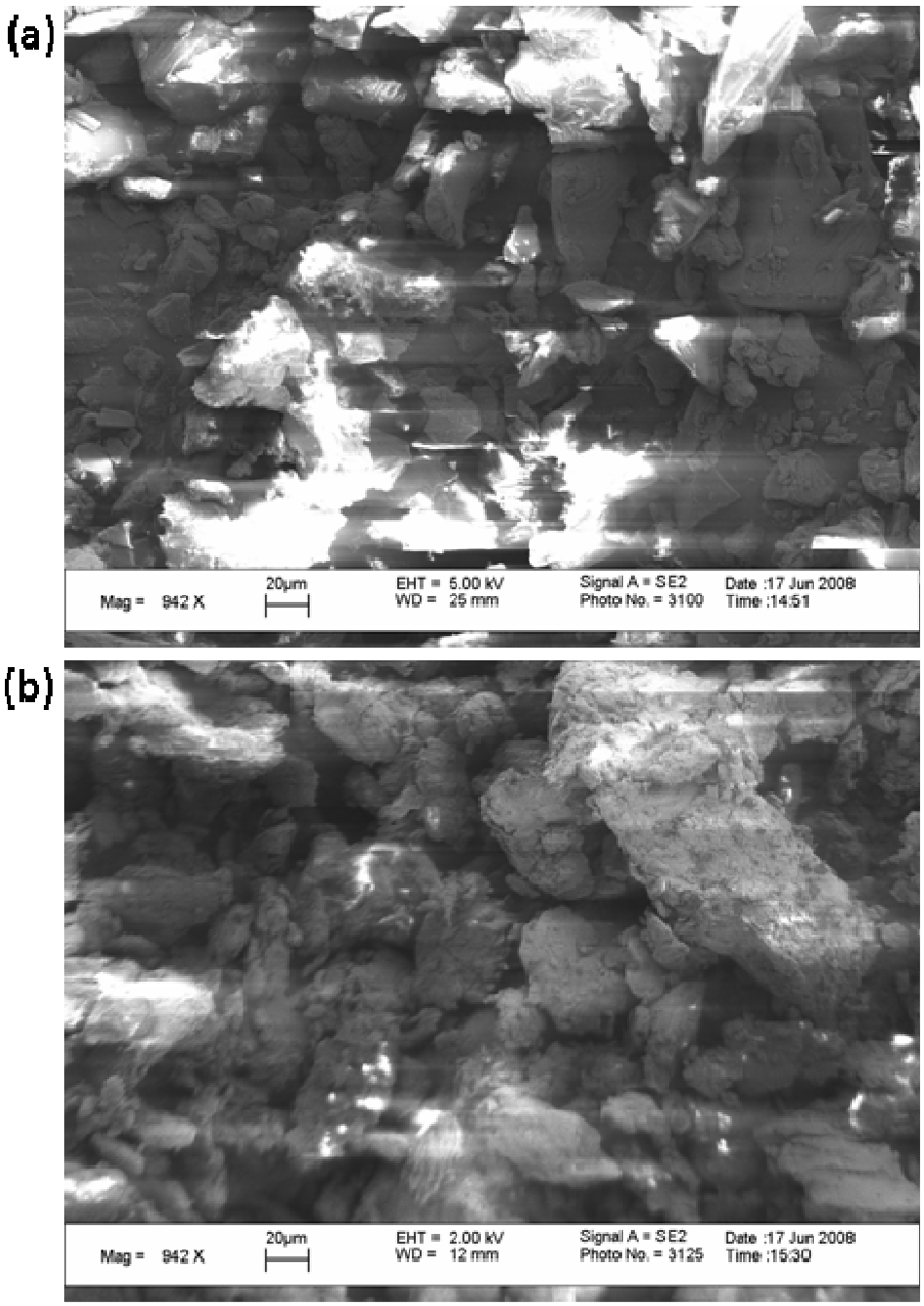

Figure 4.17 SEM micrograph comparison of (a) P(MAA-g-EG) and (b) P(MAA-co-NVP)

Comparison of micrographs show different surface features and surface textures between P(MAA-g-EG) and P(MAA-co-NVP).

REFERENCES

1. Cleland, J.L., Daugherty, A., Mrsny, R., *Emerging protein delivery methods.* Curr. Opin. Biotech., 2001. **12**(2): p. 212-219.

2. Ziv, E., Lior, O., and Kidron, M., *Absorption of protein via the intestinal wall : A quantitative model.* Biochem. Pharmacol., 1987. **36**(7): p. 1035-1039.

3. Anderson, J.M., and Van Itallie, C.M., *Tight junctions and the molecular basis for regulation of paracellular permeability.* Am. J. Physiol.-Gastr. L., 1995. **269**(4): p. G467-475.

4. Kan, K.S., and Coleman, R., *The calcium ionophore A23187 increases the tight-junctional permeability in rat liver.* Biochem. J., 1988. **256**(3): p. 1039-1041.

5. Qiu, Y., and Park, K., *Environment-sensitive hydrogels for drug delivery.* Adv. Drug Deliver. Rev., 2001. **53**(3): p. 321-339.

6. Lowman, A.M., Morishita, M., Kajita, M., Nagai, T., and Peppas, N.A., *Oral delivery of insulin using pH-responsive complexation gels.* J. Pharm. Sci., 1999. **88**(9): p. 933-937.

7. Peppas, N.A., *Hydrogels*. Biomaterials Science, ed. B.D. Ratner, Hoffman, A., Schoen, F., and Lemons, J. 2004, San Diego, CA: Elsevier Academic Press. pp. 100-106.

8. Peppas, N.A., Bures, P., Leobandung, W., and Ichikawa, H., *Hydrogels in pharmaceutical formulations.* Eur. J. Pharm. Biopharm., 2000. **50**(1): p. 27-46.

9. Hoffman, A.S., *Hydrogels for biomedical applications.* Adv. Drug Deliver. Rev., 2002. **54**(1): p. 3-12.

10. Gupta, P., Vermani, K., and Garg, S., *Hydrogels: from controlled release to pH-responsive drug delivery.* Drug Discov. Today, 2002. **7**(10): p. 569-579.

11. Wichterle, O., and Lim, D., *Hydrophilic Gels for Biological Use.* Nature, 1960. **185**(4706): p. 117-118.

12. Lim, F., and Sun, A.M., *Microencapsulated islets as bioartificial endocrine pancreas.* Science, 1980. **210**(4472): p. 908-910.

13. Yannas, I.V., Lee, E., Orgill, D.P., Skrabut, E.M., and Murphy, G.F., *Synthesis and Characterization of a Model Extracellular Matrix that Induces Partial Regeneration of Adult Mammalian Skin.* P. Natl. Acad. Sci. U.S.A., 1989. **86**(3): p. 933-937.

14. Liang-chang, D., Qi, Y., and Hoffman, A.S., *Controlled release of amylase from a thermal and pH-sensitive, macroporous hydrogel.* J. Control. Release, 1992. **19**(1-3): p. 171-177.

15. Morishita, M., Goto, T., Peppas, N.A., Joseph, J.I., Torjman, M.C., Munsick, C., Nakamura, K., Yamagata, T., Takayama, K., and Lowman, A.M., *Mucosal insulin delivery systems based on complexation polymer hydrogels: effect of particle size on insulin enteral absorption.* J. Control. Release, 2004. **97**(1): p. 115-124.

16. Brannon-Peppas, L., and Peppas, N.A., *Time-dependent response of ionic polymer networks to pH and ionic strength changes.* Int. J. Pharm., 1991. **70**(1-2): p. 53-57.

17. Khare, A.R., Peppas, N.A., Massimo, G., and Colombo, P., *Measurement of the swelling force in ionic polymeric networks I. Effect of pH and ionic content.* J. Control. Release, 1992. **22**(3): p. 239-244.

18. am Ende, M.T., Hariharan, D., and Peppas, N.A., *Factors influencing drug and protein transport and release from ionic hydrogels.* React. Polym., 1995. **25**(2-3): p. 127-137.

19. Bell, C.L., and Peppas, N.A., *Water, solute and protein diffusion in physiologically responsive hydrogels of poly(methacrylic acid-g-ethylene glycol).* Biomaterials, 1996. **17**(12): p. 1203-1218.

20. Yamagata, T., Morishita, M., Kavimandan, N.J., Nakamura, K., Fukuoka, Y., Takayama, K., and Peppas, N.A., *Characterization of insulin protection properties of complexation hydrogels in gastric and intestinal enzyme fluids.* J. Control. Release, 2006. **112**(3): p. 343-349.

21. Peppas, N.A., and Sahlin, J.J., *Hydrogels as mucoadhesive and bioadhesive materials: a review.* Biomaterials, 1996. **17**(16): p. 1553-1561.

22. Serra, L., Domenech, J., and Peppas, N.A., *Design of poly(ethylene glycol)-tethered copolymers as novel mucoadhesive drug delivery systems.* Eur. J. Pharm. Biopharm., 2006. **63**(1): p. 11-18.

23. Lowman, A.M., and Peppas, N.A., *Molecular analysis of interpolymer complexation in graft copolymer networks.* Polymer, 2000. **41**(1): p. 73-80.

CHAPTER 5

SYNTHESIS AND CHARACTERIZATION OF PROTEIN-TRANSPORTER CONJUGATES FOR ORAL DELIVERY USING COMPLEXATION HYDROGELS

5.1 Introduction

Bioavailability of orally administered therapeutic proteins depends on several factors such as protein degradation and residence time at the site of absorption. However, the factor which most directly affects absorption into the bloodstream is transport across the epithelial cell layer. Protection of the protein ensures that more protein reaches the site of absorption and increasing residence time in the small intestine ensures more time for absorption. However, the epithelial cell layer is designed to absorb only required nutrients such as vitamins and minerals and to expel unrecognized or unwanted entities such as toxins or viruses.

Under normal conditions, the tight junctions will only permit the transport of molecules with radii <11 Å [1]. Because of its ability to limit transport of large molecules, an unmodified epithelial cell layer will still significantly decrease potential bioavailability by inhibiting transport of most therapeutic proteins, even if 100% of the protein survives the transit through the GI tract and has an extended residence time in the small intestine. To design an effective oral protein delivery formulation, epithelial transport must be significantly increased.

In earlier chapters, the use of hydrogels was suggested as a possible delivery mechanism to increase bioavailability of administered proteins. Hydrogels have been proven to effectively protect the protein [2] as well as increase residence time in the small intestine [3], but are less adept at promoting epithelial transport. Specifically, anionic hydrogels can act as permeation enhancers by binding positively-charged extracellular calcium. The depletion of extracellular calcium causes calcium within the cells to also be depleted due to diffusion. The levels of intracellular calcium play a

significant role in the maintenance of the tight junctions between the cells, and a decrease in calcium levels will loosen the tight junctions [4]. While this effect has been shown to increase transport of therapeutic proteins across the epithelial cell layer, the increase is not significant enough to achieve a high bioavailability. To design a highly effective oral protein delivery system, design strategies must be employed which increase epithelial transport even further beyond the effect achieved using only hydrogels.

In recent years, many design strategies have been implemented by researchers to increase epithelial transport and ultimately raise bioavailability of orally administered proteins. One strategy employed by several scientists is encapsulation of the therapeutic protein in nanoparticle carriers to improve transport [5]. Because of their size, nanoparticle carriers are thought to be uptaken more readily by epithelial cells than any microparticle formulation, increasing the chance of transcytosis of the protein.

Another set of strategies involve modification of the protein to improve transport characteristics. Hinds et al. [6] investigated the effect of poly(ethylene glycol) (PEG) conjugation to insulin, a common therapeutic protein. The presence of a grafted PEG chain significantly reduced the tendency of the insulin to agglomerate. Also, the conjugated PEG-insulin entity exhibited reduced immunogenicity, allergenicity, and antigenicity. The addition of PEG to insulin also increased the circulation time of the conjugate relative to unmodified insulin after subcutaneous injection. While many of these properties are desirable, there is no significant effect on the epithelial transport properties resulting from PEG conjugation.

A large portion of the design strategies to improve epithelial transport focuses on protein transport through the tight junctions which exist between the cells within the monolayer. In other words, the protein can absorbed through the *paracellular* route, or route between the cells. System designs based on large molecule absorption through the paracellular route contain an inherent disadvantage. Based on the regulation mechanism of the tight junctions, proteins are known to transport poorly across

unmodified epithelial cell layers, requiring the tight junctions be disrupted or loosened to promote absorption. However, the tight junctions between the cells control the influx of outside entities into the bloodstream and are a natural barrier to toxins or viruses entering the bloodstream. Monolayer disruption may result in increased protein absorption, but the trade-off is a decreased capacity for the cell monolayer to inhibit absorption of other undesirable entities. Even if the loosening of the tight junctions is quick and reversible, the underlying fact is that the monolayer is disrupted in a manner that is non-specific to the administered protein, creating a possibly safety concern from entering viruses or toxins.

An alternative to protein absorption through the paracellular route is to absorb the protein through the cell itself, utilizing the *transcellular* route for absorption. There are many ways in which a molecule can undergo transcellular transport. The simplest type of transcellular transport is passive diffusion, or diffusion through a cell based on a concentration gradient. This type of transport requires no real response from the cell, but is typically limited to very small molecules such as carbon dioxide and oxygen.

Another type of transcellular transport is efflux transport in which a molecule is brought into the cell, some action is often performed, and then the molecule is expelled on the same side. However, efflux transport does not result in transcytosis, limiting its useful potential for protein absorption into the bloodstream. There are two more types of transcellular transport, both of which involve more complex cell interactions: carrier-mediated transport and receptor-mediated transcytosis. Both processes involve the molecule interacting with the lipid bilayer and reversibly binding to either a carrier molecule or a specific receptor.

In carrier-mediated transport, the molecule-carrier complex dissociates after transporting the molecule inside the cell, allowing the molecule to drift to the other side and engage in a similar carrier-mediated process to exit the cell [7]. However, in receptor-mediated transcytosis, a specific molecule binds to a specific receptor on the cell surface due to its high affinity for the receptor. The molecule-receptor complex is

then transported into the cell and remains intact until it dissociates on the opposite side of the cell. Both processes often involve the uptake of very large molecules which are similar in size to therapeutic proteins, demonstrating the potential for the utilization of both transport pathways for protein delivery.

The transcellular mechanism of absorption receiving the most consideration for use in protein delivery systems is receptor-mediated transcytosis. Receptor-mediated transcytosis benefits from several advantages. Because the protein is being transported through the cells, the tight junctions are left mostly unaffected and are not disrupted. Keeping the tight junctions unmodified and functioning is essential to ensuring the lowest probability of toxins entering. Perhaps the most important advantage is the specificity with which the protein is being transported. If transport occurs only by a specific receptor-ligand interaction, then the protein is being transcytosed in a manner specific to only the protein and nearly all chance of toxins entering is eliminated. Also, because of the specific targeting associated with receptor-mediated transcytosis, the overall transport and bioavailability of the administered protein is likely to increase relative to paracellular mechanisms of absorption.

To utilize receptor-mediated transcytotic pathways, scientists have attempted to form reversible covalent bonds between therapeutic proteins and transporter molecules [8]. The chosen transporter molecule acts as a ligand for a specific receptor which is expressed on human epithelial cells. Assuming the ligand-receptor affinity is unaffected by the conjugation reaction, the resulting transport is specific to the bioconjugate of interest. Xia et al. [9] developed an insulin conjugate by binding it to transferrin and observed the hypoglycemic effect after administration to rats. Also, Russell-Jones [10] demonstrated that erythropoietin can be conjugated to vitamin B_{12} and absorbed through the vitamin B_{12} uptake system. Both systems attempted to improve epithelial transport of the respective therapeutic protein, but neither facilitated the delivery of the bioconjugate to the site of absorption by use of carrier or any other means.

Within this thesis, the proposed strategy to increase epithelial transport was to utilize receptor-mediated endocytosis by conjugating therapeutic proteins of interest to transferrin. Transferrin (~80 kDa) is a single chain protein naturally occurring in the human body which has the ability to bind to two iron ions per transferrin molecule. Transferrin bound with two iron ions (holo-transferrin) has a greater affinity for the transferrin-receptor than transferrin bound with one iron ion (mono-transferrin) or no iron ions (apo-transferrin) [11]. Transferrin-receptors are expressed on many types of cells in the human body, including intestinal epithelial cells. The transferrin-receptor is a homodimer comprised of two identical subunit monomers of approximately 90 kDa each [9]. When iron bound transferrin binds to the transferrin-receptor on the apical side of the cell layer, the complex can undergo either endocytosis (i.e. transport into the cell), or transcytosis (i.e. transport to the basolateral side of the cell layer) [12]. Due to its ability to serve as a transporter targeting ligand for specific cellular uptake as well as its ability to resist trypsin and chymotrypsinogen degradation [13], transferrin remains an attractive option for circumventing the limited transport of the epithelium for drug delivery applications.

This work focuses on forming insulin-transferrin bioconjugates as well as calcitonin-transferrin bioconjugates. The potential advantages of forming these bioconjugates include further protection from degradation by digestive enzymes, increased epithelial transport, and specific targeting of the bioconjugates. Moreover, the incorporation of synthesized bioconjugates in complexation hydrogel carriers increase the probability of stable, intact conjugates reaching the site of absorption. However, forming bioactive conjugates which effectively transport into the bloodstream requires overcoming several challenges. The most important challenge in synthesizing bioconjugates is to form an entity which still retains the bioactivity of both the protein and the transporter ligand. Both bioactivities are essential because lack of protein activity results in inefficient treatment of the disease and lack of transporter activity leads to minimal to no transport into the bloodstream. Also, it is important to examine

whether the conjugate is only being endocytosed, or if it is eventually transcytosed into the bloodstream.

In this chapter, the conjugation reactions to synthesize insulin-transferrin conjugates and calcitonin-transferrin conjugates are discussed. In both cases, the proteins were conjugated by the protein conjugation method first proposed by Carlsson et al [14]. The protein conjugation scheme involves conjugation of the two proteins by the protein crosslinker N-succinimidyl 3-(2-pyridyldithio)propionate (SPDP). SPDP is a heterobifunctional crosslinker which can react with a primary amine group and a sulfohydryl group on two separate proteins. The heterobifunctionality ensures minimal formation of homoconjugates, or conjugates consisting of the same protein. Instead, it promotes synthesis of heteroconjugates, or conjugates consisting of one of each protein. The final result is a bioconjugate which connects both proteins with disulfide linkages. The newly formed disulfide linkages can be broken to separate the proteins under certain conditions such as incubation in blood plasma [15].

The purpose of synthesizing protein-transporter conjugates is to effectively increase epithelial transport. While similar strategies have been employed by several researchers, they have been met with limited success as oral delivery systems due to lack of consideration for other barriers to oral delivery such as degradation in the stomach and intestinal motility. However, utilizing a combinatorial approach of synthesizing protein-transporter conjugates and loading them inside complexation hydrogel carriers presents the ideal opportunity to obtain acceptable overall bioavailability values. The combination of the known abilities of the hydrogel carriers to protect from degradation in the stomach as well as create adhesion near the site of absorption with the increased epithelial transport of using the specific targeting characteristics of protein-transporter conjugates merits the investigation and optimization of the oral protein delivery system explored in this thesis.

5.2 Materials and Methods

5.2.1 Synthesis of Insulin-Transferrin Conjugates

The method for protein conjugation outlined in this section was originally developed by Carlsson et al [14]. The protein conjugation method was first utilized for the conjugation of insulin to transferrin by Shah and Shen [9]. The conjugation scheme consists of using N-succinimidyl 3-(2-pyridyldithio)propionate (SPDP) as a protein crosslinker to conjugate insulin (Ins) to transferrin (Tf) to form insulin-transferrin (Ins-Tf) heteroconjugates. The structure of SPDP is shown as Figure 5.1. The final form of the conjugate is comprised of insulin molecules bound to a transferrin molecule by disulfide linkages.

Step I: Insulin modification by DMMA: The n-terminals of the insulin chains were effectively "blocked" by reaction of insulin with dimethylmaleic anhydride (DMMA, Fluka/Sigma Aldrich Inc., St. Louis, MO), excluding possible reactive sites for SPDP. Step I of the conjugation reaction is illustrated in Figure 5.2. To begin Step I of the conjugation reaction, a sample of 25 mg of bovine insulin (Sigma Aldrich Inc., St. Louis, MO) was added to an acidic solution consisting of 3 mL PBS buffer solution (pH 6.9, Fisher Scientific, Fair Lawn, NJ) and 1.5 mL 1 N HCl (Fisher Scientific, Fair Lawn, NJ). After the insulin had completely dissolved in the acidic solution, 1.5 mL 1 N NaOH (Fisher Scientific, Fair Lawn, NJ) was added to bring the solution back to pH 6.9. A sample of 3.5 mg of DMMA was then added to the solution of dissolved insulin and allowed to react under constant stirring for 0.5 h.

During the reaction period, the pH was monitored using a micro-pH meter (IQ Scientific Instruments, San Diego, CA) and was maintained within the pH range of 6.8-6.9 by adding small volumes of a 1 M Na_2CO_3 (Fisher Scientific, Fair Lawn, NJ) solution. After the reaction finished within 0.5 h, the process of adding 3.5 mg DMMA and maintaining the pH of the solution was repeated two more times. At the end of the final reaction period, the resultant solution was transferred to dialysis tubing (MWCO 3,500,

Spectrum Laboratories Inc., Rancho Dominguez, CA) and dialyzed against PBS buffer (pH 6.9) for approximately 24 hours. Dialysis is performed on the product to remove trace contaminants as well as unreacted DMMA.

Step II: PDP Addition to Insulin: After dialysis of the product, insulin-DMMA was reacted with SPDP (Pierce Biotechnology Inc., Rockford, IL) to add disulfide bonds to the remaining unblocked primary amine at B29-Lysine. The newly introduced disulfide bond serves as the conjugation site for the later addition of transferrin. Step II of the conjugation reaction is illustrated in Figure 5.3. The insulin-DMMA product formed from Step I was removed from dialysis and cooled to 4°C and placed under constant stirring in an Erlenmeyer flask. The pH of the insulin solution was then raised to 9.0 by adding small volumes of 1 M Na_2CO_3. Before its addition to the reaction mixture, 6.0 mg of SPDP was dissolved in 150 μL of dimethyl formamide (DMF, Fisher Scientific, Fair Lawn, NJ). Upon dissolving, the SPDP solution was added in its entirety to the insulin-DMMA solution. The combined solution was allowed to react for 2 hours under constant temperature and stirring. The pH of the solution was maintained within the pH range of 8.8-9.0 for the duration of the reaction using a micro-pH meter. Upon completion of the reaction time period, the insulin-PDP product was transferred to dialysis tubing (MWCO 3,500) and allowed to dialyze at 4°C for 24 hours. Dialysis of insulin-PDP ensures the removal of trace contaminants as well as excess SPDP reagent.

Step III: Transferrin modification by SPDP: In addition to the insulin modification reactions, transferrin was also reacted with SPDP to form PDP groups on the transferring molecule. After forming PDP groups, the newly formed Tf-PDP was reduced by reaction with dithiothreitol (DTT, Sigma Aldrich Inc., St. Louis, MO). Step III of the conjugation reaction is illustrated in Figure 5.4. To begin Step III of the conjugation reaction, a sample of 120 mg of human holo-transferrin (Tf, Sigma Aldrich Inc., St. Louis, MO) was added to a solution consisting of PBS buffer (pH 7.0). Before its addition to the

reaction mixture, 8.0 mg of SPDP was dissolved in 100 μL DMF. The SPDP/DMF solution was added to the transferrin solution and allowed to react for 2 hours under constant stirring and at approximately 4°C. After the completion of the reaction period, the product solution was removed and placed in dialysis tubing (MWCO 12,000-14,000, Spectrum Laboratories Inc., Rancho Dominguez, CA) in a solution of PBS buffer (pH 8.0). The Tf-PDP product was dialyzed overnight to remove any unreacted SPDP.

After formation of PDP groups on transferrin, the modified protein must be reduced to alter the PDP groups and to form sulfohydryl groups. To reduce Tf-PDP, a solution consisting of 1 M DTT in H_2O was first prepared. After 24 hours of dialysis, the Tf-PDP solution was reduced using the prepared 1 M DTT solution. The solutions were combined and allowed to react for 1 h. The newly formed product was a solution of transferrin with attached sulfohydryl groups (Tf-SH) and was allowed to dialyze for 24 h to remove unreacted DTT.

Step IV: Combination of modified proteins: Upon completion of Step III, the Tf-SH product was purified by elution from D-Salt Dextran Desalting Columns (10 mL, Pierce Biotechnology Inc., Rockford, IL). To achieve a high level of purity, four columns were connected in series. During elution from the columns, small 1 mL fractions were obtained using a fractional collector (CF-1, Spectrum Chromatography, Rancho Dominguez, CA). A PBS buffer solution (pH 8.0, 3mM EDTA) was used to elute the modified protein from the columns. Each fraction was analyzed using UV spectroscopy and the fractions having relatively higher absorbances at a wavelength of 280 nm indicating higher protein concentration and were collected for further use. The presence of EDTA in the PBS solution used to elute the columns is necessary to prevent any metal-catalyzed oxidation of free sulfohydryl groups into disulfide bonds, thereby reducing the possibility of forming any crosslinked transferrin complexes.

Step IV of the conjugation reaction consists of combining the two modified proteins to form a final conjugate product. Step IV of the reaction is illustrated in Figure

5.5. To initiate the final step in the conjugation reaction, the product solutions of Ins-PDP and Tf-SH were combined into one Erlenmeyer flask. The reaction is allowed to proceed under constant stirring. The reaction progress can be monitored by first taking small samples of the reaction mixture at any desired time point of the reaction period. Each sample can be analyzed by UV spectroscopy to determine its absorbance.

When Ins-PDP reacts with Tf-SH, the chromophore 2-pyridinethione is released. The concentration of 2-pyridinethione can be determined by measuring the absorbance of the reaction mixture at 343 nm. The concentration of 2-pyridinethione can be compared to the concentration of transferrin in the solution to determine how many average insulin molecules are attaching to each transferrin molecule. It is desirable to limit the number of insulin molecules per transferrin molecule to prevent the conjugate from being too large. The reaction can be stopped at any point by the addition of n-ethylmaleimide (NEM, ACROS Organics, Geel, Belgium), which reacts with free thiol groups [16] and prevents further crosslinking. Typically, the reaction was stopped by addition of NEM after a period of 90 minutes to prevent bulkiness of the conjugate product. After the reaction had been halted, the product was transferred to dialysis tubing (MWCO 12,000-14,000) and allowed to dialyze for 48 hours to remove unreacted reagents. To determine the concentration of the conjugate solution, the product was analyzed using HPLC (Waters Corporation, Milford, MA). After analysis, the conjugate solution was refrigerated until further use.

5.2.2 Synthesis of Calcitonin-Transferrin Conjugates

The protein conjugation method explored in this section was originally developed by Carlsson et al [14]. The conjugation scheme for the formation of calcitonin-transferrin bioconjugates is similar to the reaction scheme employed to make insulin-transferrin conjugates by Shah and Shen [8] as well as Kavimandan et al [17]. The conjugation scheme consists of using the protein crosslinker SPDP to conjugate calcitonin (Calc) to transferrin (Tf) to form calcitonin-transferrin (Calc-Tf)

heteroconjugates. The final product of the reaction is a conjugate molecule consisting of calcitonin molecules conjugated to a transferring molecule by disulfide linkages.

Step I: Calcitonin modification by SPDP: The primary amines on calcitonin were reacted with SPDP to provide disulfide linkages for subsequent protein conjugation. Step I of the calcitonin-transferrin conjugation reaction is illustrated in Figure 5.6. To begin Step I of the conjugation reaction, a sample of 25 mg of salmon calcitonin (EMD Biosciences Inc., Darmstadt, Germany) was added to a solution consisting of 5% by volume acetic acid (Fisher Scientific, Fair Lawn, NJ) in 6 mL of PBS buffer (pH 8.0) and allowed to dissolve. The presence of acetic acid in the initial solution is necessary to facilitate the dissolution of calcitonin. After calcitonin had successfully been dissolved, a reagent solution consisting of 6 mg SPDP in 150 μL DMF was prepared. The SPDP/DMF solution is added to the calcitonin solution and allowed to react for 2 hours under constant stirring and at 4°C. At the end of the final reaction period, the Calc-PDP solution was transferred to dialysis tubing (Spectrum Laboratories Inc., Rancho Dominguez, CA) and dialyzed against PBS buffer (pH 8.0) for approximately 24 hours. Dialysis is performed on the product to remove trace contaminants as well as unreacted SPDP.

Step II: PDP Addition to Transferrin: Transferrin is modified by the addition of PDP groups to later allow for conjugation to calcitonin. The newly introduced PDP group is reduced in a later step to allow for reaction with modified Calc-PDP. Step II of the calcitonin-transferrin conjugation reaction is illustrated in Figure 5.7. To begin the modification of transferrin, a sample of 125 mg of transferrin is added to a PBS buffer solution (pH 6.9). Before its addition to the reaction mixture, 6.0 mg of SPDP was dissolved in 150 μL of DMF. Upon dissolving, the SPDP solution was added in its entirety to the transferrin solution. The combined solution was allowed to react for 2 hours under constant stirring and at 4°C. After the reaction was complete, the transferrin-PDP product was transferred to dialysis tubing (MWCO 12,000-14,000) and allowed to

dialyze at 4°C for 24 hours. Dialysis of transferrin-PDP ensures the removal of trace contaminants as well as excess SPDP reagent.

Step III: Reduction of Transferrin-PDP by DTT: After forming PDP groups, modified transferrin (Tf-PDP) was reduced by reaction with DTT. Reduction of Tf-PDP by DTT allows the replacing of PDP groups with sulfohydryl groups (-SH) to form another modified transferrin molecule (Tf-SH). Step III of the calcitonin-transferrin conjugation reaction is illustrated in Figure 5.8. To reduce Tf-PDP, a solution consisting of 1 M DTT in H_2O was first prepared. After 24 hours of dialysis, the Tf-PDP solution was reduced using the prepared 1 M DTT solution. The 1 M DTT solution was added to the Tf-PDP solution and allowed to react for 1 hour under constant stirring. The newly formed product was a solution of transferrin with attached sulfohydryl groups (Tf-SH) and was placed in dialysis tubing (MWCO 12,000-14,000) for 24 h to remove unreacted DTT.

Step IV: Combination of modified proteins: Upon completion of Step III, the Tf-SH product was purified by elution from D-Salt Dextran Desalting Columns. To achieve a high level of purity, four columns were connected in series. During elution from the columns, small 1 mL fractions were obtained using a fractional collector. A PBS buffer solution (pH 8.0, 3mM EDTA) was used to elute the modified protein from the columns. Each fraction was analyzed using UV spectroscopy and the fractions having relatively higher absorbances at a wavelength of 280 nm indicating higher protein concentration and were collected for further use. The presence of EDTA in the PBS solution used to elute the columns is necessary to prevent any metal-catalyzed oxidation of free sulfohydryl groups into disulfide bonds, thereby reducing the possibility of forming any crosslinked transferrin complexes.

Step IV of the calcitonin-transferrin conjugation reaction consists of combining modified calcitonin (Calc-PDP) with modified transferrin (Tf-SH) to form a final conjugate. Step IV of the reaction is illustrated in Figure 5.9. The final step of the calcitonin-

transferrin conjugation reaction is initiated by combining both product solutions (Calc-PDP and Tf-SH) into one Erlenmeyer flask. The reaction is then allowed to proceed under constant stirring. The reaction progress can be monitored by first taking small samples of the reaction mixture at any desired time point of the reaction period. Each sample can be analyzed by UV spectroscopy to determine its absorbance. When Calc-PDP reacts with Tf-SH, the chromophore 2-pyridinethione is released. The concentration of 2-pyridinethione can be determined by measuring the absorbance of the reaction mixture at 343 nm. The concentration of 2-pyridinethione can be compared to the concentration of transferrin in the solution to determine how many average calcitonin molecules are attaching to each transferrin molecule. It is desirable to limit the number of calcitonin molecules per transferrin molecule to prevent the conjugate from being too large. The reaction can be stopped at any time by the addition of NEM which will prevent any further crosslinking. Generally, the reaction was stopped by addition of NEM after a period of 90 minutes to prevent bulkiness of the calcitonin-transferrin product. At the completion of the reaction period, the product was transferred to dialysis tubing (MWCO 12,000-14,000) and allowed to dialyze for 48 hours to remove unreacted reagents. To determine the concentration of the calcitonin-transferrin conjugate solution, the product was analyzed using HPLC. The final conjugate solution was refrigerated until further use.

5.2.3 Analysis of Protein-Transporter Conjugates

Throughout the steps of the conjugation reactions, intermediates as well as the final conjugate products were characterized to gain insight into the nature of the crosslinking bonds as well as to verify the synthesis of a confirmed protein-transporter conjugate. Characterization methods include UV spectroscopic analysis of intermediates to determine nature of modified proteins and analysis by HPLC to verify synthesis of the final product.

Conjugate Analysis using UV Spectroscopy: As an analysis of Step II of the conjugation reaction, it is possible to use UV spectroscopy to determine the average number of PDP groups that are bound to each insulin molecule (PDP:Insulin ratio). Upon reduction of Ins-PDP with DTT, there is a release of 2-pyridinethione, a chromophore whose concentration can be measured by analyzing absorbance of the solution at a wavelength of 343 nm (A_{343}). To analyze the Ins-PDP solution, a small volume of approximately 40 μL was obtained and subsequently reduced with 25mM DTT. After reduction of the sample, the absorbance was measured using a microplate reader (Synergy HT, Bio-Tech Instruments, Winooski, VT) at a wavelength of 280 nm (A_{280}) to determine protein concentration and at a wavelength of 343 nm (A_{343}) to obtain chromophore concentration. Molar extinction coefficients of 8.08 x 10^3 $M^{-1}cm^{-1}$ at 343 nm ($\varepsilon_{343,TP}$) and 5.10 x 10^3 $M^{-1}cm^{-1}$ at 280 nm ($\varepsilon_{280,TP}$) were used for the calculations for the chromophore [14, 18]. Insulin concentration was determined by measuring the absorbance at 280 nm (A_{280}). The molar extinction coefficient used for proteins was 5.8 x 10^3 $M^{-1}cm^{-1}$ at 280 nm ($\varepsilon_{280,INS}$). The sample of 40 µl reduced Ins-PDP solution was diluted to 700 µl and the absorbance was measured in triplicates at 343 nm and 280 nm. The PDP:Insulin ratio was calculated using Equation 1 shown below:

$$\text{PDP : Insulin ratio} = \frac{A_{343} \text{ x } \varepsilon_{280,INS}}{\left(A_{280} \text{ x } \varepsilon_{343,TP} - A_{343} \text{ x } \varepsilon_{280,TP}\right)} \qquad (1)$$

Similar to the UV spectroscopic analysis after Step II, Step III can be analyzed by determining the average number of PDP groups attached to each transferrin molecule (PDP:Tf ratio). As with insulin, reduction of transferrin with DTT releases 2-pyridinethione, a chromophore whose concentration can be measured by analyzing absorbance of the solution. After completion of Step III, a small volume of 40 μL was extracted from the already reduced Tf-PDP solution, now denoted as Tf-SH. The small sample was diluted to 700 μL and the absorbance was measured in triplicates at wavelengths of 280 nm and 343 nm using a microplate reader. The PDP:Tf ratio was

calculated using Equation 1 from the previous section. The molar extinction coefficients for the chromophore were the same as those used to find the PDP:Insulin ratio, but the molar extinction coefficient used for transferrin was 93.0 x 10^3 $M^{-1}cm^{-1}$ ($\varepsilon_{280,TF}$).

HPLC Analysis of Protein-Transporter Conjugates: High Performance Liquid Chromatography (HPLC) was used to verify production of both insulin-transferrin and calcitonin-transferrin conjugates as well as for quantification of reaction yield and final concentration of conjugate solutions. The HPLC equipment used consists of a Waters 2695 Separation Module (Waters Corporation, Milford, MA) attached to a Waters 2487 Dual λ Absorbance Detector (Waters Corporation, Milford, MA). Characterization is performed using a reverse-phase analytical HPLC method designed to elute a wide range of proteins within a specified time period. The method includes the use of water (HPLC Grade, Fisher Scientific, Fair Lawn, NJ) with 0.1% by volume trifluoroacetic acid (TFA, ACROS Organics, Geel, Belgium) as Solvent A and acetonitrile (Optima, Fisher Scientific, Fair Lawn, NJ) with 0.08% by volume TFA as Solvent B. During the separation process, the mobile phase begins at a composition of 70% Solvent A and 30% Solvent B. The mobile phase changes composition using a gradient to 40% Solvent A and 60% Solvent B within 6 minutes. The mobile phase composition is then returned to initial conditions of 70% Solvent A and 30% Solvent B for the next sample to be analyzed. The mobile phase was introduced at a constant flow rate of 0.6 mL/min. All separations are performed using a Symmetry300^{TM} C4 column (particle size 5 μm, 3.9 mm I.D. x 150 mm length, Waters Corporation, Milford, MA) held at a constant temperature of 40°C. After separation of proteins, absorbance of the solution was detected at a wavelength of 220 nm. All instrument and processing methods were controlled and specified using the Empower software.

5.3 Results and Discussion

5.3.1 Synthesis of Insulin-Transferrin Conjugates

By using the conjugation scheme outlined by Carlsson et al. [14], insulin was conjugated to transferrin by disulfide linkages from use of the protein crosslinker SPDP. SPDP is classified as a heterobifunctional crosslinker because of its ability to react with two different types of functional groups. As can be seen in Figure 5.1, SPDP can react with amine groups near the region of the n-hydroxysuccinimide (NHS) ester. After reaction occurs by nucleophilic attack from the nitrogen to the carbonyl group, the amine group is modified and now contains a reactive 2-pyridyldithio group. The free 2-pyridyldithio group provides the other half of the reactivity of SPDP and is reactive with sulfohydryl groups. By using SPDP, it is possible to crosslink a protein with primary amine groups with a different protein which contains sulfohydryl groups. The heterobifunctional properties of SPDP ensure the formation of heteroconjugates, or conjugates consisting of two different proteins. At the same time, using SPDP to form protein conjugates also excludes formation of homoconjugates, or conjugates consisting of multiple molecules of the same protein, due to SPDP not having two amine reactive sites or two sulfohydryl reactive sites.

The result of binding two proteins using SPDP is conjugation by disulfide linkages. The prospect of protein conjugation by disulfide linkages is especially relevant considering the inherent instability and tendency of disulfide bonds to cleave within blood plasma [19]. Due to the instability of disulfide bonds in blood plasma, the conjugated proteins may be cleaved once they reach systemic circulation, thus releasing free insulin [8, 20, 21]. In fact, Xia et al. [15] showed that free insulin is released after only 5 minutes of incubation of insulin-transferrin conjugates in rat liver slices. Also, free insulin was detected in the rat serum up to 4 hours after insulin-transferrin conjugates were orally administered.

Step I of the insulin-transferrin conjugation reaction involves the “blocking” of two primary amine groups of insulin by reaction with DMMA. Insulin has three primary

amine moieties which are reactive with DMMA. The three primary amine groups are located at A1-Glycine (A1-Gly), B1-Phenylalanine (B1-Phe), and B29-Lysine (B29-Lys). The same three primary amine moieties are also reactive with the protein crosslinker SPDP. However, the amine groups can only react with SPDP or with DMMA at a pH which will make the amine group deprotonated and able to act as a nucleophile. The NH_2 group, acting as a nucleophile, can react with the electron-deficient carbon atom in the succinimidyl group of SPDP or the carbon atom in either carbonyl group of DMMA. The nucleophilic attack of DMMA is shown in Figure 5.2 and the attack of SPDP is shown in Figure 5.3. However, Lindsay and Shall [22] reported that conjugation of a large molecule to the A1-Glycine residue of insulin can significantly reduce its bioactivity. Due to the specificity requirement of the conjugation site, a method had to be devised to selectively conjugate transferrin to insulin at either the B1-Phenylalanine site or the B29-Lysine site while inhibiting reaction at the A1-Glycine site. The chosen strategy to overcome this barrier is to first conjugate a small molecule, such as DMMA, to the primary amine at A1-Glycine to prevent subsequent reaction with SPDP. However, a factor had to be found which controlled the reactivities of the possible conjugation sites such that all three possible conjugation sites are not blocked by DMMA. A major factor differentiating the conjugation sites is the pKa of the primary amine groups. A1-Glycine and B1-Phenylalanine, which are n-terminal residues, have a pKa of 7.5-8.0 while the primary amine at B29-Lysine has a pKa around 10.5 [23]. Thus, control of the reaction pH can be used to selectively react either the two n-terminal primary amines or only the primary amine at B29-Lysine. The structure of insulin along with labeling of its possible conjugation sites for DMMA and SPDP is presented as Figure 5.10. The pH of Step I of the conjugation reaction is maintained between pH 6.8-6.9, ensuring a significant portion of the n-terminal primary amines are deprotonated and can react with DMMA, thus preventing subsequent reaction with SPDP. However, the reaction pH is significantly below the pKa of the primary amine residue at B29-Lysine, ensuring that there will be little to no reaction at that site.

After successfully blocking the n-terminal primary amine residues of insulin, Step II involves raising the reaction pH and reacting the remaining primary amine located at B29-Lysine with SPDP. At the completion of Step I of the insulin-transferrin conjugation reaction, insulin had been modified by conjugating DMMA molecules to A1-Glycine and B1-Phenylalanine (Insulin-DMMA). With the n-terminal primary amines effectively "blocked", the pH of the solution was raised to 9.0 to allow a significant number of the amines at B29-Lysine to become deprotonated and able to react. The reaction pH was maintained within the range of 8.8-9.0 during the addition and reaction of SPDP to Insulin-DMMA. SPDP will react with any primary amine which has not previously been conjugated to DMMA, forming another modified insulin intermediate (Insulin-PDP). The PDP groups on insulin still possess free 2-pyridyldithio groups, which are reactive to sulfohydryl groups. The other half of the bioconjugate, transferrin, will be modified to contain sulfohydryl groups.

Step III of the insulin-transferrin conjugation reaction involves modification of transferrin, a second protein implemented to improve insulin transport. The objective in Step III is to modify transferrin in such a way as to add sulfohydryl groups (-SH), making it reactive to Insulin-PDP. Sulfohydryl groups were added by the addition and subsequent reduction of SPDP, the same protein crosslinker used in previous steps. Due mostly to the size of insulin (5.8 kDa) relative to transferrin (80 kDa), conjugation at any primary amine would most likely not hinder bioactivity. Since there is no need to perform site-specific conjugation, the pH is not controlled as SPDP is added to transferrin. At the conclusion of the reaction, a modified transferrin is formed which contains PDP groups (Transferrin-PDP), similar to Insulin-PDP formed at the conclusion of Step II. To reduce Transferrin-PDP, the reducing agent DTT is added to cleave the disulfide bonds and create sulfohydryl groups. DTT is added to the solution at a concentration low enough to prevent cleavage of the internal disulfide bonds of the transferrin molecule. After reduction with DTT, Transferrin-SH is formed and is now reactive with PDP-modified proteins.

Step IV of the insulin-transferrin conjugation reaction is the final step and involves combination of both modified proteins in an effort to form a single conjugate. For the final reaction, approximately two moles of Insulin-PDP were added for every one mole of Transferrin-SH. During the reaction, the release of 2-pyridinethione relative to transferrin was monitored to prevent the addition of too many insulin molecules to each transferrin molecule. Typically, the reaction was stopped by the addition of NEM within 90 minutes to reduce bulkiness of the conjugate. If the conjugate were to become too large, the transport properties would be greatly affected and diffusion within the polymer network could be greatly reduced, thus adversely affecting loading and release characteristics. Also, Shah and Shen [8] showed that insulin-transferrin conjugates with too many insulin molecules attached could not be effectively transported across a Caco-2 cell monolayer using a transcellular mechanism. The final product of Step IV of the conjugation reaction is a newly formed insulin-transferrin conjugate with on average 2 insulin molecules attached to each transferrin molecule.

5.3.2 Synthesis of Calcitonin-Transferrin Conjugates

Calcitonin was conjugated to transferrin to form active bioconjugates using the protein crosslinker SPDP and the conjugation scheme first outlined by Carlsson et al [14]. SPDP is a useful crosslinker for forming hetero conjugates because of its heterobifunctional characteristics, which means it can react with two different types of functional groups. As demonstrated in Figure 5.1, the region of the n-hydroxy succinimide (NHS) ester of SPDP can react with primary amine groups. This reaction occurs by nucleophilic attack from the amine nitrogen to the carbonyl group and the result is a modified amine group which now contains a reactive 2-pyridyldithio group. The free 2-pyridyldithio group provides the other half of the reactivity of SPDP and is reactive with sulfohydryl groups. By using SPDP, it is possible to crosslink a protein with primary amine groups with a different protein which contains sulfohydryl groups. This characteristic of SPDP ensures the formation of heteroconjugates, or conjugates

consisting of two different proteins. At the same time, because SPDP does not have two amine reactive sites or two sulfohydryl reactive sites, the use of SPDP excludes formation of homoconjugates, or conjugates consisting of multiple molecules of the same protein.

The result of binding two proteins using SPDP is conjugation by disulfide linkages. The method of protein conjugation by disulfide linkages is especially useful considering tendency of disulfide bonds to cleave within blood plasma [19]. Due to the instability of disulfide bonds in blood plasma, the conjugated proteins may be cleaved once they reach systemic circulation, thus releasing free calcitonin [8, 20, 21].

Step I of the calcitonin-transferrin conjugation reaction involves the reaction of calcitonin with SPDP to form a modified protein with PDP groups attached (Calcitonin-PDP). In contrast to the insulin-transferrin conjugation reaction, the initial step of blocking reactive amines relating to protein activity with DMMA was not taken for this conjugation reaction. There is no known adverse effect to the activity of calcitonin due to large molecule conjugation at any specific site. Therefore, conjugation of transferrin to calcitonin does not have to be site-specific and SPDP can react freely with any primary amine group on calcitonin. Thus there is no need for rigid control of reaction pH, allowing the majority of the amine groups to react with SPDP. The intermediate product from Step I is Calcitonin-PDP.

Step II of the calcitonin-transferrin conjugation reaction involves initial modification of transferrin, a transporter protein intended to improve calcitonin transport. Step II is very similar to Step I in that SPDP is used to add PDP groups to modify a protein. However, Step II involves modifying transferrin which will later be reacted with modified Calcitonin-PDP. Due mostly to the size of calcitonin (3.4 kDa) relative to transferrin (80 kDa), conjugation at any primary amine would most likely not hinder bioactivity or reduce affinity for the transferrin receptor. Since there is no need to perform site-specific conjugation, the pH is not controlled as SPDP is added to transferrin. At the conclusion of the reaction, a modified transferrin is formed which

contains PDP groups (Transferrin-PDP), similar to Calcitonin-PDP formed at the conclusion of Step I.

Step III of the calcitonin-transferrin conjugation reaction involves the reduction of Transferrin-PDP to form a modified transferrin with sulfohydryl groups (Transferrin-SH). The newly modified Transferrin-SH is reactive with the free 2-pyridyldithio groups on Calcitonin-PDP. Sulfohydryl groups can be formed by the reduction of already existing PDP groups on the transferrin molecule. To reduce Transferrin-PDP, the reducing agent DTT is added to cleave the disulfide bonds and create sulfohydryl groups. DTT is added to the solution at a concentration low enough to prevent cleavage of the internal disulfide bonds of the transferrin molecule. After reduction with DTT, Transferrin-SH is formed and is now reactive with PDP-modified proteins.

Step IV of the calcitonin-transferrin conjugation reaction is the final step and involves combination of both modified proteins in an effort to form a single conjugate. For the final reaction, approximately two moles of Calcitonin-PDP were added for every one mole of Transferrin-SH. During the reaction, the release of 2-pyridinethione relative to transferrin was monitored to prevent the addition of too many calcitonin molecules to each transferrin molecule. The reaction was typically stopped by the addition of NEM within 90 minutes to reduce bulkiness of the conjugate and to minimize complex aggregation. If the conjugate were to become too large, the transport properties would be greatly affected and diffusion within the polymer network could be greatly reduced, thus adversely affecting loading and release characteristics. The final product of Step IV of the conjugation reaction is a newly formed calcitonin-transferrin conjugate with on average 2 calcitonin molecules attached to each transferrin molecule.

5.3.3 Analysis of Protein Transporter Conjugates

At the completion as well as during the insulin-transferrin and calcitonin-transferrin conjugation reactions, specific analyses were performed to quantify the amount of conjugate produced as well as verify the combination of the two proteins.

After addition of SPDP to each protein, PDP:Protein ratios were calculated using Equation 1. Also, at the completion of each conjugation reaction, the final product was analyzed using HPLC to verify the conjugation process as well as to quantify the absolute yield of the reaction.

PDP Modification Analysis by UV Spectroscopy: The addition of SPDP to insulin in Step II of the insulin-transferrin conjugation reaction as well as the addition of SPDP to transferrin in Step III of the insulin-transferrin conjugation reaction and Step II of the calcitonin-transferrin conjugation reaction was analyzed using UV spectroscopy. After addition of SPDP to the respective proteins, a small aliquot of the product was reduced with 25 mM DTT to release the chromophore 2-pyridinethione. The DTT was introduced to the solution at a concentration low enough to only break the disulfide bonds on the PDP groups and not cleave the internal disulfide bonds which may exist within the protein structure. The absorbance of each solution was measured at 280 nm and 343 nm and the PDP:Protein ratio was calculated using Equation 1 and same molar extinction coefficients given previously. The PDP:Insulin ratio determined after Step II of the insulin-transferrin conjugation reaction was found to be 1.09. Under ideal conditions, the primary amines located at A1-Glycine and B1-Phenylalanine would be blocked by DMMA, leaving only one possible conjugation site for SPDP at B29-Lysine and giving an ideal PDP:Insulin ratio of 1.00. An experimental PDP:Insulin ratio of 1.09:1 means that Step I and Step II were carried out properly, with only a small portion of insulin molecules having more than one PDP group. The experimental PDP:Transferrin ratio for both conjugation reactions was found to be approximately 7.5:1. Assuming all PDP groups on transferrin are reduced to sulfohydryl groups, the existence of over seven possible conjugation sites provides opportunity for insulin molecules to successfully bind to transferrin. In comparison to insulin, the amount of PDP groups on calcitonin is less important due to the lack of requirements for site-specific conjugation. Therefore, the PDP:Calcitonin ratio was not determined.

Insulin-Transferrin Conjugate Verification Analysis by HPLC: Synthesized insulin-transferrin conjugates were examined by HPLC after purification and dilution. The verification of a successful conjugation reaction is indicated by a significant shift from the typical transferrin HPLC peak. The HPLC chromatogram for the insulin-transferrin conjugate is shown as Figure 5.11. As evident in the chromatogram, the HPLC analysis of the insulin-transferrin conjugate shows a peak that elutes a full minute later than the unmodified transferrin peak. The shift in elution time indicates a significant structure modification as to strengthen the interaction with the separations column, forcing it to elute later. Also, the shift can also indicate an increase in size, causing the conjugate to elute later from the column than unmodified transferrin. Simple modification of transferrin by adding PDP groups or reducing them to –SH groups does not result in any noticeable shift. Only after the addition of insulin to the transferrin molecules is such a shift observed. While the HPLC analysis does not specifically determine the number of insulin molecules attached to each transferrin molecule, it does confirm the combination of insulin and transferrin molecules into a single conjugate.

Calcitonin-Transferrin Conjugate Verification Analysis by HPLC: HPLC analysis was used to verify the synthesis of calcitonin-transferrin conjugates after their purification and necessary dilution. Similar to the insulin-transferrin conjugation reaction, the verification of a successful conjugation reaction should be indicated by a significant shift from the typical transferrin HPLC peak. The HPLC chromatogram for the calcitonin-transferrin conjugate is shown as Figure 5.12. The chromatogram shows a shift of over one minute from unmodified transferrin to the calcitonin-transferrin conjugate. Such a significant shift in elution time of the conjugate relative to transferrin means that the transferrin is undergoing a significant change to its size and structure. As the transferrin molecule grows in size from the addition of calcitonin molecules and the surface properties change as well, the interaction of the conjugate with the column will change and cause it to elute later. In fact, the unmodified transferrin peak shown may also be

partially attributed to unreacted Transferrin-PDP or Transferrin-SH. This means that modification of large proteins such as transferrin with small groups such as PDP groups or –SH groups will not noticeably change the elution peak. Therefore, the significant shift in elution time confirms the addition of another large molecule such as insulin to transferrin to form a single conjugate.

Conjugation Reaction Yield Quantification by HPLC: The final products from both conjugation reactions were analyzed by HPLC to verify the reaction was successful. The same analysis can also be used to quantify the amount of conjugate synthesized in each reaction. By determining the concentration of the sample using HPLC, the amount of conjugate can be back-calculated and compared to the initial amounts of reagents used to determine a reaction yield. The reaction yields for both conjugation reactions are shown as Figure 5.13. The insulin-transferrin conjugation reaction achieved the higher overall yield of the two reactions. Since the protein reactivities with SPDP are fairly similar and the transferrin portion of the reaction is the same, the difference can most readily be attributed to the differences in solubility. Neither insulin nor calcitonin will dissolve in neutral PBS buffer. Insulin dissolution requires the addition of acid to lower the pH and dissolving calcitonin requires making the solution 5% acetic acid. Based on the overall yields, one can observe that insulin most likely dissolves more readily than calcitonin using the protocols outlined earlier in this chapter. However, both overall reaction yields are relatively high, indicating a significant amount of conjugate is being produced. Due to the high expense of the proteins involved, a significant yield is important and necessary to designing a practical and useful protein-transporter conjugate for therapeutic applications.

5.4 Conclusions

Protein-transporter conjugates consisting of therapeutic proteins bound to transporter proteins were designed and investigated. Insulin-transferrin and calcitonin-

transferrin conjugates were synthesized using the protein crosslinker SPDP and the bound proteins are connected by disulfide linkages. Each conjugation reaction was analyzed using UV spectroscopy, HPLC for conjugate verification, and HPLC for quantification of overall reaction yield. Based on the analyses, it was shown that intact conjugates were indeed synthesized in a controlled, repeatable manner which gave significant reaction yields. The conjugates synthesized and investigated in this chapter will provide a greater specificity for drug uptake as well as provide potential for increased transport. The conjugates will be incorporated into the polymer hydrogel carriers explored in Chapter 4 and the *in vitro* loading and release characteristics will be examined along with the hydrogel systems optimized in the following chapters.

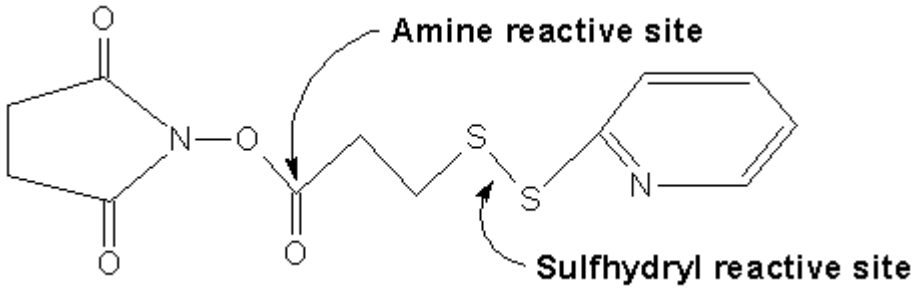

Figure 5.1 Structure and reactive sites of succinimidyl 3-(2-pyridyldithio) propionate (SPDP).

SPDP is a cleavable heterobifunctional crosslinker for conjugating proteins. Contains an amine-reactive N-hydroxysuccinimide (NHS) ester, and sulfohydryl reactive pyridyldithio groups.

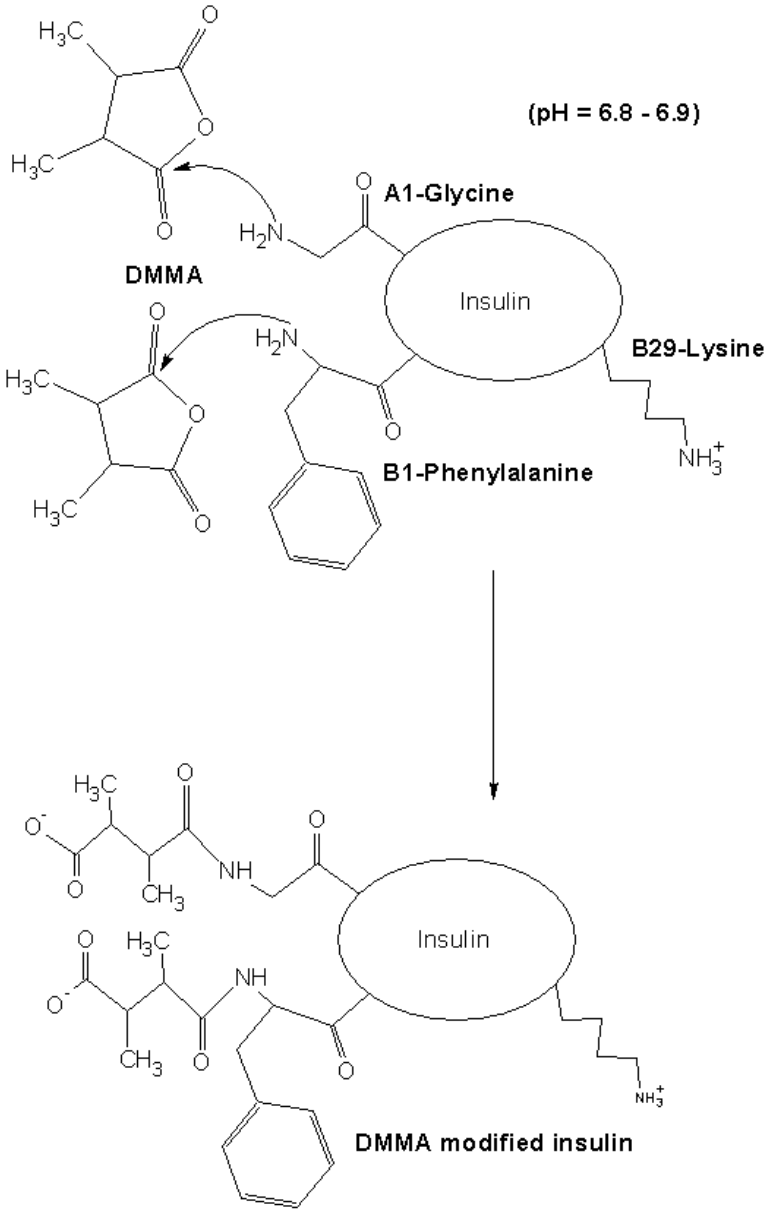

Figure 5.2 Step I of insulin-transferrin conjugation reaction

In this step, the primary n-terminal amines of insulin are "blocked" with DMMA to prevent transporter conjugation. Reaction carried out at pH of 6.8-6.9 to ensure n-terminal amines are deprotonated and will react while the amine group at B29-Lysine is protonated and unreactive.

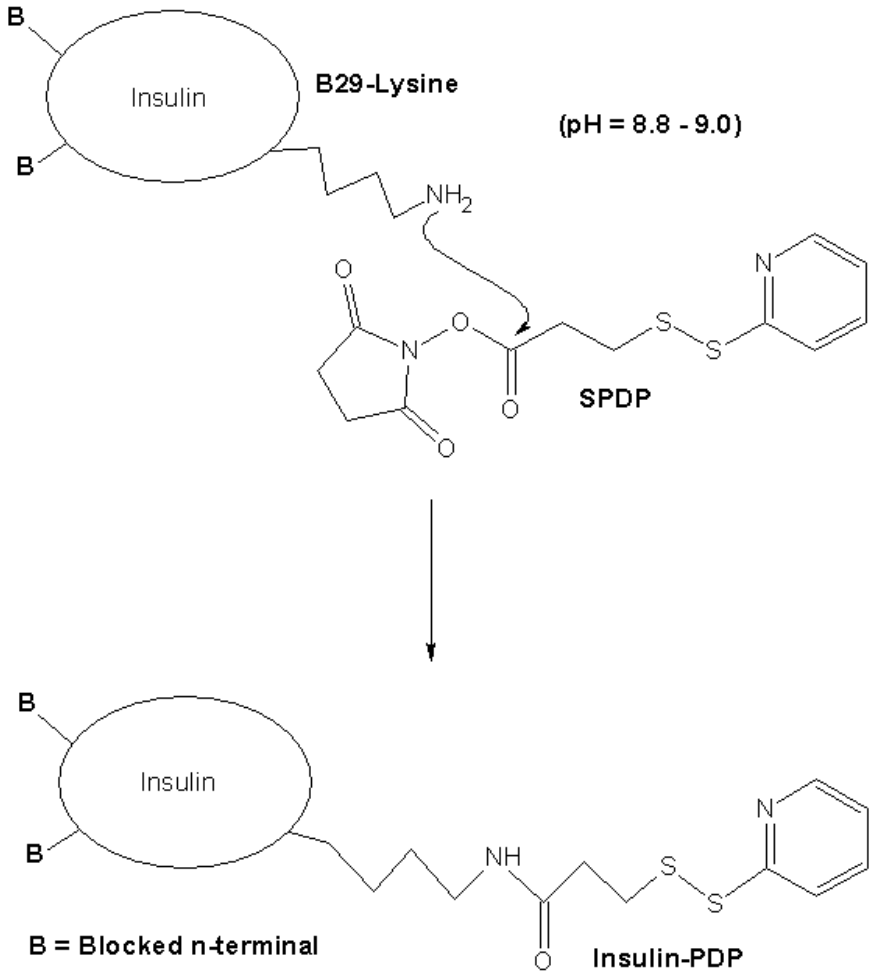

Figure 5.3 Step II of insulin-transferrin conjugation reaction

In this step, the remaining primary amine at the B29-Lysine position is reacted with the crosslinker SPDP. Reaction carried out at pH of 8.8-9.0 to ensure the primary amine at B29-Lysine is deprotonated and will react.

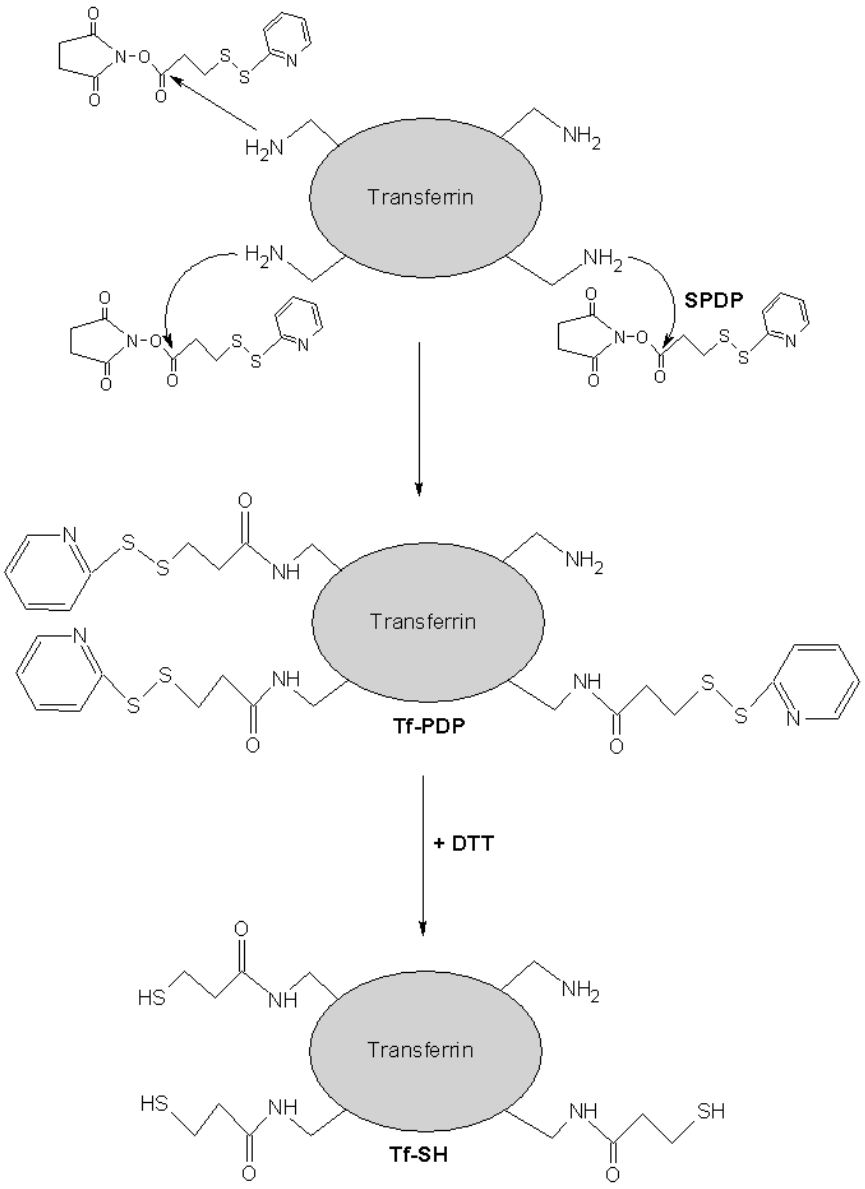

Figure 5.4 Step III of insulin-transferrin conjugation reaction

In this step, the primary amines of transferrin are reacted with SPDP to form Tf-PDP. Transferrin-PDP is reduced with DTT to form sulfohydryl groups on the modified transferrin.

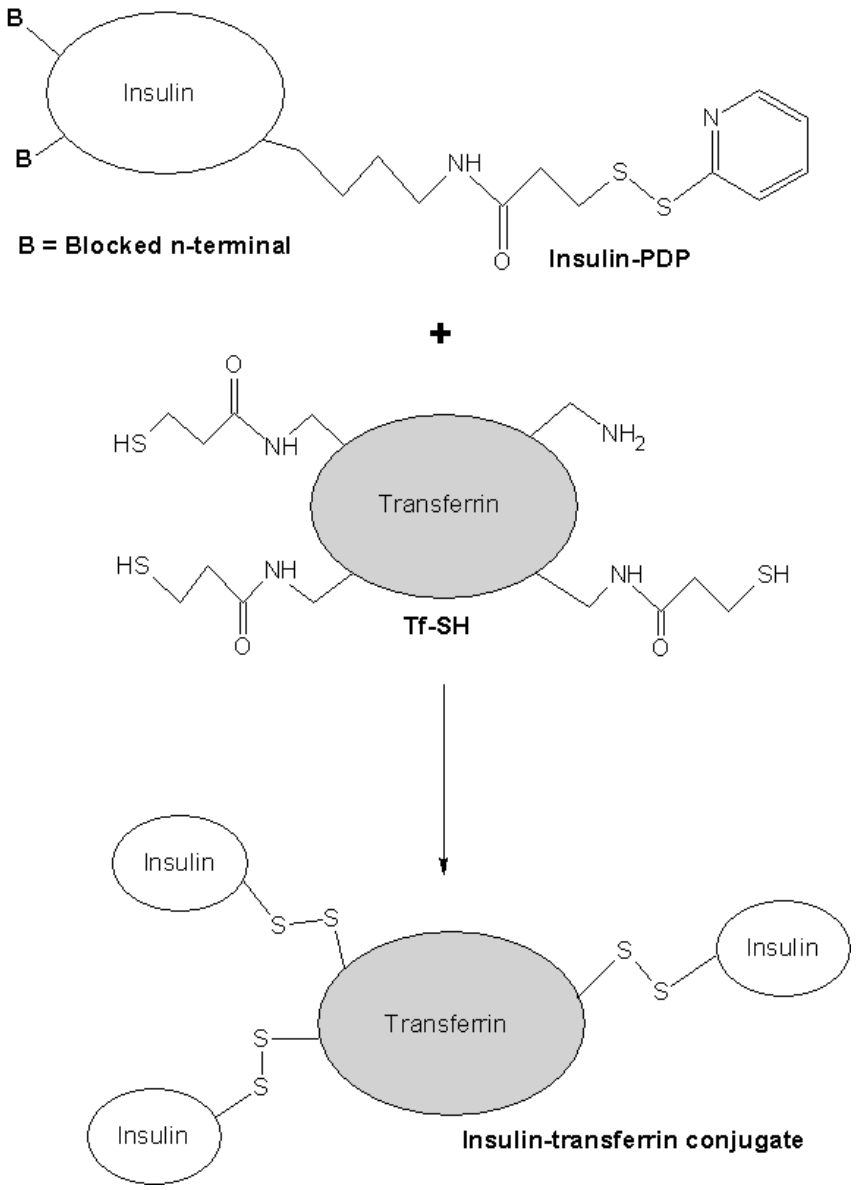

Figure 5.5 Step IV of insulin-transferrin conjugation reaction

In this step, the modified transferrin and modified insulin are combined to form an insulin-transferrin conjugate bound by cleavable disulfide linkages.

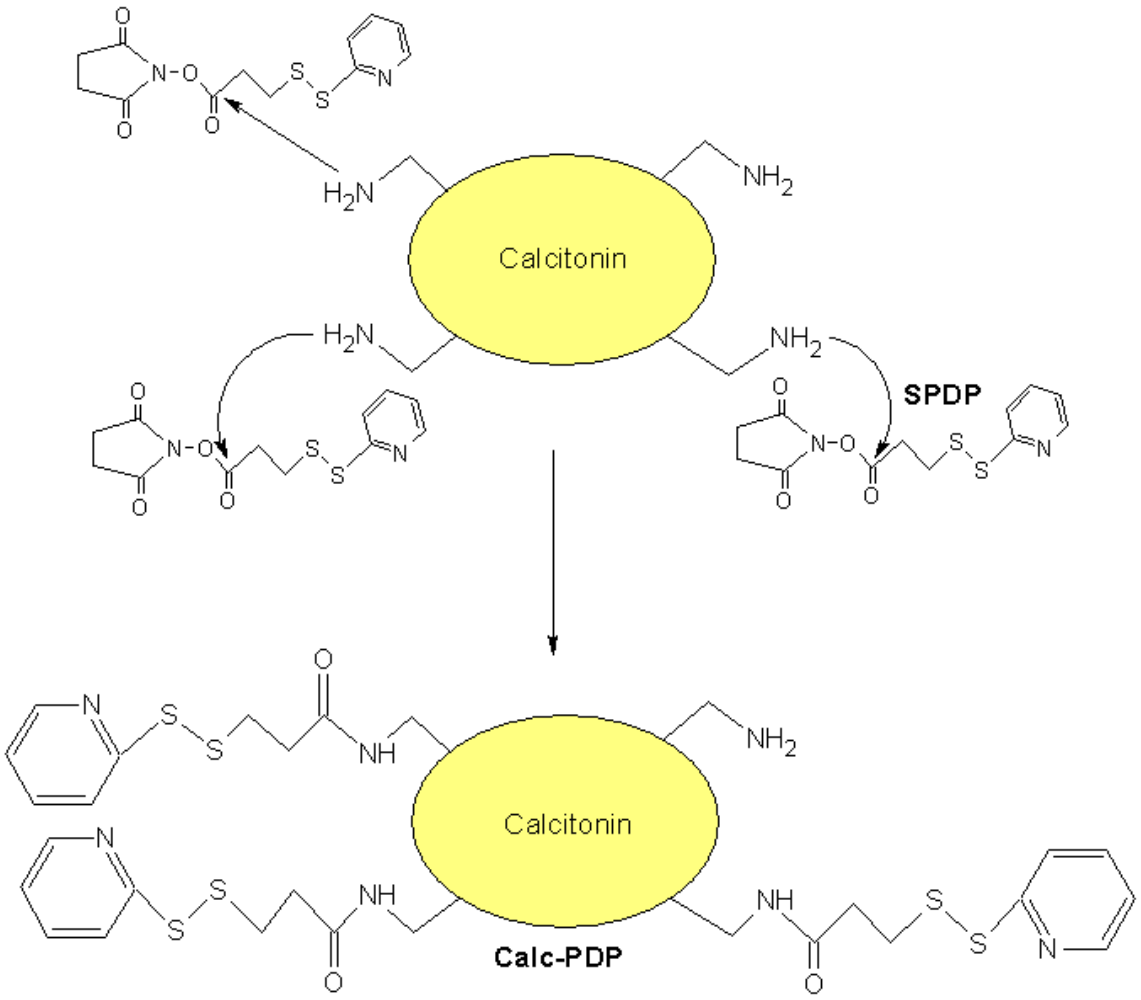

Figure 5.6 Step I of calcitonin-transferrin conjugation reaction

In this step, the primary amines of calcitonin are reacted with SPDP to form Calc-PDP.

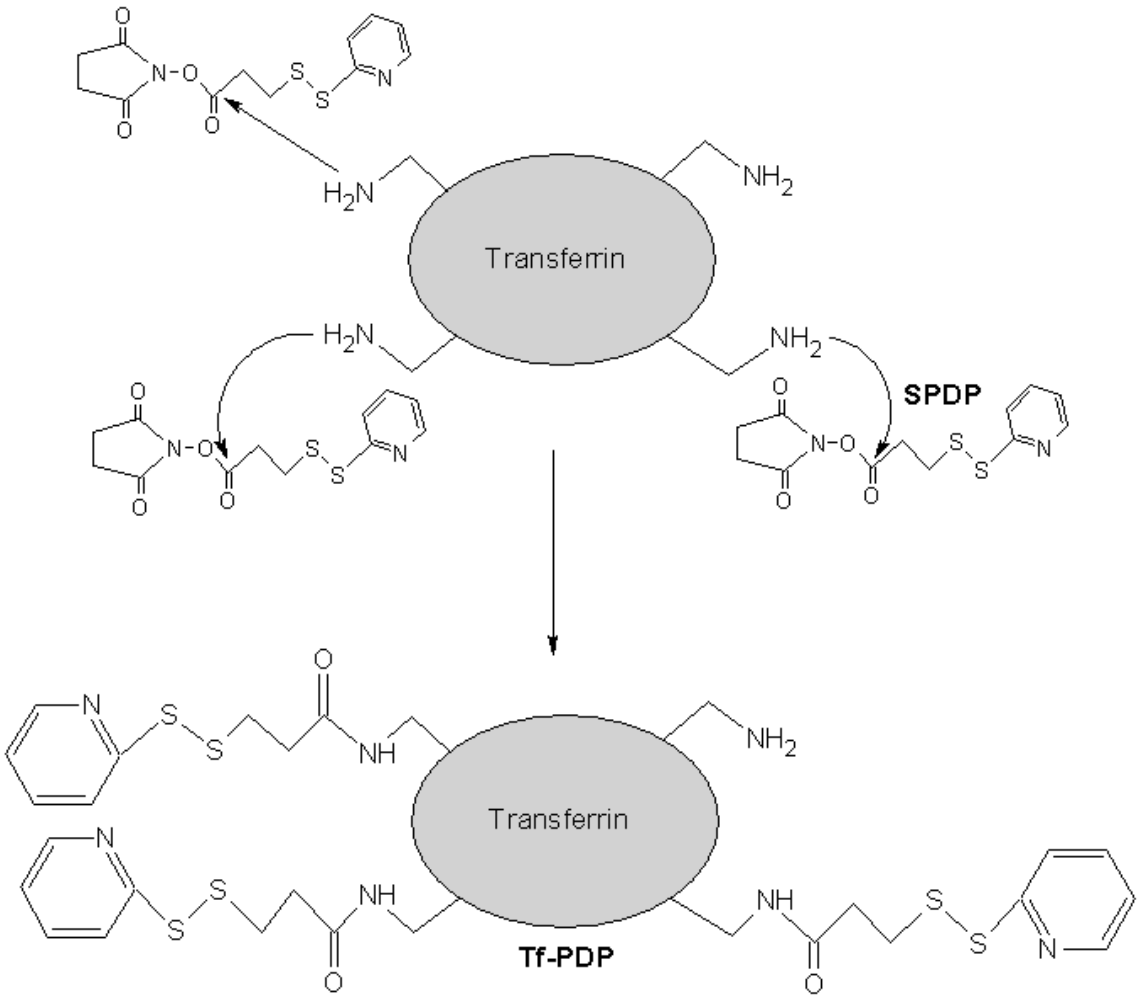

Figure 5.7 Step II of calcitonin-transferrin conjugation reaction

In this step, the primary amines of transferrin are reacted with SPDP to form Tf-PDP.

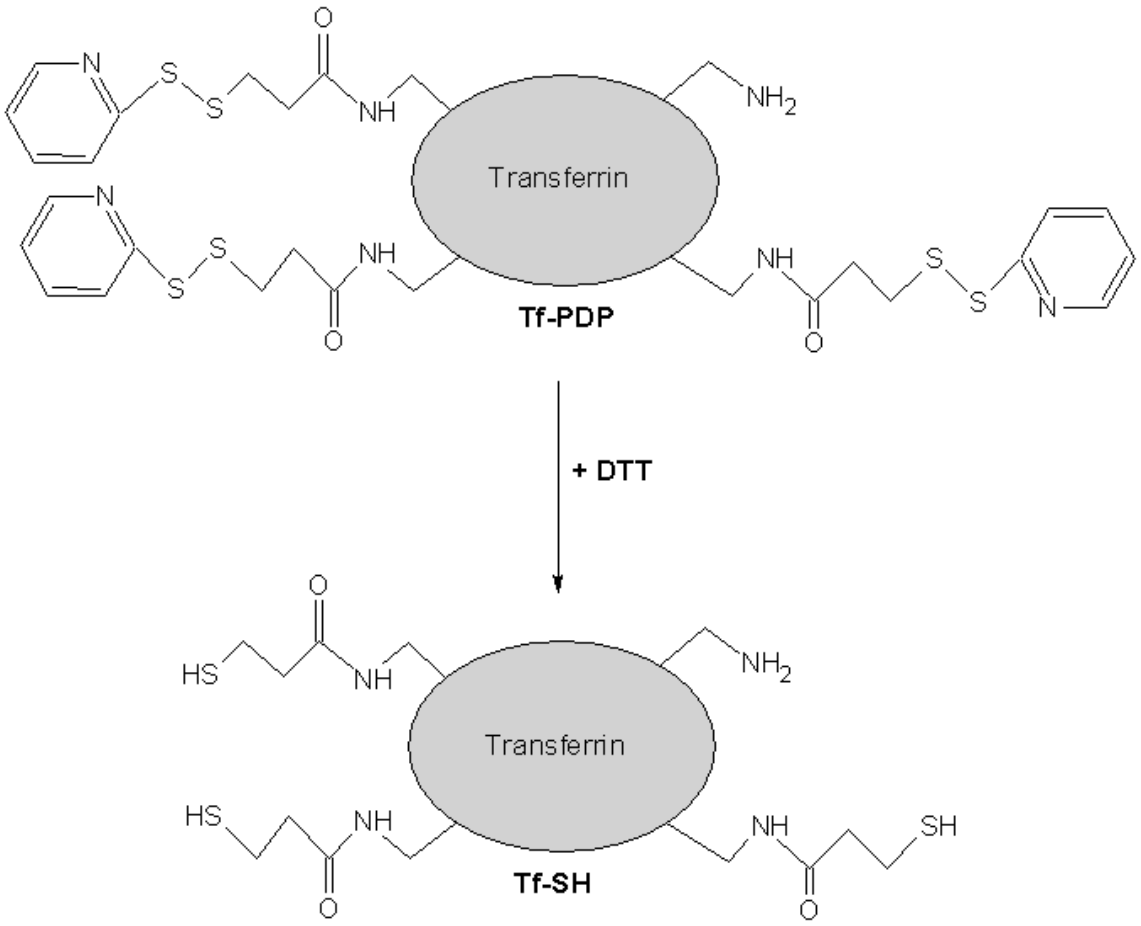

Figure 5.8 Step III of calcitonin-transferrin conjugation reaction

In this step, transferrin-PDP is reduced with DTT to form sulfohydryl groups on the modified transferrin (Tf-SH).

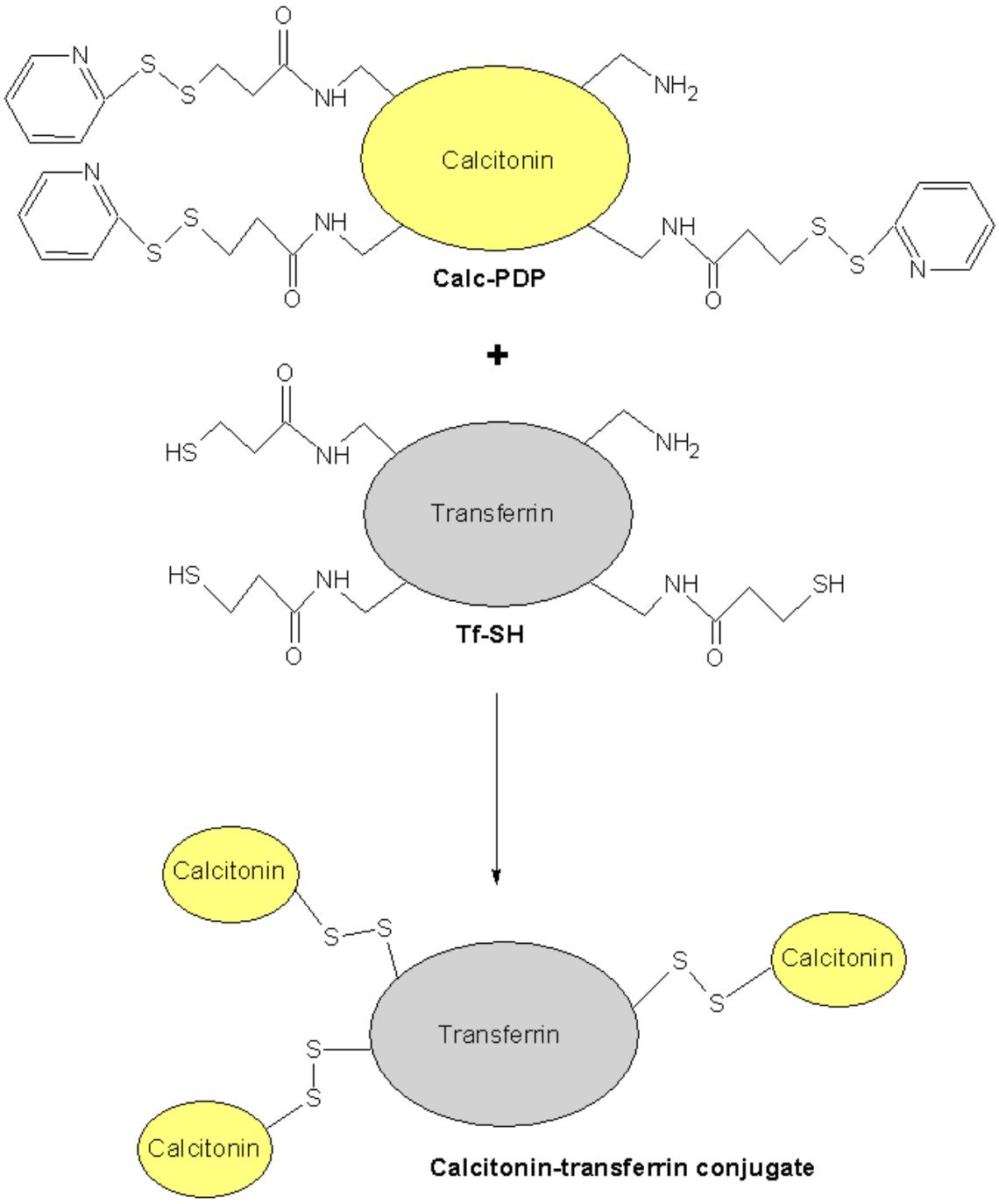

Figure 5.9 Step IV of calcitonin-transferrin conjugation reaction

In this step, the modified transferrin and modified calcitonin are combined to form a calcitonin-transferrin conjugate bound by cleavable disulfide linkages.

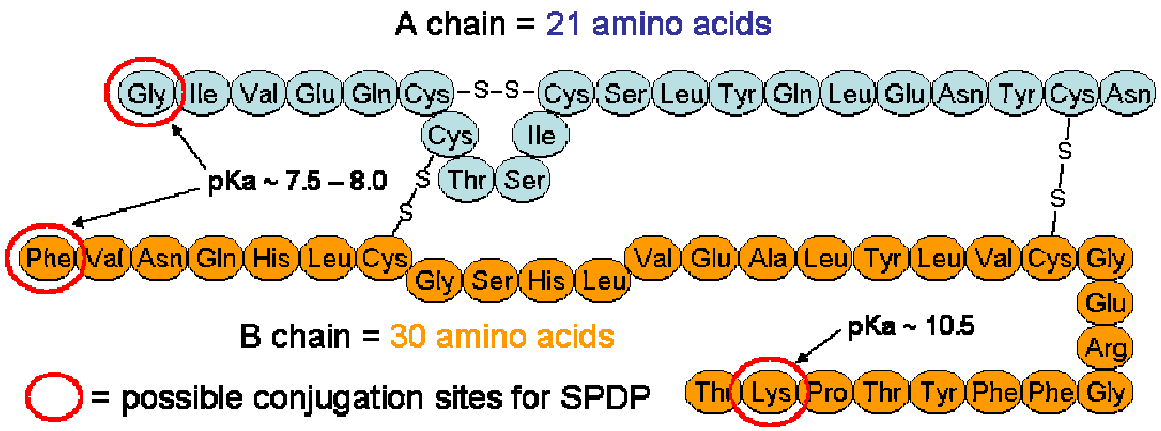

Figure 5.10 Structure and conjugation reactivity of insulin.

Insulin contains two chains of amino acids connected by disulfide linkages. A1-Glycine, B1-Phenylalanine, and B29-Lysine are possible conjugation sites if using the heterobifunctional crosslinker SPDP. B29-Lysine has a significantly different pKa than A1-Glycine and B1-Phenylalanine, allowing for the possibility of site-specific conjugation.

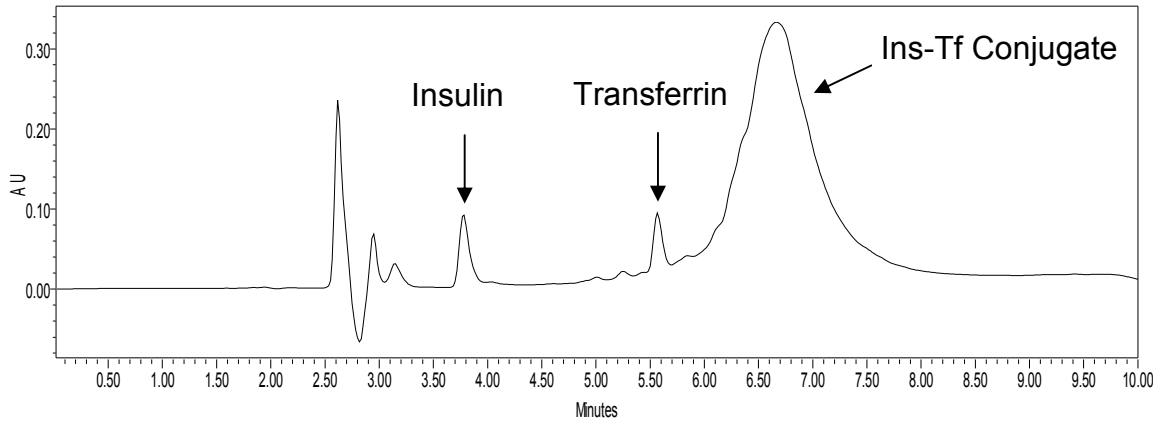

Figure 5.11 HPLC chromatogram showing elution times for insulin, transferrin, and the insulin-transferrin conjugate.

The chromatogram was the result of an HPLC analysis following the final step of the insulin-transferrin conjugation reaction.

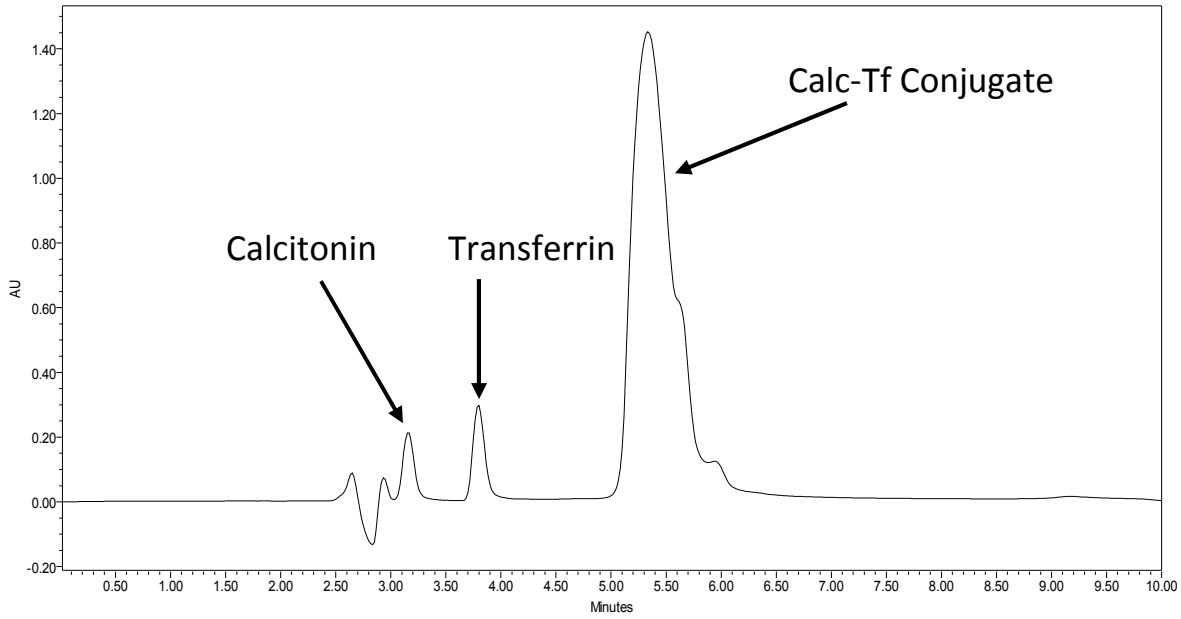

Figure 5.12 HPLC chromatogram showing elution times for calcitonin, transferrin, and the calcitonin-transferrin conjugate.

The chromatogram was the result of an HPLC analysis of the final product following the final step of the calcitonin-transferrin conjugation reaction.

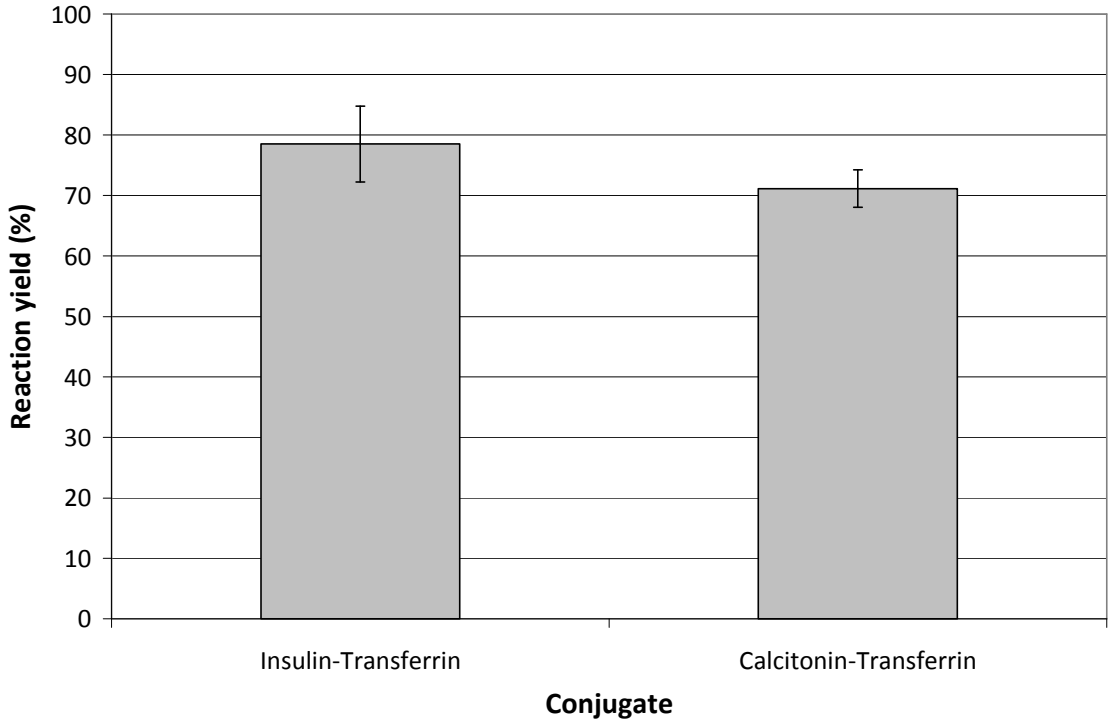

Figure 5.13 Average reaction yields for both the insulin-transferrin conjugation reaction and the calcitonin-transferrin conjugation reaction.

REFERENCES

1. Fasano, A., *Novel approaches for oral delivery of macromolecules.* J. Pharm. Sci., 1998. **87**(11): p. 1351-1356.

2. Yamagata, T., Morishita, M., Kavimandan, N.J., Nakamura, K., Fukuoka, Y., Takayama, K., and Peppas, N.A., *Characterization of insulin protection properties of complexation hydrogels in gastric and intestinal enzyme fluids.* J. Control. Release, 2006. **112**(3): p. 343-349.

3. Peppas, N.A., and Sahlin, J.J., *Hydrogels as mucoadhesive and bioadhesive materials: a review.* Biomaterials, 1996. **17**(16): p. 1553-1561.

4. Kan, K.S., and Coleman, R., *The calcium ionophore A23187 increases the tight-junctional permeability in rat liver.* Biochem. J., 1988. **256**(3): p. 1039-1041.

5. des Rieux, A., Fievez, V., Garinot, M., Schneider, Y., and Préat, V., *Nanoparticles as potential oral delivery systems of proteins and vaccines: A mechanistic approach.* J. Control. Release, 2006. **116**(1): p. 1-27.

6. Hinds, K.D., and Kim, S.W., *Effects of PEG conjugation on insulin properties.* Adv. Drug Deliver. Rev., 2002. **54**(4): p. 505-530.

7. Blanchette, J., Kavimandan, N.J., and Peppas, N.A., *Principles of transmucosal delivery of therapeutic agents.* Biomed. Pharmacother., 2004. **58**(3): p. 142-151.

8. Shah, D., and Shen, W.C., *Transcellular delivery of an insulin-transferrin conjugate in enterocyte-like Caco-2 cells.* J. Pharm. Sci., 1996. **85**: p. 1306-1311.

9. Widera, A., Norouziyan, F., and Shen, W.C., *Mechanisms of TfR-mediated transcytosis and sorting in epithelial cells and applications toward drug delivery.* Adv. Drug Deliver. Rev., 2003. **55**(11): p. 1439-1466.

10. Russell-Jones, G.J., Westwood, S.W., and Habberfield, A.D., *Vitamin B12 Mediated Oral Delivery Systems for Granulocyte-Colony Stimulating Factor and Erythropoietin.* Bioconjugate Chem., 1995. **6**(4): p. 459-465.

11. Huebers, H.A., Csiba, E., Huebers, E., and Finch, C.A., *Competitive advantage of diferric transferrin in delivering iron to reticulocytes.* P. Natl. Acad. Sci.-Biol., 1983. **80**(1): p. 300-304.

12. Jones, A.T., Gumbleton, M., and Duncan, R., *Understanding endocytic pathways and intracellular trafficking: a prerequisite for effective design of advanced drug delivery systems.* Adv. Drug Deliver. Rev., 2003. **55**(11): p. 1353-1357.

13. Azari, P. R., and Feeney, R. E., *Resistance of Metal Complexes of Conalbumin and Transferrin to Proteolysis and to Thermal Denaturation.* J. Biol. Chem., 1958. **232**(1): p. 293-302.

14. Carlsson, J., Drevin, H. and Axen, R., *Protein thiolation and reversible protein-protein conjugation. N-Succinimidyl 3-(2-pyridyldithio)propionate, a new heterobifunctional reagent.* Biochem. J., 1978. **173**: p. 723-737.

15. Xia, C.Q., Wang, J., and Shen, W.C., *Hypoglycemic Effect of Insulin-Transferrin Conjugate in Streptozotocin-Induced Diabetic Rats.* J. Pharmacol. Exp. Ther., 2000. **295**(2): p. 594-600.

16. Faulstich, H., Zobeley, S., Heintz, D., and Drewes, G., *Probing the phalloidin binding site of actin.* FEBS Lett., 1993. **318**(3): p. 218-222.

17. Kavimandan, N.J., Losi, E., Wilson, J.J., Brodbelt, J.S., and Peppas, N.A., *Synthesis and Characterization of Insulin-Transferrin Conjugates.* Bioconjugate Chem., 2006. **17**(6): p. 1376-1384.

18. Stuchbury, T., Shipton, M., Norris, R., Malthouse, J.P., Brocklehurst, K., Herbert, J.A., and Suschitzky, H., *A reporter group delivery system with both absolute and selective specificity for thiol groups and an improved fluorescent probe containing the 7-nitrobenzo-2-oxa-1,3-diazole moiety.* Biochem. J., 1975. **151**: p. 417-432.

19. Melton, R.G., and Sherwood, R.F., *Antibody-Enzyme Conjugates for Cancer Therapy.* J. Natl. Cancer Inst., 1996. **88**(3-4): p. 153-165.

20. Saito, G., Swanson, J.A., and Lee, K., *Drug delivery strategy utilizing conjugation via reversible disulfide linkages: role and site of cellular reducing activities.* Adv. Drug Deliver. Rev., 2003. **55**(2): p. 199-215.

21. Thorpe, P.E., Wallace, P.M., Knowles, P.P., Relf, M.G., Brown, A.N.F., Watson, G.J., Knyba, R.E., Wawrzynczak, E.J., and Blakey, D.C., *New Coupling Agents for the Synthesis of Immunotoxins Containing a Hindered Disulfide Bond with Improved Stability in Vivo.* Cancer Res., 1987. **47**(22): p. 5924-5931.

22. Lindsay, D.G., and Shall, S., *The acetylation of insulin.* Biochem. J., 1971. **121**(5): p. 737-745.

23. Mohammed, A., and Dent, A., *Bioconjugation: protein coupling techniques for the biomedical sciences*. Grove's Dictionaries. 1998: New York.

CHAPTER 6

LOADING AND RELEASE CHARACTERISTICS OF INSULIN-TRANSFERRIN CONJUGATES FROM COMPLEXATION HYDROGELS

6.1 Introduction

Before administration to human or animal subjects, newly synthesized drugs and polymer systems for oral delivery must first be combined and tested in the laboratory to determine the interactions and how they relate to overall efficacy. Specifically, the protein of interest can be loaded into the hydrogel carrier using laboratory procedures and subsequently released in conditions which are designed to mimic physiological conditions.

The simulated conditions used in release studies can mimic important stages of the transit through the GI tract such as the periods spent in the stomach or small intestine. The results from these loading and release studies are valuable to understanding the effect that the hydrogel carrier has on the encapsulated protein as well as obtaining insight on how to improve the system to achieve optimal efficacy.

After selecting an optimal system design for the loading and release of the specific protein, the formulation can be then tested using cell culture models to determine interaction with the cell monolayer. While synthesis of polymer carriers and protein bioconjugates is based on theoretical predictions, loading and release studies on these entities provide initial insight into properties relating to actual performance of the delivery system.

In the previous chapter, insulin was bound to transferrin to create a protein-transporter conjugate designed to improve specificity of uptake as well as overall transport. The major advantage of the addition of the transferrin molecule to the therapeutic insulin protein is utilized during the interaction of the protein with the epithelial cell monolayer lining the small intestine. However, in terms of loading the

conjugate into the polymer carrier, transit through the GI tract, and eventually release in the small intestine, the formation of a conjugate has little strategic utility. In fact, relative to unmodified insulin, the use of a much larger conjugate molecule can possibly hinder diffusion, thus adversely affecting loading and release characteristics. Loading and release studies on the insulin-transferrin conjugate are explored in this chapter to determine the existence of a possible detrimental effect of the conjugate on system characteristics as well as to alter the polymer carrier in such a way as to minimize this effect and to maximize potential bioavailability.

The process of loading refers to the incorporation of the conjugate into or onto the polymer component to form a single system. In general, there are many different ways in which a molecule can be loaded into the system. In some systems, drugs are often covalently bound to polymers to better take advantage of improved properties such as improved transport and better stealth characteristics [1-3]. In systems with a larger polymer component, such as a carrier, the conjugate could still be covalently bound but is often times loaded into the polymer using diffusion. However, once inside, it is extremely limited diffusion which keeps the conjugate molecule contained within the carrier [4-6]. Because the diffusion characteristics of the conjugate within the polymer network can be significantly changed using pH-responsive hydrogel carriers, the loading performed in this chapter is based on diffusion and occurs through equilibrium partitioning.

Release of the encapsulated therapeutic could also happen in a number of different ways. Typically, release is simply the reverse process of the loading mechanism. In the case of covalently bound therapeutic drugs, the bond is typically broken by the presence of certain conditions or molecules and the drug can be released freely. In the case of systems in which the drug was loaded using diffusion, the release typically occurs in one of two ways. The mechanism of release can be initiated from a contraction of the polymer carrier, resulting in a burst release of loaded therapeutics [7-10]. The mechanism of release can also be triggered from an expansion of the polymer

system, increasing diffusion in and out of the system and allowing the therapeutic entity to diffuse out. In this chapter, release of insulin-transferrin conjugates is triggered by an expansion of the hydrogel carrier and subsequent increase in diffusive properties of the conjugate.

The loading and release characteristics of insulin-transferrin conjugates in complexation hydrogels are affected by a number of factors inherent to the system design. A primary concern in designing a system to have desirable loading and release properties is selecting materials while understanding that possible interactions may occur between the polymer and the conjugate. For example, a common interaction which has a profound effect on loading and release is the surface charge interaction of both the polymer and the conjugate. The forces which occur due to opposite charge attraction or like charge repulsion will have a significant effect on the rate at which the conjugate loads and releases as well as how much is loaded and released. Also important in selecting materials for use is the hydrophilicity of both materials. Because loading and release is performed in solution, the respective hydrophilicities of both the polymer and conjugate play a significant role in whether the conjugate can load into the polymer properly.

Another set of factors can influence the diffusion coefficient of the insulin-transferrin conjugate into and out of the polymer network, greatly affecting loading and release. A major factor affecting diffusion within the system is the mesh size of the polymer network. The mesh size refers to the average space between crosslinks of the polymer network, or how much space there is for the conjugate to diffuse. The mesh size of the polymer is a direct function of the materials used and synthesis parameters of the polymer formation and can be easily controlled.

Another factor affecting diffusion is the size of the conjugate molecule itself. The larger the molecule, the more difficult it is for it to diffuse through a given mesh size. While the size of the insulin-transferrin conjugate is mostly limited by the choice of therapeutic and transporter proteins, it can be somewhat controlled by limiting the

number of insulin molecules that attach to each transferrin molecule. The insulin to transferrin ratio can be easily controlled by using specific protocol during the conjugate synthesis.

The factors which affect loading and release of a system can be controlled by selecting the correct design specifications. For example, the diffusion within the system can be controlled by selecting a number of specifications. Diffusion of the insulin-transferrin conjugate within the system can be increased by increasing the effective mesh size of the polymer network. By increasing the length of the crosslinker, the mesh size can also be increased, leading to better overall release. Also, by lowering the monomer-to-solvent ratio during polymerization, the system becomes more porous and open, leading to better overall release. Diffusion can also be increased by limiting the size of the synthesized conjugate. To limit the size of the conjugate, the conjugation reaction can be stopped before the complex becomes too bulky. Crosslinker length, monomer-to-solvent ratio, and conjugate size are all controllable synthesis parameters which can be manipulated to achieve optimal diffusivity of the conjugate within the system.

Apart from factors affecting diffusion within the system, other controllable parameters can also affect loading and release. Selection of the proper particle size has an effect on diffusion as well. However, particle size does not affect the rate at which the conjugate diffuses, but rather the diffusion path length necessary for the conjugate to be released. Smaller particle sizes translate to a shorter, less tortuous path to release, leading to a quicker release and a better overall release in a specified time [11]. Interactions between the conjugate and polymer network can also have an effect on loading and release and can be controlled by the selection of materials.

In this chapter, insulin-transferrin conjugates were tested with both P(MAA-g-EG) and P(MAA-co-NVP) polymer networks to determine which system has more desirable interactions with the conjugate molecule. In fact, P(MAA-co-NVP) polymers are thought to have a stronger interpolymer complexation [12] but it is relatively

unknown if they will have a desirable interaction with insulin-transferrin conjugates. Particle size and selected materials are two controllable synthesis parameters which have an effect on overall loading and release but are not related to changing the diffusivity of the insulin-transferrin conjugate.

The objectives of the studies performed in this chapter are related to determining performance of the insulin-transferrin conjugate with the hydrogel carriers already synthesized with respect to loading and release and also optimizing the system based on the results. Because the polymer networks are usually used for smaller proteins such as insulin, they must first be tested on much larger molecules to determine if loading and release is feasible. After testing a large molecule and appropriately adjusting synthesis protocol, insulin-transferrin conjugates will be loaded and released from a variety of polymer networks to examine performance and efficiency as well as to determine which synthesis parameters lead to an optimal system. At the conclusion of the studies in this chapter, the goal is to find a polymer network which can successfully load insulin-transferrin conjugates and can also quickly release a large portion of the loaded conjugate in conditions simulating the small intestine. The ideal polymer for use with the insulin-transferrin conjugate will consist of specially selected materials and will be a precise combination of a number of synthesis parameters based on loading and release experiments performed in this chapter.

6.2 Materials and Methods

6.2.1 Polymer Microparticle Formation by UV Polymerization

P(MAA-g-EG) and P(MAA-co-NVP) were prepared using a free radical UV polymerization in solution. P(MAA-g-EG) was prepared by mixing MAA (Sigma-Aldrich Inc., St. Louis, MO) with poly(ethylene glycol) monomethyl ether monomethacrylate with a approximate molecular weight of 1000 (PEGMA1000, Polysciences Inc., Warrington, PA) in a 1:1 molar ratio of MAA:EG. P(MAA-co-NVP) was prepared by mixing MAA with NVP (Sigma-Aldrich Inc., St. Louis, MO) in a 1:1 molar ratio of

MAA:NVP. Crosslinkers were then added into the monomer mixtures consisting of MAA/EG or MAA/NVP. The crosslinkers used within this study were tetraethylene glycol dimethacrylate (TEGDMA, Sigma-Aldrich Inc., St. Louis, MO) and poly(ethylene glycol) dimethacrylate with an approximately molecular weight of 1000 (PEGDMA1000, Polysciences Inc., Warrington, PA). The amount of crosslinker added to each monomer mixture was equal to 1 mol% of the total amount of monomer (MAA/EG or MAA/NVP). In order to eventually initiate the polymerization, the photoinitiator 1-hydroxycyclohexyl phenyl ketone (Irgacure 184, Sigma-Aldrich Inc., St. Louis, MO) was added to the polymerization mixture in the amount of 1 wt% of the total monomer added (MAA/EG or MAA/NVP). A solvent mixture consisting of 50:50 by weight deionized water (Milli-Q Plus system, Millipore) and ethanol (AAPER Alcohol, Shelbyville, KY) was added to the polymer mixture in the amounts of either 50:50, 60:40, or 67:33 by weight polymer mixture to solvent mixture. The presence of the solvent is essential to carry out the polymerization in solution, to prevent autopolymerization, and to produce a workable thin polymer film.

To ensure all components dissolved and went into a homogenous solution, the polymer mixture was sonicated for 15 minutes. After sonication, nitrogen was bubbled through the polymer solution within a nitrogen environment to eliminate oxygen. Oxygen is a free radical scavenger and significant oxygen levels could prematurely end the polymerization process. After removal of oxygen by nitrogen purging, the polymer mixture is poured between two glass slides (153 x 153 x 3 mm) separated by a Teflon spacer (0.7 mm) while still in a nitrogen environment. The glass slide apparatus containing the polymer solution spread into a thin film was then placed under a UV light source while still in a nitrogen environment. The solution was allowed to polymerize under the light source within an intensity range of 16-17 mW/cm^2 for 30 minutes. After the polymerization was completed, the polymer gels were removed from the nitrogen environment, separated from the glass slides, and placed in deionized water. The polymer films were washed in the deionized water for 7 days to remove excess

monomer and contaminants. After washing was completed, the polymers were dried in a vacuum oven at approximately 30° C for 2 days.

After completely drying the polymer films, they were removed from the vacuum oven and crushed into microparticles using a mortar and pestle. The crushed microparticles were then sieved into appropriate size ranges of either less than 75 microns, 90-150 microns, or 150-212 microns. The crushed and sieved microparticles were then stored in a vial within a desiccator to prevent moisture entering until further use.

6.2.2 Loading Time Determination for Large Molecules (Transferrin)

Diffusion into the polymer network is largely based upon the size of the molecule being loaded. Because P(MAA-g-EG) and P(MAA-co-NVP) were largely designed for smaller therapeutic proteins such as insulin, the loading of a larger molecule such as transferrin or insulin-transferrin conjugates would take significantly longer than the typical insulin loading period (2 hours). Instead of using expensive insulin-transferrin conjugates for this determination, transferrin was used as an analog to represent a size similar to insulin-transferrin conjugates.

Transferrin (Sigma-Aldrich Inc., St. Louis, MO) stock solutions were prepared by dissolving transferrin in 20 mL PBS buffer (pH 7.4, Fisher Scientific, Fair Lawn, NJ) at a concentration of 1 mg/mL. To initiate the loading process, 140 mg of P(MAA-g-EG) microparticles were added to each transferrin stock solution to reach a concentration of 7 mg/mL. Two different formulations of P(MAA-g-EG), differing by crosslinker length, were added to two separate transferrin stock solutions. The concentrated transferrin solutions were allowed to load into the microparticles through equilibrium partitioning for an extended period of time. Small samples of 0.2 mL were withdrawn using syringes (1 mL, Norm-Ject, Henke Sass Wolf, Tuttlingen, Germany) at time points of 0.25, 0.5, 1, 2, 3, 6, 12 hours for subsequent analysis by HPLC (Waters Corporation, Milford, MA). Also, a final sample was taken for analysis the following day. All withdrawn samples were

filtered through syringe filters (PVDF, 0.22 μm, Millipore, Jaffrey, NH) to ensure only free protein is being analyzed. Transferrin loading was carried out in siliconized glass beakers using Sigmacote (Sigma-Aldrich Inc., St. Louis, MO) to prevent any inaccurate concentration values due to protein adhesion to the glass.

To determine initial concentration, an initial sample was taken before addition of microparticles and analyzed by HPLC. Based on the concentration of the initial sample, the calculated concentrations of free transferrin in solution at each time point provided a comparison or ratio to determine percentage transferrin loaded at that specific time. Based on the loading efficiencies at each interval, the time point at which the loading efficiency had reached a value close to the equilibrium loading efficiency was chosen as the ideal loading period for large molecules similar to transferrin.

6.2.3 Loading of Transferrin into Polymer Microparticles

After determination of an ideal loading time for large molecules, the protocols for loading and releasing insulin-transferrin conjugates were sufficiently corrected. However, before performing any loading and release tests on the insulin-transferrin conjugate, the molecule transferrin was tested in loading and release scenarios to determine if the polymer microparticles were capable of effectively loading and releasing large molecules similar to transferrin. While the loading time for transferrin was already determined, it was also necessary to determine if transferrin could remain within the particle after collapse as well as through the filtering and lyophilization processes.

Transferrin stock solutions were prepared by dissolving the protein in 20 mL PBS buffer at a concentration of 1 mg/mL. The stock solutions were placed in glass beakers which were siliconized using Sigmacote to reduce protein adhesion to the glass. To initiate the loading process, 140 mg of P(MAA-g-EG) microparticles were added to each transferrin stock solution to reach a concentration of 7 mg/mL. Two different formulations of P(MAA-g-EG), differing by crosslinker length, were added to two

separate transferrin stock solutions. The transferrin in each solution was allowed to load by equilibrium partitioning for 4 hours under constant stirring. At the conclusion of the loading period, 20 mL of 0.1 N HCl (Fisher Scientific, Fair Lawn, NJ) was added to the solution to lower the pH and collapse the particles. After allowing the particles to fully collapse, the loaded microparticles were filtered by passing the solution through filter paper. The particles were then washed using 10 mL deionized water (Milli-Q Plus system, Millipore) to remove any excess transferrin adhered to the surface of the particle. The collected microparticles are then frozen at -80° C and lyophilized overnight to remove any excess water content. Once the lyophilization process has completed, the loaded microparticles are stored in desiccator in a freezer until further use.

To determine initial concentration, an initial sample was taken before addition of microparticles and analyzed by HPLC. In order to calculate loading efficiencies at various time points of the loading process, additional samples were withdrawn after the end of the loading period, after the addition of HCl, and after the filtering of microparticles. Sampling at the end of the loading period gives an initial loading efficiency based solely on equilibrium partitioning. Taking a sample after the addition of HCl allows observation of the difference in loading from expulsion of protein molecules due to particle collapse. The final sample after filtering is used to determine a final loading percentage and also to determine the initial amount of transferrin being introduced in the release study. All withdrawn samples were filtered through syringe filters (PVDF, 0.22 μm) to ensure only free protein is being analyzed. All four samples for each loading procedure were analyzed using HPLC.

6.2.4 Transferrin Release Studies

In preparing P(MAA-g-EG) and P(MAA-co-NVP) microparticles for use with insulin-transferrin conjugates, it was important to know if a large molecule such as transferrin could be released from the microparticles effectively and in a timely manner, or if the transferrin would simply be too large to diffuse out in an appreciable amount.

Release studies using transferrin-loaded microparticles were performed to determine if large molecules would release in a desirable manner, creating potential for the system to achieve high bioavailability.

Transferrin release studies were performed by placing approximately 10 mg of transferrin-loaded microparticles in 50 mL of PBS buffer (pH 7.4) in a dissolution apparatus (Distek Model 2100B, Distek Inc., North Brunswick, NJ). The dissolution apparatus water bath was maintained at 37° C and the experimental solutions were kept under constant stirring using impellers at 100 rpm. As the microparticles began to swell and release transferrin after addition to neutral buffer, small samples of 0.2 mL were taken at time points of 5, 10, 15, 30, 60, and 120 minutes to obtain release profiles versus time. The volume of the solution was maintained at 50 mL by addition of 0.2 mL of PBS buffer after each sample withdrawal. Needles were used with the syringes to minimize particle uptake and the sample volume was passed through syringe filters (PVDF, 0.22 μm) to ensure only free transferrin was being analyzed.

The initial amount of transferrin in the mass of particles added to the release study was determined by the data obtained from loading experiments. Based on this initial mass of transferrin available for release, the free transferrin concentration at each time point was used to calculate a percentage of transferrin released up to that point. By analyzing several time points using HPLC to determine transferrin concentration in solution, it was possible to generate a release profile which indicates the rate at which transferrin is released as well as the total overall amount released.

6.2.5 Loading of Insulin-Transferrin Conjugates into Polymer Microparticles

Loading and release studies performed on transferrin verified the possibility of incorporating large molecules such as insulin-transferrin conjugates into the synthesized hydrogel carriers. Based on the success of P(MAA-g-EG) being able to load large molecules, insulin-transferrin conjugates were loaded into a number of polymer formulations. The polymer formulations included P(MAA-g-EG) and P(MAA-co-NVP) and

varied by synthesis parameters such as crosslinker length, monomer-to-solvent ratio, and particle size. Due to transferrin previously being effectively loaded and release, a similar protocol was used to load insulin-transferrin conjugates with only slight modifications.

As a result of the previous conjugation reaction, insulin-transferrin conjugates were already dissolved in a PBS buffer (pH 7.4) at a known concentration as measured by HPLC. Insulin-transferrin stock solutions were prepared by diluting the conjugate solutions with PBS buffer (pH 7.4) to a concentration of 1 mg/mL and a volume of 40 mL. The stock solutions were placed in glass beakers which were siliconized using Sigmacote to reduce protein adhesion to the glass. To initiate the loading process, 280 mg of P(MAA-g-EG) or P(MAA-co-NVP) microparticles were added to each insulin-transferrin stock solution to reach a concentration of 7 mg/mL. Within the insulin-transferrin loading experiments, the conjugates were loaded into numerous different polymer formations which differed by crosslinker length, monomer-to-solvent ratio, particle size, and comonomer used. The insulin-transferrin conjugates in each solution were allowed to load by equilibrium partitioning for 4 hours under constant stirring. At the conclusion of the loading period, 40 mL of 0.1 N HCl was added to the solution to lower the pH and collapse the particles. After allowing the particles to fully collapse, the loaded microparticles were filtered by passing the solution through filter paper. The particles were then washed using 2 mL deionized water to remove any excess insulin-transferrin conjugates adhered to the surface of the particle. The collected microparticles were then frozen at -80° C and lyophilized overnight to remove any excess water content. Once the lyophilization process had completed, the loaded microparticles were stored in a desiccator in a freezer until further use.

To determine initial concentration, an initial sample was taken before addition of microparticles and analyzed by HPLC. In order to calculate loading efficiencies at various time points of the loading process, additional samples were withdrawn after the end of the loading period, after the addition of HCl, and after the filtering of microparticles.

Sampling at the end of the loading period gives an initial loading efficiency based solely on equilibrium partitioning. Taking a sample after the addition of HCl allows observation of the difference in loading from expulsion of protein molecules due to particle collapse. The final sample after filtering is used to determine a final loading percentage and also to determine the initial amount of insulin-transferrin conjugate being introduced in the release study. All withdrawn samples were filtered through syringe filters (PVDF, 0.22 μm) to ensure only free protein is being analyzed. All four samples for each loading procedure were analyzed using HPLC.

6.2.6 Insulin-Transferrin Conjugate Release Studies

Release studies for a therapeutic protein loaded into a polymer carrier are essential to understanding the dynamics of the system as well as to gain insight on the possible performance of the formulation when administered to human subjects. Specifically, release studies are necessary to shed light on two different properties of the system. The first property is the speed at which the conjugate is released. If diffusion is too slow and significant release takes over an hour, then very little conjugate will be absorbed because of a finite residence time in the small intestine due to intestinal motility. Also, the overall amount of conjugate released into solution is very important as well. If a significant portion of loaded conjugate is not released from the microparticle within the residence time at the site of absorption, the chances for achieving a useful bioavailability in the bloodstream drops significantly.

Insulin-transferrin conjugate release studies were performed by placing approximately 10 mg of conjugate-loaded microparticles in 50 mL of PBS buffer (pH 7.4) in a dissolution apparatus. The dissolution apparatus water bath was maintained at 37° C and the experimental solutions were kept under constant stirring using impellers at 100 rpm. As the microparticles began to swell and release insulin-transferrin conjugates after addition to neutral buffer, small samples of 0.2 mL were taken at time points of 5, 10, 15, 30, 60, and 120 minutes to obtain release profiles versus time. The volume of

the solution was maintained at 50 mL by addition of 0.2 mL of PBS buffer after each sample withdrawal. Needles were used with the syringes to minimize particle uptake and the sample volume was passed through syringe filters (PVDF, 0.22 μm) to ensure only free insulin-transferrin conjugates were being analyzed.

The initial amount of insulin-transferrin conjugates in the mass of particles added to the release study was determined by the data obtained from the previous insulin-transferrin loading experiments. Based on this initial mass of conjugate available for release, the free insulin-transferrin concentration at each time point was used to calculate a percentage of insulin-transferrin released up to that point. By analyzing several time points using HPLC to determine conjugate concentration in solution, it was possible to generate a release profile which indicates the rate at which insulin-transferrin is released as well as the total overall amount released.

6.2.7 Protein Sample Concentration Analysis by HPLC

High Performance Liquid Chromatography (HPLC) was used to analyze samples containing either transferrin or insulin-transferrin conjugates dissolved in PBS buffer (pH 7.4). The samples analyzed came from nearly every procedure listed in this chapter including determination of loading time for large molecules, transferrin loading and release, and insulin-transferrin conjugate loading and release. HPLC analysis was used for each sample to determine concentration based on absorbance values relative to absorbances of standard samples of known concentrations. Determining sample concentrations allows for the calculation of free protein in solution as well as loading efficiencies and release profiles.

The HPLC equipment used consists of a Waters 2695 Separation Module (Waters Corporation, Milford, MA) attached to a Waters 2487 Dual λ Absorbance Detector (Waters Corporation, Milford, MA). Analysis is performed using a reverse-phase analytical HPLC method designed to elute a wide range of proteins within a specified time period. The method includes the use of water (HPLC Grade, Fisher Scientific, Fair

Lawn, NJ) with 0.1% by volume trifluoroacetic acid (TFA, ACROS Organics, Geel, Belgium) as Solvent A and acetonitrile (Optima, Fisher Scientific, Fair Lawn, NJ) with 0.08% by volume TFA as Solvent B. During the separation process, the mobile phase begins at a composition of 70% Solvent A and 30% Solvent B. The mobile phase changes composition using a gradient to 40% Solvent A and 60% Solvent B within 6 minutes. The mobile phase composition is then returned to initial conditions of 70% Solvent A and 30% Solvent B for the next sample to be analyzed. The mobile phase was introduced at a constant flow rate of 0.6 mL/min. All separations are performed using a Symmetry300^{TM} C4 column (particle size 5 μm, 3.9 mm I.D. x 150 mm length, Waters Corporation, Milford, MA) held at a constant temperature of 40°C. After separation of proteins, absorbance of the solution was detected at a wavelength of 220 nm. All instrument and processing methods were controlled and specified using the Empower software.

6.3 Results and Discussion

6.3.1 Polymer Microparticle Formation by UV Polymerization

A number of different systems of polymer microparticles were synthesized for use in the loading and release experiments conducted in this chapter. Many different polymers were created including P(MAA-g-EG) and P(MAA-co-NVP) while also varying synthesis parameters such as crosslinker length (4 repeat units and 23 repeat units), monomer-to-solvent ratio (67:33, 60:40, and 50:50), and particle size (less than 75 microns, 90-150 microns, and 150-212 microns). The use of different systems yielded a range of results based on the effect of the synthesis parameters on loading and release studies. At the conclusion of the studies, a specific polymer formulation was chosen as the optimal formulation for use with insulin-transferrin conjugates. All formulations were successfully synthesized and determined to be usable for demonstrating loading and release characteristics of insulin-transferrin conjugates in conditions which mimic physiological environments.

6.3.2 Loading Time Determination for Large Molecules (Transferrin)

Transferrin was used as a model protein analog for the insulin-transferrin conjugate based on its similar size and properties. Before performing loading and release on transferrin, it was necessary to determine a suitable loading period which would allow the molecule to diffuse into the polymer network for subsequent incorporation. The loading period for a molecule is very much dependent on its diffusion coefficient within the polymer network, which in turn is very dependent on molecule size and surface properties. Using transferrin as a model analog, the loading time determination experiment consisted of loading transferrin for an extended period over 24 hours. Samples were taken at various time points to determine free transferrin concentration in solution as well as the loading efficiency at each time point. The graph showing the loading efficiency profiles versus time is shown as Figure 6.1.

As seen in Figure 6.1, the percentage of transferrin loaded sharply increases within the first few hours of the loading period. The goal of the experiment was to select a cutoff at which point the percentage of transferrin loaded would be a stable value which would not differ greatly from the equilibrium value. Based on this criteria, the selected loading period for future loading experiments with insulin-transferrin conjugates was chosen to be 4 hours. As evident in Figure 6.1, the cutoff at four hours is well after the initial sharp increase and also occurs at a value which is within 10-15% of the equilibrium value. Four hours allows sufficient time for a large molecule such as insulin-transferrin conjugates to diffuse far enough into the polymer network to not be removed with washing but still be able to release in a reasonable amount of time.

If one were to attempt to have a longer loading period, it would indeed translate to more efficient loading, but loading for too long, or overloading, typically has an adverse effect on release of the protein. In fact, the microparticles loaded with transferrin from Figure 6.1 for over 29 hours were collapsed, filtered, and lyophilized for use in a subsequent release study. The results from the release study using the overloaded microparticles are shown as Figure 6.2. As seen in Figure 6.2, there is a

significant delay in the release of transferrin using the overloaded microparticles. It appears as if it takes at least 15 minutes for the system to release any appreciable amount of encapsulated protein. The lag in release can most likely be attributed to increased time for diffusion during loading, allowing transferrin to diffuse deeper into the network from which it takes more time and a more tortuous path to diffuse out. The ramifications of loading for too long are evident in that even if the release of protein is satisfactory but delayed only 15 minutes, the chance for absorption will still be greatly decreased due to intestinal motility and the brevity of the residence time at the site of absorption. Because of the disadvantages of loading for too short of a period (bad loading) and loading for too long (bad release), the ideal loading time was found to be approximately 4 hours.

6.3.3 Loading of Transferrin into Polymer Microparticles

Transferrin was used as an analog protein to determine if a large molecule could be effectively loaded and released with P(MAA-g-EG), a polymer system previously used in this laboratory for loading and release of much smaller proteins. Before performing loading and release studies on transferrin, the ideal loading time for large molecules such as transferrin was first investigated and found to be 4 hours. After appropriately modifying the protocol to reflect the longer loading period, the protein transferrin was loaded into two different formulations of P(MAA-g-EG) to test its loading capabilities. Loading efficiencies can be calculated by taking the ratio of the difference between initial protein concentration in solution (C_0) and the final free protein concentration in solution (C_f) to the initial protein concentration. The loading efficiencies were calculated using Equation 6.1 as shown below:

$$\text{Loading Efficiency} = \frac{C_0 - C_f}{C_0} \times 100\% \qquad (6.1)$$

The loading efficiencies of transferrin in the two different formulations are shown as Figure 6.3.

As seen in Figure 6.3, P(MAA-g-EG) microparticles are capable of effectively loading large molecules such as transferrin. Also, modification of synthesis parameters such as crosslinker length can have a significant effect on the results of the loading experiments. The graph also shows that a significant portion of protein is lost due to particle collapse and surface washing. Particle collapse often squeezes out a significant amount of protein and surface washing removes the majority of any surface-adhered protein, greatly reducing the loading efficiency. However, while a high final loading efficiency makes for a more efficient overall process, it is the subsequent release performance that is the most important when deciding an ideal polymer carrier. Protein which is not loaded can still potentially be recovered and reused in an industrial process where protein which is not released in the body is considered wasted therapeutics. The important results obtained from the transferrin analog loading experiment are that an appreciable amount is loaded into the network, meaning it will not require a huge mass of polymer to deliver a relatively small amount of insulin-transferrin conjugate. Also, the performance appears to depend significantly on the synthesis parameters of the polymer carriers.

Another indication of performance in loading studies is the polymer weight fraction of transferrin, or the weight fraction of the loaded microparticles which can be attributed to the presence of transferrin molecules. Because of the nature of loading protocols, the polymer weight fraction for most proteins is typically somewhat low (0.04-0.14). However, if the polymer weight fraction of a protein is extremely low, then it would take a large amount of polymer to deliver a small amount of therapeutic protein, translating to an increased materials cost as well as large dosage forms. Polymer weight fractions were calculated by taking the difference between the initial mass of protein in solution (M_0) and the final mass of protein in the solution (M_f) and

dividing by the same difference ($M_0 - M_f$) added to the weight of polymer in the solution (M_p). Polymer weight fractions were calculated using Equation 6.2 as shown below:

$$\text{Polymer Weight Fraction} = \frac{M_0 - M_f}{(M_0 - M_f) + M_p} \qquad (6.2)$$

The polymer weight fractions of transferrin in each formulation are shown as Figure 6.4.

Figure 6.4 gives additional insight into the performance of P(MAA-g-EG) with respect to loading of large molecules. The polymer weight fractions generally reflect trends observed in loading efficiencies but are also very important because the specific values of the polymer weight fraction of a protein determine if delivering the protein will be cost-effective as well as mass-effective. In this case, the graph shows that P(MAA-g-EG) have potential to act as carriers for a large molecule such as insulin-transferrin conjugates. The calculation of exact mass of dosage form required also depends on other factors such as amount released, epithelial transport, and bioavailability. However, the polymer weight fractions of transferrin are within a reasonable range, indicating potential use of P(MAA-g-EG) with insulin-transferrin conjugates and allowing for progression of the project into observing large molecule performance in release studies.

6.3.4 Transferrin Release Studies

Transferrin-loaded P(MAA-g-EG) microparticles were placed in PBS buffer (pH 7.4) to determine if transferrin, acting as a protein analog for insulin-transferrin, could be effectively released from the polymer carriers in a reasonable period of time. After successfully loading transferrin into the P(MAA-g-EG), it was expected that the transferrin could diffuse out of the polymer network just as easily. However, the extent to which it diffuses out is still an important factor in selecting a system for use. Release studies were performed with transferrin inside two different formulations of P(MAA-g-EG) to determine the potential effect on synthesis parameters on overall release. The

percentage released at any time point during the experiment is simply a ratio of the free transferrin in solution to the amount of transferrin initially present in the mass of microparticles added. The generated release profiles of transferrin in the two formulations of P(MAA-g-EG) are shown in Figure 6.5.

As evident in Figure 6.5, P(MAA-g-EG) microparticles are capable of effectively releasing large molecules similar to transferrin from within the polymer network. Also, it can be observed that synthesis parameters such as crosslinker length have a significant effect on the overall results of the release study. The graph shows that approximately 75% of the transferrin is released from one of the formulations within one hour. A one hour window is a conservative representation of the useful residence time at the site of absorption before intestinal motility causes the removal of the microparticles from the mucus. Under the right conditions, the residence time can be more than one hour, but 1-1.5 hours is a fair time range to use to judge the release study results. With 75% of the transferrin released in the first hour, P(MAA-g-EG) microparticles demonstrate potential to deliver large amounts of insulin-transferrin conjugate to the small intestine. The protein which remains trapped in the polymer network at the end of the useful residence time continues through the digestive tract and is considered wasted therapeutics. Therefore, in a system that achieves 75% release the maximum bioavailability is also 75%. The 1:1 ratio of amount released to maximum bioavailability illustrates the importance of the release properties of the system. Also, it is advantageous for the release properties of a system to be easily manipulated simply through the changing of various synthesis parameters. The transferrin release studies performed in this section have demonstrated that the potential bioavailability of the system will not be seriously hindered by the limited diffusion and release kinetics of large molecules such as insulin-transferrin conjugates and also that the system can be fine-tuned using synthesis parameters to achieve the best possible release and thus the highest potential bioavailability.

6.3.5 Loading of Insulin-Transferrin Conjugates into Polymer Microparticles

The viability of P(MAA-g-EG) microparticles for loading and release of large molecules such as insulin-transferrin conjugates was demonstrated through loading and release of transferrin as a protein analog. To determine the performance of insulin-transferrin conjugates, they were loaded into P(MAA-g-EG) formulations. Several formulations were investigated to determine the effect of various synthesis parameters on loading and release characteristics of the system. The polymer microparticles tested included varying crosslinker lengths (4 repeat units and 23 repeat units), monomer-to-solvent ratios (67:33, 60:40, and 50:50), particle size (less than 75 microns, 90-150 microns, and 150-212 microns), and comonomer used (to form both P(MAA-g-EG) and P(MAA-co-NVP)). Based on the results from the investigation of each synthesis parameter, an ideal formulation in terms of loading can be identified for use with insulin-transferrin conjugates.

Analysis of the Effect of Crosslinker Length on Insulin-Transferrin Loading: Insulin-transferrin conjugates were loaded into two different P(MAA-g-EG) formulations which differed only in the length of the crosslinker. The crosslinkers used were TEGDMA (4 ethylene glycol repeat units) and PEGDMA1000 (approximately 23 ethylene glycol repeat units). Loading efficiencies were calculated at specific points throughout the loading process for both formulations using Equation 6.1 shown above. The loading efficiencies for insulin-transferrin in the specified formulations are shown as Figure 6.6.

Figure 6.6 shows that a significant portion of the insulin-transferrin conjugate was loaded using the experimental protocol designated for large molecules. Also, it shows that the presence of a longer crosslinker had a significant effect on the amount of conjugate loaded into the polymer network. Specifically, the use of a shorter crosslinker resulted in a final loading efficiency that is well over double the loading efficiency obtained using a much longer crosslinker. The reason for the noticeable difference is twofold. The use of a shorter crosslinker creates a tighter, more rigid polymer network,

forcing conjugate which has diffused into the network to most likely remain in the polymer network due to the tortuous path to diffuse out. Also, upon particle collapse and surface rinsing, the longer crosslinker network is more open and loose, allowing more protein to be squeezed out due to deswelling. However, as previously mentioned, conjugate which is not loaded can potentially be recovered in an industrial process. The full analysis of crosslinker length with respect to optimization of the system can only occur after examining the subsequent release studies. While release studies have a major effect on maximum potential bioavailability, loading studies theoretically do not. However, loading efficiencies are important to understand and these experiments demonstrate that a significant portion of conjugate can be loaded.

Additional insight into the effect of crosslinker length on loading of insulin-transferrin conjugates was gained by observing the polymer weight fractions as calculated by Equation 6.2 shown above. The polymer weight fractions for insulin-transferrin loaded in both formulations are shown in Figure 6.7. The graph shows that a larger fraction of the hypothetical dosage form will be comprised of therapeutic insulin-transferrin conjugates in systems which contain shorter crosslinkers. While this trend mirrors the trend seen in the graph of loading efficiencies, it also brings to the forefront the possibility of having to create larger dosage forms if the use of a longer crosslinker proves optimal based on release studies. However, based on the value of the polymer weight fraction for the longer crosslinked system, a significant portion of the total dosage form is still insulin-transferrin, albeit reduced from the shorter crosslinked system. While adjusting synthesis parameters, the benefits and drawbacks are often linked in such a way that the optimal system requires a balance of specific synthesis parameters.

Analysis of the Effect of Monomer-to-Solvent Ratios on Insulin-Transferrin Loading: Loading studies were performed by loading insulin-transferrin conjugates into three P(MAA-g-EG) polymer formulations which differed only by monomer-to-solvent ratios

used during the synthesis procedure. The formulations included monomer-to-solvent ratios of 67:33, 60:40, and 50:50. Loading efficiencies were calculated at specific points throughout the loading process for all formulations using Equation 6.1. The loading efficiencies for insulin-transferrin conjugates in the specified formulations are shown as Figure 6.8.

As can be seen in Figure 6.8, all three formulations were able to successfully load a large portion of the insulin-transferrin conjugates. Also, it is clear that the monomer-to-solvent ratio had little pronounced effect on the obtained loading efficiencies. Changing the monomer-to-solvent ratio during the synthesis of the polymer in effect changes the way in which diffusion occurs within the system. If a polymer network is formed with very little solvent and mostly monomer, such as in the 67:33 formulation, then the diffusion is based solely on the effective mesh size of the network and the conjugate must be able to diffuse between the crosslinked polymer strands. However, if the synthesis is carried out with the presence of more solvent, such as in the 50:50 formulation, the polymer network is forced to form *around* the solvent molecules, creating a more porous and open network. The additional solvent increases the "effective mesh size" of the system by allowing conjugates to diffuse through larger spaces, or pores, created by the presence of solvent. However, it appears that the different types of diffusion had little influence in the loading of insulin-transferrin conjugates but may still play a role in release of the conjugate molecules.

The effect of the monomer-to-solvent ratios on loading of insulin-transferrin conjugates was observed further by examining the polymer weight fractions of the conjugate-loaded microparticles as calculated by Equation 6.2. The polymer weight fractions for insulin-transferrin loaded in all three formulations are shown in Figure 6.9. Similar to the loading efficiencies, there is little variation between the polymer weight fractions of insulin-transferrin conjugates in the three formulations. However, it is important to note that roughly 7-8% of the weight of the loaded microparticle can be attributed to the presence of the conjugate, indicating its potential to be used in a

practical therapeutic dosage form. While release characteristics remain the most direct contributor to potential bioavailability, the three formulations examined in this section performed extremely well throughout the loading process.

Analysis of the Effect of Particle Size on Insulin-Transferrin Loading: Insulin-transferrin conjugates were loaded into three P(MAA-g-EG) formulations differing only in the average size of the microparticles. The three particle size ranges of formulations tested include less than 75 microns, 90-150 microns, and 150-212 microns. Loading efficiencies were calculated at specific points throughout the loading process for all formulations using Equation 6.1. The loading efficiencies for insulin-transferrin conjugates in the specified formulations are shown as Figure 6.10.

Figure 6.10 illustrates that a significant portion of insulin-transferrin conjugates were successfully loaded into all three formulations. Also, the difference in particle size appears to have a slight effect in initial loading efficiencies, but little to no pronounced effect on the final loading efficiencies. The effect of changing the particle size of polymer formulations can be described in terms of volume or in terms of diffusion path length. As the diameter of the particle is increased, the volume of the particle increases exponentially and is able to carry more conjugate molecules. However, conjugate molecules which are loaded into the center of the polymer network of a larger particle have a longer diffusion path length in order to diffuse out of the system. The longer diffusion path means a more tortuous journey for the molecule and thus a slower and less complete release. In terms of loading, the effect of particle size is mostly directly related to the volume that the particle can hold. Specifically, the surface area-to-volume ratio has some effect on the amount of conjugate loaded in each formulation. Among the three formulations, the smallest particles achieved the lowest initial loading efficiency compared to the other larger particles. This can be most readily explained by volume considerations and surface area-to-volume ratios. However, it is interesting to note that after particle collapse and surface rinsing, the final loading efficiencies were

nearly identical. The minimization of differences among the formulations in terms of final loading efficiencies can most likely be attributed to the decreasing differences in particle size in the collapsed state. Because the final loading efficiency is the most important practical value for industrial processes, the particle size had minimal effect on the loading process.

Additional insight into the effect of particle size on the loading of insulin-transferrin conjugates in P(MAA-g-EG) microparticles was gained by analyzing the polymer weight fractions of the conjugate as calculated by Equation 6.2. The polymer weight fractions for insulin-transferrin conjugates loaded in all three formulations are shown in Figure 6.11. As evident in the figure, the polymer weight fraction which can be attributed to the presence of the insulin-transferrin conjugate decreased as the particle size was increased. Based on these results, use of smaller microparticles as carriers for insulin-transferrin conjugates is preferential due to the practical advantage of being able to formulate smaller dosage forms. Also, the final loading efficiencies of the three particle size ranges were nearly identical, eliminating any informed selection based on loading efficiencies alone. In contrast, the effect of particle size on the release of conjugate will most likely stem from factors related to diffusion path length within the particle and will also be the determining factor when optimizing particle size due to the direct relationship between release studies and potential bioavailability.

Analysis of the Effect of the Replacement of PEG Comonomer with NVP Comonomer on Insulin-Transferrin Loading: Loading studies were performed by loading insulin-transferrin conjugates into P(MAA-g-EG) and P(MAA-co-NVP) polymer microparticles which differed only by the comonomer used. Loading efficiencies were calculated at specific points throughout the loading process for both formulations using Equation 6.1. The loading efficiencies for insulin-transferrin conjugates in P(MAA-g-EG) and P(MAA-co-NVP) are shown as Figure 6.12.

As can be seen in Figure 6.12, both P(MAA-g-EG) and P(MAA-co-NVP) were able to effectively load the majority of insulin-transferrin conjugates placed in solution. Also, the difference between the two formulations with respect to loading efficiencies was only evident in the initial loading efficiencies. After the particles were collapsed and surface rinsed, the difference in loading efficiencies between the systems became minimal. Differences in loading between the systems can be attributed to interactions between the insulin-transferrin conjugate and either the PEG tethers or NVP repeat units. Interactions which may have an effect include surface charge interactions, physical hindrance, hydrophilicity, and interpolymer interactions. However, because the loading efficiencies were very similar between the systems, it is reasonable to conclude that the interactions based on the presence of the comonomer had little effect on the loading process. However, the presence of a specific comonomer is more likely to play a role in the subsequent release studies because of the importance of the interpolymer interactions governing the rate of swelling as well as the hydrophilicity of each group significantly affecting the release properties.

The effect of the presence of the PEG and NVP comonomers on the loading of insulin-transferrin conjugates was further investigated by determining the polymer weight fractions of insulin-transferrin as calculated by Equation 6.2. The polymer weight fractions for insulin-transferrin conjugates loaded in both P(MAA-g-EG) and P(MAA-co-NVP) are shown in Figure 6.13. Similar to the final loading efficiencies, little difference could be observed between the polymer weight fraction of the insulin-transferrin conjugate in P(MAA-g-EG) and P(MAA-co-NVP). However, it is important to note that both polymer formulations had polymer weight fractions within the range of 0.07-0.08, indicating that both polymers could serve as potential carriers for insulin-transferrin conjugates in a dosage form. As with all four synthesis parameters investigated, the selection of the optimal system will most likely depend on the release characteristics in simulated physiological conditions because of the direct link to potential bioavailability. However, loading studies are important to perform with respect to each synthesis

parameter in order to verify loading of a significant amount of conjugate, to determine if the polymer weight fraction is enough to warrant a practical dosage form, and to better understand how each manipulated synthesis parameter affects the diffusion of the conjugate within the polymer network.

6.3.6 Insulin-Transferrin Conjugate Release Studies

Insulin-transferrin conjugates were loaded into a number of different polymer formulations including P(MAA-g-EG) and P(MAA-co-NVP) synthesized using a number of different synthesis parameters. The formulations were found to all be able to load an appreciable amount of insulin-transferrin conjugate in solution as well as having a significant polymer weight fraction attributed to the protein. The conjugate-loaded microparticles from each formulation were then investigated using release studies. The formulations included systems with varying crosslinker lengths (4 repeat units and 23 repeat units), monomer-to-solvent ratios (67:33, 60:40, and 50:50), particle size (less than 75 microns, 90-150 microns, and 150-212 microns), and comonomer used (to form both P(MAA-g-EG) and P(MAA-co-NVP)). Based on the results obtained from the investigation of the loading and release studies for each synthesis parameter, an optimal polymer formulation to achieve maximum potential bioavailability was identified and chosen for future use with insulin-transferrin conjugates.

Analysis of the Effect of Crosslinker Length on the Release of Insulin-Transferrin: Insulin-transferrin conjugates were previously loaded into two different P(MAA-g-EG) formulations which differed only in the length of the crosslinker. The crosslinkers used were TEGDMA (4 ethylene glycol repeat units) and PEGDMA1000 (approximately 23 ethylene glycol repeat units). Release studies were performed by placing the conjugate-loaded microparticles in PBS buffer (pH 7.4) and measuring the conjugate concentration in solution over time. The percentage released at each time point was calculated by taking a ratio of the amount of conjugate at the specified time to the initial amount of

conjugate present in the loaded particles. The release profiles for insulin-transferrin as released from the specified formulations are shown as Figure 6.14.

Figure 6.14 shows that while both formulations released a significant amount of conjugate within 2 hours, the system which was crosslinked with PEGDMA1000 released approximately 10% more than the system crosslinked with TEGDMA by the conclusion of the release period. The difference in release is a result of the effect of a longer crosslinker on the polymer network. The crosslinker PEGDMA1000 is significantly longer than TEGDMA, creating a polymer network with a larger mesh size which is more open to diffusion of a large molecule such as the conjugate. The increased distance between polymer strands allows loaded conjugate in the PEGDMA1000 crosslinked formulation to diffuse out of the system quicker and in a higher quantity over a short time period. Even though the loading and polymer weight fraction is preferential for the TEGDMA crosslinked system, the release profile clearly justifies the use of longer crosslinkers for polymer carriers for insulin-transferrin conjugates. Because of the improved release using a longer crosslinker, even longer crosslinkers such as PEGDA4000 were used as crosslinkers in some experimental systems. However, the resultant polymer films were not rigid enough and were unmanageable due to the introduction of an extremely long crosslinker. However, the additional insulin-transferrin conjugate released in the case of the PEGDMA1000 crosslinked formulation relative to the TEGDMA crosslinked formulation equates to higher potential bioavailability and increased potential efficacy of a possible oral formulation.

Analysis of the Effect of Monomer-to-Solvent Ratios on the Release of Insulin-Transferrin: Insulin-transferrin conjugates were previously loaded into three different P(MAA-g-EG) formulations which differed only in the monomer-to-solvent ratios used during synthesis. The formulations included monomer-to-solvent ratios of 67:33, 60:40, and 50:50. Release studies were performed by placing the conjugate-loaded microparticles in PBS buffer (pH 7.4) and measuring the conjugate concentration in

solution over time. The percentage released at each time point was calculated by taking a ratio of the amount of conjugate at the specified time to the initial amount of conjugate present in the loaded particles. The release profiles for insulin-transferrin as released from the specified formulations are shown as Figure 6.15.

Figure 6.15 illustrates that all three formulations were able to release at least a sizable portion of the loaded insulin-transferrin conjugates. However, the data also clearly shows that as more solvent relative to monomer is introduced to the prepolymer mixture, the release characteristics benefit greatly. Changing the balance of the monomer-to-solvent ratio in the prepolymer mixture in effect changes the way in which diffusion occurs throughout the system. If a large amount of monomer relative to solvent is used, such as in the 67:33 formulation, then diffusion characteristics are based solely on the effective mesh size of the network, forcing the conjugate to diffuse within the spaces created between the crosslinked polymer strands. However, if the monomer-to-solvent ratio is changed to favor adding more solvent, such as in the 50:50 formulation, the polymer network forms around the solvent molecules, creating a more porous and open network. The additional solvent increases the "effective mesh size" of the system by allowing conjugates to diffuse through larger spaces, or pores, created by the presence of solvent in the prepolymer mixture. The loading characteristics varied very little between the three formulations, but the release profiles clearly require that the monomer-to-solvent ratio of the prepolymer mixture must be as low as possible to achieve an optimal system. Because more solvent present in the synthesis led to better release, experimental systems were synthesis with monomer-to-solvent ratios of 40:60 and 33:67. However, the syntheses produced films which were gel-like and unmanageable in terms of washing excess monomer and subsequent crushing. The formulation successfully synthesized using the lowest monomer-to-solvent ratio, which was 50:50, was chosen as the optimal system because of the significantly more probable prospect of achieving high bioavailability versus the other two formulations.

Analysis of the Effect of Particle Size on the Release of Insulin-Transferrin: Insulin-transferrin conjugates were previously loaded into three different P(MAA-g-EG) formulations which differed only in particle size. The formulations included P(MAA-g-EG) microparticles in size ranges of less than 75 microns, 90-150 microns, and 150-212 microns. Release studies were performed by placing the conjugate-loaded microparticles in PBS buffer (pH 7.4) and measuring the conjugate concentration in solution over time. The percentage released at each time point was calculated by taking a ratio of the amount of conjugate at the specified time to the initial amount of conjugate present in the loaded particles. The release profiles for insulin-transferrin as released from the specified formulations are shown as Figure 6.16.

As can be seen in Figure 6.16, all three formulations were able to release at least a small portion of the loaded insulin-transferrin conjugate. However, there is a large increase in the overall amount of conjugate released as the particle size decreases. The relationship between amount of conjugate released and particle size of the carrier can best be described by the concept of diffusion path length. In smaller particles, the loaded conjugate has a shorter distance to diffuse before being completely released from the system. In contrast, a large molecule presents a more tortuous and longer path for the release of conjugate, translating to slower release and a reduction in overall release over a short period. The diffusion path length plays a considerable role in the release characteristics of the conjugate whereas the particle size effect on loading is best described by volume considerations as mentioned previously. Based on the results, the ideal particle size for polymer carriers for insulin-transferrin conjugates was determined to be less than 75 microns. It is difficult to reduce the upper end of the size range due to the difficulty in creating smaller particles using the crushing method of using a mortar and pestle. If a different type of polymerization were used which could control the size down to a smaller range, the release of conjugates would likely see even greater benefit. However, using the specific protocol outlined in Chapter 4, the

microparticles of size range of less than 75 microns were used to achieve the highest potential bioavailability.

Analysis of the Effect of the Replacement of PEG Comonomer with NVP Comonomer on the Release of Insulin-Transferrin: Insulin-transferrin conjugates were previously loaded into P(MAA-g-EG) and P(MAA-co-NVP) formulations which differed only by the comonomer used. Release studies were performed by placing the conjugate-loaded microparticles in PBS buffer (pH 7.4) as well as PBS buffer (pH 3.2) and measuring the conjugate concentration in solution over time. The release studies performed under acidic conditions were performed to examine how the particles would perform in the collapsed state, or to observe if any conjugate was prematurely released in conditions mimicking the stomach. The percentage released at each time point was calculated by taking a ratio of the amount of conjugate at the specified time to the initial amount of conjugate present in the loaded particles. The release profiles for insulin-transferrin as released from the specified formulations are shown as Figure 6.17.

Figure 6.17 illustrates that both P(MAA-g-EG) and P(MAA-co-NVP) polymer formulations were able to release a portion of the loaded insulin-transferrin conjugate under neutral pH conditions and that both formulations were able to prevent any release of conjugate under acidic conditions. Also, while no free conjugate could be detected in solution under acidic conditions for both formulations, the P(MAA-g-EG) polymer formulation far outperformed the P(MAA-co-NVP) formulation by releasing much more conjugate under neutral conditions. The major difference between these two comonomers is the interpolymer interactions and the resultant degree of complexation. NVP is thought to have a higher degree of complexation with MAA than PEG does, allowing for the interpolymer bonds in P(MAA-co-NVP) to be stronger than those in P(MAA-g-EG). The selection of NVP as a possible replacement for the PEG comonomer was based on its degree of complexation and such a property was determined to have an advantageous effect on protection of the conjugate under acidic

conditions. However, it was the strong interpolymer interactions which most likely limited the release of conjugate from P(MAA-co-NVP) particles. While the degree of complexation in the collapsed state may have been higher in P(MAA-co-NVP), the P(MAA-g-EG) particles also prevented *any* release of conjugate under acidic conditions. Therefore, the additional complexation in the collapsed state was unnecessary for protection of a large molecule such as the insulin-transferrin conjugate. In fact, the strong complexation most likely limited the release of the conjugate under neutral conditions. If the therapeutic were a smaller protein, such as insulin by itself, the additional protection from the complexation of P(MAA-co-NVP) may be necessary. Moreover, in the less complexed system of P(MAA-g-EG), the insulin may be able to diffuse out under acidic conditions. However, for the specific case of the insulin-transferrin conjugate, the P(MAA-g-EG) microparticles were found to be the desired formulation as a carrier for the conjugate because of the much improved release and concurrently the much improved potential bioavailability of an oral formulation.

Determination of an Optimal Polymer Formulation for the Delivery of Insulin-Transferrin Conjugates: Several polymer formulations were synthesized in an effort to determine an optimal polymer formulation to achieve high bioavailability of orally delivered insulin-transferrin conjugates. The polymer formulations included P(MAA-g-EG) and P(MAA-co-NVP) while also varying synthesis parameters such as crosslinker length (4 repeat units and 23 repeat units), monomer-to-solvent ratio (67:33, 60:40, and 50:50), and particle size (less than 75 microns, 90-150 microns, and 150-212 microns). Each formulation was loaded with insulin-transferrin conjugates and subsequently released to determine loading efficiencies and release profiles. As each synthesis parameter was investigated, all other synthesis parameters and values were held constant. At the conclusion of the studies, the release characteristics were the determining factor in selecting an optimal carrier. The loading efficiencies and polymer weight fractions were

determined to verify that each formulation could indeed load a significant portion of conjugate.

The investigation of the effect of crosslinker length yielded that the longest crosslinker (PEGDMA1000) would provide the best release characteristics. After testing monomer-to-solvent ratios, it was found necessary to include as much solvent as possible in the prepolymer mixture (50:50 monomer-to-solvent) to achieve desirable release profiles. The experiments on the effect of particle size of the carrier demonstrated that the smallest particles (less than 75 microns) achieved the highest overall release. The studies in which the PEG comonomer was replaced with the NVP comonomer illustrated that while NVP may complex better under acidic conditions, the extra protection in unnecessary in the case of a large molecule such as insulin-transferrin conjugates and that P(MAA-g-EG) particles are preferred as carriers due to the much improved release characteristics. Within the parameters specified in this chapter and manipulation only to the extent that polymers could be successfully synthesized, the ideal polymer carrier for oral delivery of insulin-transferrin conjugates was found to be P(MAA-g-EG) particles synthesized using a monomer-to-solvent ratio of 50:50, crosslinked with PEGDMA1000, and having a particle size of less than 75 microns.

6.3.7 Protein Sample Concentration Analysis by HPLC

All samples obtained from loading and release studies were analyzed by HPLC. The concentration of each sample was determined by comparisons to standards of known concentrations. The experimental concentration of each sample was used to calculate the free protein concentration in the solution at the time the sample was withdrawn. In the cases of values of zero concentration as in the release studies performed under acidic conditions, the free protein in the samples was at a concentration low enough to be undetectable by HPLC.

6.4 Conclusions

Insulin-transferrin conjugates were successfully synthesized and required investigation into the *in vitro* characteristics with relation to loading and release in polymer microparticle carriers. To determine if polymer carriers typically used for smaller proteins such as insulin were able to carry large molecules, a protocol was designed for transferrin and it was tested as a protein analog to determine its loading and release characteristics. The polymer carriers were found to perform well with a large molecule, allowing for investigation into the loading and release of insulin-transferrin conjugates in the polymer carriers. To determine the ideal polymer formulation to use as a carrier for the conjugate, several polymer formulations were tested using loading and release studies to gauge performance. The polymer formulations included P(MAA-g-EG) and P(MAA-co-NVP) and also differed in synthesis parameters such as crosslinker length, monomer-to-solvent ratio, and particle size. Loading studies performed on all formulations confirmed that each formulation was capable of loading a significant amount of insulin-transferrin conjugates. Upon performing release studies, the optimal release characteristics for obtaining high bioavailability upon administration were obtained using the specific optimal formulation of P(MAA-g-EG) microparticles less than 75 microns in size, crosslinked with PEGDMA1000, and synthesized using a 50:50 monomer-to-solvent ratio. The selected optimized polymer carrier along with the synthesized insulin-transferrin conjugate received further investigation into their properties and potential to achieve high bioavailability upon administration by evaluation via cell studies performed in a later chapter.

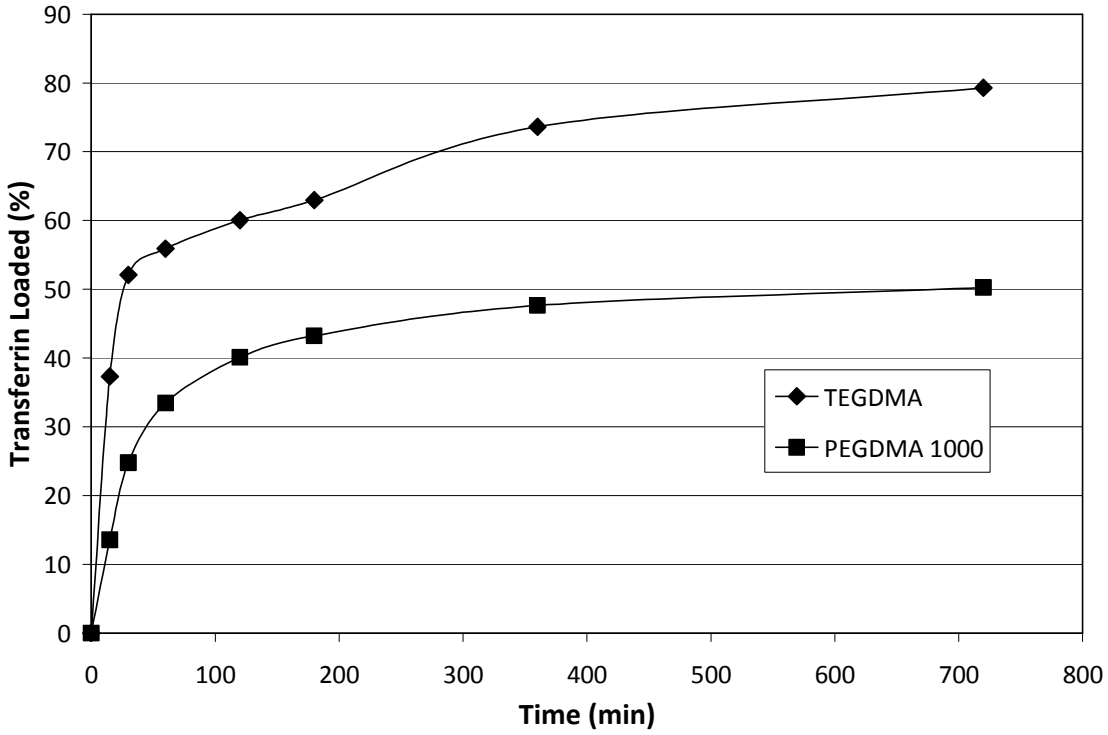

Figure 6.1 Loading profiles versus time for transferrin loading in P(MAA-g-EG) in PBS buffer (pH 7.4).

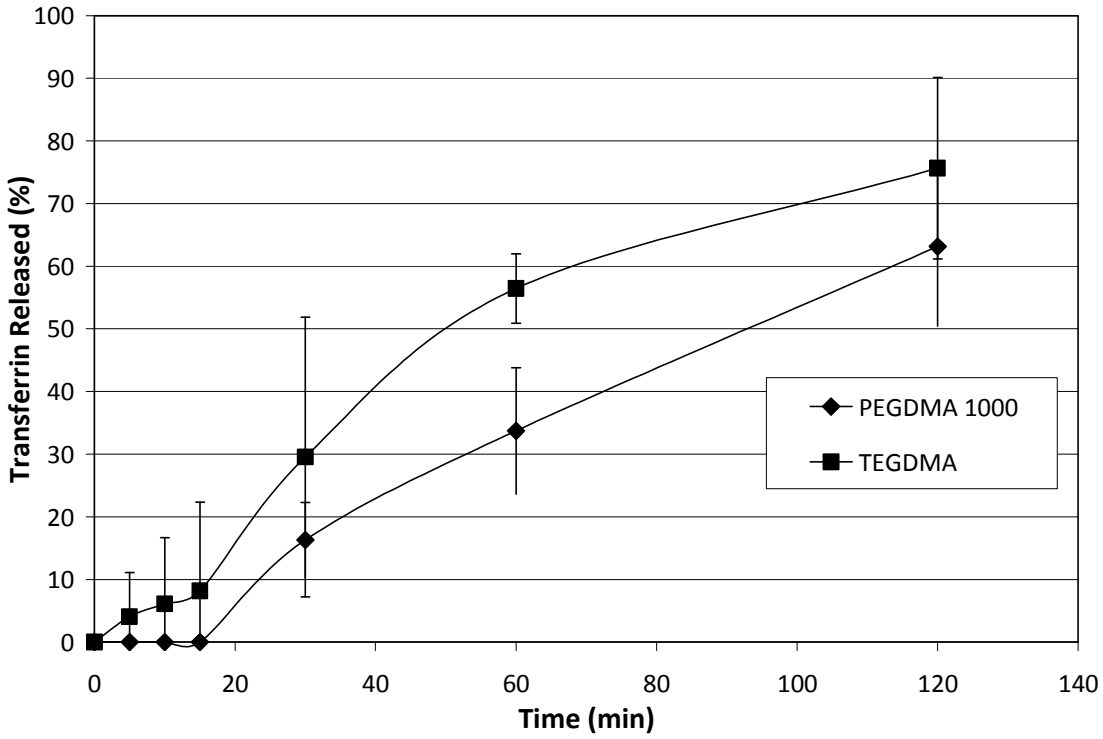

Figure 6.2 Release profiles for transferrin-loaded microparticles from an extended loading experiment incorporating transferrin in P(MAA-g-EG) for over 29 hours.

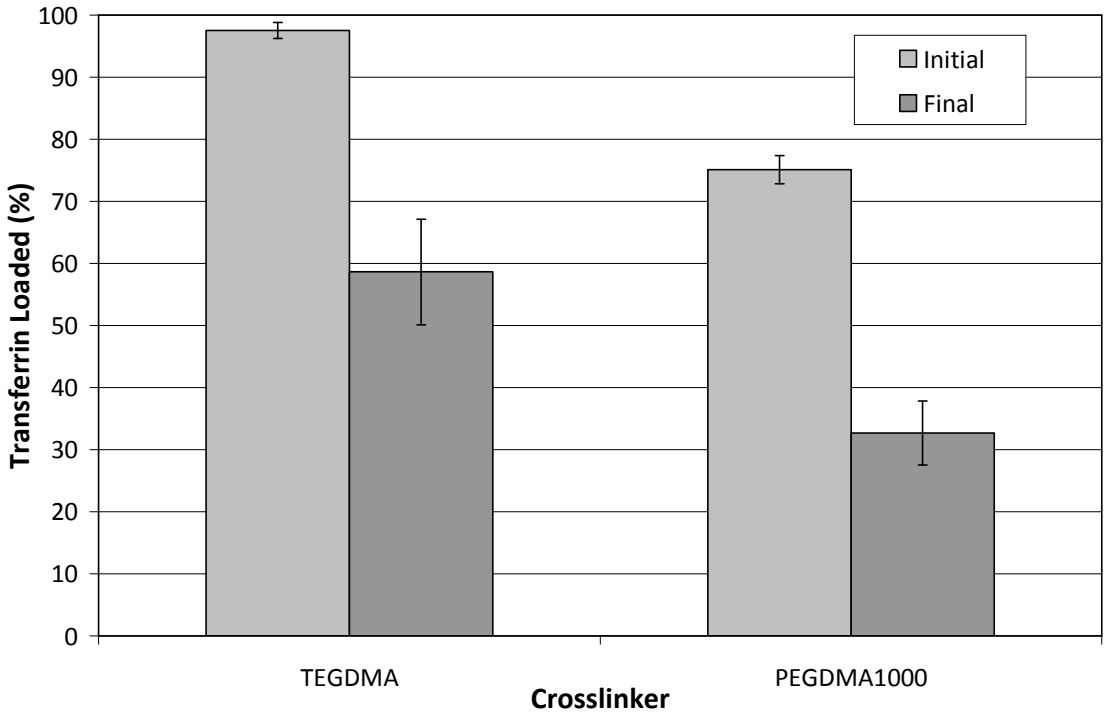

Figure 6.3 Loading efficiencies of transferrin in P(MAA-g-EG) before and after particle collapse and surface washing.

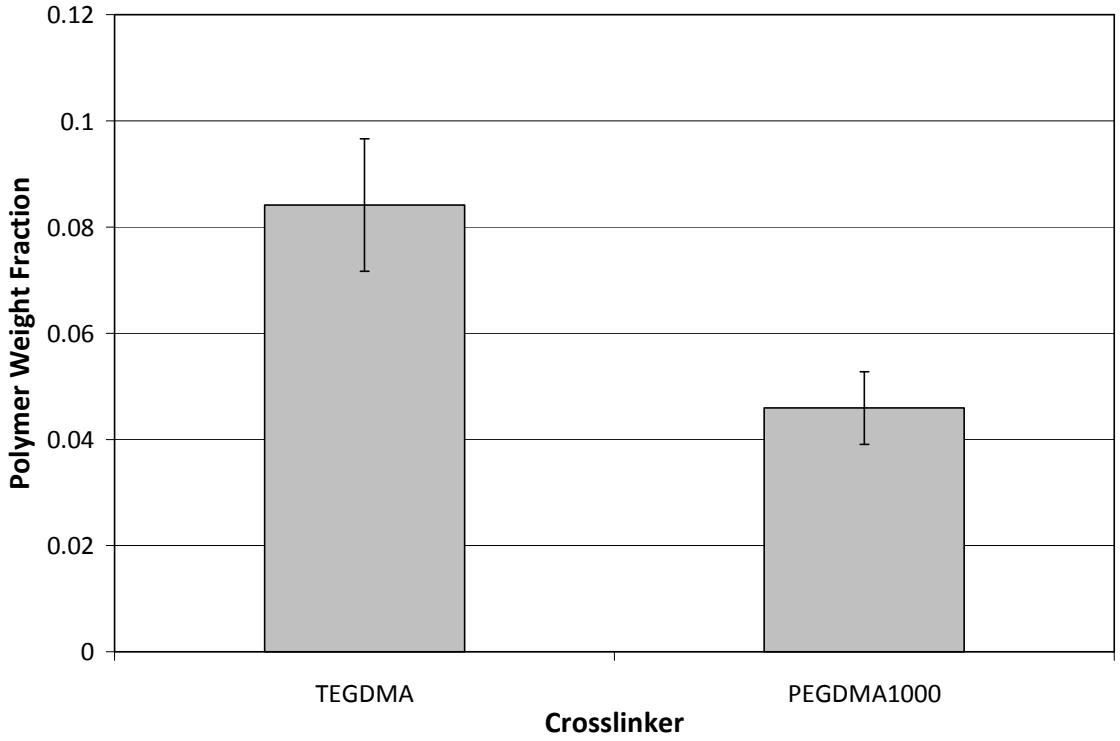

Figure 6.4 Polymer weight fractions of transferrin in loaded P(MAA-g-EG) microparticles.

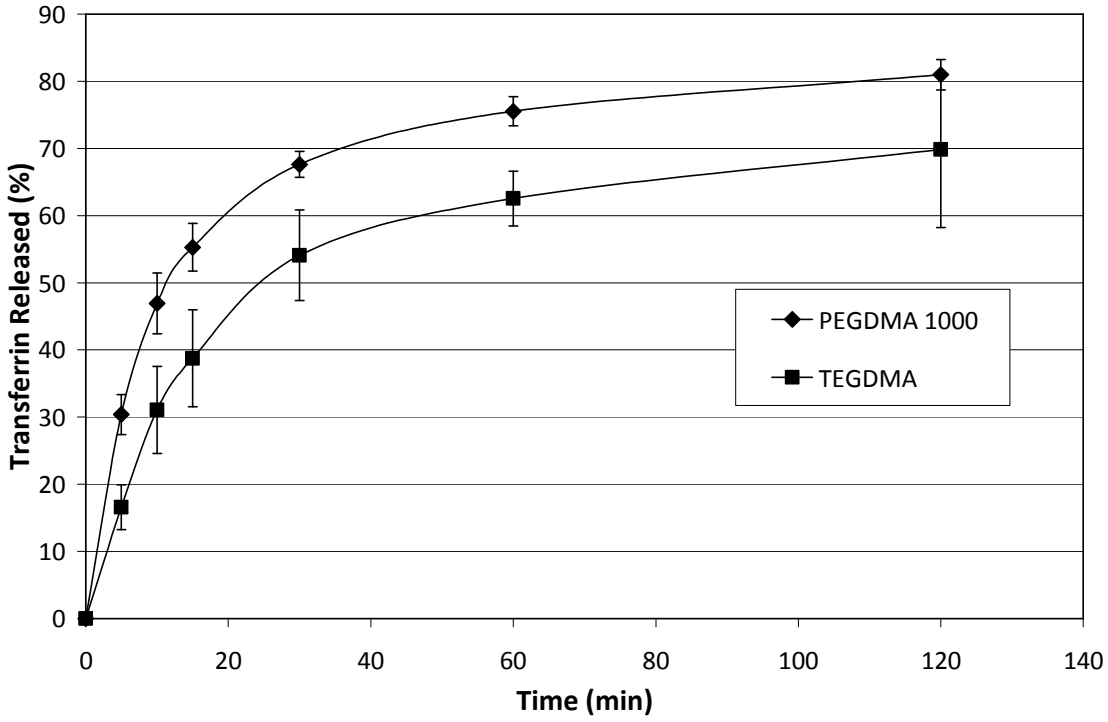

Figure 6.5 Release profiles of transferrin loaded in P(MAA-g-EG) microparticles and placed in PBS buffer (pH 7.4).

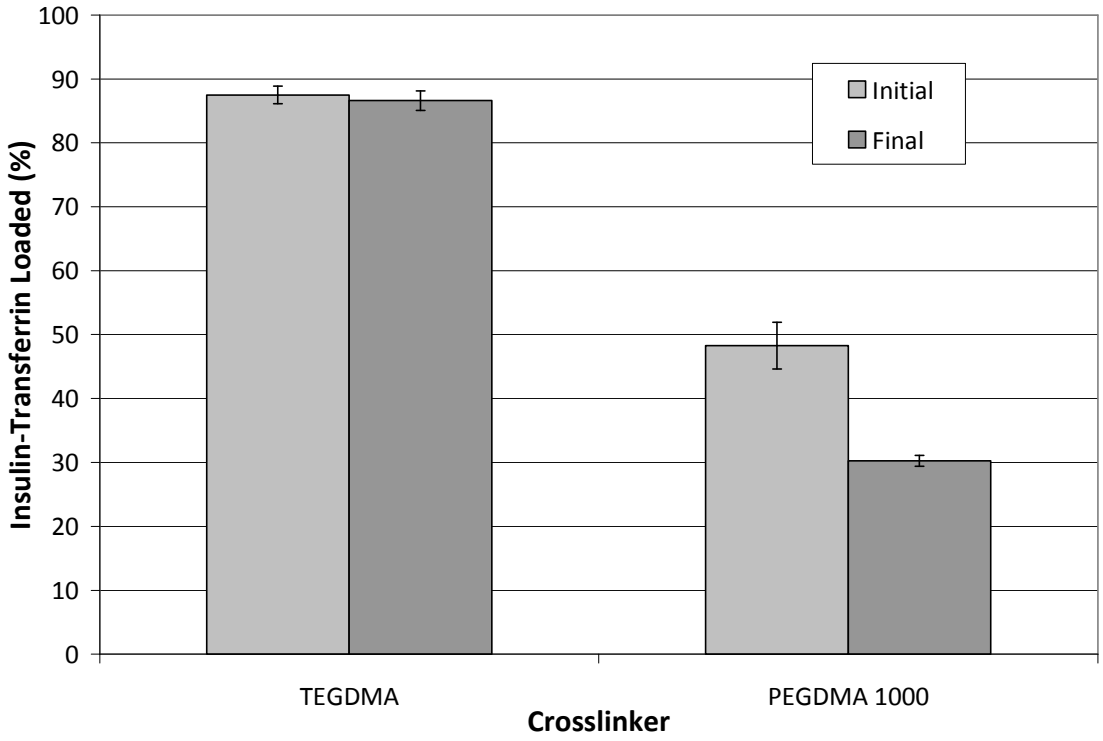

Figure 6.6 Loading efficiencies of insulin-transferrin conjugates in P(MAA-g-EG) microparticles of differing crosslinker lengths before and after particle collapse and surface washing.

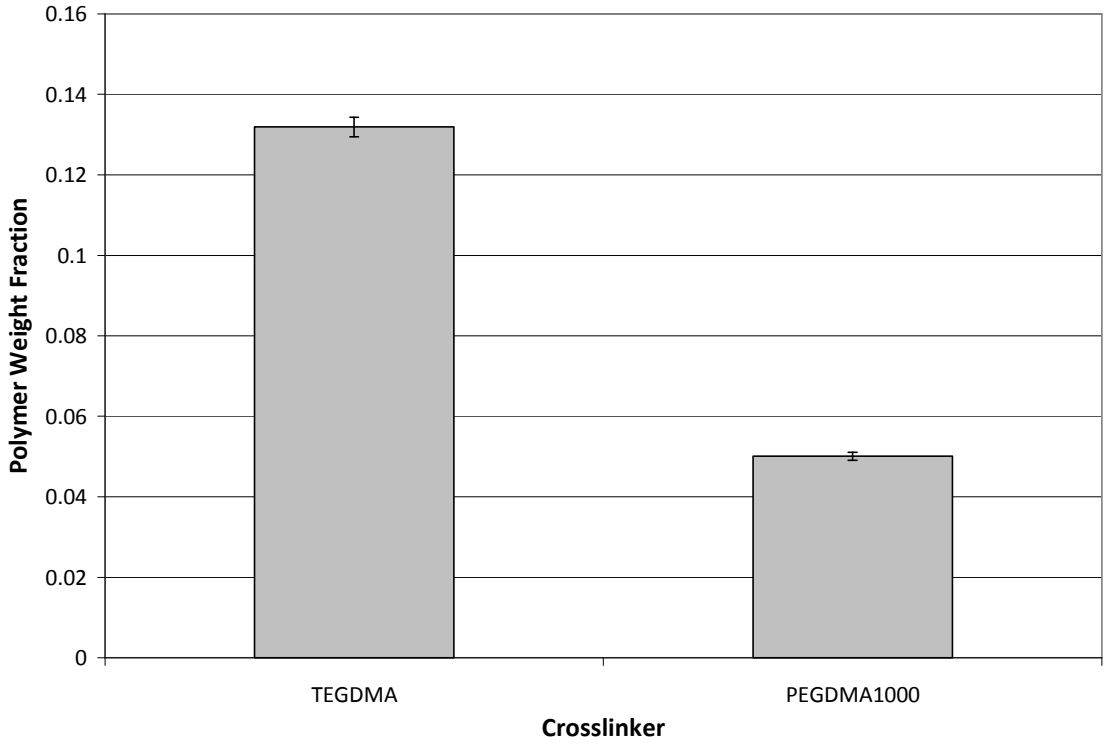

Figure 6.7 Polymer weight fractions of insulin-transferrin conjugates in P(MAA-g-EG) formulations of differing crosslinker lengths.

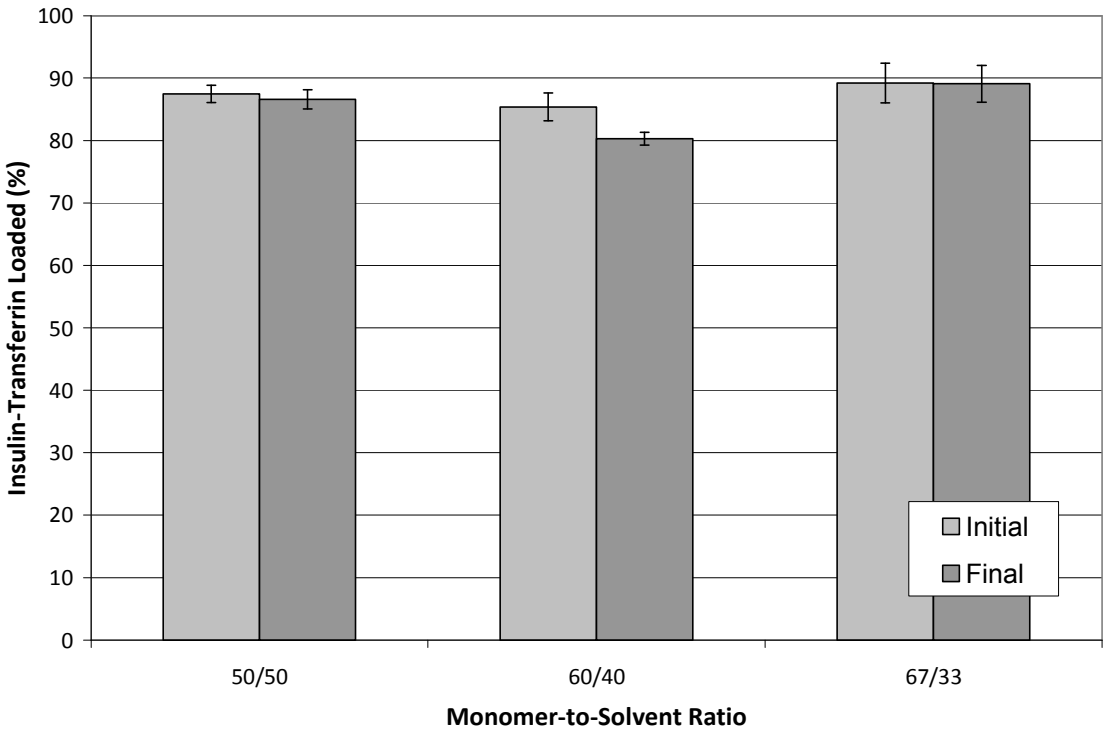

Figure 6.8 Loading efficiencies of insulin-transferrin conjugates in P(MAA-g-EG) formulations of differing monomer-to-solvent ratios before and after particle collapse and surface washing.

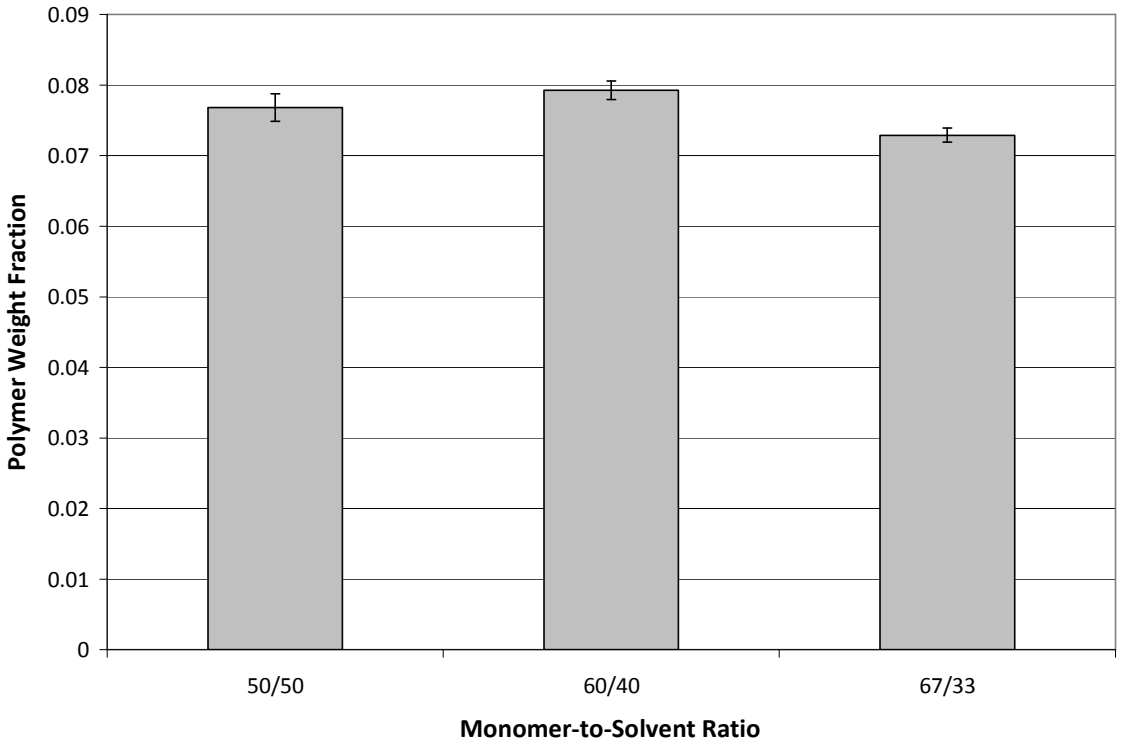

Figure 6.9 Polymer weight fractions of insulin-transferrin conjugates in P(MAA-g-EG) formulations synthesized using different monomer-to-solvent ratios.

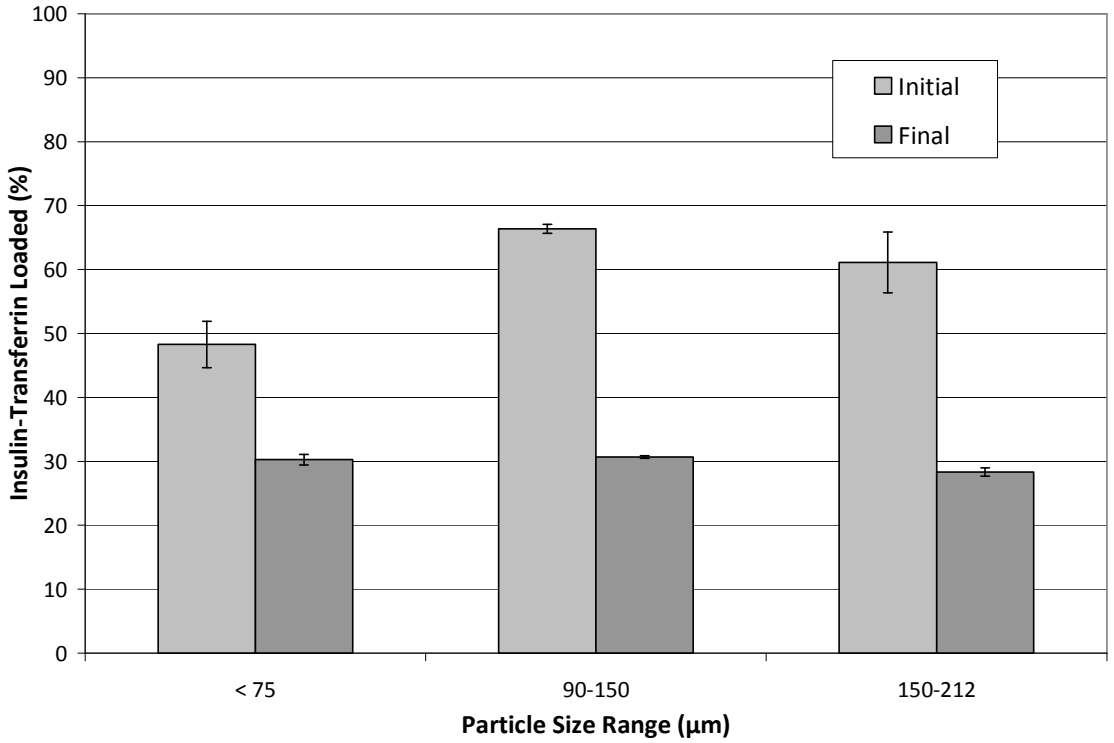

Figure 6.10 Loading efficiencies of insulin-transferrin conjugates in P(MAA-g-EG) formulations of differing particle sizes before and after particle collapse and surface washing.

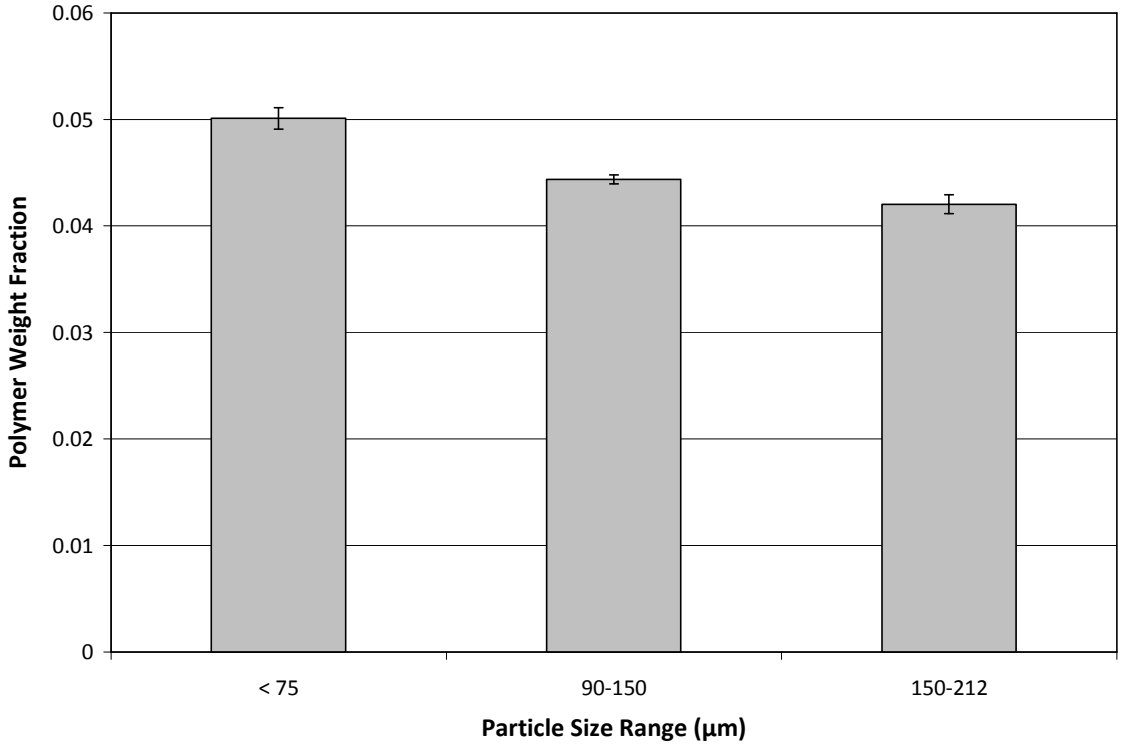

Figure 6.11 Polymer weight fractions of insulin-transferrin conjugates in P(MAA-g-EG) formulations of different particle size ranges.

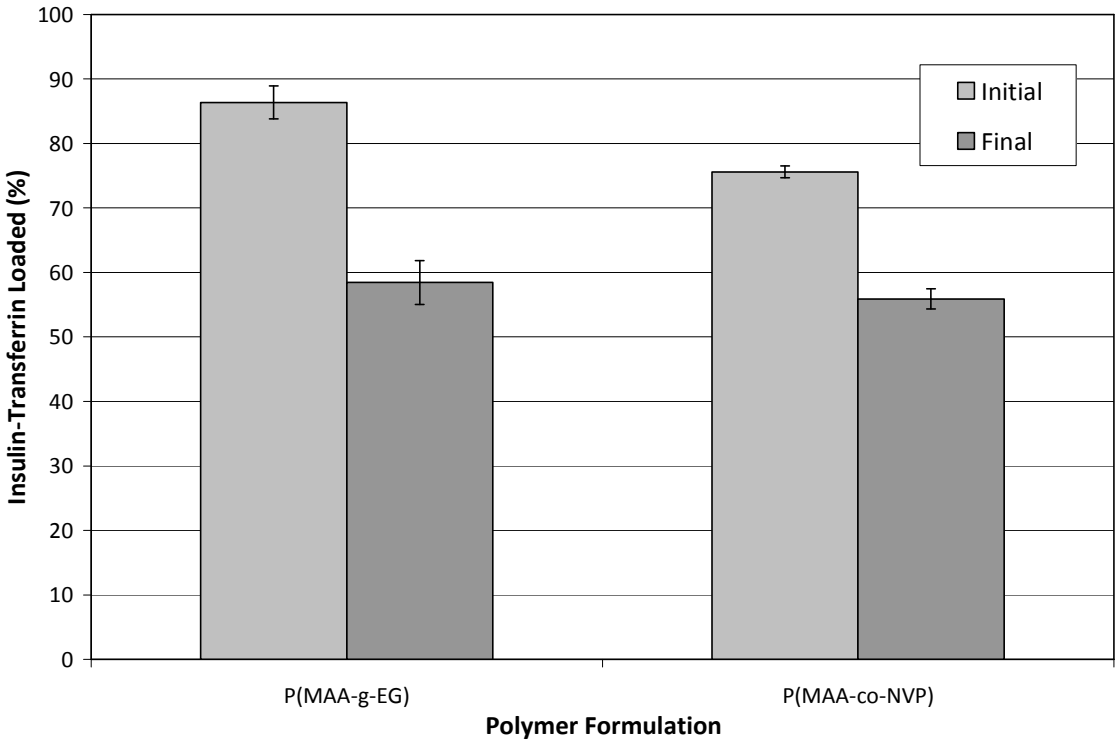

Figure 6.12 Loading efficiencies of insulin-transferrin conjugates in P(MAA-g-EG) and P(MAA-co-NVP) polymer formulations before and after particle collapse and surface washing.

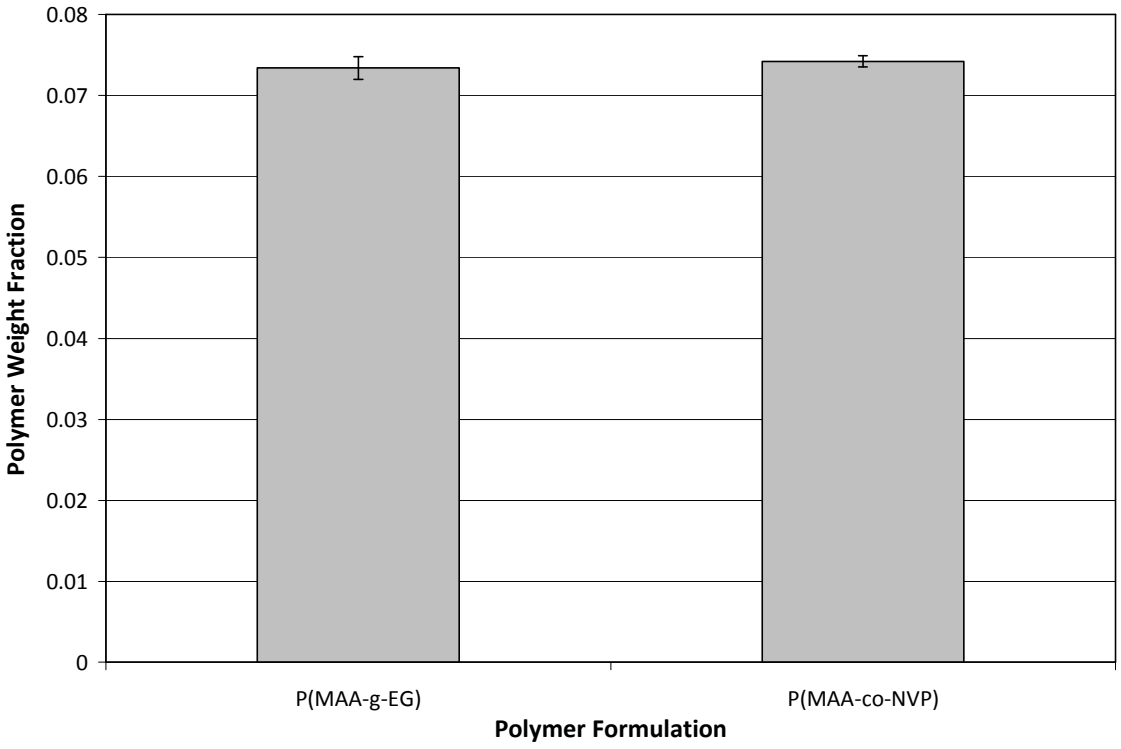

Figure 6.13 Polymer weight fractions of insulin-transferrin conjugates in P(MAA-g-EG) and P(MAA-co-NVP) polymer formulations.

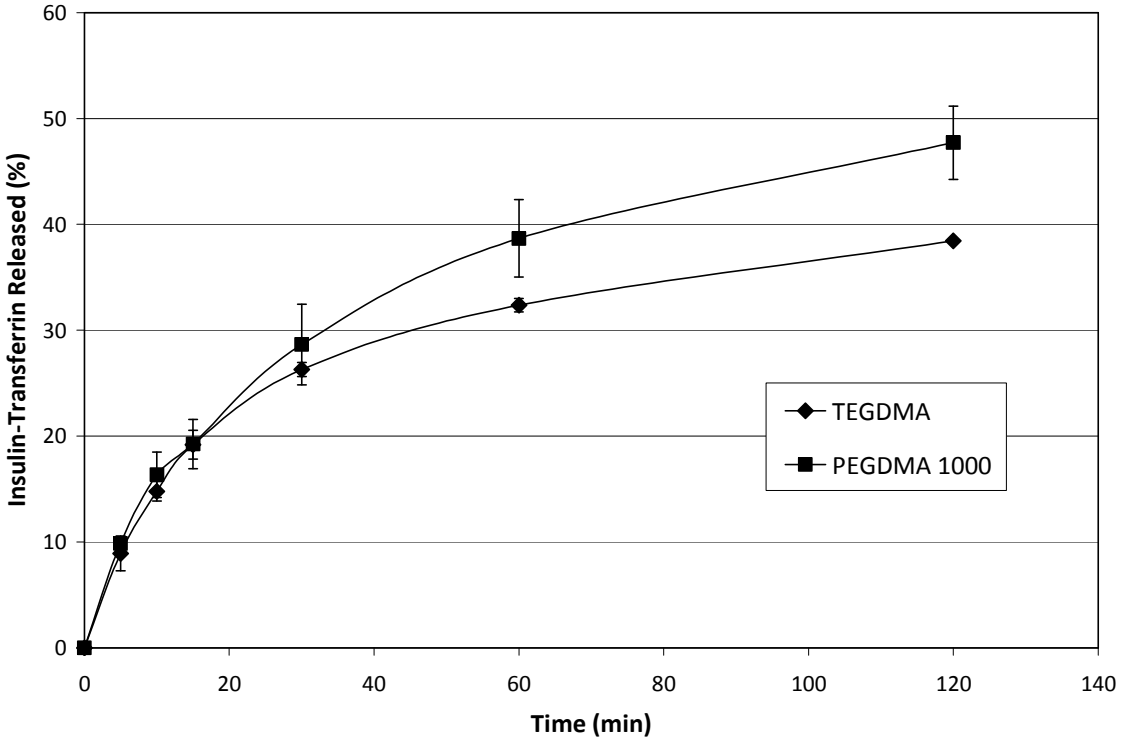

Figure 6.14 Release profiles of insulin-transferrin conjugates loaded in P(MAA-g-EG) microparticles of differing crosslinker lengths and placed in PBS buffer (pH 7.4).

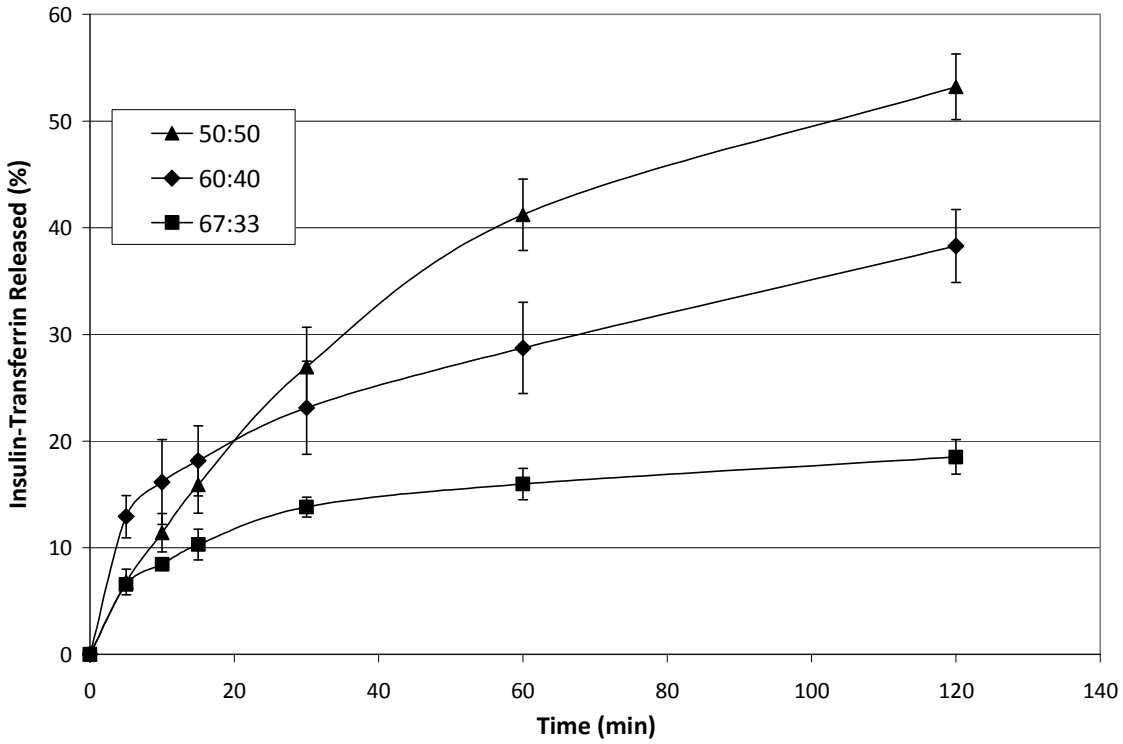

Figure 6.15 Release profiles of insulin-transferrin conjugates loaded in P(MAA-g-EG) microparticles of differing monomer-to-solvent ratios and placed in PBS buffer (pH 7.4).

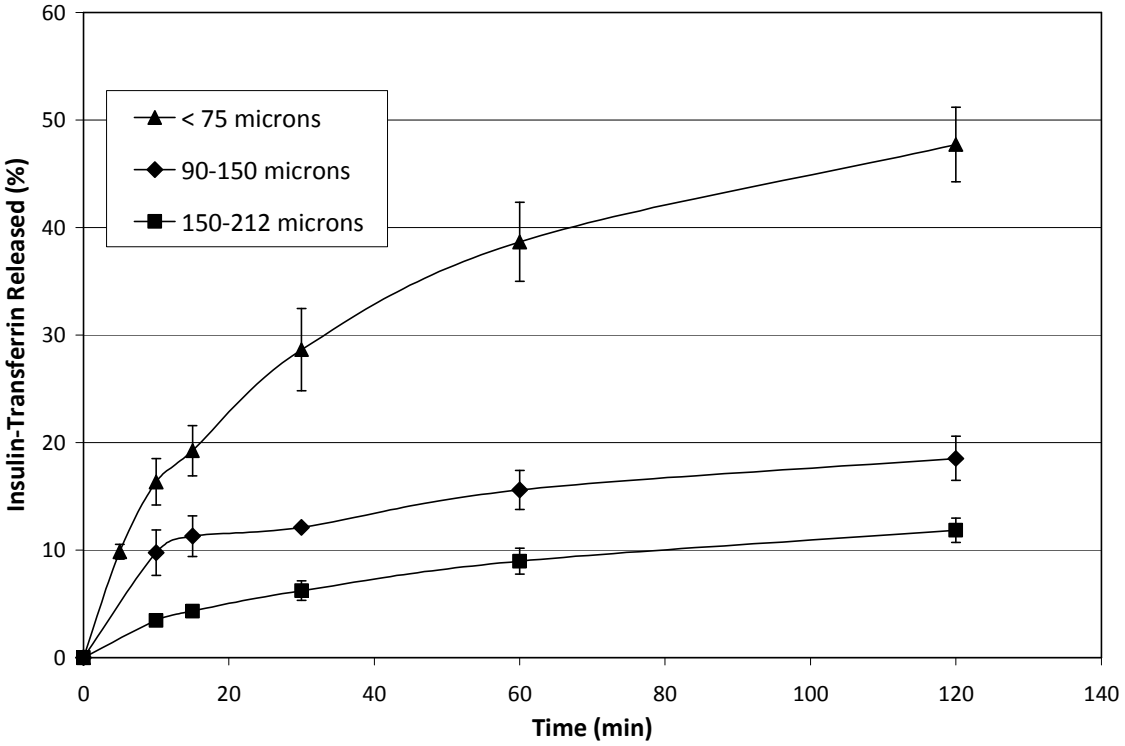

Figure 6.16 Release profiles of insulin-transferrin conjugates loaded in P(MAA-*g*-EG) microparticles of differing particle sizes and placed in PBS buffer (pH 7.4).

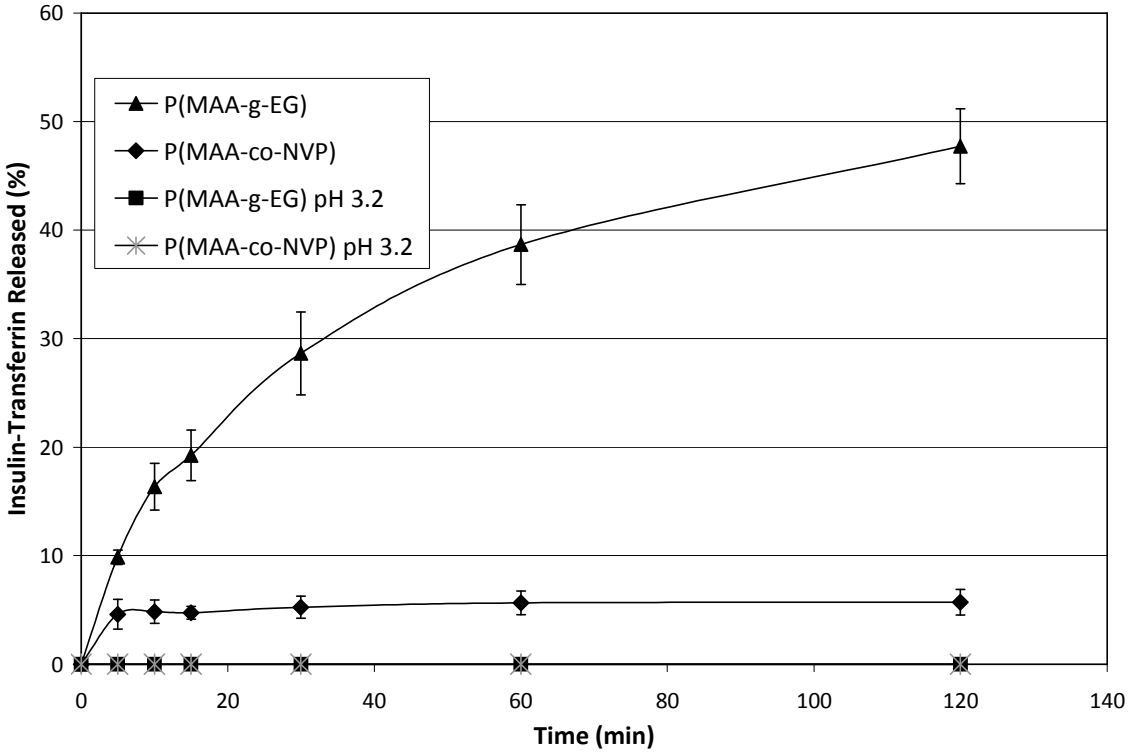

Figure 6.17 Release profiles of insulin-transferrin conjugates loaded in P(MAA-g-EG) and P(MAA-co-NVP) microparticles and placed in either PBS buffer (pH 7.4) or PBS buffer (pH 3.2).

REFERENCES

1. Khandare, J., and Minko, T., *Polymer-drug conjugates: Progress in polymeric prodrugs.* Prog. Polym. Sci., 2006. **31**(4): p. 359-397.

2. Li, C., and Wallace, S., *Polymer-drug conjugates: Recent development in clinical oncology.* Adv. Drug Deliver. Rev., 2008. **60**(8): p. 886-898.

3. Pasut, G., and Veronese, F.M., *Polymer-drug conjugation, recent achievements and general strategies.* Prog. Polym. Sci., 2007. **32**(8-9): p. 933-961.

4. Nakamura, K., Morishita, M., Ehara, J., Onuki, Y., Yamagata, T., Kamei, N., Lowman, A.M., Peppas, N.A., and Takayma, K., *Key functions in polymer carriers for intestinal absorption of insulin.* Int. J. Pharm., 2008. **354**(1-2): p. 135-142.

5. Wood, K.M., Stone, G., and Peppas, N.A., *Lectin functionalized complexation hydrogels for oral protein delivery.* J. Control. Release, 2006. **116**(2): p. e66-e68.

6. Lowman, A.M., Morishita, M., Kajita, M., Nagai, T., and Peppas, N.A., *Oral delivery of insulin using pH-responsive complexation gels.* J. Pharm. Sci., 1999. **88**(9): p. 933-937.

7. Duncan, G., Jess, T.J., Mohamed, F., Price, N.C., Kelly, S.M., and van der Walle, C.F., *The influence of protein solubilisation, conformation and size on the burst release from poly(lactide-co-glycolide) microspheres.* J. Control. Release, 2005. **110**(1): p. 34-48.

8. Hasan, A.S., Socha, M., Lamprecht, A., Ghazouani, F.E., Sapin, A., Hoffman, M., Maincent, P., and Ubrich, N., *Effect of the microencapsulation of nanoparticles on the reduction of burst release.* Int. J. Pharm., 2007. **344**(1-2): p. 53-61.

9. Huang, X., and Brazel, C.S., *On the importance and mechanisms of burst release in matrix-controlled drug delivery systems.* J. Control. Release, 2001. **73**(2-3): p. 121-136.

10. Luan, X., Skupin, M., Siepmann, J., and Bodmeier, R., *Key parameters affecting the initial release (burst) and encapsulation efficiency of peptide-containing poly(lactide-co-glycolide) microparticles.* Int. J. Pharm., 2006. **324**(2): p. 168-175.

11. Morishita, M., Goto, T., Peppas, N.A., Joseph, J.I., Torjman, M.C., Munsick, C., Nakamura, K., Yamagata, T., Takayama, K., and Lowman, A.M., *Mucosal insulin delivery systems based on complexation polymer hydrogels: effect of particle size on insulin enteral absorption.* J. Control. Release, 2004. **97**(1): p. 115-124.

12. Lowman, A.M., and Peppas, N.A., *Molecular analysis of interpolymer complexation in graft copolymer networks.* Polymer, 2000. **41**(1): p. 73-80.

CHAPTER 7

EVALUATION OF CALCITONIN-TRANSFERRIN CONJUGATES BY INVESTIGATION INTO LOADING AND RELEASE PROPERTIES FROM COMPLEXATION HYDROGELS

7.1 Introduction

In determining the potential efficacy of a new drug formulation being released from a polymer carrier, it is first necessary to investigate the interactions that occur between the carrier and the drug formulations as well as to understand the effect in will have on final bioavailability. Investigation into the interactions can consist of several different approaches. To determine how effectively the drug formulation will be incorporated into the polymer network, studies can be performed to load the formulation into the carrier in a manner similar to the way it would be carried out in preparation of the dosage form in an industrial setting. Once present within the polymer network, further studies can be performed to examine drug-polymer interactions with relation to release of the formulation from the carrier. Such investigations would typically be performed under conditions which are made to closely mimic the physiological conditions that would be relevant at the time of release within actual patients. Based on the results from the studies, either the formulation or the polymer carrier can be altered in such a way as to propagate the positive results and to create an optimal system for achieving maximum efficacy.

In Chapter 5, the therapeutic protein calcitonin was bound to transferrin to create a protein-transporter conjugate designed to improve specificity of the uptake as well as to increase transport of calcitonin into the bloodstream. The addition of transferrin to the therapeutic calcitonin offers a couple of advantages. Transferrin is resistant to tryptic and chymotryptic degradation [1], thereby protecting calcitonin and making the conjugate itself also resistant to degradation. Also, the ligand-receptor interaction which exists between transferrin and the transferrin receptor can be used to

increase specificity of the uptake as well to improve overall transport. However, the addition of transferrin to calcitonin also drastically increases the size of the molecule being loaded and released from the polymer carriers. In most cases, the increase in size of the encapsulated entity will have an adverse effect on the loading and release characteristics of the system. To determine the effect of the incorporation of the calcitonin-transferrin conjugate on the system properties, loading and release studies need to be performed to gain insight on potential performance of the conjugates under relevant conditions. Ideally, a large portion of the conjugate can be easily loaded into the network over a reasonable loading period and nearly all of the conjugate would be released within an hour upon introduction of the loaded particles into liquid simulating the small intestine.

The process of loading refers to the incorporation of the conjugate into or onto the polymer component to form a single system. Loading can occur in a number of different ways depending on the properties and requirements of the system. In some systems, therapeutic molecules are bound to polymers to enhance system properties such as improved transport and better stealth characteristics [2-4]. If the therapeutic drug needs to be protected, such as with most proteins, some systems will contain a larger polymer component such as a carrier network. In this case, the conjugate could still be covalently bound but are often times loaded into the polymer using diffusion. However, once loaded into the polymer network, it is also a lack of diffusion under certain conditions which keeps the conjugate molecule contained within the carrier [5, [6, 7]. Because the diffusion characteristics of the calcitonin-transferrin conjugate within the polymer network can be significantly altered using pH-responsive hydrogel carriers, the loading explored in this chapter is based on diffusion and occurs through equilibrium partitioning.

Release of the loaded therapeutic entity could also occur in a number of different ways. Most times, the release mechanism is simply the reverse process of the loading mechanism. In the case of covalently bound therapeutic drugs, the bond is

typically broken by the presence of certain conditions or molecules and the drug can be released freely. In the case of systems in which the drug was loaded using diffusion, the release also occurs based on diffusion but can be categorized in one of two ways. The mechanism of release can be initiated from a contraction or deswelling of the polymer carrier, resulting in a burst release of loaded therapeutics [8-11]. In contrast, the mechanism of release can also be triggered by an expansion or swelling of the polymer system, increasing the effective diffusion in and out of the system and allowing the therapeutic entity to diffuse out. In this chapter, release of calcitonin-transferrin conjugates from the polymer carriers is triggered by an expansion of the hydrogel carrier and subsequent increase in the effective diffusion of the conjugate.

Analysis of the loading and release processes for calcitonin-transferrin conjugates presents a unique challenge based on the properties of the calcitonin molecule. Unlike other therapeutic proteins such as insulin, calcitonin has an unusually high isoelectric point (pI) of approximately 8.0 [12]. In a loading process using calcitonin and anionic polymer hydrogels such as P(MAA-g-EG), the calcitonin molecules will contain a net positive charge due to the isoelectric point and the polymer carriers would contain overall negative charges in neutral media. The opposite charge interaction that exists between calcitonin and the polymer carriers would make loading incredibly effective and fast.

However, in release studies which are also performed in neutral media, the opposite charges create an attractive force which causes the calcitonin to remain in the polymer network, preventing any significant release. Modification of calcitonin by conjugation to a molecule such as transferrin can help to overcome this unique challenge inherent to calcitonin. Because of the drastically increased size and volume of transferrin relative to calcitonin, the addition of transferrin to calcitonin translates to a new molecule which takes on properties more similar to the original properties of transferrin. As demonstrated in earlier chapters, transferrin can be easily loaded and released from anionic hydrogels. The formation of calcitonin-transferrin conjugates,

while intended to increase specificity and overall transport, also serves the purpose of allowing efficient loading and release of therapeutic calcitonin with hydrogel carriers.

The loading and release characteristics of calcitonin-transferrin conjugates in complexation hydrogels are affected by a number of factors inherent to the system design. For example, it is essential to have an understanding of the possible interactions which may occur between the polymer and the conjugate when selecting materials on which to base a system. A common interaction which has a profound effect on loading and release characteristics is the surface charge interaction of both the polymer and the conjugate. The electrostatic forces which occur due to opposite charge attraction or like charge repulsion will have a significant effect on the rate and efficiency with which the conjugate loads and releases as well as how much is loaded and released. Also important in selecting materials for use is the hydrophilicity of both materials. Because loading and release is performed in solution, the respective hydrophilicities of both the polymer and conjugate play a significant role in whether the conjugate can load into the polymer properly.

Another set of factors which can influence the loading and release of calcitonin-transferrin conjugates are factors which relate to the diffusivity of the conjugate into and out of the polymer network. A major factor affecting diffusion within the system is the mesh size of the polymer network. The mesh size refers to the average space between crosslinks of the polymer network, or how much space there is for the conjugate to diffuse. The mesh size of the polymer is a direct function of the synthesis parameters of the polymer formation and can be easily controlled. Another factor affecting diffusion is the size of the conjugate molecule itself. The larger the molecule, the more difficult it is for it to diffuse through a given space based on a known mesh size. While the size of the calcitonin-transferrin conjugate is mostly limited by the choice of therapeutic and transporter proteins, it can be partially controlled by limiting the number of calcitonin molecules that attach to each transferrin molecule. The calcitonin

to transferrin ratio can be easily controlled by using specific protocol during the combination of the two modified proteins during the conjugate synthesis.

The factors which affect loading and release of a system can generally be controlled by modifying specific design specifications. For example, the diffusion within the system can be either enhanced or limited by controlling a number of specifications. Diffusion of the calcitonin-transferrin conjugate within the system can be increased by increasing the effective mesh size of the polymer network. A method to accomplish increasing the mesh size is to lengthen the crosslinker used to connect the polymer network, which will ultimately make the mesh size larger and can lead to better overall release. Also, by lowering the monomer-to-solvent ratio, the system becomes more porous and open and also leads to better overall release. Diffusion can also be increased by limiting the final size of the synthesized conjugate product. During the conjugation reaction of calcitonin-transferrin, the conjugate size is limited by stopping the reaction within 90 minutes. Crosslinker length, monomer-to-solvent ratio, and conjugate size are all controllable synthesis parameters which can be manipulated to achieve optimal diffusivity of the conjugate within the system.

Apart from factors affecting diffusivity within the system, other controllable parameters can also affect loading and release. Manipulation of the carrier particle size has an effect on diffusion as well. However, particle size does not affect the rate at which the conjugate diffuses, but rather the diffusion path length necessary for the conjugate to be released. Smaller particle sizes translate to a shorter, less tortuous path to release, leading to a quicker release and a better overall release in a given time [13]. Interactions which occur between the conjugate and polymer network can also have an effect on loading and release and can be controlled by the selection of materials for use in the system.

In this chapter, calcitonin-transferrin conjugates are tested with both P(MAA-g-EG) and P(MAA-co-NVP) polymer networks to determine which system has more desirable interactions with the conjugate molecule. In fact, P(MAA-co-NVP) polymers

are thought to have a stronger interpolymer complexation [14] but it is relatively unknown if they will have a desirable interaction with calcitonin-transferrin conjugates. Particle size and the materials selected for use with the system are two controllable synthesis parameters which have an effect on overall loading and release but are not related to changing the diffusivity of the calcitonin-transferrin conjugate.

The overall objectives of the studies performed in this chapter are to determine the performance with respect to loading and release of the calcitonin-transferrin conjugates with the hydrogel carriers already synthesized and also to optimize the system based on the results. In a previous chapter, the polymer carriers which are typically used to load and release smaller proteins such as insulin were tested with transferrin, a large protein, and the protocols were sufficiently adjusted to achieve desirable loading and release characteristics. In this chapter, calcitonin-transferrin conjugates will be loaded and released from a variety of polymer networks to examine performance and efficiency as well as determine which synthesis parameters lead to an optimal system. At the conclusion of the studies in this chapter, the goal is to find a polymer network which can successfully load calcitonin-transferrin conjugates and can also quickly release a large portion of the loaded conjugate in conditions simulating the small intestine. The ideal polymer for use with the calcitonin-transferrin conjugate will consist of specially selected materials and will be a precise combination of a number of synthesis parameters based on loading and release experiments performed in this chapter.

7.2 Materials and Methods

7.2.1 Polymer Microparticle Formation by UV Polymerization

P(MAA-g-EG) and P(MAA-co-NVP) were prepared using a free radical UV polymerization in solution. P(MAA-g-EG) was prepared by mixing MAA (Sigma-Aldrich Inc., St. Louis, MO) with poly(ethylene glycol) monomethyl ether monomethacrylate with a approximate molecular weight of 1000 (PEGMA1000, Polysciences Inc.,

Warrington, PA) in a 1:1 molar ratio of MAA:EG. P(MAA-co-NVP) was prepared by mixing MAA with NVP (Sigma-Aldrich Inc., St. Louis, MO) in a 1:1 molar ratio of MAA:NVP. Crosslinking agents were then added into the monomer mixtures consisting of MAA/EG or MAA/NVP. The crosslinking agents used within this study were tetraethylene glycol dimethacrylate (TEGDMA, Sigma-Aldrich Inc., St. Louis, MO) and poly(ethylene glycol) dimethacrylate with an approximately molecular weight of 1000 (PEGDMA1000, Polysciences Inc., Warrington, PA). The amount of crosslinker added to each monomer mixture was equal to 1 mol% of the total amount of monomer (MAA/EG or MAA/NVP). In order to eventually initiate the polymerization, the photoinitiator 1-hydroxycyclohexyl phenyl ketone (Irgacure 184, Sigma-Aldrich Inc., St. Louis, MO) was added to the polymerization mixture in the amount of 1 wt% of the total monomer added (MAA/EG or MAA/NVP). A solvent mixture consisting of 50:50 by weight deionized water (Milli-Q Plus system, Millipore) and ethanol (AAPER Alcohol, Shelbyville, KY) was added to the polymer mixture in the amounts of either 50:50, 60:40, or 67:33 by weight polymer mixture to solvent mixture. The presence of the solvent solution is essential to prevent autopolymerization as well as to produce a workable thin polymer film.

To ensure all components dissolved and went into a homogenous solution, the polymer mixture was sonicated for 15 minutes. After sonication, nitrogen was bubbled through the polymer solution within a nitrogen environment to eliminate oxygen. Oxygen is a free radical scavenger and significant oxygen levels could prematurely end the polymerization process. After removal of oxygen by nitrogen purging, the polymer mixture is poured between two glass slides (153 x 153 x 3 mm) separated by a Teflon spacer (0.7 mm) while still in a nitrogen environment. The glass slide apparatus containing the polymer solution spread into a thin film was then placed under a UV light source while still in a nitrogen environment. The solution was allowed to polymerize under the light source within an intensity range of 16-17 mW/cm^2 for 30 minutes. After the polymerization was completed, the polymer gels were removed from the nitrogen

environment, separated from the glass slides, and placed in deionized water. The polymer films were washed in the deionized water for 7 days to remove excess monomer and contaminants. After washing was completed, the polymers were dried in a vacuum oven at approximately 30° C for 2 days.

After completely drying the polymer films, they were removed from the vacuum oven and crushed into microparticles using a mortar and pestle. The crushed microparticles were then sieved into appropriate size ranges of either less than 75 microns, 90-150 microns, or 150-212 microns. The crushed and sieved microparticles were then stored in a vial within a desiccator to prevent moisture entering until further use.

7.2.2 Loading of Calcitonin-Transferrin Conjugates into Polymer Microparticles

Based on the previously established success of P(MAA-g-EG) being able to load large molecules, calcitonin-transferrin conjugates were loaded into a number of polymer formulations. The polymer formulations included P(MAA-g-EG) and P(MAA-co-NVP) and varied by synthesis parameters such as crosslinker length, monomer-to-solvent ratio, and particle size.

As a result of the previous conjugation reaction, calcitonin-transferrin conjugates were already dissolved in a PBS buffer (pH 7.4) at a known concentration as measured by HPLC. Calcitonin-transferrin stock solutions were prepared by diluting the conjugate solutions with PBS buffer (pH 7.4) to a concentration of 1 mg/mL and a volume of 40 mL. The stock solutions were placed in glass beakers which were siliconized using Sigmacote to reduce protein adhesion to the glass. To initiate the loading process, 280 mg of P(MAA-g-EG) or P(MAA-co-NVP) microparticles were added to each calcitonin-transferrin stock solution to reach a concentration of 7 mg/mL. Within the calcitonin-transferrin loading experiments, the conjugates were loaded into numerous different polymer formations which differed by crosslinker length, monomer-to-solvent ratio, particle size, and comonomer used. The calcitonin-transferrin conjugates in each

solution were allowed to load by equilibrium partitioning for 4 hours under constant stirring. At the conclusion of the loading period, 40 mL of 0.1 N HCl was added to the solution to lower the pH and collapse the particles. After allowing the particles to fully collapse, the loaded microparticles were filtered by passing the solution through filter paper. The particles were then washed using 2 mL deionized water to remove any excess calcitonin-transferrin conjugates adhered to the surface of the particle. The collected microparticles were then frozen at -80° C and lyophilized overnight to remove any excess water content. Once the lyophilization process had completed, the loaded microparticles were stored in a desiccator in a freezer until further use.

To determine initial concentration, an initial sample was taken before addition of microparticles and analyzed by HPLC. In order to calculate loading efficiencies at various time points of the loading process, additional samples were withdrawn after the end of the loading period, after the addition of HCl, and after the filtering of microparticles. Sampling at the end of the loading period gives an initial loading efficiency based solely on equilibrium partitioning. Taking a sample after the addition of HCl allows observation of the difference in loading from expulsion of protein molecules due to particle collapse. The final sample after filtering is used to determine a final loading percentage and also to determine the initial amount of calcitonin-transferrin conjugate being introduced in the release study. All withdrawn samples were filtered through syringe filters (PVDF, 0.22 µm) to ensure only free protein is being analyzed. All four samples for each loading procedure were analyzed using HPLC.

7.2.3 Calcitonin-Transferrin Conjugate Release Studies

Release studies for a therapeutic protein loaded into a polymer carrier are essential to understanding the dynamics of the system as well as to gain insight on the possible performance of the formulation when administered to human subjects. Specifically, release studies are necessary to shed light on two different properties of the system. The first property is the speed at which the conjugate is released. If

diffusion is too slow and significant release takes over an hour, then very little conjugate will be absorbed because of a finite residence time in the small intestine due to intestinal motility. Also, the overall amount of conjugate released into solution is very important as well. If a significant portion of loaded conjugate is not released from the microparticle within the residence time at the site of absorption, the chances for achieving a useful bioavailability in the bloodstream drops significantly.

Calcitonin-transferrin conjugate release studies were performed by placing approximately 10 mg of conjugate-loaded microparticles in 50 mL of PBS buffer (pH 7.4) in a dissolution apparatus. The dissolution apparatus water bath was maintained at 37° C and the experimental solutions were kept under constant stirring using impellers at 100 rpm. As the microparticles began to swell and release calcitonin-transferrin conjugates after addition to neutral buffer, small samples of 0.2 mL were taken at time points of 5, 10, 15, 30, 60, and 120 minutes to obtain release profiles versus time. The volume of the solution was maintained at 50 mL by addition of 0.2 mL of PBS buffer after each sample withdrawal. Needles were used with the syringes to minimize particle uptake and the sample volume was passed through syringe filters (PVDF, 0.22 μm) to ensure only free calcitonin-transferrin conjugates were being analyzed.

The initial amount of calcitonin-transferrin conjugates in the mass of particles added to the release study was determined by the data obtained from the previous calcitonin-transferrin loading experiments. Based on this initial mass of conjugate available for release, the free calcitonin-transferrin concentration at each time point was used to calculate a percentage of calcitonin-transferrin released up to that point. By analyzing several time points using HPLC to determine conjugate concentration in solution, it was possible to generate a release profile which indicates the rate at which calcitonin-transferrin is released as well as the total overall amount released.

7.2.4 Protein Sample Concentration Analysis by HPLC

High Performance Liquid Chromatography (HPLC) was used to analyze samples containing calcitonin-transferrin conjugates dissolved in PBS buffer (pH 7.4). The samples analyzed came from the loading and release studies for the calcitonin-transferrin conjugate. HPLC analysis was used for each sample to determine concentration based on absorbance values relative to absorbances of standard samples of known concentrations. Determining sample concentrations allows for the calculation of free protein in solution as well as loading efficiencies and release profiles.

The HPLC equipment used consists of a Waters 2695 Separation Module (Waters Corporation, Milford, MA) attached to a Waters 2487 Dual λ Absorbance Detector (Waters Corporation, Milford, MA). Analysis is performed using a reverse-phase analytical HPLC method designed to elute a wide range of proteins within a specified time period. The method includes the use of water (HPLC Grade, Fisher Scientific, Fair Lawn, NJ) with 0.1% by volume trifluoroacetic acid (TFA, ACROS Organics, Geel, Belgium) as Solvent A and acetonitrile (Optima, Fisher Scientific, Fair Lawn, NJ) with 0.08% by volume TFA as Solvent B. During the separation process, the mobile phase begins at a composition of 70% Solvent A and 30% Solvent B. The mobile phase changes composition using a gradient to 40% Solvent A and 60% Solvent B within 6 minutes. The mobile phase composition is then returned to initial conditions of 70% Solvent A and 30% Solvent B for the next sample to be analyzed. The mobile phase was introduced at a constant flow rate of 0.6 mL/min. All separations are performed using a Symmetry300^{TM} C4 column (particle size 5 μm, 3.9 mm I.D. x 150 mm length, Waters Corporation, Milford, MA) held at a constant temperature of 40°C. After separation of proteins, absorbance of the solution was detected at a wavelength of 220 nm. All instrument and processing methods were controlled and specified using the Empower software.

7.3 Results and Discussion

7.3.1 Polymer Microparticle Formation by UV Polymerization

A number of different formulations of polymer microparticles were synthesized for use in the loading and release experiments conducted in this chapter. Many different formulations were created including P(MAA-g-EG) and P(MAA-co-NVP) while also varying synthesis parameters such as crosslinker length (4 repeat units and 23 repeat units), monomer-to-solvent ratio (67:33, 60:40, and 50:50), and particle size (less than 75 microns, 90-150 microns, and 150-212 microns). The use of different systems yielded different results based on the effect of the synthesis parameters on loading and release studies. At the conclusion of the studies, a specific polymer formulation was chosen as the optimal formulation for use with calcitonin-transferrin conjugates. All formulations were successfully synthesized and determined to be usable for demonstrating loading and release characteristics of calcitonin-transferrin conjugates in conditions which mimic physiological environments.

7.3.2 Loading of Insulin-Transferrin Conjugates into Polymer Microparticles

To determine the performance characteristics of calcitonin-transferrin conjugates, they were loaded into P(MAA-g-EG) formulations. Several formulations were investigated to determine the effect of various synthesis parameters on loading and release characteristics of the system. The polymer microparticles tested included varying crosslinker lengths (4 repeat units and 23 repeat units), monomer-to-solvent ratios (67:33, 60:40, and 50:50), particle size (less than 75 microns, 90-150 microns, and 150-212 microns), and comonomer used (to form both P(MAA-g-EG) and P(MAA-co-NVP)). Based on the results from the investigation of each synthesis parameter, an ideal formulation in terms of loading can be identified for use with calcitonin-transferrin conjugates.

Analysis of the Effect of Crosslinker Length on Calcitonin-Transferrin Loading: Calcitonin-transferrin conjugates were loaded into two different P(MAA-g-EG) formulations which differed only by the length of the crosslinker. The crosslinkers used were TEGDMA (4 ethylene glycol repeat units) and PEGDMA1000 (approximately 23 ethylene glycol repeat units). Loading efficiencies were calculated at specific points throughout the loading process for both formulations using Equation 7.1 as shown below:

$$\text{Loading Efficiency} = \frac{C_0 - C_f}{C_0} \times 100\% \qquad (7.1)$$

The loading efficiencies for calcitonin-transferrin in the specified formulations are shown as Figure 7.1.

Figure 7.1 shows that a significant portion of the calcitonin-transferrin conjugates were effectively loaded into the P(MAA-g-EG) microparticles. Also, it shows that the presence of a longer crosslinker had a significant effect on the amount of conjugate loaded into the polymer network. The system that is crosslinked with the much shorter crosslinker TEGDMA achieves a final loading efficiency that is well over double the loading efficiency of the PEGDMA1000 crosslinked system. The reason for the noticeable difference is twofold. The use of a shorter crosslinker creates a more rigid network, forcing conjugate already loaded into the network to most likely remain in the polymer network due to the difficult path to diffuse out of the network. Also, upon particle collapse and surface rinsing, the longer crosslinker network is more open and loose, allowing more protein to be squeezed out due to contraction of the network. It is also interesting to note that a slightly higher loading efficiency in the TEGDMA crosslinked system is achieved *after* addition of acid.

The additional loaded conjugate can most likely be attributed to an increased charge interaction due to the presence of calcitonin and the significant lowering of solution pH. However, the increase is only minimal and is within the error of the data

samples. In comparing the two polymer formulations, the loading efficiencies are important to obtain but less important in choosing an ideal polymer for carrying calcitonin-transferrin conjugates. As previously mentioned, conjugate which is not loaded can potentially be recovered in an industrial process. The full analysis of crosslinker length with respect to optimization of the system can only occur after examining the subsequent release studies. While release studies have a major effect on maximum potential bioavailability, loading studies theoretically do not. However, loading efficiencies are important to understand and these experiments demonstrate that a significant portion of conjugate can be loaded.

Another indication of performance in loading studies is the polymer weight fraction of calcitonin-transferrin conjugates, or the weight fraction of the loaded microparticles which can be attributed to the presence of calcitonin-transferrin molecules. Because of the nature of loading protocols, the polymer weight fraction for most proteins is typically somewhat low (0.04-0.14) relative to the weight of the polymer. However, if the polymer weight fraction of a protein is even lower, then it would take a large amount of polymer to deliver a small amount of therapeutic protein, translating to an increased materials cost as well as larger dosage forms. Polymer weight fractions were calculated by taking the difference between the initial mass of protein in solution (M_0) and the final mass of protein in the solution (M_f) and dividing by the same difference ($M_0 - M_f$) added to the weight of polymer in the solution (M_p). Polymer weight fractions were calculated using Equation 7.2 as shown below:

$$\text{Polymer Weight Fraction} = \frac{M_0 - M_f}{(M_0 - M_f) + M_p} \qquad (7.2)$$

The polymer weight fractions of calcitonin-transferrin in each formulation previously mentioned are shown as Figure 7.2.

Figure 7.2 demonstrates that a larger fraction of a possible dosage form will be comprised of therapeutic calcitonin-transferrin conjugates in systems which contain shorter crosslinkers. A similar tendency can be observed in the loading efficiencies, but

the polymer weight fraction analysis also demonstrates the need to create larger dosage forms if the use of a longer crosslinker proves optimal based on release studies. However, the value of the polymer weight fraction for the longer crosslinked system indicates that a significant portion of the total dosage form is still calcitonin-transferrin, even though it is a reduced fraction relative to the shorter crosslinked system. While adjusting synthesis parameters, the benefits and drawbacks are often linked in such a way that the optimal system requires a balance of specific synthesis parameters.

Analysis of the Effect of Monomer-to-Solvent Ratios on Calcitonin-Transferrin Loading: Loading studies were performed by loading calcitonin-transferrin conjugates into three P(MAA-g-EG) polymer formulations which differed only by monomer-to-solvent ratios used during the synthesis procedure. The formulations included monomer-to-solvent ratios of 67:33, 60:40, and 50:50. Loading efficiencies were calculated at specific points throughout the loading process for all formulations using Equation 7.1. The loading efficiencies for calcitonin-transferrin conjugates in the specified formulations are shown as Figure 7.3.

As can be seen in Figure 7.3, all three of the polymer formulations were able to successfully load a large portion of the calcitonin-transferrin conjugates. Also, it is clear that the monomer-to-solvent ratio had a significant effect on the loading efficiencies of calcitonin-transferrin. The effect of monomer-to-solvent ratio on conjugate loading differs significantly in the case of the calcitonin-transferrin conjugate compared to the insulin-transferrin conjugate where there was no effect. In the case of calcitonin-transferrin conjugates, it appears that the addition of more monomer relative to solvent significantly decreases the loading efficiencies, particularly the final loading efficiency values. Changing the monomer-to-solvent ratio during the synthesis of the polymer in effect changes the way in which diffusion occurs within the system. If a polymer network is formed with very little solvent and mostly monomer, such as in the 67:33 formulation, then the diffusion is based solely on the effective mesh size of the network

and the conjugate must be able to diffuse between the crosslinked polymer strands. However, if the synthesis is carried out with the presence of more solvent, such as in the 50:50 formulation, the polymer network is forced to form *around* the solvent molecules, creating a more porous and open network. The additional solvent increases the "effective mesh size" of the system by allowing conjugates to diffuse through larger spaces, or pores, created by the presence of solvent. In this case, the system in which diffusion is based on porosity of the network achieved higher loading of calcitonin-transferrin conjugates than the systems where diffusion is based primarily on a smaller mesh size. In order to optimize the polymer carriers with respect to monomer-to-solvent ratios, it is necessary to examine the effect of the monomer-to-solvent ratio on release of the conjugates from the polymer carriers.

The effect of the monomer-to-solvent ratios on loading of calcitonin-transferrin conjugates was observed further by examining the polymer weight fractions of the conjugate-loaded microparticles as calculated by Equation 7.2. The polymer weight fractions for calcitonin-transferrin loaded in all three formulations are shown in Figure 7.4. Similar to the loading efficiencies, there a significant effect of the monomer-to-solvent ratio on the polymer weight fraction. The highest polymer weight fraction exists in the system which used the most solvent in the prepolymer mixture. The use of a system with high polymer weight fraction attributed to the conjugate translates to a more practical therapeutic dosage form.

Analysis of the Effect of Particle Size on Calcitonin-Transferrin Loading: Calcitonin-transferrin conjugates were loaded into three P(MAA-g-EG) formulations differing only in the average size of the microparticles. The three particle size ranges of formulations tested include less than 75 microns, 90-150 microns, and 150-212 microns. Loading efficiencies were calculated at specific points throughout the loading process for all formulations using Equation 7.1. The loading efficiencies for calcitonin-transferrin conjugates in the specified formulations are shown as Figure 7.5.

Figure 7.5 illustrates that a significant portion of calcitonin-transferrin conjugates were successfully loaded into all three polymer formulations. Also, the difference in particle size appears to have an effect on both the initial and final loading efficiencies. The effect of the particle size of a polymer carrier can be described in terms of volume or in terms of diffusion path length. As the diameter of the particle is increased, the volume of the particle increases exponentially and is able to carry or load more conjugate molecules.

However, conjugate molecules which are loaded into the center of the polymer network of a larger particle have a longer diffusion path length in order to diffuse out of the system. The longer diffusion path means a more tortuous journey for the conjugate molecules and thus a slower and less complete release. In terms of loading, the effect of particle size is most directly related to the volume that the particle can hold. Specifically, the surface area-to-volume ratio has some effect on the amount of conjugate loaded in each formulation. Among the three formulations, the smallest particles achieved the both the highest initial and final loading efficiencies compared to the larger particles. In the case of loading calcitonin-transferrin conjugates, the initial loading efficiencies were similar, indicating that volume considerations and surface area-to-volume ratios have little to do with the initial loading of this particular conjugate. However, the effect of particle size can be observed after collapse and surface washing of the microparticles. With respect to final loading efficiencies, the smaller particles exhibited more desirable loading characteristics for loading calcitonin-transferrin conjugates. To fully optimize the system with respect to particle size, release studies must be performed to determine the full effect of the particle size of the carrier.

Additional insight into the effect of particle size on the loading of calcitonin-transferrin conjugates in P(MAA-g-EG) microparticles was gained by analyzing the polymer weight fractions of the conjugate as calculated by Equation 7.2. The polymer weight fractions for calcitonin-transferrin conjugates loaded in all three formulations are shown in Figure 7.6. As evident in the figure, the polymer weight fraction due to the

calcitonin-transferrin conjugate decreased as the particle size was increased. Therefore, use of smaller microparticles as carriers for calcitonin-transferrin conjugates is more desirable due to the practical advantage of being able to administer smaller dosage forms. Also, the polymer weight fractions attributed to the conjugate in the cases of the two larger particle sizes are low (<0.035), which means an effective dosage form would require much more polymer and consequently would be much larger, decreasing effectiveness and potential profit margins.

Analysis of the Effect of the Replacement of PEG Comonomer with NVP Comonomer on Calcitonin-Transferrin Loading: Loading studies were performed by loading calcitonin-transferrin conjugates into P(MAA-g-EG) and P(MAA-co-NVP) polymer microparticles which differed only by the comonomer used. Loading efficiencies were calculated at specific points throughout the loading process for both formulations using Equation 7.1. The loading efficiencies for calcitonin-transferrin conjugates in P(MAA-g-EG) and P(MAA-co-NVP) are shown as Figure 7.7.

As can be seen in Figure 7.7, both P(MAA-g-EG) and P(MAA-co-NVP) were able to effectively load a significant portion of calcitonin-transferrin conjugates placed in solution. Also, the difference between the two formulations with respect to loading efficiencies was evident in both the initial and final loading efficiencies. While P(MAA-g-EG) had higher initial and final loading efficiencies, it is interesting to note that there was virtually no decrease in loading efficiency before and after particle collapse and surface washing for P(MAA-co-NVP). The differences in loading between the systems can be attributed to the different interactions between the calcitonin-transferrin conjugate and either the PEG tethers or NVP repeat units. Interactions which may have an effect include surface charge interactions, physical hindrance, hydrophilicity, and interpolymer interactions. Based on the results, the loading efficiencies were significantly affected by the interactions based on the presence of the comonomer both before and after particle collapse and surface washing. The presence of a specific

comonomer is likely to have an even more significant role in the subsequent release studies because of the importance of the interpolymer interactions governing the rate of swelling as well as the hydrophilicity of each group significantly affecting the release properties.

The effect of the presence of the PEG and NVP comonomers on the loading of calcitonin-transferrin conjugates was further investigated by determining the polymer weight fractions of calcitonin-transferrin as calculated by Equation 7.2. The polymer weight fractions for calcitonin-transferrin conjugates loaded in both P(MAA-g-EG) and P(MAA-co-NVP) are shown in Figure 7.8. Similar to the loading efficiencies, a significant difference was observed between the polymer weight fractions of the calcitonin-transferrin conjugate in P(MAA-g-EG) and P(MAA-co-NVP). The polymer weight fraction of calcitonin-transferrin in P(MAA-g-EG) was well over double of the polymer weight fraction of the conjugate in P(MAA-co-NVP). Also, it is important to note that P(MAA-g-EG) had a polymer weight fraction above 0.08, indicating that the polymer could serve as a potential carrier for calcitonin-transferrin conjugates in a dosage form. As with all four synthesis parameters investigated, system optimization will most likely depend more on the release characteristics in simulated physiological conditions because of the increased effect on potential bioavailability. However, loading studies are important to perform with respect to each synthesis parameter in order to verify loading of a significant amount of conjugate, to obtain polymer weight fractions to better envision the possibility of an effective and practical dosage form, and to better understand how each manipulated synthesis parameter affects the diffusion of the conjugate within the polymer network.

7.3.3 Calcitonin-Transferrin Conjugate Release Studies

Calcitonin-transferrin conjugates were loaded into a number of different polymer formulations including P(MAA-g-EG) and P(MAA-co-NVP) synthesized using a number of different synthesis parameters. The formulations were found to all be able

to load an appreciable amount of calcitonin-transferrin conjugate in solution as well as having a significant polymer weight fraction attributed to the protein. The conjugate-loaded microparticles from each formulation were then investigated using release studies. The formulations included systems with varying crosslinker lengths (4 repeat units and 23 repeat units), monomer-to-solvent ratios (67:33, 60:40, and 50:50), particle size (less than 75 microns, 90-150 microns, and 150-212 microns), and comonomer used (to form both P(MAA-g-EG) and P(MAA-co-NVP)). Based on the results obtained from the investigation of the loading and release studies for each synthesis parameter, an optimal polymer formulation to achieve maximum potential bioavailability was identified and chosen for future use with calcitonin-transferrin conjugates.

Analysis of the Effect of Crosslinker Length on the Release of Calcitonin-Transferrin: Calcitonin-transferrin conjugates were previously loaded into two different P(MAA-g-EG) formulations which differed only in the length of the crosslinker. The crosslinkers used were TEGDMA (4 ethylene glycol repeat units) and PEGDMA1000 (approximately 23 ethylene glycol repeat units). Release studies were performed by placing the conjugate-loaded microparticles in PBS buffer (pH 7.4) and measuring the conjugate concentration in solution over time. The percentage released at each time point was calculated by taking a ratio of the amount of conjugate at the specified time to the initial amount of conjugate present in the loaded particles. The release profiles for calcitonin-transferrin as released from the specified formulations are shown as Figure 7.9.

Figure 7.9 shows that while both formulations released a significant amount of conjugate within 2 hours, the longer crosslinked system released approximately 30% more than the system crosslinked with TEGDMA by the conclusion of the release period. The significant difference in release is a result of the effect of incorporation of a longer crosslinker within the polymer network. The crosslinker PEGDMA1000 is over 5 times longer than TEGDMA, creating a polymer network with a larger mesh size which

consequently is more open to diffusion of a large molecule such as the conjugate. The increased space between polymer strands allows loaded conjugate in the PEGDMA1000 crosslinked formulation to diffuse out of the system much quicker and in a higher quantity over a specified time period. The loading and polymer weight fraction results demonstrate a preference for using the TEGDMA crosslinked system, but the release profiles clearly justify the use of longer crosslinkers for polymer carriers for insulin-transferrin conjugates. From within 10 minutes into the study to the conclusion, the amount of calcitonin-transferrin conjugate released from the PEGDMA1000 crosslinked system is an additional 50% relative to the amount released from the TEGDMA crosslinked system. Because of the improved release using a longer crosslinker, even longer crosslinkers such as PEGDA4000 were used as crosslinkers in some experimental systems. However, the resultant polymer films were not rigid enough and were unmanageable due to the introduction of an extremely long crosslinker. However, the additional calcitonin-transferrin conjugate released in the case of the PEGDMA1000 crosslinked formulation relative to the TEGDMA crosslinked system equates to higher potential bioavailability and increased potential efficacy of a possible oral formulation.

Analysis of the Effect of Monomer-to-Solvent Ratios on the Release of Calcitonin-Transferrin: Calcitonin-transferrin conjugates were previously loaded into three different P(MAA-*g*-EG) formulations which differed only in the monomer-to-solvent ratios used during synthesis. The formulations included monomer-to-solvent ratios of 67:33, 60:40, and 50:50. Release studies were performed by placing the conjugate-loaded microparticles in PBS buffer (pH 7.4) and measuring the conjugate concentration in solution over time. The percentage released at each time point was calculated by taking a ratio of the amount of conjugate at the specified time to the initial amount of conjugate present in the loaded particles. The release profiles for calcitonin-transferrin as released from the specified formulations are shown as Figure 7.10.

Figure 7.10 illustrates that all three formulations were able to release at least a sizable portion of the loaded calcitonin-transferrin conjugates. The data also shows that changing the monomer-to-solvent ratio has very little effect on release of calcitonin-transferrin other than a quicker initial release in the case of the system which contained the most solvent (50:50). Changing the balance of the monomer-to-solvent ratio in the prepolymer mixture in effect changes the way in which diffusion occurs throughout the system. If a large amount of monomer relative to solvent is used, such as in the 67:33 formulation, then diffusion characteristics are based solely on the effective mesh size of the network, forcing the conjugate to diffuse within the spaces created between the crosslinked polymer strands. However, if the monomer-to-solvent ratio is changed to favor adding more solvent, such as in the 50:50 formulation, the polymer network forms around the solvent molecules, creating a more porous and open network. The additional solvent increases the "effective mesh size" of the system by allowing conjugates to diffuse through larger spaces, or pores, created by the presence of solvent in the prepolymer mixture. In the case of the release of calcitonin-transferrin, the increased "effective mesh size" and increased diffusion only generated the small effect of increasing the amount released with 10-15 minutes. However, even though the release characteristics varied very little between the three formulations, the loading studies combined with a higher initial release clearly require that the monomer-to-solvent ratio of the prepolymer mixture must be as low as possible to achieve an optimal system. Because more solvent present in the synthesis led to preferable system properties, experimental systems were synthesis with monomer-to-solvent ratios of 40:60 and 33:67. However, the syntheses produced films which were gel-like and unmanageable in terms of washing excess monomer and subsequent crushing. The formulation successfully synthesized using the lowest monomer-to-solvent ratio, which was 50:50, was chosen as the optimal system because of the significantly better loading characteristics as well as the prospect of delivering more calcitonin-transferrin to the site of absorption over a short time period.

Analysis of the Effect of Particle Size on the Release of Calcitonin-Transferrin: Calcitonin-transferrin conjugates were previously loaded into three different P(MAA-g-EG) formulations which differed only in particle size. The formulations included P(MAA-g-EG) microparticles in size ranges of less than 75 microns, 90-150 microns, and 150-212 microns. Release studies were performed by placing the conjugate-loaded microparticles in PBS buffer (pH 7.4) and measuring the conjugate concentration in solution over time. The percentage released at each time point was calculated by taking a ratio of the amount of conjugate at the specified time to the initial amount of conjugate present in the loaded particles. The release profiles for calcitonin-transferrin as released from the specified formulations are shown as Figure 7.11.

As can be seen in Figure 7.11, all three formulations were able to release a significant portion of the loaded calcitonin-transferrin conjugate. However, there is a substantial increase in the overall amount of conjugate released as the particle size becomes smaller and smaller. The relationship between amount of conjugate released and particle size of the carrier can best be described by the concept of diffusion path length. In smaller particles, the loaded conjugate has a shorter distance to diffuse before being completely released from the system. In contrast, a large molecule presents a more tortuous and longer path for the release of conjugate, translating to slower release and a reduction in overall release over a short period. The diffusion path length plays a considerable role in the release characteristics of the conjugate and can drastically change the release profiles of the dosage form. Based on the results, the ideal particle size for polymer carriers for calcitonin-transferrin conjugates was determined to be less than 75 microns. It is difficult to reduce the upper end of the size range due to the difficulty in creating smaller particles using the crushing method which uses a mortar and pestle. If a different type of polymerization were used which could control the size down to a smaller range, the release of conjugates would likely see even greater benefit. However, using the specific protocol outlined in Chapter 4, the

microparticles of size range of less than 75 microns were used to achieve the highest potential bioavailability.

Analysis of the Effect of the Replacement of PEG Comonomer with NVP Comonomer on the Release of Calcitonin-Transferrin: Calcitonin-transferrin conjugates were previously loaded into P(MAA-g-EG) and P(MAA-co-NVP) formulations which differed only by the comonomer used. Release studies were performed by placing the conjugate-loaded microparticles in PBS buffer (pH 7.4) as well as PBS buffer (pH 3.2) and measuring the conjugate concentration in solution over time. The release studies performed under acidic conditions were performed to examine how the particles would perform in the collapsed state, or to observe if any conjugate was prematurely released in conditions mimicking the stomach. The percentage released at each time point was calculated by taking a ratio of the amount of conjugate at the specified time to the initial amount of conjugate present in the loaded particles. The release profiles for calcitonin-transferrin as released from the specified formulations are shown as Figure 7.12.

Figure 7.12 illustrates that both P(MAA-g-EG) and P(MAA-co-NVP) polymer formulations were able to release a portion of the loaded calcitonin-transferrin conjugate under neutral pH conditions. However, release studies performed under acidic conditions showed that P(MAA-g-EG) released a minute fraction of the loaded conjugate while P(MAA-co-NVP) did not release any conjugate under acidic conditions. Also, the release studies performed under neutral conditions showed that the P(MAA-g-EG) polymer formulation far outperformed the P(MAA-co-NVP) formulation by releasing much more conjugate over the entire release period. The major difference between these two comonomers is the interpolymer interactions and the resultant degree of complexation. NVP is thought to have a higher degree of complexation with MAA than PEG does, allowing for the interpolymer bonds in P(MAA-co-NVP) to be stronger than those in P(MAA-g-EG). The selection of NVP as a possible replacement for the PEG comonomer was based on its degree of complexation and such a property was

determined to have an advantageous effect on protection of the conjugate under acidic conditions. However, it was the strong interpolymer interactions which also most likely limited the release of conjugate from P(MAA-co-NVP) particles. While the degree of complexation in the collapsed state may have been higher in P(MAA-co-NVP), the P(MAA-g-EG) particles released very little of the conjugate under acidic conditions, demonstrating that the P(MAA-g-EG) system also has a suitably high degree of complexation. Therefore, the additional complexation in the collapsed state in the P(MAA-co-NVP) system was deemed unnecessary for protection of a large molecule such as the calcitonin-transferrin conjugate. In fact, the strong complexation in the P(MAA-co-NVP) system most likely limited the release of the conjugate under neutral conditions while the relatively weaker complexation allowed for greater release in the P(MAA-g-EG) system. If the therapeutic were a smaller protein, such as insulin by itself, the additional protection from the complexation of P(MAA-co-NVP) may be necessary. Moreover, in the less complexed system of P(MAA-g-EG), the insulin may be able to diffuse out under acidic conditions. However, for the specific case of the calcitonin-transferrin conjugate, the P(MAA-g-EG) microparticles were found to be the preferred formulation as a carrier for the conjugate because of the significantly improved release and concurrently the improved potential bioavailability of a possible oral formulation.

Determination of an Optimal Polymer Formulation for the Delivery of Calcitonin-Transferrin Conjugates: Several polymer formulations were synthesized in an effort to determine an optimal polymer formulation to achieve high bioavailability of orally delivered calcitonin-transferrin conjugates. The polymer formulations included P(MAA-g-EG) and P(MAA-co-NVP) while also varying synthesis parameters such as crosslinker length (4 repeat units and 23 repeat units), monomer-to-solvent ratio (67:33, 60:40, and 50:50), and particle size (less than 75 microns, 90-150 microns, and 150-212 microns). Each formulation was loaded with calcitonin-transferrin conjugates and subsequently released to determine loading efficiencies and release profiles. As each synthesis

parameter was investigated, all other synthesis parameters and values were held constant. At the conclusion of the studies, the release characteristics were the primary determining factor in selecting an optimal carrier. The loading efficiencies and polymer weight fractions were determined to verify that each formulation could indeed load a significant portion of conjugate and also the loading studies were used as a secondary criteria for selecting the optimal polymer carrier for calcitonin-transferrin conjugates.

The investigation of the effect of crosslinker length yielded that the longest crosslinker (PEGDMA1000) would provide the best release characteristics. After testing monomer-to-solvent ratios, it was determined that release profiles differed very little but including as much solvent as possible in the prepolymer mixture (50:50 monomer-to-solvent) was chosen to obtain a quicker initial release and more desirable loading characteristics. The experiments on the effect of particle size of the carrier demonstrated that the smallest particles (less than 75 microns) achieved the highest overall release. The studies in which the PEG comonomer was replaced with the NVP comonomer illustrated that while NVP may complex better under acidic conditions, the extra protection in mostly unnecessary in the case of a large molecule such as calcitonin-transferrin conjugates and that P(MAA-g-EG) particles are preferred as carriers due to the much improved release characteristics. Within the parameters specified in this chapter and manipulation only to the extent that polymers could be successfully synthesized, the ideal polymer carrier for oral delivery of calcitonin-transferrin conjugates was found to be P(MAA-g-EG) particles synthesized using a monomer-to-solvent ratio of 50:50, crosslinked with PEGDMA1000, and having a particle size of less than 75 microns.

7.3.4 Protein Sample Concentration Analysis by HPLC

All samples obtained from loading and release studies were analyzed by HPLC. The concentration of each sample was determined by comparisons to standards of known concentrations. The experimental concentration of each sample was used to

calculate the free protein concentration in the solution at the time the sample was withdrawn. In the cases of values of zero concentration as in the release studies performed under acidic conditions, the free protein in the samples was at a concentration low enough to be undetectable by HPLC.

7.4 Conclusions

Calcitonin-transferrin conjugates were successfully synthesized and required investigation into the *in vitro* characteristics with relation to loading and release in polymer microparticle carriers. To determine the ideal polymer formulation to use as a carrier for the conjugate, several polymer formulations were tested using loading and release studies to obtain performance characteristics. The polymer formulations included P(MAA-g-EG) and P(MAA-co-NVP) and also differed in synthesis parameters such as crosslinker length, monomer-to-solvent ratio, and particle size. Loading studies performed on all formulations verified that each formulation was capable of loading a significant amount of calcitonin-transferrin conjugates and that a few polymer formulations were marginally better at loading calcitonin-transferrin conjugates. Upon performing release studies, the selected polymer formulation for optimal release characteristics for obtaining high bioavailability upon administration was P(MAA-g-EG) microparticles less than 75 microns in size, crosslinked with PEGDMA1000, and synthesized using a 50:50 monomer-to-solvent ratio. The selected optimized polymer carrier along with the synthesized calcitonin-transferrin conjugates received further investigation into their properties and potential to achieve high bioavailability upon administration by evaluation via cell studies performed in a later chapter.

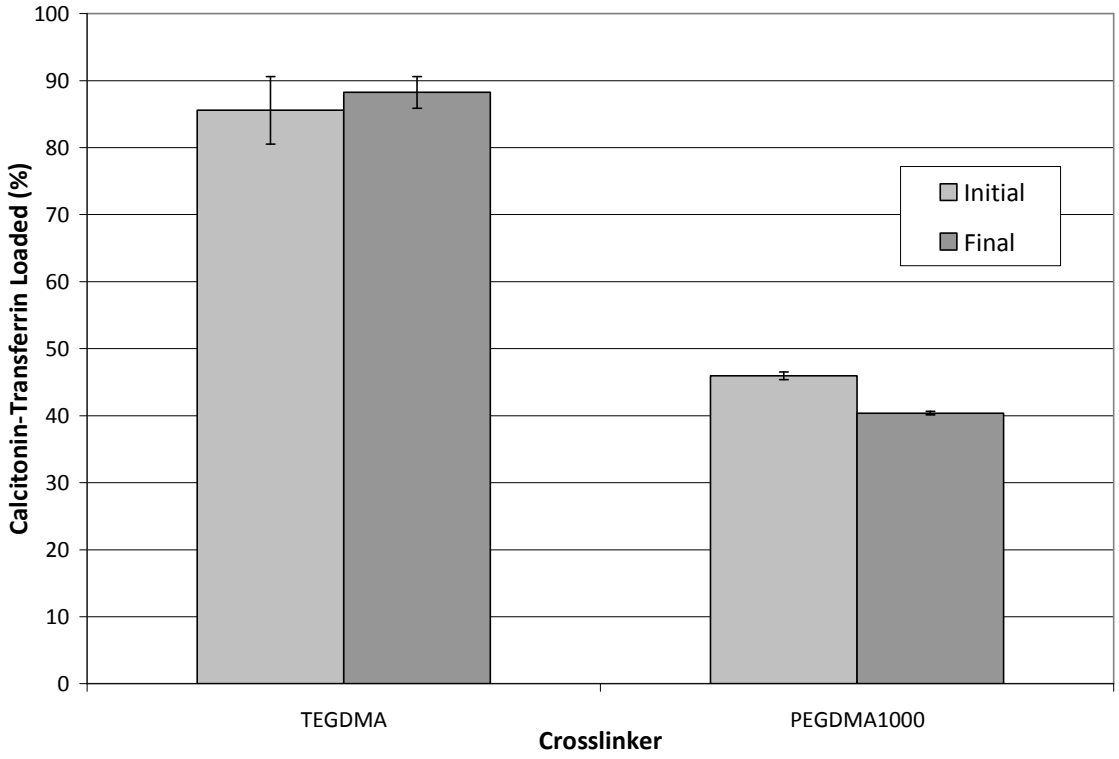

Figure 7.1 Loading efficiencies of calcitonin-transferrin conjugates in P(MAA-g-EG) microparticles of differing crosslinker lengths before and after particle collapse and surface washing.

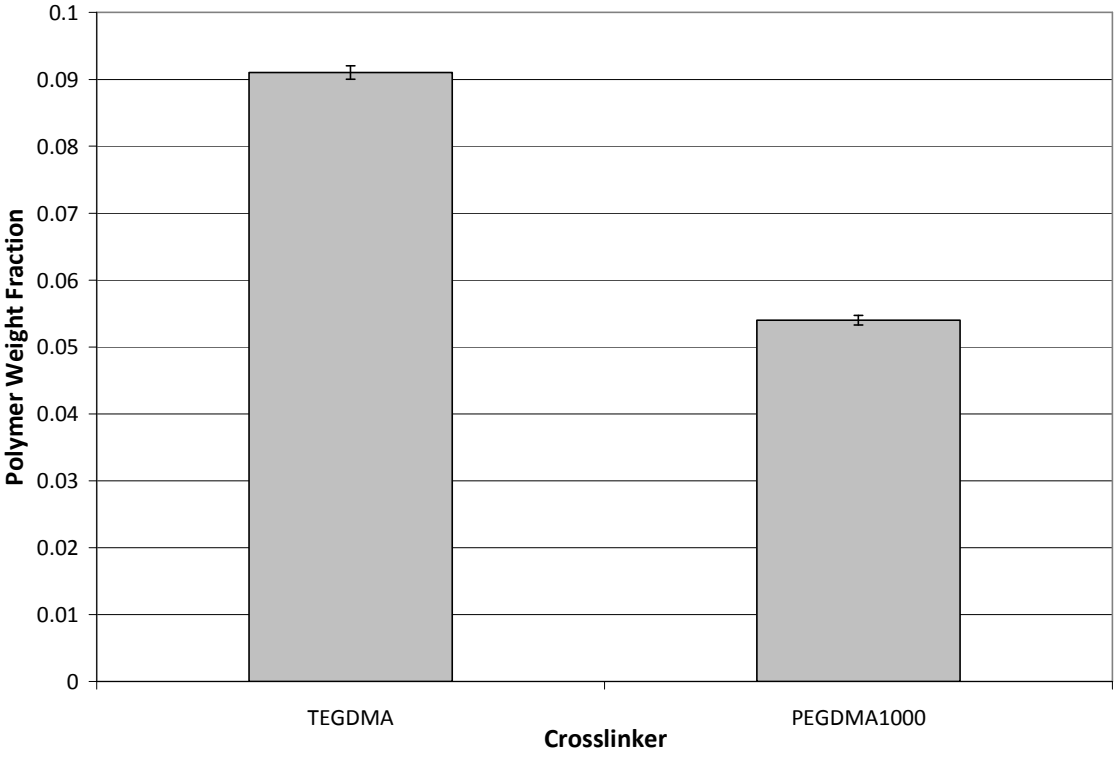

Figure 7.2 Polymer weight fractions of calcitonin-transferrin in loaded P(MAA-g-EG) formulations of differing crosslinker lengths.

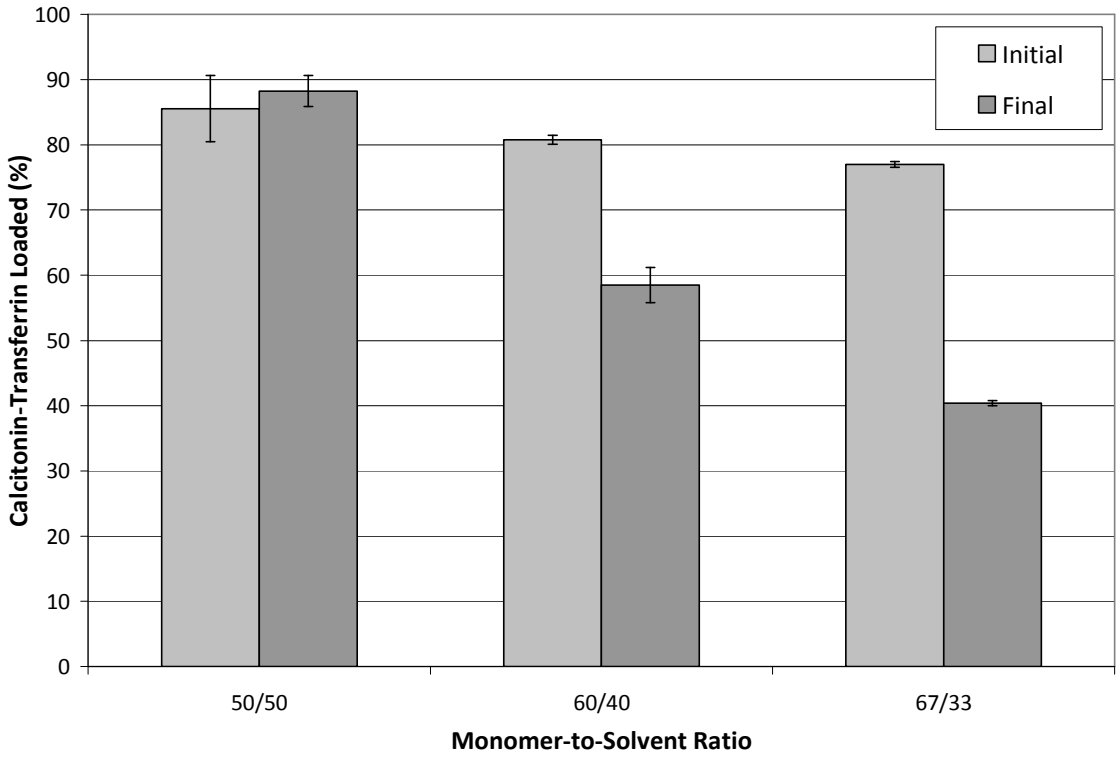

Figure 7.3 Loading efficiencies of calcitonin-transferrin conjugates in P(MAA-g-EG) formulations of differing monomer-to-solvent ratios before and after particle collapse and surface washing.

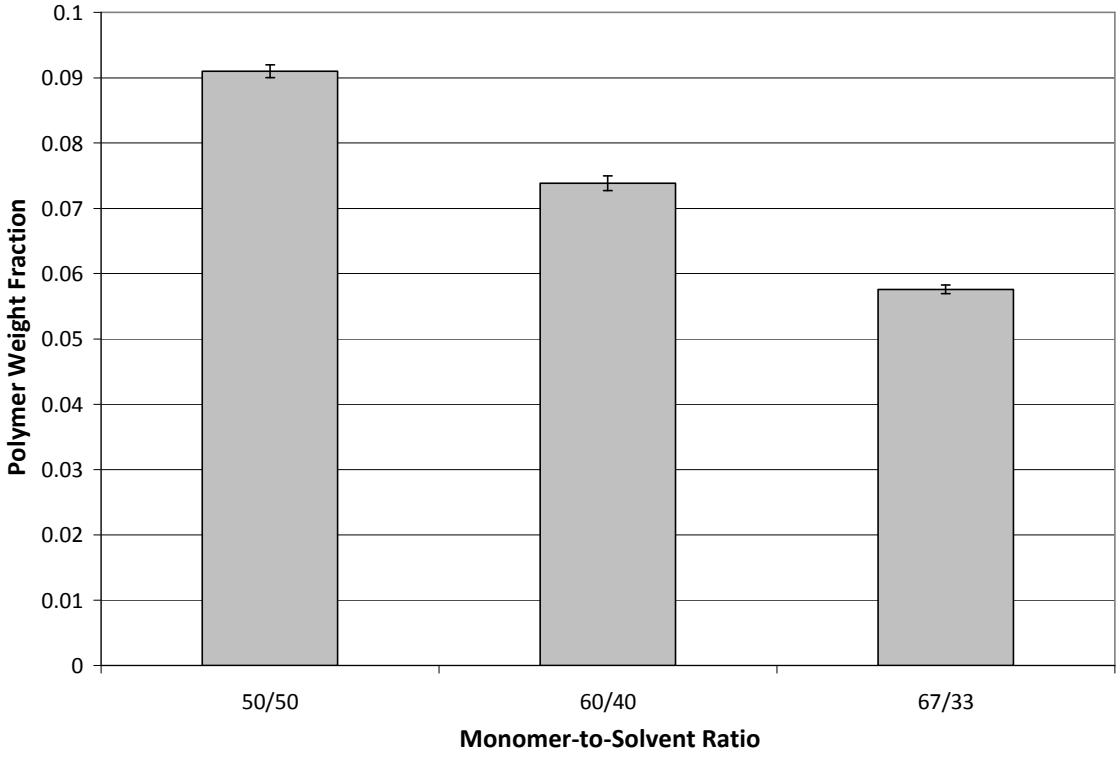

Figure 7.4 Polymer weight fractions of calcitonin-transferrin conjugates in P(MAA-g-EG) formulations synthesized using different monomer-to-solvent ratios.

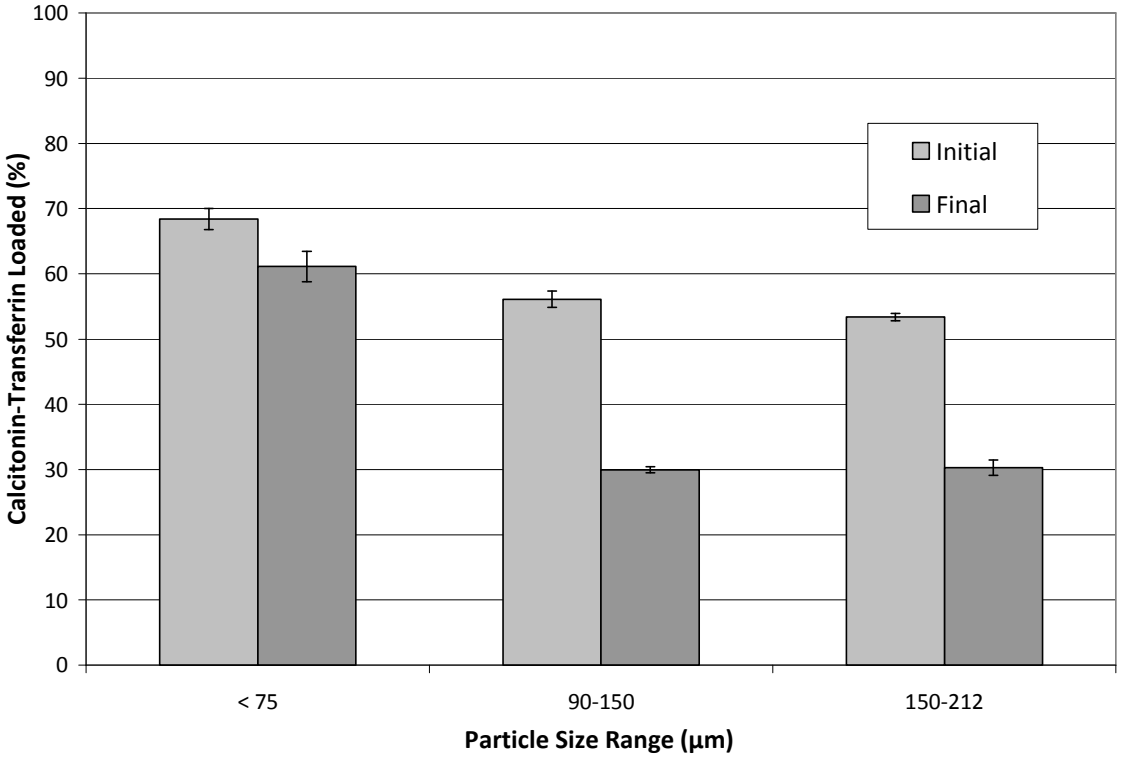

Figure 7.5 Loading efficiencies of calcitonin-transferrin conjugates in P(MAA-g-EG) formulations of differing particle sizes before and after particle collapse and surface washing.

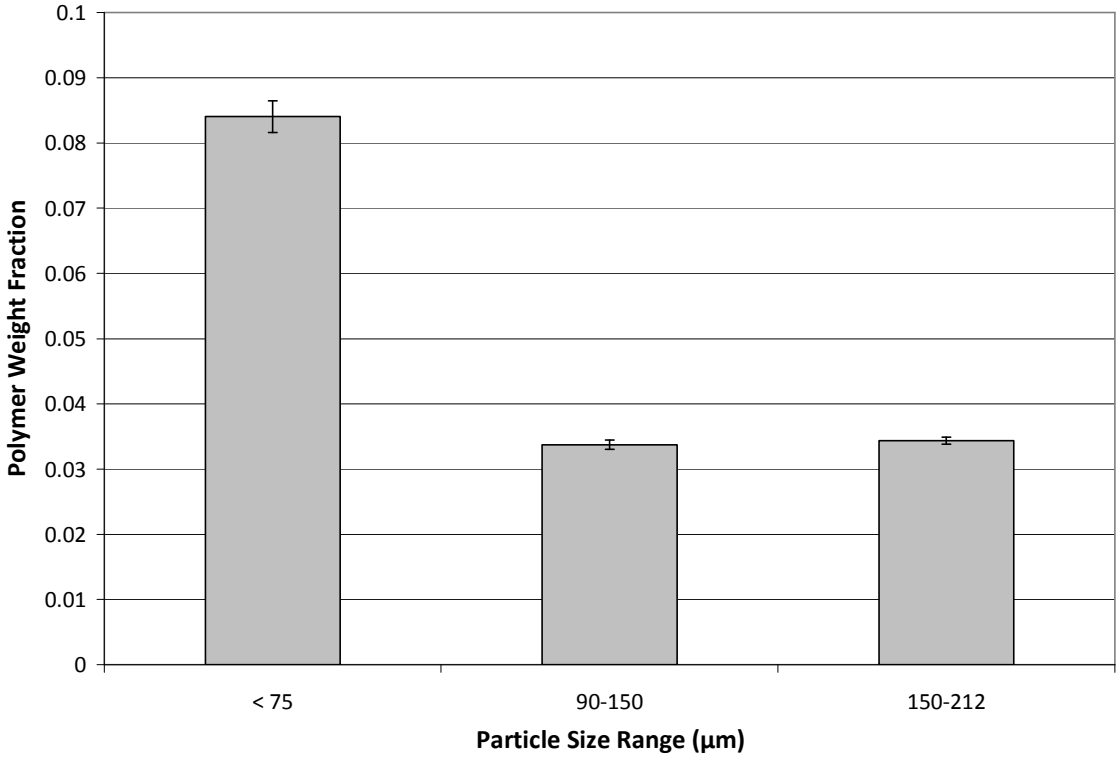

Figure 7.6 Polymer weight fractions of calcitonin-transferrin conjugates in P(MAA-g-EG) formulations of different particle size ranges.

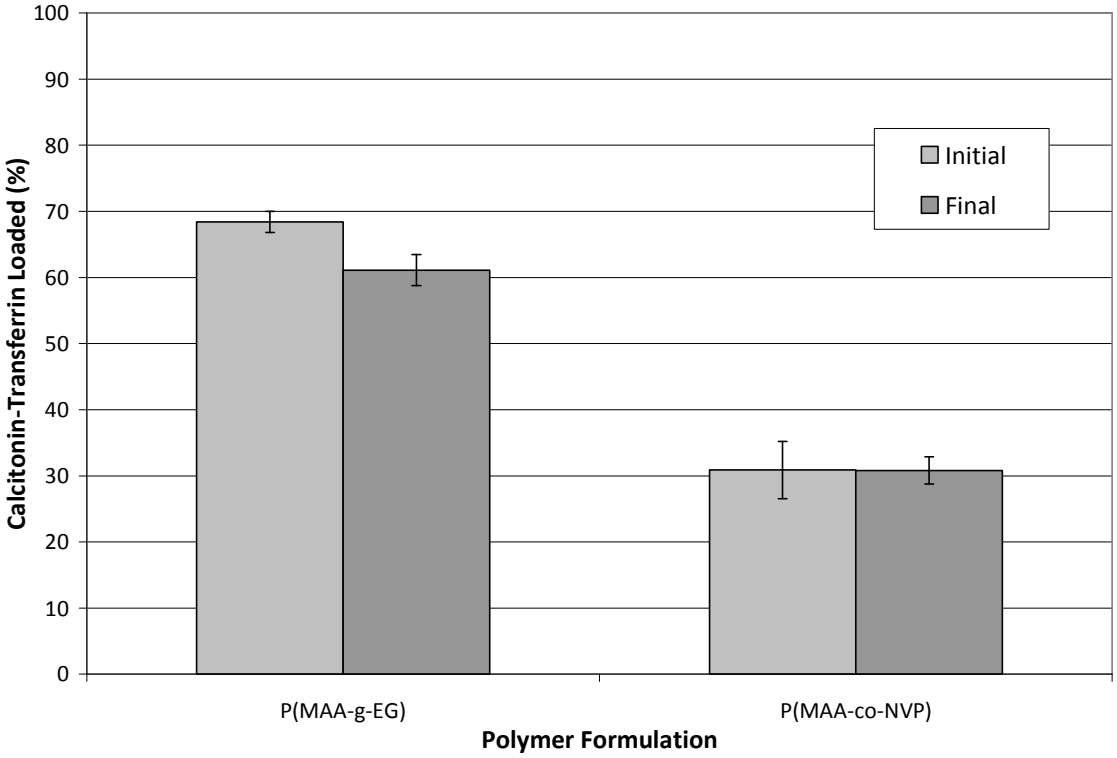

Figure 7.7 Loading efficiencies of calcitonin-transferrin conjugates in P(MAA-g-EG) and P(MAA-co-NVP) polymer formulations before and after particle collapse and surface washing.

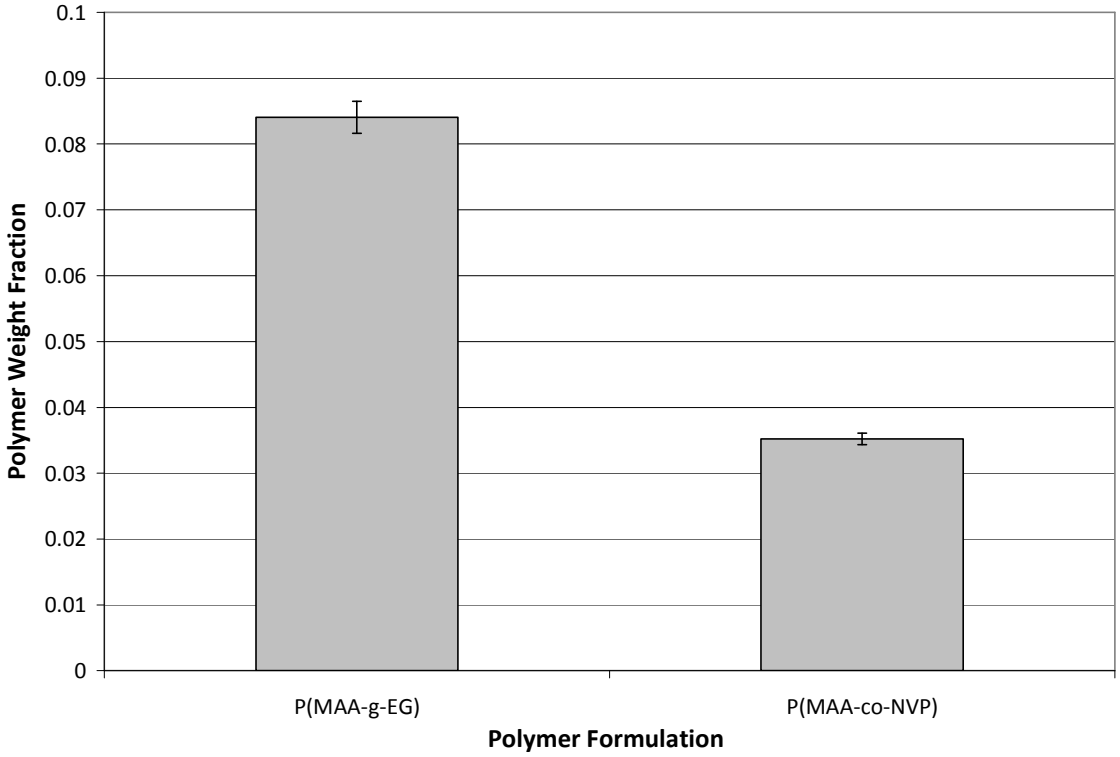

Figure 7.8 Polymer weight fractions of calcitonin-transferrin conjugates in P(MAA-g-EG) and P(MAA-co-NVP) polymer formulations.

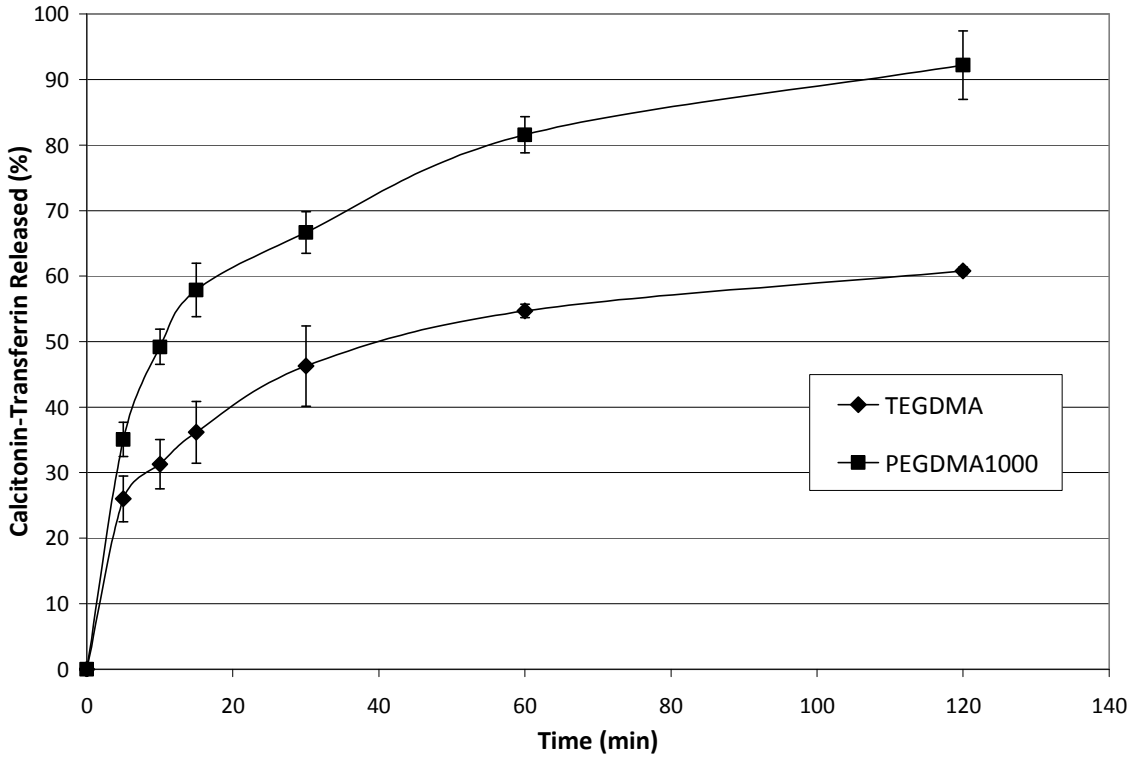

Figure 7.9 Release profiles of calcitonin-transferrin conjugates loaded in P(MAA-g-EG) microparticles of differing crosslinker lengths and placed in PBS buffer (pH 7.4).

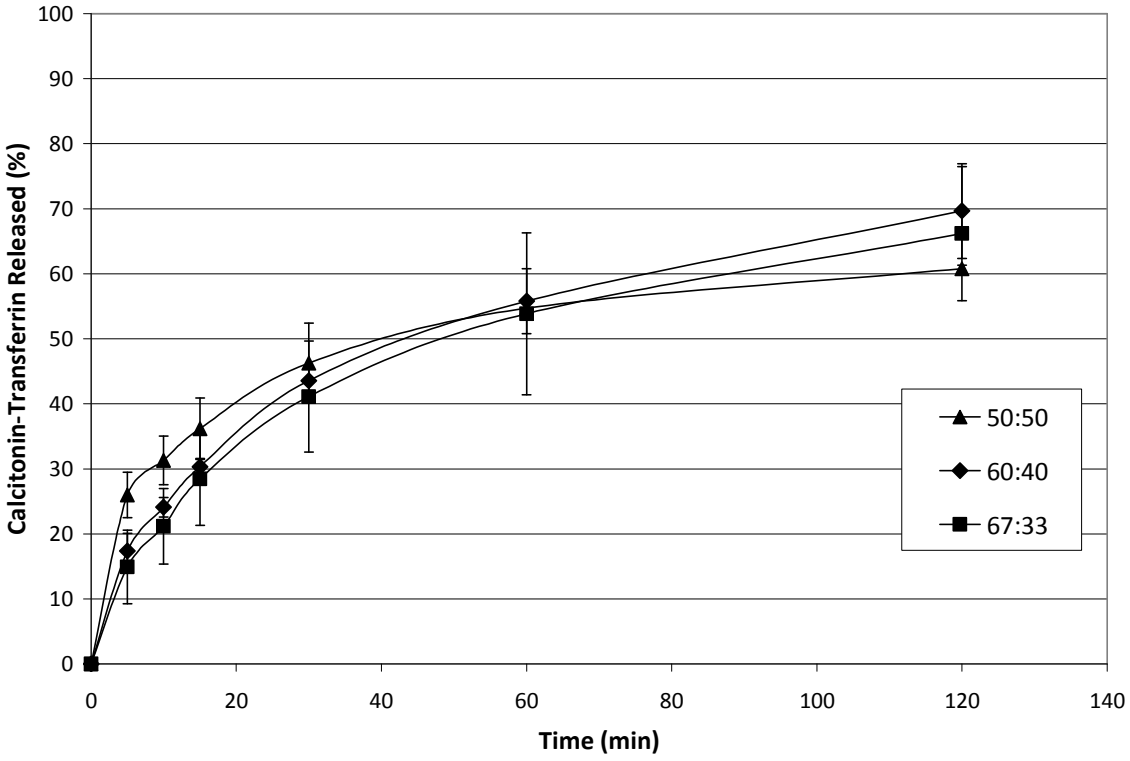

Figure 7.10 Release profiles of calcitonin-transferrin conjugates loaded in P(MAA-g-EG) microparticles of differing monomer-to-solvent ratios and placed in PBS buffer (pH 7.4).

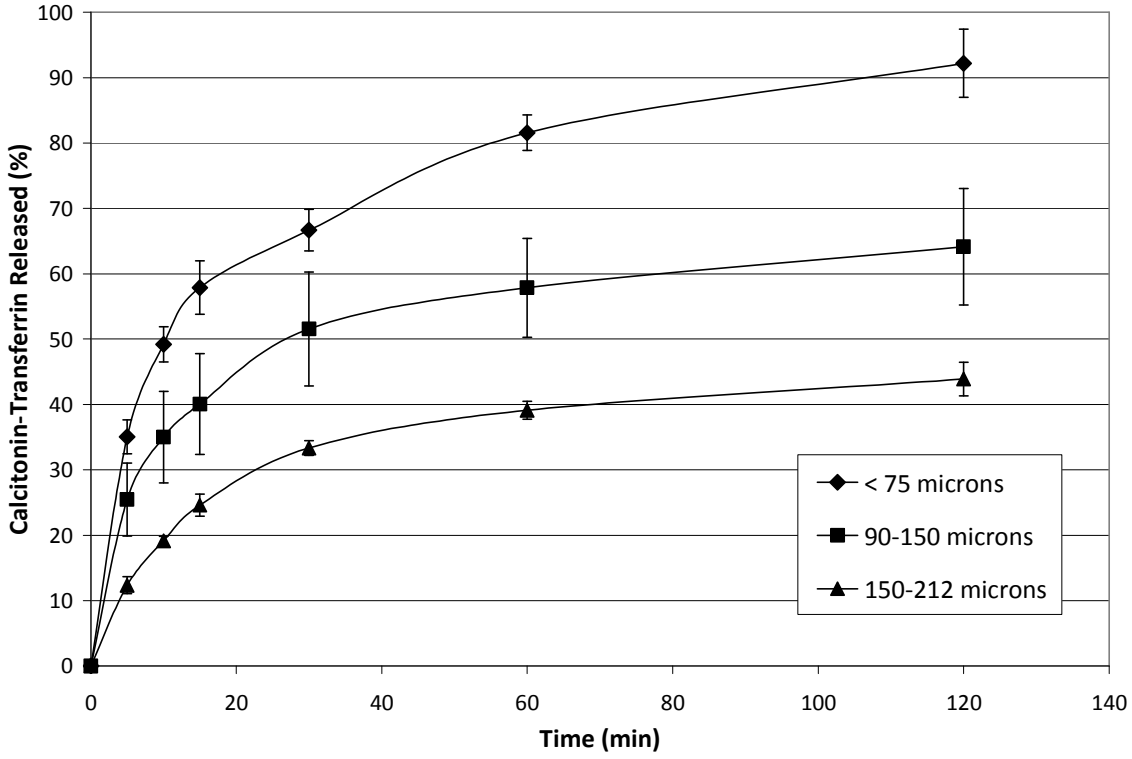

Figure 7.11 Release profiles of calcitonin-transferrin conjugates loaded in P(MAA-g-EG) microparticles of differing particle sizes and placed in PBS buffer (pH 7.4).

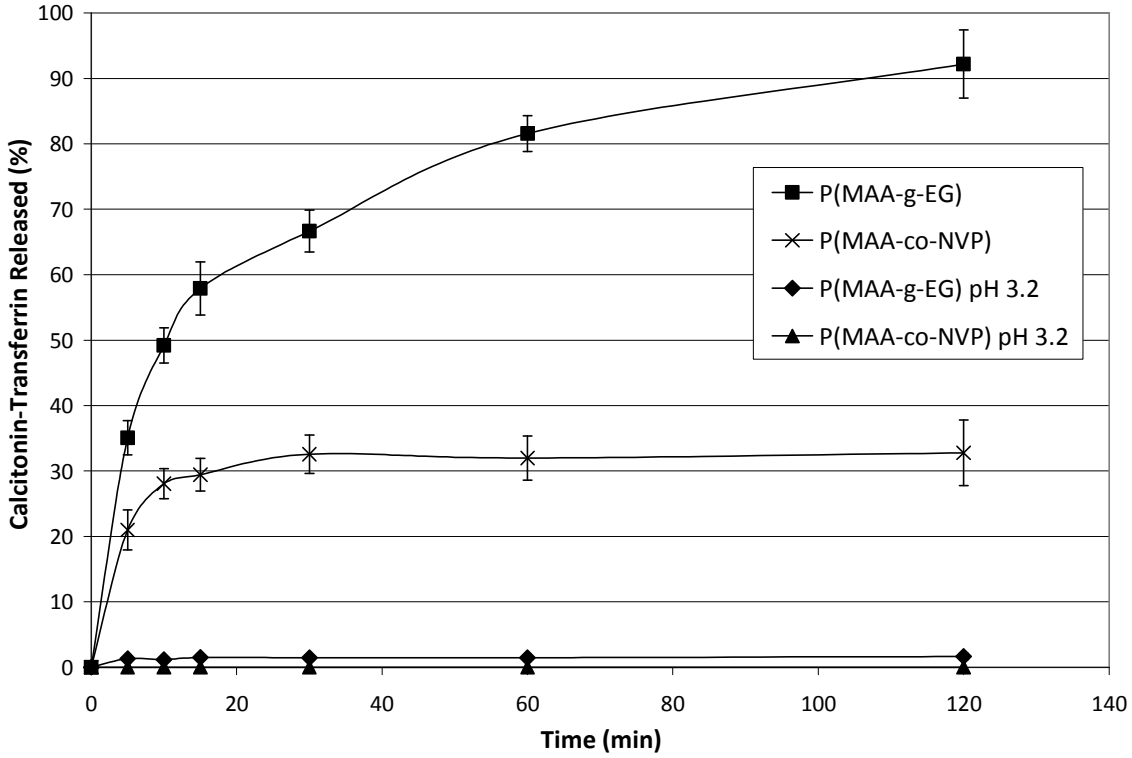

Figure 7.12 Release profiles of calcitonin-transferrin conjugates loaded in P(MAA-g-EG) and P(MAA-co-NVP) microparticles and placed in either PBS buffer (pH 7.4) or PBS buffer (pH 3.2).

REFERENCES

1. Azari, P. R., and Feeney, R. E., *Resistance of Metal Complexes of Conalbumin and Transferrin to Proteolysis and to Thermal Denaturation.* J. Biol. Chem., 1958. **232**(1): p. 293-302.

2. Khandare, J., and Minko, T., *Polymer-drug conjugates: Progress in polymeric prodrugs.* Prog. Polym. Sci., 2006. **31**(4): p. 359-397.

3. Li, C., and Wallace, S., *Polymer-drug conjugates: Recent development in clinical oncology.* Adv. Drug Deliver. Rev., 2008. **60**(8): p. 886-898.

4. Pasut, G., and Veronese, F.M., *Polymer-drug conjugation, recent achievements and general strategies.* Prog. Polym. Sci., 2007. **32**(8-9): p. 933-961.

5. Nakamura, K., Morishita, M., Ehara, J., Onuki, Y., Yamagata, T., Kamei, N., Lowman, A.M., Peppas, N.A., and Takayma, K., *Key functions in polymer carriers for intestinal absorption of insulin.* Int. J. Pharm., 2008. **354**(1-2): p. 135-142.

6. Wood, K.M., Stone, G., and Peppas, N.A., *Lectin functionalized complexation hydrogels for oral protein delivery.* J. Control. Release, 2006. **116**(2): p. e66-e68.

7. Lowman, A.M., Morishita, M., Kajita, M., Nagai, T., and Peppas, N.A., *Oral delivery of insulin using pH-responsive complexation gels.* J. Pharm. Sci., 1999. **88**(9): p. 933-937.

8. Duncan, G., Jess, T.J., Mohamed, F., Price, N.C., Kelly, S.M., and van der Walle, C.F., *The influence of protein solubilisation, conformation and size on the burst release from poly(lactide-co-glycolide) microspheres.* J. Control. Release, 2005. **110**(1): p. 34-48.

9. Hasan, A.S., Socha, M., Lamprecht, A., Ghazouani, F.E., Sapin, A., Hoffman, M., Maincent, P., and Ubrich, N., *Effect of the microencapsulation of nanoparticles on the reduction of burst release.* Int. J. Pharm., 2007. **344**(1-2): p. 53-61.

10. Huang, X., and Brazel, C.S., *On the importance and mechanisms of burst release in matrix-controlled drug delivery systems.* J. Control. Release, 2001. **73**(2-3): p. 121-136.

11. Luan, X., Skupin, M., Siepmann, J., and Bodmeier, R., *Key parameters affecting the initial release (burst) and encapsulation efficiency of peptide-containing poly(lactide-co-glycolide) microparticles.* Int. J. Pharm., 2006. **324**(2): p. 168-175.

12. Tobler, P.H., Jöhl, A., Born, W., Maier, R., and Fishcer, J.A., *Identity of calcitonin extracted from normal human thyroid glands with synthetic human calcitonin-(1-32).* BBA-Protein Struct. M., 1982. **707**(1): p. 59-65.

13. Morishita, M., Goto, T., Peppas, N.A., Joseph, J.I., Torjman, M.C., Munsick, C., Nakamura, K., Yamagata, T., Takayama, K., and Lowman, A.M., *Mucosal insulin delivery systems based on complexation polymer hydrogels: effect of particle size on insulin enteral absorption.* J. Control. Release, 2004. **97**(1): p. 115-124.

14. Lowman, A.M., and Peppas, N.A., *Molecular analysis of interpolymer complexation in graft copolymer networks.* Polymer, 2000. **41**(1): p. 73-80.

CHAPTER 8

EVALUATION OF INSULIN-TRANSFERRIN CONJUGATES BY INVESTIGATION USING CELLULAR MODELS AND *IN VIVO* ANIMAL MODELS

8.1 Introduction

When evaluating the potential of a novel oral dosage form for oral delivery, it is necessary to examine cellular interactions with the therapeutic entity using cellular models as well as to determine performance of the drug *in vivo* using animal models. Investigation of the insulin-transferrin conjugate using cellular and animal models can give insight into a number of important factors governing efficacy and bioavailability of the potential drug formulation.

The mechanism of absorption of insulin-transferrin conjugate can be determined by comparing the permeability alone and in the presence of excess transferrin which would act as a competitive binding agent. Verification of transcellular transport of the insulin-transferrin conjugate is essential towards demonstrating the potential for use of protein-transporter conjugates for oral delivery.

Cellular models can be used to compare the permeability and transport of insulin-transferrin conjugates to native insulin. If comparison of the two reveals increased transport in the case of the insulin-transferrin conjugate, then transcellular transport holds greater potential to achieve high bioavailability than systems based on paracellular transport.

Cellular studies performed in the presence of the P(MAA-g-EG) microparticles will also give insight into the effect of complexation hydrogels on the integrity of the epithelial cell monolayer. Also, preliminary studies performed using animal models can be used to verify the synthesis of insulin-transferrin conjugates as well as to confirm the therapeutic bioactivity of insulin. As a result from evaluation of the insulin-transferrin conjugate using cellular and animal models, it can be determined whether the use of

protein-transporter conjugates as a strategy to increase bioavailability of orally delivered proteins is a viable concept and whether the system design deserves consideration for further testing and implementation into other existing pharmaceutical processes.

In previous chapters, insulin-transferrin conjugates were synthesized, characterized, and then loaded and released from complexation hydrogel carriers to determine the optimal carrier for the conjugates. Assuming optimal release characteristics are achieved, a large portion of therapeutic conjugate will arrive in the small intestine at the site of absorption upon administration. However, to determine the nature and degree of the absorption of the conjugate into the bloodstream, it is necessary to examine the interaction between the conjugate and the cell monolayer which lines the small intestine. The epithelium lining the small intestine contains a cell monolayer which consists of six different types of cells: enterocytes (absorptive cells), goblet cells (produce mucus), endocrine cells, paneth cells, M cells, and tuft and cup cells [1]. To investigate epithelial cellular interactions with therapeutics, cell monolayers can be constructed *in vitro* to simulate interactions which may occur in the small intestine of a typical patient. However, it is extremely difficult to form cellular models using all six types of intestinal epithelial cells in the proper proportions, forcing most cellular models to be designed as a simplified system while still being representative of *in vivo* characteristics and interactions.

A common cellular model used to evaluate therapeutics is the Caco-2 cell line. Caco-2 cells, extracted from a human colon, act as an analog to intestinal epithelial enterocyte cells and are the most widely used cells for determining permeability of a specified molecule [2-5]. More specifically, Caco-2 cell lines are used as a tool for rapid screening when comparing the transport or permeability of various drugs and therapeutics [6]. Caco-2 cell lines are generally used as cellular models by growing a monolayer of the cells on a permeable support. After a rigid monolayer has formed, a drug or therapeutic can be placed on the apical (top) side of the monolayer. Over time,

a portion of the drug will be transported to the basolateral (bottom) side, allowing for the calculation of permeability and the observation of transport characteristics.

The use of Caco-2 cell lines for cellular studies also has some disadvantages. While Caco-2 cells accurately represent the absorptive enterocytes of the small intestine, the use of Caco-2 cells as a model does not account for contributions from the other five types of cells present in the intestinal epithelium. For example, in the epithelium of the small intestine, the enterocytes are covered by mucus which is secreted by the goblet cells. The presence of mucus has been found to have a profound effect on the diffusion of drugs across the epithelial cell barrier [7, 8].

In an effort to create more realistic cellular models, co-cultures have been developed consisting of Caco-2 cells and HT29-MTX cells (mucus secreting goblet cells) [9]. Due to the large size of the insulin-transferrin conjugate, it is essential to provide accurate conditions for diffusion of the large molecule in order to calculate reasonable and meaningful permeability values. To more closely mimic the conditions of the small intestine, a co-culture of Caco-2/HT29-MTX cells were used as the cellular model for all investigations.

Transport of orally administered therapeutics into the bloodstream can occur through a number of different mechanisms of absorption [10] as shown in Figure 8.1. Drug molecules can be absorbed either through the cell membranes (transcellular transport) or through the tight junctions between the cells (paracellular transport).

Transcellular transport can be further classified as either passive diffusion, efflux transport, carrier-mediated transcytosis, or receptor-mediated endocytosis. Past work involving oral delivery of insulin using P(MAA-g-EG) hydrogels has relied on paracellular transport for the absorption of insulin. Furthermore, the presence of the hydrogels has been to shown to approximately double paracellular transport of insulin due to the capacity of the hydrogels to bind calcium, which is vital to maintenance of the tight junctions [11]. However, paracellular transport of insulin has a few inherent disadvantages.

Even with increased absorption due to the presence of the hydrogels, the bioavailability of insulin is still low in most cases. Also, paracellular transport is not specific to insulin molecules, allowing the possible introduction of viruses or toxins into the bloodstream during the period in which the integrity of the tight junctions is lowered. The development of protein-transporter conjugates allows for utilization of transcellular pathways. Specifically, binding therapeutic proteins to transporter ligands utilizes the specificity of the receptor-ligand interaction to transport the therapeutic protein using receptor-mediated endocytosis. Increased specific targeting of the protein-transporter conjugate should minimize risk of introduction of viruses or toxins as well as to potentially increase bioavailability in the bloodstream.

Important information about the insulin-transferrin conjugate can be ascertained by simulating cellular transport under a number of different conditions. By placing only the protein on the apical side of the chamber, it is possible to compare the permeability of insulin and insulin-transferrin conjugates as to determine if the presence of transferrin increases absorption. By performing similar tests but in the presence of P(MAA-g-EG) microparticles, it is also possible to determine if the calcium binding effect of the hydrogel will change the amount of drug transported in either/both cases. Lastly, by performing a transport study with excess transferrin in solution with the conjugate, insight can be gained as to the mechanism of absorption. If the permeability of insulin-transferrin conjugates is significantly lowered because of the introduction of excess transferrin, transcellular transport must be occurring to some degree due to the drop in conjugate transport from competitive binding at receptor sites. By comparing transport studies, valuable information related to potential bioavailability of insulin-transferrin conjugates can be obtained.

While cellular models are designed to mimic physiological conditions within the small intestine, they cannot predict the reaction of a living organism to the therapeutic drug and they cannot help to validate the efficacy or bioactivity of the therapeutic protein. To validate the potential use of insulin-transferrin conjugates, studies were

performed *in vivo* to verify the synthesis of the bioconjugate and to evaluate bioactivity of the insulin molecule. Upon administration of insulin-transferrin conjugates into the bloodstream, subsequent reduction of blood-glucose level would demonstrate that insulin-transferrin conjugates were successfully synthesized (insulin alone would have been dialyzed out) and that insulin is still bioactive despite having undergone an extensive conjugation reaction. Animal studies designed to evaluate efficacy and bioactivity are an essential step towards gaining the necessary level of understanding needed to further pursue the investigation of a novel therapeutic for practical applications.

The overall objectives of the studies performed in this chapter are to evaluate the performance of insulin-transferrin conjugates using *in* vitro cellular models and *in vivo* animal models. In this chapter, insulin-transferrin conjugates will be evaluated using a Caco-2/HT29-MTX co-culture under differing conditions such as using pure insulin versus using insulin-transferrin conjugates, introducing the P(MAA-g-EG) microparticles, and introducing excess transferrin for competitive binding. Also, this chapter will determine the *in vivo* reaction of animal models to administration of insulin-transferrin conjugates. The cellular studies will shed light on the degree of increased transport due to transferrin, the effect of the presence of the microparticles, and the mechanism of absorption. The animal studies will give some idea as to the potential efficacy of the drug as well as to determine if the therapeutic insulin is still bioactive. If the data from this chapter and the previous chapters proves that the use of insulin-transferrin conjugates is a significant improvement to previously designed systems for oral insulin delivery, then the concept of protein-transporter conjugates merits further investigation and possible implementation into other pharmaceutical designs as well.

8.2 Materials and Methods

8.2.1 Development of Caco-2/HT29-MTX Monolayers

To effectively perform the transport studies using insulin-transferrin conjugates, monolayers consisting of a co-culture of Caco-2/HT29-MTX cells had to be formed. To form the monolayer, both types of cells were initially cultured in culturing flasks (75 cm^2, VWR Scientific, West Chester, PA) with 10 mL of culture media (DMEM, Biofluids Inc., Rockville, MD). The DMEM culture media was also supplemented with 10% fetal bovine serum and 1% non-essential amino acids (penicillin, streptomycin, amphotericin B) (Mediatech, Inc., Manassas, VA). Cultivation was performed at a seeding density of 2.5 x 10^5 cells per flask for the Caco-2 cells and 1.25 x 10^5 cells per flask for the HT29-MTX cells. During cultivation, the cells were incubated at 37° C, 95% relative humidity, and 5% CO_2 while the culture media was replaced every other day until the cells reached 70-80% confluency. After reaching the desired confluency, the cells were passaged by rinsing 3 times with DPBS and subsequent trypsinization via exposure to a trypsin-EDTA solution (0.05% w/v trypsin, 0.02% w/v EDTA, MP Biomedical, Solon, OH) for 5 minutes. Both types of cells were passaged at least once prior to combination of the cell types. The Caco-2 cells had passage numbers between 77 and 78 while the HT29-MTX cells had passage numbers between 17 and 19. After passaging, the Caco-2 and HT29-MTX cells were transferred at the desired seeding density to experimental wells in a 1:1 ratio as to obtain a 50% Caco-2/50% HT29-MTX experimental co-culture monolayer.

For the transport studies, a co-culture of Caco-2/HT29-MTX cells was grown in 6-well Transwell® plates (4.71 cm^2/well, Costar Corning Inc., Corning, NY). The cell density in the experimental wells was approximately 3 x 10^5 cells/well with the composition being 50% of each cell type. The co-culture was grown in the culture medium for approximately 21-23 days until the monolayer achieved a constant transepithelial electrical resistance (TEER) as measured by a chopstick electrode (World Precision Instrument, Sarasota, FL). Typically, a constant TEER value indicates that the monolayer

has formed tight junctions [12, 13]. During the formation of the monolayer, the culture media was changed every other day and the TEER was monitored regularly.

Each experimental well is composed of two compartments: an apical (top) side which represents the small intestine, and a basolateral (bottom) side which potentially represents transport to the bloodstream. The apical and basolateral compartments were separated only by the cell monolayer which was grown on a porous membrane support. The experiment setup for transport studies for each well can be seen as Figure 8.2.

Upon the formation of tight junctions, the transport studies began by allowing the cells to equilibrate with Hank's Balanced Salt Solution (HBSS, HyClone, Logan, UT), the experimental medium for the study. The HBSS also contained Ca^{2+} ions to ensure regulation of intracellular Ca^{2+} ions, which are instrumental in maintaining the integrity of the tight junctions. A volume of 1.5 mL of HBSS was added to both the apical and basolateral chambers. The TEER of the cell monolayer was monitored for the next hour with samples withdrawn at 0, 15, 30, 45, and 60 minutes. At the conclusion of the equilibration period, the TEER had achieved and maintained a constant value, indicating adjustment to the HBSS solution as well as the ability to begin the transport studies.

8.2.2 Protein Transport Across the Cell Monolayer

Three transport studies were performed using only protein in the apical chamber. An insulin control study was performed to determine the permeability of insulin alone. A study using insulin-transferrin conjugates was performed to determine if there is increased transport due to the presence of transferrin. A final transport study was performed with insulin-transferrin conjugates in the presence of excess transferrin as to determine the mechanism of absorption of the conjugate. Excess transferrin should serve as a competitive binding entity, thus lowering the permeability of insulin-transferrin conjugates if the transport is indeed transcellular.

For the studies, insulin or insulin-transferrin was dissolved in warm HBSS at a concentration of 0.2 mg/mL. For the study with excess transferrin, insulin-transferrin was dissolved at a concentration of 0.2 mg/mL while transferrin was dissolved at a concentration of 2.0 mg/mL. To begin the study, the previous HBSS solution was removed from the apical chamber. Approximately 1.5 mL of the solution containing either the insulin, insulin-transferrin, or conjugate and excess transferrin was then placed in the apical chamber. The Transwell® plates were then placed in an incubator at 37° C. Samples of 100 µL were withdrawn from the basolateral chambers at time points of 0, 0.5, 1, 2, and 3 hours after the addition of protein solution to the well. Also, samples of 100 µL were withdrawn from the apical chambers at time points of 0 and 3 hours to observe any change in apical protein concentration. The TEER of the monolayer was also measured at the withdrawal of each sample. Throughout the course of the transport study, all measurements were taken while maintaining the Transwell® plate at 37° C, ensuring no changes in the integrity of the tight junctions or in the amount of transcellular transport as both vary significantly as temperature varies. The samples were placed in small vials and refrigerated until they could be analyzed. Analysis of protein concentration of the apical chamber was performed by HPLC and protein concentration in the basolateral chamber was determined by use of an ELISA kit.

8.2.3 Protein Transport Across the Cell Monolayer in the Presence of P(MAA-g-EG) Microparticles

In addition to transport studies using only proteins, more transport studies were performed to determine the effect of the presence of P(MAA-g-EG) microparticles on the cellular transport of both insulin and insulin-transferrin conjugates. Because the P(MAA-g-EG) microparticles are anionic, the local negative charges throughout the polymer network attract positively charged extracellular Ca^{2+} ions, thereby lowering intracellular Ca^{2+} concentrations. Intracellular Ca^{2+} is vital to maintaining the integrity of the tight junctions, thus causing P(MAA-g-EG) microparticles to act as a transport

enhancer for paracellular transport. Since the mechanism of absorption for insulin is thought to be paracellular, insulin transport should benefit from the presence of anionic polymer microparticles. However, because insulin-transferrin conjugates are thought to undergo transcellular transport, the presence of P(MAA-g-EG) microparticles should have no effect on the transcellular transport of the conjugate. Alternatively, there may be a combinatorial effect of transcellular transport as well as paracellular transport due to the presence of the microparticles.

The polymer microparticles used in this study are the exact same microparticles which were determined optimal for the loading and release of insulin-transferrin conjugates in Chapter 6. As with the previous transport studies, solutions of either insulin or insulin-transferrin conjugates were prepared at a concentration of 0.2 mg/mL in warm HBSS. After removing the HBSS used for equilibration of the monolayer from the apical chamber, approximately 1.5 mL of either of the protein solutions was added to refill the apical chamber with sample. Immediately after addition of the protein solutions to the apical side, dry P(MAA-g-EG) microparticles were added to the apical chamber at a concentration of 1 mg/mL. Sampling of both the apical and basolateral chambers occurred in the same manner as previously described and all samples were analyzed by either HPLC (apical samples) or using an ELISA kit (basolateral samples).

8.2.4 Apical Sample Protein Concentration Analysis by HPLC

High Performance Liquid Chromatography (HPLC) was used to analyze samples from the apical chamber containing either insulin or insulin-transferrin conjugates dissolved in HBSS. HPLC analysis was used for each sample to determine concentration based on absorbance values relative to absorbances of standard samples of known concentrations. Protein concentrations in the apical chamber as determined by HPLC are values used to calculate permeability values of the transported protein.

The HPLC equipment used consists of a Waters 2695 Separation Module (Waters Corporation, Milford, MA) attached to a Waters 2487 Dual λ Absorbance Detector

(Waters Corporation, Milford, MA). Analysis is performed using a reverse-phase analytical HPLC method designed to elute a wide range of proteins within a specified time period. The method includes the use of water (HPLC Grade, Fisher Scientific, Fair Lawn, NJ) with 0.1% by volume trifluoroacetic acid (TFA, ACROS Organics, Geel, Belgium) as Solvent A and acetonitrile (Optima, Fisher Scientific, Fair Lawn, NJ) with 0.08% by volume TFA as Solvent B. During the separation process, the mobile phase begins at a composition of 70% Solvent A and 30% Solvent B. The mobile phase changes composition using a gradient to 40% Solvent A and 60% Solvent B within 6 minutes. The mobile phase composition is then returned to initial conditions of 70% Solvent A and 30% Solvent B for the next sample to be analyzed. The mobile phase was introduced at a constant flow rate of 0.6 mL/min. All separations are performed using a Symmetry300^{TM} C4 column (particle size 5 μm, 3.9 mm I.D. x 150 mm length, Waters Corporation, Milford, MA) held at a constant temperature of 40°C. After separation of proteins, absorbance of the solution was detected at a wavelength of 220 nm. All instrument and processing methods were controlled and specified using the Empower software.

8.2.5 Measurement of Transported Insulin and Insulin-Transferrin Conjugate Using ELISA Assay Kits

The concentration of free insulin as well as transferrin-bound insulin transported across the cell monolayer was determined using an enzyme-linked immunosorbent assay (ELISA) for detection of bovine insulin (Mercodia AB, Uppsala, Sweden). ELISA uses the direct sandwich technique in which two monoclonal antibodies are directed towards two different antigenic determinants on the insulin molecule. Insulin in the sample initially reacts with peroxidase-conjugated anti-insulin antibodies bound to the bottom of each well. After washing out unbound antibody, the insulin-antibody complex is detected by reaction with 3,3'-5,5'-tetramethylbenzidine (TMB). The reaction can be stopped with the addition of an acidic stop solution which gives a

colorimetric endpoint which can be read using spectrophotometry. A standard curve can be generated using the provided calibrator solutions of known concentrations.

Preliminary experiments were performed to determine the dilution factors necessary to adjust the sample concentrations within a detectable range for the assay. The basolateral samples were diluted using HBSS to several different concentrations and then analyzed spectrophotometrically. Based on the results of the experiments, all samples were diluted by a factor of 300 times to ensure proper measurement of the sample insulin concentration.

The experimental process for using the ELISA assay to determine insulin concentration was performed using the materials provided in the assay kit and according to the provided instructions. A volume of 25 μL of either calibrator solutions or basolateral samples was placed in each well for analysis. Approximately 100 μL of enzyme conjugate solution containing peroxidase-conjugated anti-insulin antibodies was added to each well and the entire plate was incubated on a plate shaker (Model 4625, Lab-Line Instruments Inc., Melrose Park, IL) for 2 hours at room temperature. After incubation, the wells were washed 6 times using a wash buffer to remove excess unreacted antibody. After emptying all excess fluid, 200 μL of the substrate TMB was added to each well and the plate was incubated for 15 minutes at room temperature. At the conclusion of the incubation period, 50 μL of acidic stop solution was added to each well and placed on the plate shaker for 5 seconds to reach the colorimetric endpoint. Each well was analyzed using a microplate reader (Synergy HT, Bio-Tech Instruments, Winooski, VT) at a wavelength of 450 nm. The absorbance of each sample was compared to calibrator absorbances to determine the concentration of each sample well.

8.2.6 *In Vivo* Animal Studies

Preliminary animal studies were performed to measure the bioactivity and to verify the synthesis of insulin-transferrin conjugates. The animal studies were

performed under compliance with the regulations of the Committee on Ethics in the Care and Use of Laboratory Animals. The animal models were male Sprague–Dawley rats (Tokyo Laboratory Animals Science Co., Ltd., Tokyo, Japan) weighing between 180–220 g and were housed in rooms controlled between 23 ± 1 °C and 55 ± 5% relative humidity. The rats also had free access to water and food during acclimatization. Following anesthetization by intraperitoneal injection of sodium pentobarbital (50 mg/kg of body weight; Dainippon Pharmaceutical Co., Ltd., Osaka, Japan), rats were held in a supine position on a thermostatically controlled board at 37 °C. Additional intraperitoneal injections of sodium pentobarbital (12.5 mg/kg) were used every hour to maintain the appropriate level of anesthesia.

The studies were performed by administering insulin-transferrin conjugates through the subcutaneous route. Subcutaneous injection ensures reasonable bioavailability of the conjugates in the bloodstream such that the effect on blood glucose level can be observed. Solutions for injection of insulin-transferrin conjugates were prepared at approximate conjugate concentrations of 0.125 mg, 0.25 mg, and 0.5 mg per kilogram of rat body weight. The three concentrations of conjugates in solution roughly correspond to insulin dosages of 0.5 IU/kg, 1.0 IU/kg, and 2.0 IU/kg respectively under ideal conjugation reaction conditions. As a control, recombinant human insulin was also injected at a dosage of 1.0 IU/kg.

After injection of insulin-transferrin conjugates, a sample of 0.25 mL of blood was taken from the jugular vein at time points of 0, 5, 10, 15, 30, 60, 120, 180, and 240 minutes. Tuberculin syringes (1 mL) were preheparinized by coating the syringe wall with aspirating heparin and subsequently expelling all heparin by completely depressing the plunger. Plasma was separated by centrifugation at 13,000 rpm for 1 minute. Blood glucose concentration was measured using a glucose meter (Novo Assist Plus, Novo Nordisk Pharma Ltd., Tokyo, Japan) and was used to represent the biological activity of the bound insulin within the insulin-transferrin conjugates. The hypoglycemic response

was quantified by examining the blood glucose concentration curve and calculating the area above the curve (AAC) using the trapezoidal method for the first 4 hours.

8.3 Results and Discussion

8.3.1 Development of Caco-2/HT29-MTX Monolayers

Cell monolayers consisting of a co-culture of 50% Caco-2 cells and 50% HT29-MTX cells were formed for the use of five separate transport studies. The transport studies included measuring the cellular transport of insulin and insulin-transferrin with and without the presence of polymer microparticles as well as a study with insulin-transferrin conjugates in the presence of excess transferrin. The cell monolayers for each study were constructed identically as to allow comparison between the separate transport studies.

The transepithelial electrical resistance (TEER) was monitored regularly during the formation of the cell monolayer. After 21-23 days, an equilibrium TEER value was achieved, indicating the formation of tight junctions within the monolayer. The monolayer was then allowed to equilibrate with warm HBSS, the solvent used for the transport studies. The TEER values of the monolayer were monitored for the next hour to ensure equilibration with the fluid before starting the transport studies. The average TEER values for all of the monolayers over the hour of the equilibration period are shown in Figure 8.3.

After equilibrating with HBSS, the monolayers were used for transport studies. At the conclusion of the studies, the interaction of the protein with the cell monolayers and the amount of protein transported through the monolayers provided a basis of comparison between the samples as well as evidence to differentiate between the suggested approaches for the oral delivery of insulin and to determine which approach is the most effective and useful for drug delivery applications.

8.3.2 Protein Transport Across the Cell Monolayer

Several samples including solutions of either insulin, insulin-transferrin conjugates, or insulin-transferrin conjugates with excess transferrin were investigated through transport studies. Transport studies of the different protein solutions were conducted by placing dissolved protein in the apical chamber of a Transwell® plate with a monolayer of Caco-2/HT29-MTX cells grown on a porous membrane support. Samples were withdrawn from the basolateral chamber at regular time points to determine the amount of protein transported over time. The transport profiles were fit using a linear regression model and the slope of the fit was used to calculate apparent permeability values (P_{app}) for each of the protein samples.

In order to calculate an apparent permeability for protein transport, several assumptions and simplifications must first be made. For this analysis, the cellular monolayer is assumed to be similar to a chemically homogenous layer of known thickness. Applying Fick's first law of diffusion to the protein transport, a relationship can be derived between the rate of protein transport and the concentrations of both the apical and basolateral chamber. The relationship is shown as Equation 8.1:

$$\frac{dQ(t)}{dt} = \frac{K \times D}{h} \times A \times [C_A(t) - C_B(t)] \qquad (8.1)$$

where Q(t) is the cumulative amount of protein (ng) transported at time t, K is the partition of distribution coefficient of the protein within the cell monolayer, D is the diffusion coefficient (cm^2/s), h is the height or thickness of the cell monolayer (cm), A is the area of the cell monolayer (cm^2), and $C_A(t)$ and $C_B(t)$ are the protein concentrations (ng/mL or ng/cm^3) of the apical and basolateral chambers respectively.

To simplify the expression, the first term of the expression was redefined as apparent permeability (P_{app}) using Equation 8.2 as shown below:

$$P_{app} = \frac{K \times D}{h} \qquad (8.2)$$

To further simplify the expression, the term $[C_A(t) - C_B(t)]$ can be reworked based on the relationship between the terms. Because the concentration in the apical chamber ($C_A(t)$) is measured in milligrams and the concentration in the basolateral chamber ($C_B(t)$) is measured in nanograms and is much smaller, the basolateral concentration is essentially zero. Also, because very little transport occurs relative to the initial apical concentration (C_{A0}), the term $[C_A(t) - C_B(t)]$ can be replaced by the term C_{A0}. Using the reduced version of Equation 8.1 and solving for apparent permeability (P_{app}) yields a simplified expression for determining permeability values as shown in Equation 8.3:

$$P_{app} = \frac{dQ(t)}{dt} \times \frac{1}{A \times C_{A0}} \qquad (8.3)$$

In Equation 8.3, the area of the monolayer (A) and the initial apical concentration (C_{A0}) are known values. The term dQ(t)/dt is the slope of the linear fit of the cellular transport profiles of each protein.

As an experimental control, a solution of insulin dissolved in HBSS was added to the apical chamber and was allowed to interact with the cell monolayer. The cellular transport profile of insulin from the apical to basolateral chamber for a period of 3 hours is shown as Figure 8.4. The data in Figure 8.4 confirms that insulin transport across the cell does occur. In fact, the graph shows that there may be a burst transport of insulin across the monolayer, indicated by the high amount of insulin transported within 30 minutes and a leveling off of transport over the next few hours. The apparent permeability (P_{app}) of the insulin relative to the cell monolayer was determined to be 4.95×10^{9} cm/s as calculated using Equation 8.3. The extent of transport as well as the apparent permeability of the insulin control served as a standard of comparison for the experimental protein solutions.

To determine the effect of the conjugation of a transporter protein to insulin, the transport of a solution of insulin-transferrin conjugates across the cell monolayer was measured and analyzed. The cellular transport profile of insulin-transferrin

conjugates from the apical to basolateral chamber for a period of 3 hours is shown as Figure 8.5. As evident in Figure 8.5, a significant amount of insulin-transferrin conjugate was transported across the Caco-2/HT29-MTX monolayer. In comparison to the insulin control, the transport occurred to a much greater extent and also in a much more linear fashion. The linearity of the transport can most likely be attributed to the timing of cellular mechanisms involved in transcellular transport, leading to a slower but more linear transport profile. The apparent permeability (P_{app}) of the insulin-transferrin conjugates across the Caco-2/HT29-MTX monolayer was calculated using Equation 8.3 and found to be 37.0 x 10^{9} cm/s. The increased permeability of insulin-transferrin conjugates compared to the insulin control suggests that the addition of a transporter protein such as transferrin will greatly increase the transport of a therapeutic protein like insulin across the cell monolayer. Based on the cellular permeability, the conjugation of a transporter protein to a therapeutic protein may also drastically increase the bioavailability of the drug in the bloodstream.

In an attempt to gain more knowledge about the mechanism of absorption of insulin-transferrin conjugates, transport studies were performed using a solution of insulin-transferrin conjugates with excess unmodified transferrin also in solution. The cellular transport which occurred over a period of 3 hours using insulin-transferrin conjugates with excess transferrin is shown as Figure 8.6. The data from Figure 8.6 seems to suggest that more insulin-transferrin conjugate was transported due to the presence of unmodified transferrin. However, the presence of excess transferrin was thought to have an inhibitory effect due to competitive binding of available transferrin receptors. Moreover, the transferrin molecule has no known ability to increase paracellular transport or loosen tight junctions.

The increased transport can most likely be attributed to unmodified transferrin being transported to the basolateral side as expected, but also causing non-specific binding between the transferrin in the sample solution and the antibodies lining the wells of the ELISA kit, giving a falsely high insulin-transferrin concentration. However,

the graph does allow for some useful insight. Because of the similarities between the transport profiles of the conjugate solution and the conjugate solution with excess transferrin, it seems likely that insulin-transferrin conjugates are transported using the same transcellular mechanisms as unmodified transferrin, indicating that the conjugation of insulin has little effect on the bioactivity of the transferrin molecule. The apparent permeability (P_{app}) of the proteins across the Caco-2/HT29-MTX monolayer was calculated using Equation 8.3 and found to be 76.8 x 10^9 cm/s.

While performing the transport studies, it was important to monitor the integrity of the cell monolayer and the tight junctions as to ensure that administration of such therapeutics would not cause the epithelial cell layer to have a lessened ability to expel dangerous viruses or toxins. Over the course of each transport study, the transepithelial electrical resistance was measured as a means of monitoring tight junction integrity. The TEER values throughout the three transport studies are shown as Figure 8.7. As evident in Figure 8.7, the TEER of the Caco-2/HT29-MTX monolayer stayed near 100% of the initial value throughout the course of each transport study. The maintenance of steady TEER values indicates that the proteins (insulin, insulin-transferrin, transferrin) do not have a disruptive effect on the cell monolayer, ensuring their presence upon administration will not cause illness due to uptake of dangerous toxins or viruses through a weakened epithelial cell barrier.

To compare the protein transport studies, the most simple and direct method is to compare the apparent permeability (P_{app}) values between the different protein solutions. The apparent permeability values can be directly compared by referencing Table 8.1. According to the values, the insulin-transferrin molecule has more than seven times the permeability compared to unmodified insulin. Increasing transport of a potential therapeutic more than sevenfold has dramatic potential ramifications on the bioavailability of the drug in the bloodstream. Based on the results of the transport studies conducted using solutions containing only protein, the transport of an orally administered therapeutic protein can be greatly increased by conjugating the drug to a

transporter molecule such as transferrin. Upon investigation into a specific protein for oral delivery, the use of transporter molecules merits at least investigation and experimentation if not incorporation into the system design.

8.3.3 Protein Transport Across the Cell Monolayer in the Presence of P(MAA-g-EG) Microparticles

Several transport studies were conducted on protein solutions with P(MAA-g-EG) microparticles added to the solution. The solutions investigated included a solution containing insulin in the presence of P(MAA-g-EG) microparticles and a solution containing insulin-transferrin conjugates in the presence of P(MAA-g-EG) microparticles. The studies were conducted by first preparing a solution of in which protein was dissolved in HBSS and a known mass of polymer microparticles was added. The transport study began as the prepared solution was added to the apical chamber of a Transwell® plate with a monolayer of Caco-2/HT29-MTX cells grown on a porous membrane support. Samples were withdrawn from the basolateral chamber at regular time points to determine the amount of protein transported over time. The transport profiles were fit using a linear regression model and the slope of the fit was used to calculate apparent permeability values (P_{app}) for each of the protein samples using Equation 8.3.

To determine the effect of the presence of polymer microparticles on cellular insulin transport, a prepared solution of insulin dissolved in HBSS with added P(MAA-g-EG) microparticles was added to the apical chamber and was allowed to interact with the cell monolayer. The cellular transport profile of insulin from the apical to basolateral chamber for a period of 3 hours in the presence of P(MAA-g-EG) microparticles is shown as Figure 8.8. As can be seen in Figure 8.4, insulin transport still occurs in the presence of P(MAA-g-EG) microparticles. In comparison to insulin transport with no microparticles present, the cumulative amount of insulin transported is similar and the initial burst transport of insulin within the first 30 minutes can also be

observed. To quantitatively compare insulin transport with and without the presence of P(MAA-g-EG) microparticles, the apparent permeability (P_{app}) of each study was examined. The apparent permeability (P_{app}) of the insulin in the presence of polymer microparticles was determined to be 5.20 x 10^{9} cm/s as calculated using Equation 8.3. The apparent permeability of insulin in the presence of polymer microparticles is slightly higher than the value obtained for insulin alone, indicating that the presence of the microparticles may have a slight permeation enhancing effect for the paracellular transport of insulin. A higher concentration of microparticles in solution would have most likely caused a greater increase in insulin transport due to concurrently increased calcium binding capacity, further loosening the tight junctions of the cell monolayer. In addition to protection in the stomach and adhesion near the site of absorption, P(MAA-g-EG) microparticles facilitate oral delivery of insulin even further by binding to extracellular calcium, thereby loosening the tight junctions and increasing the potential for paracellular transport.

Similar transport studies were also conducted which used solutions of insulin-transferrin conjugates in the presence of P(MAA-g-EG) microparticles to determine if the microparticles had a similar effect as was seen with insulin. The cellular transport profile of insulin-transferrin conjugates from the apical to basolateral chamber for a period of 3 hours in the presence of P(MAA-g-EG) microparticles is shown as Figure 8.9. As can be seen in Figure 8.9, the magnitude of insulin-transferrin conjugates transported across the Caco-2/HT29-MTX cell monolayer is much higher than in the other transport studies. To quantitatively compare the transport of conjugate in the presence of microparticles to the transport of conjugate alone or the transport of insulin in the presence of microparticles, it is essential to determine the apparent permeability (P_{app}) of the study. The apparent permeability (P_{app}) of the insulin-transferrin conjugates across the Caco-2/HT29-MTX monolayer in the presence of polymer microparticles was calculated using Equation 8.3 and found to be 72.8 x 10^{9} cm/s. In comparison to the transport of insulin-transferrin conjugates alone, the permeability of the conjugate

nearly doubled in the presence of polymer microparticles. Though it is not completely clear whether the presence of the microparticles enhanced transcellular transport of the conjugate or simply opened up paracellular pathways, it is evident that transport was greatly increased. Earlier studies proved that the presence of polymer microparticles helped to enhance insulin transport slightly, increasing the apparent permeability by roughly 5% at the specified microparticle concentration.

However, at the same concentration, the microparticles were able to enhance insulin-transferrin transport by nearly 100%. The drastic difference in enhanced transport suggests that P(MAA-g-EG) microparticles act as better enhancers for transcellular transport than for paracellular transport. In this study, while improved conjugate transport may be slightly attributable to newly opened paracellular pathways, it is clear that the microparticles facilitated transcellular transport, possibly through calcium binding, the consequent loss of intracellular calcium, and the resultant effect which lowered calcium has on transcytotic processes. It is also useful to compare conjugate transport to insulin transport in the presence of microparticles. Simply replacing insulin with insulin-transferrin conjugates at the same concentration but in the presence of microparticles increased the apparent permeability by a factor of nearly fourteen. Assuming that a formulation of insulin-transferrin conjugates loaded into P(MAA-g-EG) microparticles could deliver the same amount of protein to the site of absorption as an insulin-loaded microparticle, the benefit of having potentially fourteen times the cellular transport would translate into a much more effective drug with significantly higher bioavailability.

To gain a greater understanding of the effect of microparticles on the integrity of the tight junctions and the monolayer, the transepithelial electrical resistance (TEER) was measured over the course of the transport studies. The TEER values throughout the two transport studies are shown as Figure 8.10. As can be seen in Figure 8.10, the TEER of the Caco-2/HT29-MTX monolayer stayed near 100% of the initial value throughout the course of both transport studies. Steady TEER values throughout the studies

indicate little to no disruption of the monolayer in the presence of both proteins and P(MAA-g-EG) microparticles. While previous studies have shown that the TEER values and the tight junctions will be affected by the presence of polymer microparticles [11, 14], the microparticles used in this study were likely not introduced at a high enough concentration to achieve the significant disruptive effect that had been observed in previous studies.

To compare all of the transport studies quantitatively, it is important to compare the apparent permeability (P_{app}) values. The apparent permeability values for all of the transport studies can be directly examined in Table 8.1. Based on the permeability values, the insulin-transferrin conjugate alone achieves more than seven times the transport of insulin alone. Meanwhile, the addition of P(MAA-g-EG) microparticles increases insulin transport by approximately 5% while improving insulin-transferrin transport by nearly 100%. Because of the ability of the polymer microparticles to facilitate transcellular transport to such a large extent, the insulin-transferrin conjugate achieves nearly fourteen times the transport that insulin does in the presence of the microparticles. Considering all of the transport studies performed in this work, modification of therapeutic proteins by conjugation to transporter molecules remains an attractive option for increasing epithelial transport and achieving high bioavailability.

8.3.4 Apical Sample Protein Concentration Analysis by HPLC

All samples obtained during transport studies from the apical chamber were analyzed by HPLC. The concentration of each sample was determined by comparisons to standards of known concentrations. The experimental concentration of each sample was used to calculate the free protein concentration in the apical chamber at the time the sample was withdrawn. The protein concentration as determined by HPLC was used to calculate apparent permeability (P_{app}) using Equation 8.3. A table of apparent permeability values for each transport study is given as Table 8.1.

8.3.5 Measurement of Transported Insulin and Insulin-Transferrin Conjugate Using ELISA Assay Kits

The concentrations of protein transported to the basolateral chamber for all transport studies were measured using ELISA assay kits. The use of ELISA kits allows for detection of trace amounts of insulin as low as a 0.025 ng/mL. Using the protocol outlined earlier, the ELISA analysis converts insulin concentration to a colorimetric endpoint which can be observed spectrophotometrically. The insulin concentration of each sample was determined by comparison of the sample absorbance to absorbance of standards of known insulin concentration. A calibration curve was constructed to determine a relationship between absorbance and concentration. The calibration curve for all of the transport studies is shown as Figure 8.11

In addition to providing a way to measure trace amounts of insulin, the use of ELISA kits also provided indirect evidence confirming the activity of the insulin molecule despite conjugation to transferrin. Interaction with both the anti-insulin antibodies and the substrate TMB demonstrate that the active sites for both interactions remain intact and active.

8.3.6 *In Vivo* Animal Studies

Preliminary animal studies were conducted to test for the bioactivity of the insulin-transferrin conjugate as well as to verify the synthesis of the conjugate. The rat specimens were injected with three different dosages of insulin-transferrin conjugates as well as recombinant human insulin as a control. Following subcutaneous injection, the blood glucose level was monitored for four hours to determine the effect of the injected protein. Reduction of blood glucose level by injection of insulin-transferrin conjugate not only confirms bioactivity of the conjugate but also indirectly verifies the synthesis reaction by recognizing the drop in blood glucose level as detection of insulin in the conjugate.

The blood glucose levels of the rat model following injection of experimental samples of insulin-transferrin as well as the insulin control are shown as Figure 8.12. In the figure, it is clear that the two higher dosages of insulin-transferrin (1 IU/kg and 2 IU/kg) both caused a reduction in blood glucose level. In order to compare the 1 IU/kg dose of insulin-transferrin to the 1 IU/kg dose of the insulin control, the area above the curve (AAC) was calculated and the areas were compared. Based on the analysis, insulin-transferrin was found to be approximately 15% active assuming a true 1 IU/kg dose of insulin within the conjugate. However, the 1 IU/kg assumption for the insulin-transferrin dosage is based on ideal conjugation reaction conditions in which every molecule of insulin supplied to the reaction was successfully bound to a transferrin molecule. As the previously mentioned condition is the ideal reaction, it means that the insulin-transferrin dosage is at most 1 IU/kg and at least 15% active. If it were assumed that the reaction yielded one insulin molecule bound to one transferrin molecule on average, then the measure of bioactivity would rise to approximately 40%. Also, samples in this study were lyophilized as a requirement of overseas shipping, possibly denaturing a portion of the sample.

The nature of this animal study was preliminary, and to determine the true extent of the bioactivity, a much more refined and controlled sample would have to be carefully examined. However, based on the information available from the animal studies, relevant claims regarding the sample can be made. The studies proved that bioactivity of the insulin can be retained throughout the conjugation reaction. In other words, the insulin-transferrin conjugate can actually provide a therapeutic response similar to insulin. Also, during the conjugation reaction, dialysis and purification is performed to remove any proteins smaller than transferrin (i.e. unreacted insulin). An insulin-like response upon administration of insulin-transferrin conjugates suggests the presence of insulin, verifying the successful synthesis of a true protein-transporter conjugate. Based on the animal studies, it has been shown that protein-transporter

conjugates can be synthesized successfully and can still serve as therapeutics while also offering improved characteristics such as increased cellular transport.

8.4 Conclusions

Cellular evaluation of the insulin-transferrin conjugate was performed using a co-culture Caco-2/HT29-MTX cell model. The conjugate was investigated by conducting transport studies on both the insulin-transferrin conjugate and an insulin control with and without the presence of microparticles. Also, a transport study in the presence of excess transferrin was performed. Additionally, preliminary animal studies were performed by injecting the insulin-transferrin conjugate subcutaneously into rat models to verify the bioactivity of the insulin molecule within the conjugate complex. The results of the transport studies indicated a sevenfold increase in transport by replacing insulin with insulin-transferrin conjugates. Also, the presence of P(MAA-g-EG) microparticles enhanced transport for both insulin and the insulin-transferrin conjugate, but the increase in insulin transport was 5% while the increase in conjugate transport was found to be nearly 100%, indicating that the polymer microparticles may assist in transcytotic processes. Finally, the transport studies also demonstrated that a 14-fold increase in transport can be achieved by switching from insulin in the presence of polymer microparticles to insulin-transferrin conjugates in the presence of polymer microparticles. Upon administration of the insulin-transferrin conjugates to rat subjects through subcutaneous injection, the blood-glucose level was noticeably lowered, demonstrating the insulin-like therapeutic response of the conjugate as well as confirming the bioactivity of the insulin portion of the insulin-transferrin conjugate. The specific targeting, increased transport, and insulin-like therapeutic response of the insulin-transferrin conjugate in combination with the protection and site-specific release capabilities of P(MAA-g-EG) microparticles combine synergistically to form a potential dosage form which could effectively deliver therapeutics to the small intestine and across the epithelium, resulting in high bioavailability in the bloodstream.

Transport Sample	Apparent Permeability (P_{app})
Insulin (control)	4.95×10^{9} cm/s
Insulin with P(MAA-g-EG) Particles	5.20×10^{9} cm/s
Insulin-Transferrin Conjugate	37.0×10^{9} cm/s
Conjugate with P(MAA-g-EG) Particles	72.8×10^{9} cm/s
Conjugate with Excess Transferrin	76.8×10^{9} cm/s

Table 8.1 Apparent permeability values for each of the transport studies calculated using Equation 8.3

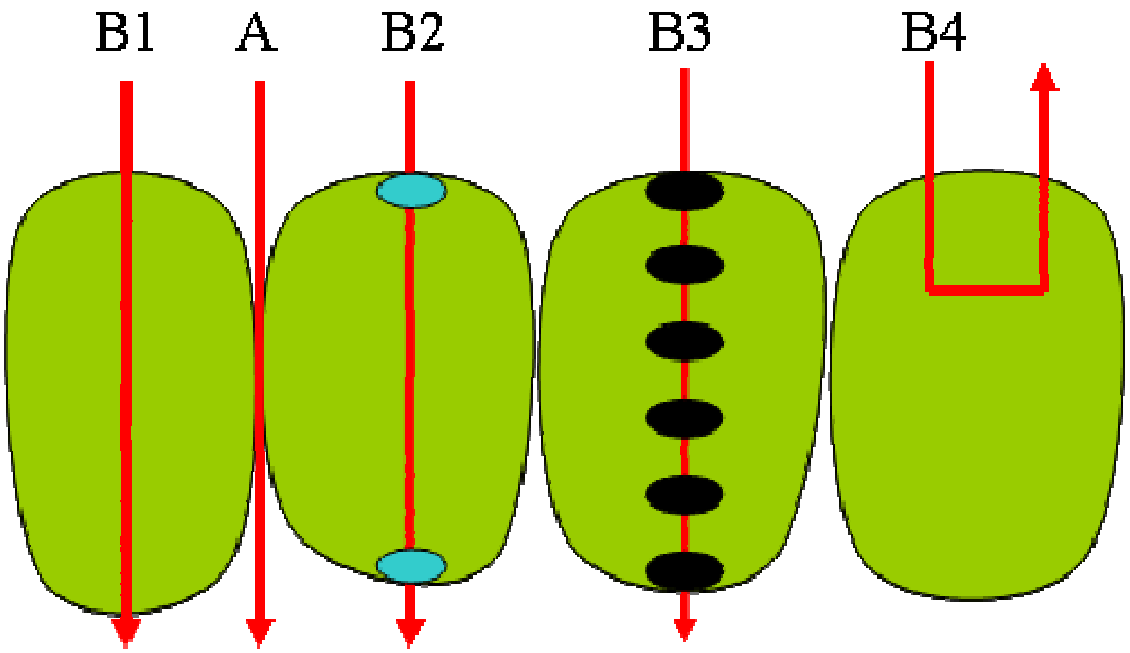

Figure 8.1 Cellular mechanisms of absorption in the small intestine.

Schematic of (A) paracellular transport and (B) transcellular transport. Specific types of transcellular transport include (B1) passive diffusion, (B2) carrier-mediated transcytosis, (B3) receptor-mediated transcytosis, and (B4) efflux transport.

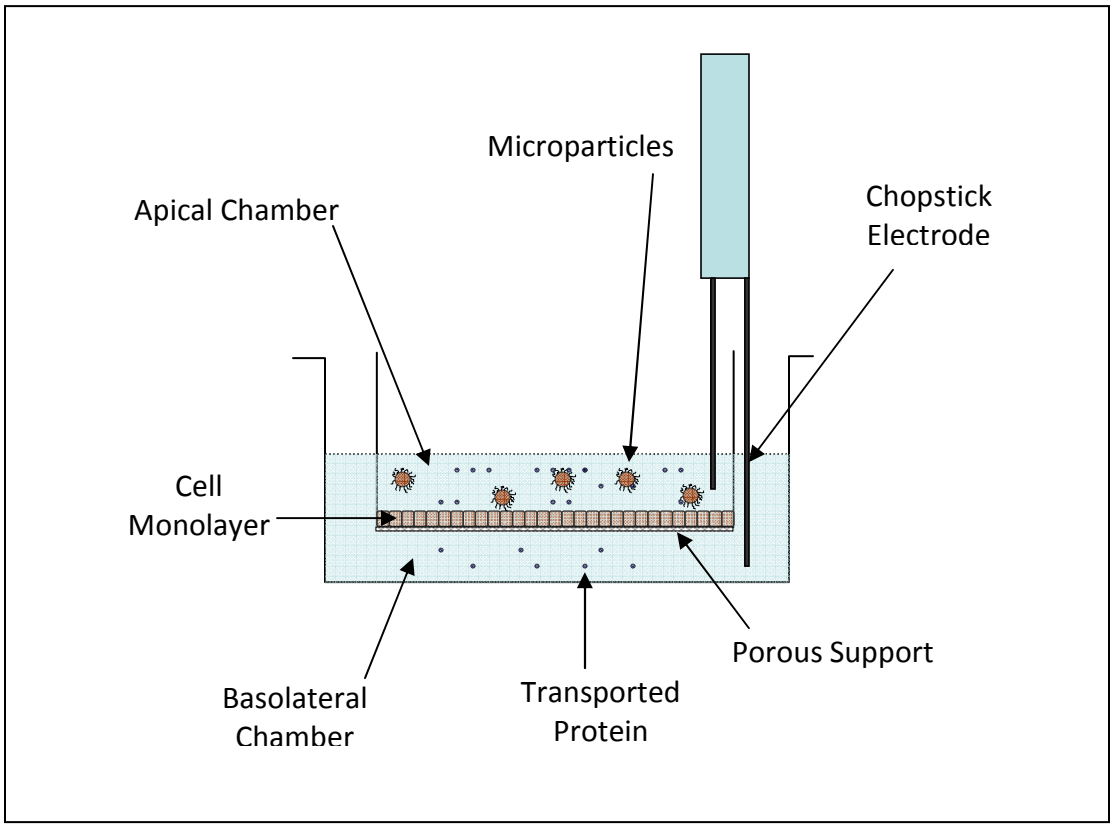

Figure 8.2 Experimental setup for transport studies using Caco-2/HT29-MTX co-culture cell models.

The cell co-culture is grown as a monolayer on a porous membrane support. Each well contains an apical (top) and a basolateral (bottom) chamber. Protein which is transported through the cells can be measured in the basolateral chamber. Transepithelial electrical resistance (TEER) is measured by the chopstick electrode.

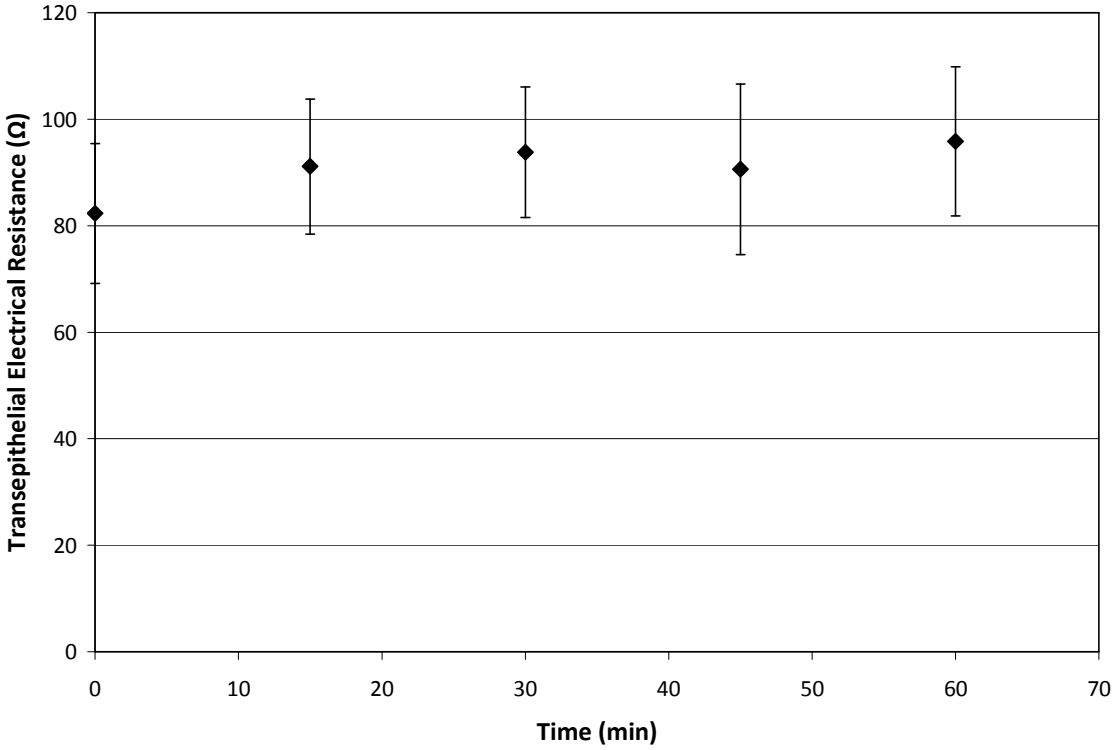

Figure 8.3 Average transepithelial electrical resistance (TEER) of cell monolayers for one hour after exposure to warm HBSS solution.

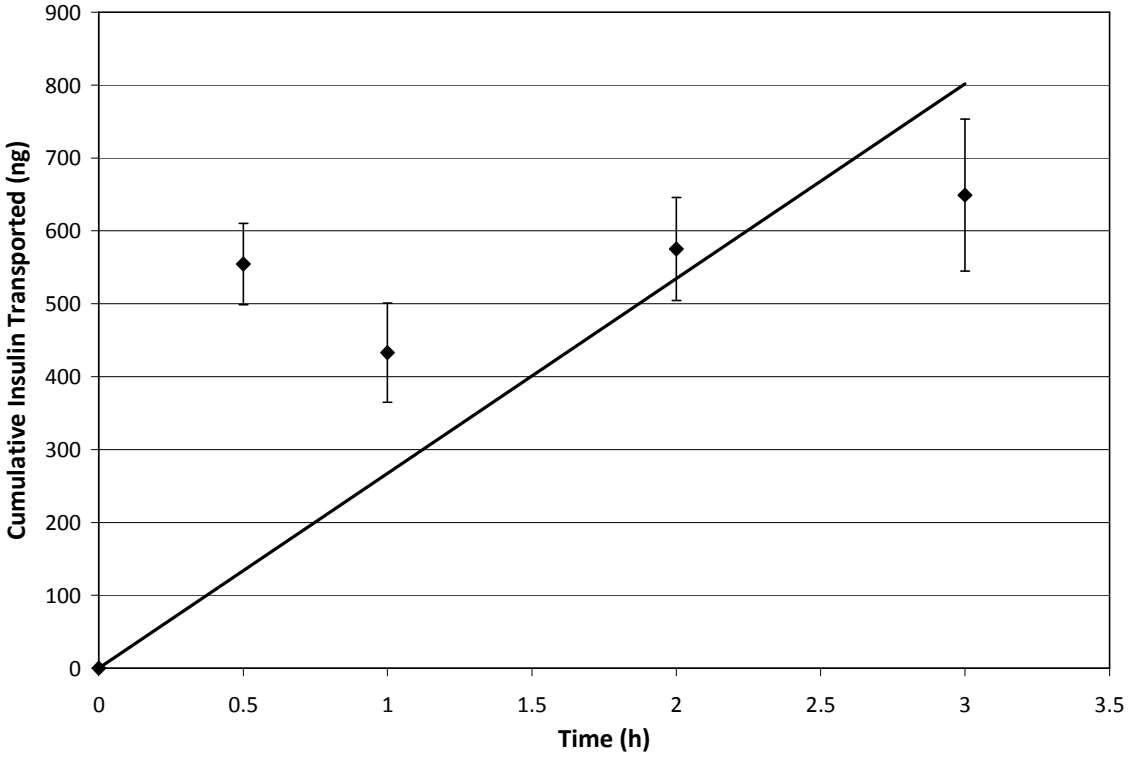

Figure 8.4 Cellular transport profile showing the cumulative amount of insulin transported across the monolayer of Caco-2/HT29-MTX cells over time.

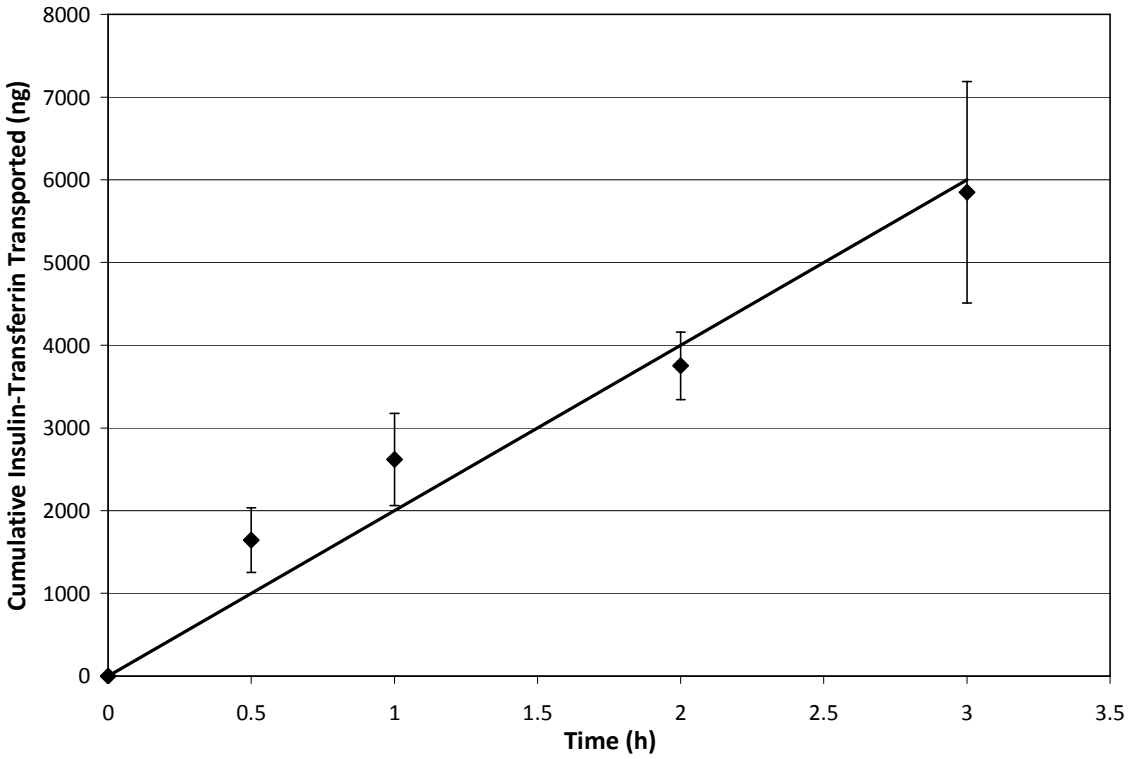

Figure 8.5 Cellular transport profile showing the cumulative amount of insulin-transferrin conjugates transported across the monolayer of Caco-2/HT29-MTX cells over time.

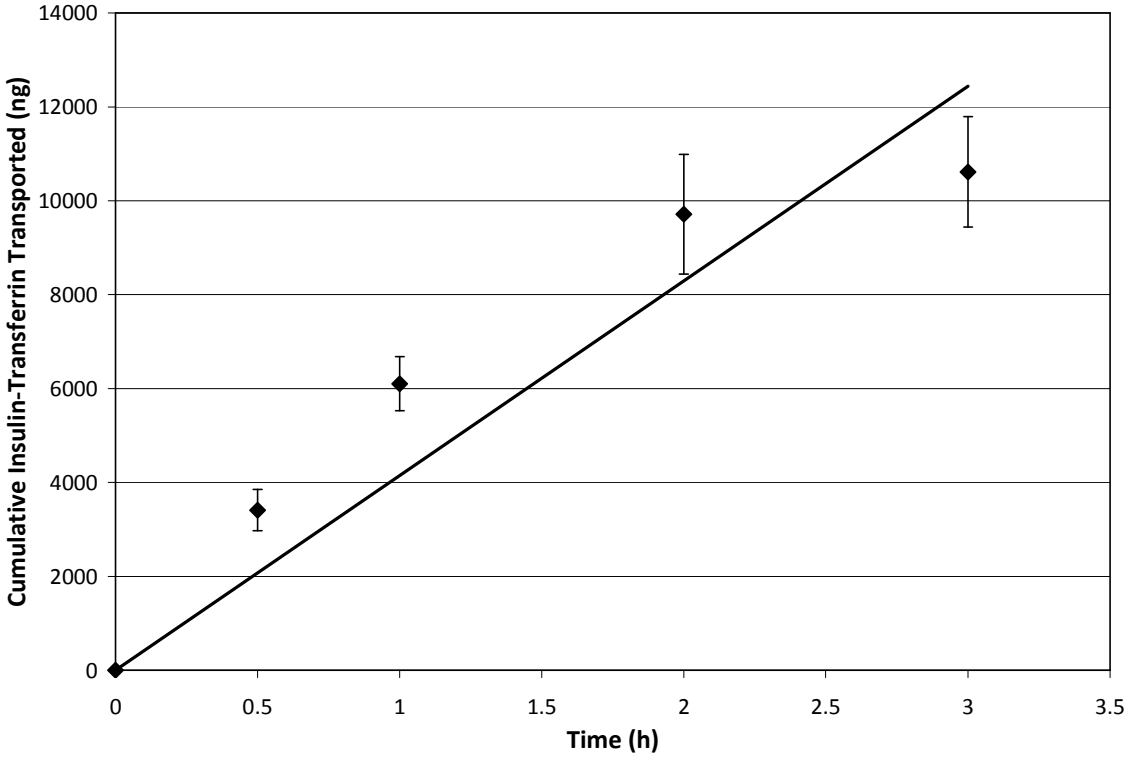

Figure 8.6 Cellular transport profile showing the cumulative amount of insulin-transferrin conjugates transported across the monolayer of Caco-2/HT29-MTX cells while in the presence of excess unmodified transferrin.

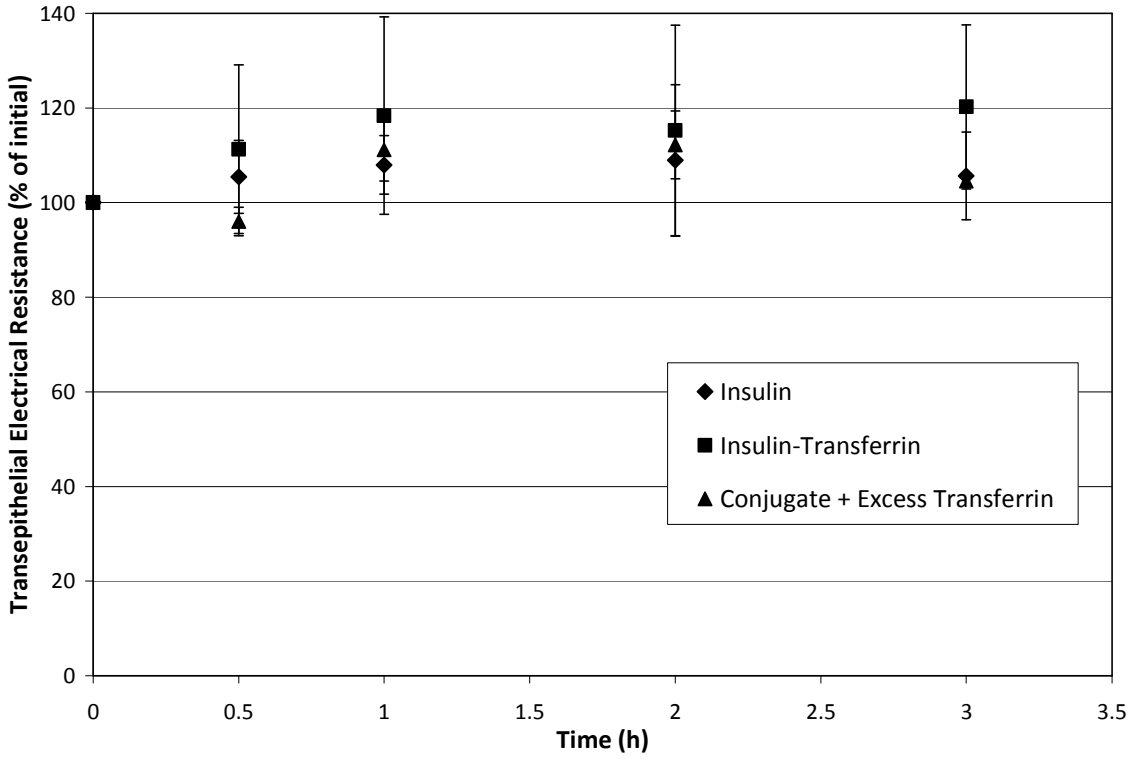

Figure 8.7 Average transepithelial electrical resistance (TEER) values throughout the duration of transport studies involving protein solutions consisting of either insulin, insulin-transferrin conjugates, or insulin-transferrin conjugates with excess unmodified transferrin.

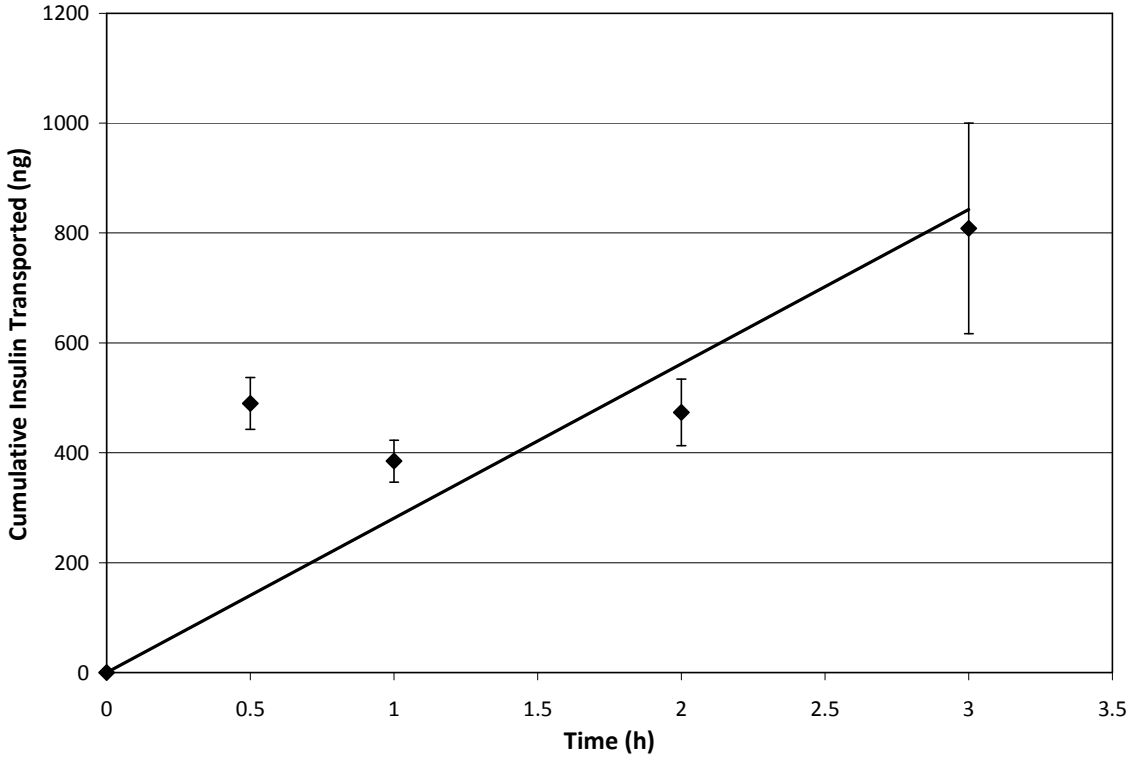

Figure 8.8 Cellular transport profile showing the cumulative amount of insulin transported across the monolayer of Caco-2/HT29-MTX cells while in the presence of P(MAA-g-EG) microparticles.

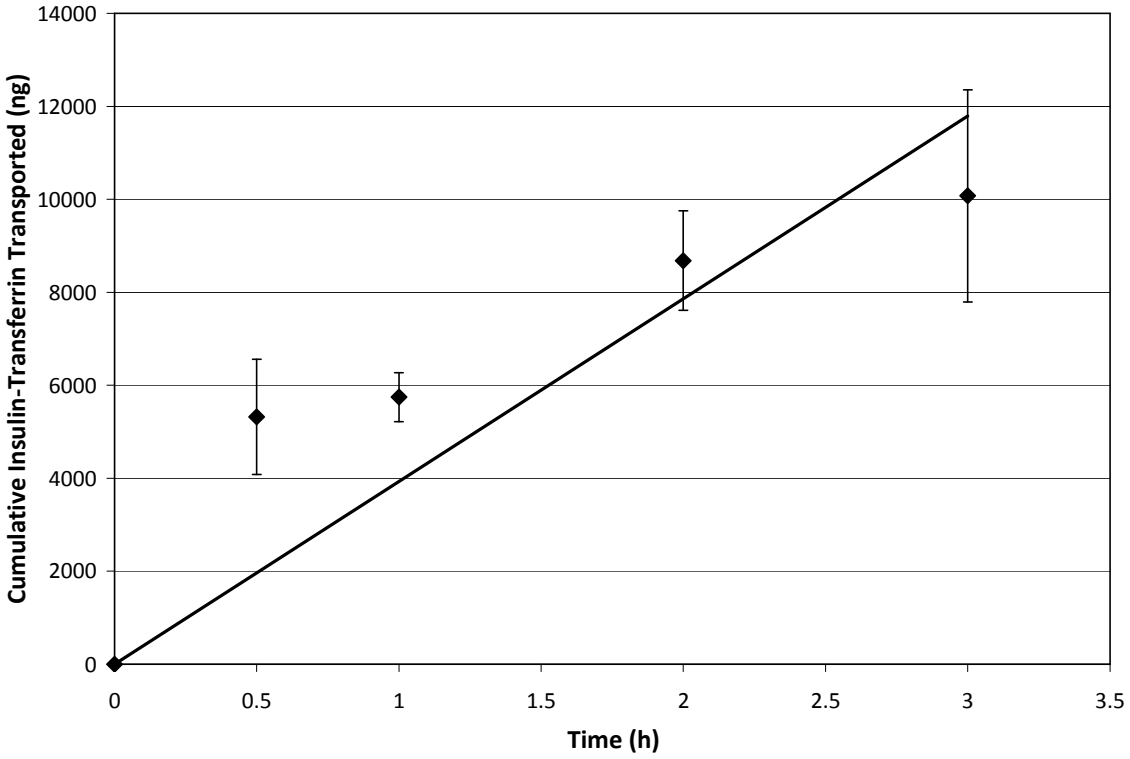

Figure 8.9 Cellular transport profile showing the cumulative amount of insulin-transferrin conjugate transported across the monolayer of Caco-2/HT29-MTX cells while in the presence of P(MAA-g-EG) microparticles.

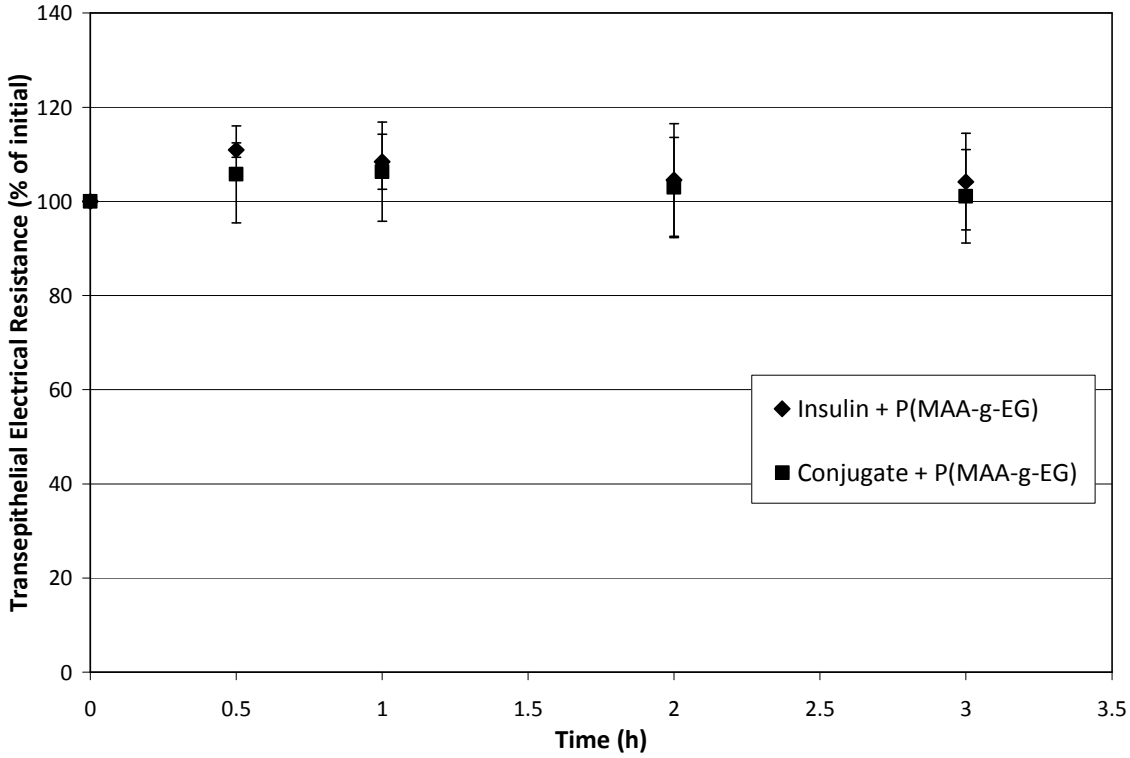

Figure 8.10 Average transepithelial electrical resistance (TEER) values throughout the duration of transport studies of insulin or insulin-transferrin conjugates in the presence of P(MAA-g-EG) microparticles.

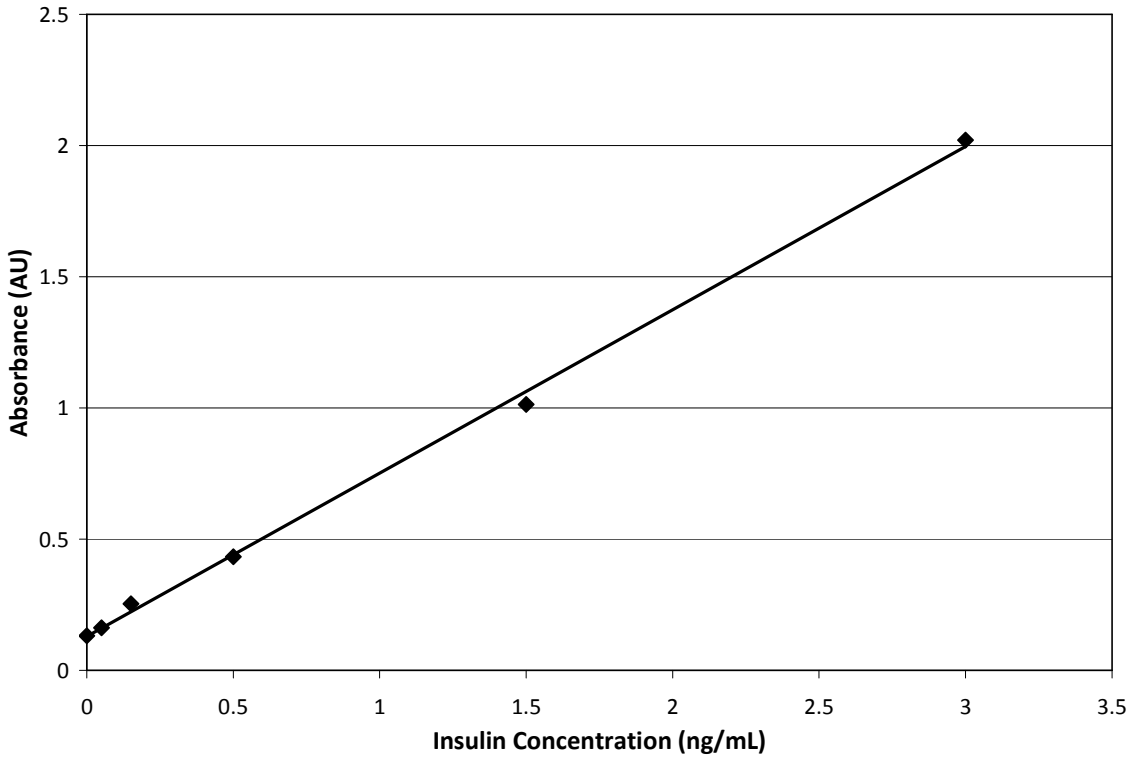

Figure 8.11 Calibration curve consisting of known concentrations of insulin in solution. Calibration curve used to determine insulin concentrations of unknown samples.

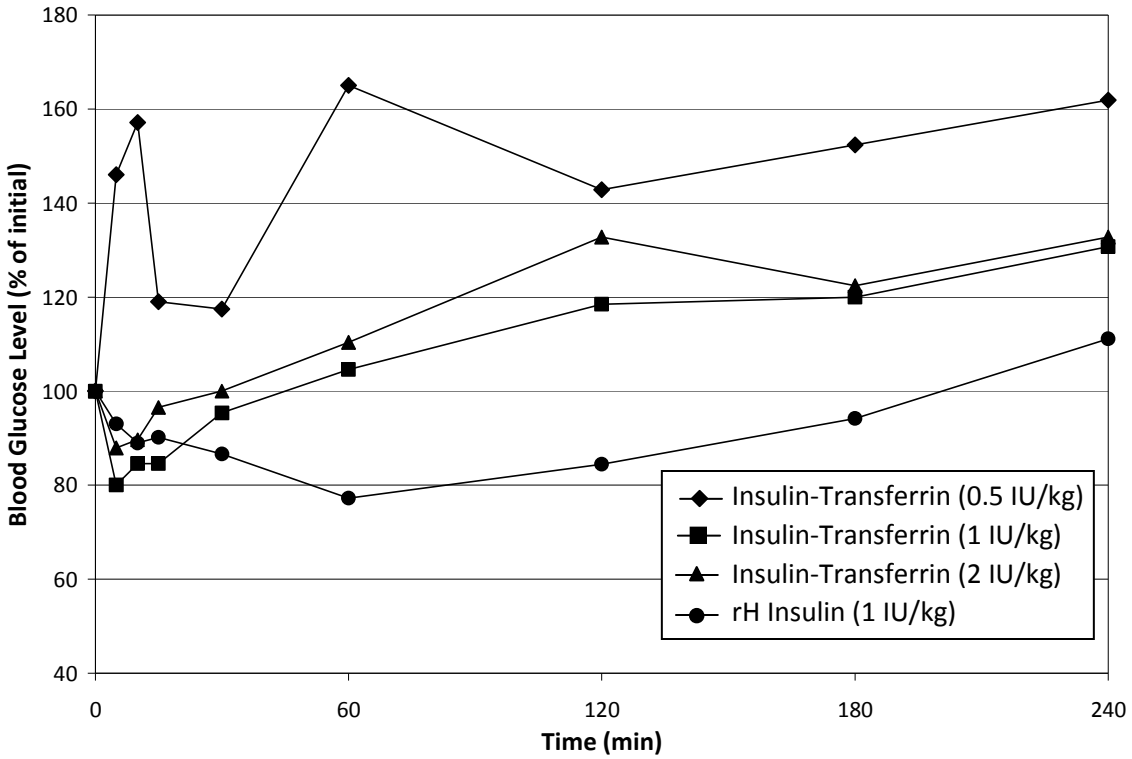

Figure 8.12 Blood glucose level of male Sprague-Dawley rats after injection of different dosages of insulin-transferrin conjugate or recombinant human insulin (control). Reduction below 100% blood glucose level indicates insulin activity.

REFERENCES

1. Madara, J.L., and Trier, J.S., *Functional morphology of the mucosa of the small intestine*. In Physiology of the Gastrointestinal Tract, ed. L.R. Johnson. 1986, New York: Raven Press.

2. Artursson, P., Lindmark, T., Davis, S.S., and Illum, L., *Effect of chitosan on the permeability of monolayers of intestinal epithelial cells (Caco-2).* Pharm. Res., 1994. **11**(9): p. 1358-1361.

3. Artursson, P., and Borchardt, R.T., *Intestinal drug absorption and metabolism in cell cultures: Caco-2 and beyond.* Pharm. Res., 1997. **14**(12): p. 1655-1658.

4. Artursson, P., Palm, K., and Luthman, K., *Caco-2 monolayers in experimental and theoretical predictions of drug transport.* Adv. Drug Deliver. Rev., 2001. **46**(1-3): p. 27-43.

5. Ungell, A.-L.B., *Caco-2 replace or refine?* Drug Discov. Today: Technologies, 2004. **1**(4): p. 423-430.

6. Audus, K.L., Bartel, R.L., Hidalgo, I.J., and Borchardt, R.T., *The use of cultured epithelial and endothelial cells for drug transport and metabolism studies.* Pharm. Res., 1990. **7**(5): p. 435-451.

7. MacAdam, A., *The effect of gastro-intestinal mucus on drug absorption.* Adv. Drug Deliver. Rev., 1993. **11**(3): p. 201-220.

8. Wikman, A., Karlsson, J., Carlstedt, I., and Artursson, P., *A drug absorption model based on the mucus layer producing human intestinal goblet cell line HT29-H.* Pharm. Res., 1993. **10**: p. 843-852.

9. Walter, E., Blake, S.J., Roessler, J., Hilfinger, J.M., and Amidon, G.L., *HT29-MTX/Caco-2 cocultures as an in vitro model for the intestinal epithelium: In vitro-in vivo correlation with permeability data from rats and humans.* J. Pharm. Sci., 1996. **85**(10): p. 1070-1076.

10. Balimane, P.V., Chong, S., and Morrison, R.A., *Current methodologies used for evaluation of intestinal permeability and absorption.* J. Pharmacol. Toxicol. Methods, 2000. **44**: p. 301-312.

11. Foss, A.C., and Peppas, N.A., *Investigation of the cytotoxicity and insulin transport of acrylic-based copolymer protein delivery systems in contact with Caco-2 cultures.* Eur. J. Pharm. Biopharm., 2004. **57**(3): p. 447-455.

12. Denker, B.M., and Nigam, S.K., *Molecular structure and assembly of the tight junction.* Am. J. Physiol. Renal Physiol., 1998. **274**(1): p. F1-9.

13. Gumbiner, B., *Structure, biochemistry, and assembly of epithelial tight junctions.* Am. J. Physiol. Cell Physiol., 1987. **253**(6): p. C749-758.

14. Ichikawa, H., and Peppas, N.A. , *Novel complexation hydrogels for oral peptide delivery: In vitro evaluation of their cytocompatibility and insulin-transport enhancing effects using Caco-2 cell monolayers.* J. Biomed. Mater. Res. Part A, 2003. **67A**(2): p. 609-617.

CHAPTER 9

CONCLUSIONS

Research in the biomedical and pharmaceutical fields has increased drastically in recent years in an attempt to develop alternative methods to injection for delivering therapeutic proteins. Research into different possible routes of administration has proved that each administration method has inherent advantages and disadvantages [1]. Among the potential types of protein delivery, oral delivery has the greatest benefits including low cost, ease of administration, and high patient compliance. Specifically, high patient compliance is essential to effective treatment because lack of proper medicine regimens can lead to serious complications in some diseases such as diabetes [2]. Lack of patient compliance is often attributed to fear or discomfort with injections [3], increasing the need for development of alternative routes of administration. However, oral delivery of proteins also has inherent challenges associated with development of a system. Due to their sensitive nature, most therapeutic proteins will be degraded or denatured by the enzymes in the stomach [4]. Also, even if the protein survives transit through the stomach, there is a narrow window for absorption in the small intestine. Finally, the epithelial cell layer lining the small intestine represents a challenging barrier to entry into the bloodstream. A successful system design for oral delivery of proteins requires protection of the protein in the stomach, increased residence time at the site of absorption, and a driving force to enhance cellular transport across the epithelial cell barrier.

To address some of the challenges associated with oral protein delivery, systems have been developed in our laboratory involving the use of complexation hydrogels as carriers for therapeutic proteins to protect in the stomach and to release at the site of absorption in the small intestine. While observing significantly increased bioavailability of therapeutic proteins in the bloodstream due to the use of hydrogels [5], the epithelial

transport barrier remains a major limiting factor for achieving bioavailability values similar to those obtained by injection. Thus, in an effort to enhance the complexation hydrogel system design, further modifications were made to the system intended to drastically increase epithelial transport into the bloodstream.

Complexation hydrogels for the oral delivery of proteins act only as a delivery vehicle to the site of absorption, prompting the need for drug modification in order to increase epithelial transport. The approach explored in this work was to conjugate a transporter molecule to the therapeutic protein to allow for specific targeting due to receptor-ligand interactions as well as increased overall epithelial transport. The major objectives of the work included the synthesis of complexation hydrogel carriers, the synthesis and characterization of multiple protein-transporter conjugates, the optimization of the polymer carriers with respect to loading and release characteristics of the conjugate formulations, and the evaluation of the transport and bioactivity of the conjugate using cellular and animal models.

Several variations of complexation hydrogel carriers were synthesized including P(MAA-g-EG) and P(MAA-co-NVP) of different crosslinker lengths, monomer-to-solvent ratios, and particle sizes. The majority of the polymers were characterized by scanning electron microscopy to investigate the size variations, morphology, and surface features of each system. Based on the characterizations, insight was gained on the type of visual differences that rigidity and tightness of the polymer network can create between systems as well as insight into mechanical properties which ultimately affect the performance of the polymer carriers.

Novel protein-transporter conjugates consisting insulin bound to transferrin and calcitonin bound to transferrin were successfully synthesized using the protein crosslinker SPDP. The final products insulin-transferrin and calcitonin-transferrin are both characterized by a disulfide bond connecting the two proteins. Each conjugation reaction was analyzed using UV spectroscopy, HPLC for conjugate verification, and HPLC for quantification of overall reaction yield. Based on the analyses, it was proven that

intact conjugates were indeed synthesized in a controlled, repeatable manner which also gave significant reaction yields. The novel conjugates synthesized were intended to provide a greater specificity for drug uptake as well as to provide potential for increased transport.

To specifically investigate the insulin-transferrin conjugates, studies were performed to gain insight into the *in vitro* characteristics with relation to loading and release in polymer microparticle carriers. Specifically, a number of experiments were run to find the optimal polymer carrier to ensure sufficient release of insulin-transferrin conjugates in the small intestine. To adjust the polymer carriers for the increased size of the conjugate relative to insulin, a protocol was designed for use with transferrin and it was tested as a protein analog to determine its loading and release characteristics. The polymer carriers were found to perform well with a large molecule, allowing for investigation into the loading and release characteristics of the specific insulin-transferrin conjugates. To optimize the polymer carrier for use with insulin-transferrin, several polymer formulations including P(MAA-g-EG) and P(MAA-co-NVP) which differed in synthesis parameters such as crosslinker length, monomer-to-solvent ratio, and particle size were investigated. Loading studies performed on all polymer systems confirmed that each system was capable of loading a significant amount of insulin-transferrin conjugates. Based on the release studies, the optimal polymer carrier for insulin-transferrin conjugates was found to be P(MAA-g-EG) microparticles less than 75 microns in size, crosslinked with PEGDMA1000, and synthesized using a 50:50 monomer-to-solvent ratio.

The calcitonin-transferrin conjugates were also investigated with relation to finding an optimal carrier for their use in oral delivery applications. The loading and release characteristics of calcitonin-transferrin conjugates in several polymer systems were examined. The polymer systems tested for optimization included P(MAA-g-EG) and P(MAA-co-NVP) which differed in synthesis parameters such as crosslinker length, monomer-to-solvent ratio, and particle size. Loading studies performed on all batches

of polymers showed that while most systems loaded a similar amount of conjugate, a few polymer formulations were marginally better at loading calcitonin-transferrin conjugate. By combining the results of the loading and release studies, the optimal polymer for use with calcitonin-transferrin conjugates was also found to be P(MAA-g-EG) microparticles less than 75 microns in size, crosslinked with PEGDMA1000, and synthesized using a 50:50 monomer-to-solvent ratio.

After determining the optimal carrier for insulin-transferrin and calcitonin-transferrin, the insulin-transferrin conjugate was chosen for evaluation of potential oral delivery characteristics using cellular and animal models. The cellular model used for evaluation was a co-culture Caco-2/HT29-MTX cell model. The insulin-transferrin conjugate was investigated by conducting transport studies on both the insulin-transferrin conjugate and an insulin control with and without the presence of microparticles. The results of the transport studies showed a *sevenfold increase* in transport by changing insulin to insulin-transferrin. Also, the presence of P(MAA-g-EG) microparticles enhanced transport for insulin by *5%* and insulin-transferrin by nearly *100%*, suggesting that the polymer may enhance transcytotic processes to some degree. The transport studies also showed that a *14-fold increase* in transport can be achieved by replacing insulin in the presence of polymer microparticles with insulin-transferrin conjugates in the presence of polymer microparticles. In addition to the cellular studies, preliminary animal studies were conducted by performing subcutaneous injections of the insulin-transferrin conjugate into rat subjects to verify the bioactivity of the insulin portion of the insulin-transferrin conjugate. The animal studies showed that injection of insulin-transferrin conjugate causes the blood-glucose level to be noticeably lowered, demonstrating a therapeutic response similar to insulin as well as confirming the bioactivity of the insulin molecule within the conjugate complex. The animal and cellular models used to evaluate the insulin-transferrin conjugate provide merit towards considering future implementation of protein-transporter conjugates into the design of new oral delivery systems.

Throughout the investigations of researchers attempting to design oral protein delivery systems, the recurring factor which limits bioavailability most frequently is epithelial transport. Within the chapters of this thesis, the idea of enhancing epithelial transport by the use of protein-transporter conjugates has been rigorously investigated. As seen in the cellular studies, the use of protein-transporter conjugates has the potential to increase epithelial transport several times over. The probability is high that such a dramatic increase in epithelial transport would translate to a drastic increase in bioavailability of the therapeutic protein. The implementation of protein-transporter conjugates into the majority of existing oral delivery system designs such as the use of complexation hydrogels certainly merits consideration if not action. In the case of this specific system, the use of insulin-transferrin conjugates in P(MAA-g-EG) microparticles as an oral insulin delivery demonstrates extreme potential. To create the most efficient system possible, more optimization experiments need to be performed with relation to some of the smaller details. Also, further testing using animal models would provide feedback on which parameters need to be altered to further improve performance *in vivo.* However, the research already performed identifies the use of protein-transporter conjugates as a viable strategy to improve epithelial transport. The combination of the benefits of the polymer carriers (protection in the gastric environment, site-specific release) with the benefits of the protein-transporter conjugates (specific uptake, increased transport, insulin-like therapeutic response) allows for the systems investigated in this work to be considered as very promising candidates for the effective oral administration of insulin.

REFERENCES

1. Berlin, C.M., et al., *Alternative Routes of Drug Administration---Advantages and Disadvantages (Subject Review).* Pediatrics, 1997. **100**(1): p. 143-152.

2. Helme, D.W., and Harrington, N.G., *Patient accounts for noncompliance with diabetes self-care regimens and physician compliance-gaining response.* Patient Educ. Couns., 2004. **55**(2): p. 281-292.

3. Zambanini, A., Newson, R.B., Maisey, M., and Feher, M.D., *Injection related anxiety in insulin-treated diabetes.* Diabetes Res. Clin. Pr., 1999. **46**(3): p. 239-246.

4. Langguth, P., Bohner, V., Heizmann, J., Merkle, H.P., Wolffram, S., Amidon, G.L., and Yamashita, S., *The challenge of proteolytic enzymes in intestinal peptide delivery.* J. Control. Release, 1997. **46**(1-2): p. 39-57.

5. Morishita, M., Goto, T., Peppas, N.A., Joseph, J.I., Torjman, M.C., Munsick, C., Nakamura, K., Yamagata, T., Takayama, K., and Lowman, A.M., *Mucosal insulin delivery systems based on complexation polymer hydrogels: effect of particle size on insulin enteral absorption.* J. Control. Release, 2004. **97**(1): p. 115-124.

.

BIBLIOGRAPHY

Agu, R.U., Ugwoke, M.I., Armand, M., Kinget, R., and Verbeke, N., *The lung as a route for systemic delivery of therapeutic proteins and peptides.* Resp. Res., 2001. **2**(4): p. 198-209.

am Ende, M.T., Hariharan, D., and Peppas, N.A., *Factors influencing drug and protein transport and release from ionic hydrogels.* React. Polym., 1995. **25**(2-3): p. 127-137.

Anderson, D.C., *Paget's Disease; evidence for a viral cause.* Bone, 1995. **17**(1): p. 97-97.

Anderson, J.M., and Van Itallie, C.M., *Tight junctions and the molecular basis for regulation of paracellular permeability.* Am. J. Physiol.-Gastr. L., 1995. **269**(4): p. G467-475.

Arora, P., Sharma, S., and Garg, S., *Permeability issues in nasal drug delivery.* Drug Discov. Today, 2002. **7**(18): p. 967-975.

Artursson, P., Lindmark, T., Davis, S.S., and Illum, L., *Effect of chitosan on the permeability of monolayers of intestinal epithelial cells (Caco-2).* Pharm. Res., 1994. **11**(9): p. 1358-1361.

Artursson, P., and Borchardt, R.T., *Intestinal drug absorption and metabolism in cell cultures: Caco-2 and beyond.* Pharm. Res., 1997. **14**(12): p. 1655-1658.

Artursson, P., Palm, K., and Luthman, K., *Caco-2 monolayers in experimental and theoretical predictions of drug transport.* Adv. Drug Deliver. Rev., 2001. **46**(1-3): p. 27-43.

Aslam, Mohammed, *Bioconjugation : protein coupling techniques for the biomedical sciences*. 1998, New York: Grove's Dictionaries.

Audus, K.L., Bartel, R.L., Hidalgo, I.J., and Borchardt, R.T., *The use of cultured epithelial and endothelial cells for drug transport and metabolism studies.* Pharm. Res., 1990. **7**(5): p. 435-451.

Avioli, L.V., *Salmon calcitonin in the prevention and treatment of osteoporosis.* Trends Endocrin. Met., 1997. **8**(3): p. 89-92.

Azari, P. R., and Feeney, R. E., *Resistance of Metal Complexes of Conalbumin and Transferrin to Proteolysis and to Thermal Denaturation.* J. Biol. Chem., 1958. **232**(1): p. 293-302.

Balimane, P.V., Chong, S., and Morrison, R.A., *Current methodologies used for evaluation of intestinal permeability and absorption.* J. Pharmacol. Toxicol. Methods, 2000. **44**: p. 301-312.

Banga, Ajay, *Theme Section: Transdermal Delivery of Proteins.* Pharm. Res., 2007. **24**(7): p. 1357-1359.

Banting, F.G., Best, C.H., Collip, J.B., Campbell, W.R., and Fletcher, A.A., *Pancreatic extracts in the treatment of diabetes mellitus: preliminary report. 1922.* Can. Med. Assoc. J., 1991. **145**(10): p. 1281-1286.

Bartha, J.L., Martinez-Del-Fresno, P., and Comino-Delgado, R., *Early diagnosis of gestational diabetes mellitus and prevention of diabetes-related complications.* Eur. J. Obstet. Gyn. R. B., 2003. **109**(1): p. 41-44.

Bell, C.L., and Peppas, N.A., *Water, solute and protein diffusion in physiologically responsive hydrogels of poly(methacrylic acid-g-ethylene glycol).* Biomaterials, 1996. **17**(12): p. 1203-1218.

Bell, J.C., Ford, J.B., Cameron, C.A., and Roberts, C.L., *The accuracy of population health data for monitoring trends and outcomes among women with diabetes in pregnancy.* Diabetes Res. Clin. Pr., 2006. **In Press**.

Berlin, C.M., et al., *Alternative Routes of Drug Administration---Advantages and Disadvantages (Subject Review).* Pediatrics, 1997. **100**(1): p. 143-152.

Bernkop-Schnurch, A., Kast, C.E., and Guggi, D., *Permeation enhancing polymers in oral delivery of hydrophilic macromolecules: thiomer/GSH systems.* J. Control. Release, 2003. **93**(2): p. 95-103.

Bezie, Y., Molina, M., Hernandez, N., Batista, R., Niang, S., and Huet, D., *Therapeutic compliance: a prospective analysis of various factors involved in the adherence rate in type 2 diabetes.* Diabetes Metab., 2006. **32**(6): p. 611-616.

Blanchette, J., Kavimandan, N.J., and Peppas, N.A., *Principles of transmucosal delivery of therapeutic agents.* Biomed. Pharmacother., 2004. **58**(3): p. 142-151.

Body, J. J., *Calcitonin for the long-term prevention and treatment of postmenopausal osteoporosis.* Bone, 2002. **30**(5, Supplement 1): p. 75-79.

Bonometti, E.C., *Medical nutrition therapy (MNT) for pre-diabetes can prevent or delay type 2 diabetes.* J. Am. Diet. Assoc., 2006. **106**(8, Supp. 1): p. A30-A30.

Boonen, S., Kaufman, J., Goemaere, S., Bouillon, R., and Vanderschueren, D., *The diagnosis and treatment of male osteoporosis: Defining, assessing, and preventing skeletal fragility in men.* Eur. J. Int. Med., 2007. **18**(1): p. 6-17.

Bottalico, J.N., *Recurrent gestational diabetes: risk factors, diagnosis, management, and implications.* Semin. Perinatol., 2007. **31**(3): p. 176-184.

Brancati, F.L., Whelton, P.K., Kuller, L.H., and Klag, M.J., *Diabetes mellitus, race, and socioeconomic status a population-based study.* Ann. Epidemiol., 1996. **6**(1): p. 67-73.

Brannon-Peppas, L., and Peppas, N.A., *Time-dependent response of ionic polymer networks to pH and ionic strength changes.* Int. J. Pharm., 1991. **70**(1-2): p. 53-57.

Brookhart, M.A., Avorn, J., Katz, J.N., Finkelstein, J.S., Arnold, M., Polinski, J.M., Patrick, A.R., Mogun, H., and Solmon, D.H., *Gaps in treatment among users of osteoporosis medications: The dynamics of noncompliance.* Am. J. Med., 2007. **120**(3): p. 251-256.

Caballero, A.E., *Long-term benefits of insulin therapy and glycemic control in overweight and obese adults with type 2 diabetes.* J. Diabetes Complicat., 2007. **In Press**.

Carino, G.P., and Mathiowitz, E., *Oral insulin delivery.* Adv. Drug Deliver. Rev., 1999. **35**(2-3): p. 249-257.

Carlsson, J., Drevin, H. and Axen, R., *Protein thiolation and reversible protein-protein conjugation. N-Succinimidyl 3-(2-pyridyldithio)propionate, a new heterobifunctional reagent.* Biochem. J., 1978. **173**: p. 723-737.

Cázares-Delgadillo, J., Naik, A., Ganem-Rondero, A., Quintanar-Guerrero, D., and Kalia, Y., *Transdermal Delivery of Cytochrome C—A 12.4 kDa Protein—Across Intact Skin by Constant–Current Iontophoresis.* Pharm. Res., 2007. **24**(7): p. 1360-1368.

Chalasani, K.B., Russell-Jones, G.J., Yandrapu, S.K., Diwan, P.V., and Jain, S.K., *A novel vitamin B12-nanosphere conjugate carrier system for peroral delivery of insulin.* J. Control. Release, 2007. **117**(3): p. 421-429.

Chalew, S.A., Gomez, R., Butler, A., Hempe, J., Compton, T., Mercante, D., Rao, J., and Vargas, A., *Predictors of glycemic control in children with Type 1 diabetes: The importance of race.* J. Diabetes Complicat., 2000. **14**(2): p. 71-77.

Chaturvedi, N., *The burden of diabetes and its complications: Trends and implications for intervention.* Diabetes Res. Clin. Pr., 2007. **76**(3, Supp. 1): p. S3-S12.

Cleland, J.L., Daugherty, A., Mrsny, R., *Emerging protein delivery methods.* Curr. Opin. Biotech., 2001. **12**(2): p. 212-219.

Colman, E., Hedin, R., Swann, J., and Orloff, D., *A brief history of calcitonin.* Lancet, 2002. **359**(9309): p. 885-886.

Cornish, J., Callon, K.E., Bava, U., Kamona, S.A., Cooper, G.J.S., and Reid, I.R., *Effects of calcitonin, amylin, and calcitonin gene-related peptide on osteoclast development.* Bone, 2001. **29**(2): p. 162-168.

Craig, M.E., Jones, T.W., Silink, M., Ping, Y.J., *Diabetes care, glycemic control, and complications in children with type 1 diabetes from Asia and the Western Pacific Region.* J. Diabetes Complicat., 2007. **21**(5): p. 280-287.

Daneman, D., *Type 1 diabetes.* Lancet. **367**(9513): p. 847-858.

Davidson, M.R., *Pharmacotherapeutics for osteoporosis prevention and treatment.* J. Midwifery Wom. Heal., 2003. **48**(1): p. 39-52.

Davis, S.N., *The role of inhaled insulin in the treatment of type 2 diabetes.* J. Diabetes Complicat. **In Press, Corrected Proof**.

Davis, S.S., *Further developments in nasal drug delivery.* Pharm. Sci. Technol. To., 1999. **2**(7): p. 265-266.

Deftos, L.J., Nolan, J.J., Seely, B.L., Clopton, P.L., Cote, G.J., Whitham, C.L., Florek, L.J., Christensen, T.A., and Hill, M.R., *Intrapulmonary drug delivery of salmon calcitonin.* Calcified Tissue Int., 1997. **61**(4): p. 345-347.

Delgado, A., Lavelle, E.C., Hartshorne, M., and Davis, S.S., *PLG microparticles stabilised using enteric coating polymers as oral vaccine delivery systems.* Vaccine, 1999. **17**(22): p. 2927-2938.

Denker, B.M., and Nigam, S.K., *Molecular structure and assembly of the tight junction.* Am. J. Physiol. Renal Physiol., 1998. **274**(1): p. F1-9.

des Rieux, A., Fievez, V., Garinot, M., Schneider, Y., and Préat, V., *Nanoparticles as potential oral delivery systems of proteins and vaccines: A mechanistic approach.* J. Control. Release, 2006. **116**(1): p. 1-27.

Dondeti, P., Zia, H., and Needham, T.E., *In vivo evaluation of spray formulations of human insulin for nasal delivery.* Int. J. Pharm., 1995. **122**(1-2): p. 91-105.

Duncan, G., Jess, T.J., Mohamed, F., Price, N.C., Kelly, S.M., and van der Walle, C.F., *The influence of protein solubilisation, conformation and size on the burst release from poly(lactide-co-glycolide) microspheres.* J. Control. Release, 2005. **110**(1): p. 34-48.

Edwards, D.A., Ben-Jebria, A., and Langer, R., *Recent advances in pulmonary drug delivery using large, porous inhaled particles.* J. Appl. Physiol., 1998. **85**(2): p. 379-385.

Efrat, S., *Beta-cell replacement for insulin-dependent diabetes mellitus.* Adv. Drug Deliver. Rev., 2008. **60**(2): p. 114-123.

Eldor, R., Stern, E., Milicevic, Z., and Raz, I., *Early use of insulin in type 2 diabetes.* Diabetes Res. Clin. Pr., 2005. **68**(Supp. 1): p. S30-S35.

Fanelli, C.G., Porcellati, F., Rossetti, P., and Bolli, G.B., *Glucagon: The effects of its excess and deficiency on insulin action.* Nutr. Metab. Cardiovas., 2006. **16**(Supplement 1): p. S28-S34.

Fasano, A., *Novel approaches for oral delivery of macromolecules.* J. Pharm. Sci., 1998. **87**(11): p. 1351-1356.

Faulstich, H., Zobeley, S., Heintz, D., and Drewes, G., *Probing the phalloidin binding site of actin.* FEBS Lett., 1993. **318**(3): p. 218-222.

Feuerstein, B.L., and Weinstock, R.S., *Diet and exercise in type 2 diabetes mellitus.* Nutrition, 1997. **13**(2): p. 95-99.

Fischer, J.A., and Born, W., *Novel peptides from the calcitonin gene: Expression, receptors and biological function.* Peptides, 1985. **6**(Supp. 3): p. 265-271.

Foss, A.C., Goto, T., Morishita, M., and Peppas, N.A., *Development of acrylic-based copolymers for oral insulin delivery.* Eur. J. Pharm. Biopharm., 2004. **57**(2): p. 163-169.

Foss, A.C., and Peppas, N.A., *Investigation of the cytotoxicity and insulin transport of acrylic-based copolymer protein delivery systems in contact with Caco-2 cultures.* Eur. J. Pharm. Biopharm., 2004. **57**(3): p. 447-455.

Franssen, O., Stenekes, R.J.H., and Hennink, W.E., *Controlled release of a model protein from enzymatically degrading dextran microspheres.* J. Control. Release, 1999. **59**(2): p. 219-228.

Gallagher, A., Butler, T.J., and Home, P.D., *The effect of the optimal use of rapid-acting insulin analogues on insulin secretion in Type 2 diabetes.* Diabetes Res. Clin. Pr., 2007. **76**(3): p. 327-334.

Galvin, R.J.S., Bryan, P., Venugopalan, M., Smith, D.P., and Thomas, J.E., *Calcitonin responsiveness and receptor expression in porcine and murine osteoclasts: a comparative study.* Bone, 1998. **23**(3): p. 233-240.

Gass, M., and Dawson-Hughes, B., *Preventing osteoporosis-related fractures: an overview.* Am. J. Med., 2006. **119**(4, Supplement 1): p. S3-S11.

Genc, S., Koroglu, T.F., and Genc, K., *Erythropoietin and the nervous system.* Brain Res., 2004. **1000**(1-2): p. 19-31.

Gritti, I., Banfi, G., and Roi, G.S., *Pepsinogens: physiology, pharmacology, pathophysiology, and exercise.* Pharm. Res., 2000. **41**(3): p. 265-281.

Group, EURODIAB ACE Study, *Variation and trends in incidence of childhood diabetes in Europe.* Lancet, 2000. **355**(9207): p. 873-876.

Gumbiner, B., *Structure, biochemistry, and assembly of epithelial tight junctions.* Am. J. Physiol. Cell Physiol., 1987. **253**(6): p. C749-758.

Gupta, P., Vermani, K., and Garg, S., *Hydrogels: from controlled release to pH-responsive drug delivery.* Drug Discov. Today, 2002. **7**(10): p. 569-579.

Habberfield, A., Jensen-Pippo, K., Ralph, L., Westwood, S.W., and Russell-Jones, G.J., *Vitamin B12-mediated uptake of erythropoietin and granulocyte colony stimulating factor in vitro and in vivo.* Int. J. Pharm., 1996. **145**(1-2): p. 1-8.

Halbron, M., Jacqueminet, S., Sachon, C., Bosquet, F., Hartemann-Heurtier, A., and Grimaldi, A., *Insulin therapy for type 2 diabetes: premixed or basal-prandial?* Diabetes Metab., 2007. **33**(4): p. 316-320.

Hasan, A.S., Socha, M., Lamprecht, A., Ghazouani, F.E., Sapin, A., Hoffman, M., Maincent, P., and Ubrich, N., *Effect of the microencapsulation of nanoparticles on the reduction of burst release.* Int. J. Pharm., 2007. **344**(1-2): p. 53-61.

Heiber, S.J., Ebert, C.D., Dave, S.C., Smith, K., Kim, S.W., and Mix, D., *In-vivo buccal delivery of calcitonin.* J. Control. Release, 1994. **28**(1-3): p. 269-271.

Helme, D.W., and Harrington, N.G., *Patient accounts for noncompliance with diabetes self-care regimens and physician compliance-gaining response.* Patient Educ. Couns., 2004. **55**(2): p. 281-292.

Hernando, M.E., Gómez, E.J., Corcoy, R., and del Pozo, F., *Evaluation of DIABNET, a decision support system for therapy planning in gestational diabetes.* Comput. Meth. Prog. Bio., 2000. **62**(3): p. 235-248.

Hill, R.A., Strat, A.L., Hughes, N.J., Kokta, T.J., Dodson, M.V., and Gertler, A., *Early insulin signaling cascade in a model of oxidative skeletal muscle: mouse Sol8 cell line.* BBA-Mol. Cell Res., 2004. **1693**(3): p. 205-211.

Hinds, K.D., and Kim, S.W., *Effects of PEG conjugation on insulin properties.* Adv. Drug Deliver. Rev., 2002. **54**(4): p. 505-530.

Hoffman, A.S., *Hydrogels for biomedical applications.* Adv. Drug Deliver. Rev., 2002. **54**(1): p. 3-12.

Hosny, E.A., Al-Shora, H.I., and Elmazar, M.M.A., *Oral delivery of insulin from enteric-coated capsules containing sodium salicylate: effect on relative hypoglycemia of diabetic beagle dogs.* Int. J. Pharm., 2002. **237**(1-2): p. 71-76.

Huang, X., and Brazel, C.S., *On the importance and mechanisms of burst release in matrix-controlled drug delivery systems.* J. Control. Release, 2001. **73**(2-3): p. 121-136.

Huebers, H.A., Csiba, E., Huebers, E., and Finch, C.A., *Competitive advantage of diferric transferrin in delivering iron to reticulocytes.* P. Natl. Acad. Sci.-Biol., 1983. **80**(1): p. 300-304.

Huebner, A.K., Keller, J., Catala-Lehnen, P., Perkovic, S., Streichert, T., Emeson, R.B., Amling, M., and Schinke, T., *The role of calcitonin and [alpha]-calcitonin gene-related peptide in bone formation.* Arch. Biochem. Biophys., 2008. **473**(2): p. 210-217.

Ichikawa, H., and Peppas, N.A. , *Novel complexation hydrogels for oral peptide delivery: In vitro evaluation of their cytocompatibility and insulin-transport enhancing effects using Caco-2 cell monolayers.* J. Biomed. Mater. Res. Part A, 2003. **67A**(2): p. 609-617.

Inoue, K., Matsumoto, M., and Kobayashi, Y., *The combination of fasting plasma glucose and glycosylated hemoglobin predicts type 2 diabetes in Japanese workers.* Diabetes Res. Clin. Pr., 2007. **77**(3): p. 451-458.

Jiamjarasrangsi, W., Lohsoonthorn, V., Lertmaharit, S., and Sangwatanaroj, S., *Incidence and predictors of abnormal fasting plasma glucose among the university hospital employees in Thailand.* Diabetes Res. Clin. Pr., 2008. **79**(2): p. 343-349.

Jones, A.T., Gumbleton, M., and Duncan, R., *Understanding endocytic pathways and intracellular trafficking: a prerequisite for effective design of advanced drug delivery systems.* Adv. Drug Deliver. Rev., 2003. **55**(11): p. 1353-1357.

Junginger, H.E., Hoogstraate, J.A., and Verhoef, J.C., *Recent advances in buccal drug delivery and absorption -- in vitro and in vivo studies.* J. Control. Release, 1999. **62**(1-2): p. 149-159.

Kan, K.S., and Coleman, R., *The calcium ionophore A23187 increases the tight-junctional permeability in rat liver.* Biochem. J., 1988. **256**(3): p. 1039-1041.

Kanis, J.A., McCloskey, E.V., Johansson, H., Oden, A., Melton Iii, L.J., and Khaltaev, N., *A reference standard for the description of osteoporosis.* Bone, 2008. **42**(3): p. 467-475.

Kavimandan, N.J., Losi, E., Wilson, J.J., Brodbelt, J.S., and Peppas, N.A., *Synthesis and Characterization of Insulin-Transferrin Conjugates.* Bioconjugate Chem., 2006. **17**(6): p. 1376-1384.

Kavimandan, N.J., Losi, E., and Peppas, N.A., *Novel delivery system based on complexation hydrogels as delivery vehicles for insulin-transferrin conjugates.* Biomaterials, 2006. **27**(20): p. 3846-3854.

Kawasaki, E., Abiru, N., and Eguchi, K., *Prevention of type 1 diabetes: from the view point of [beta] cell damage.* Diabetes Res. Clin. Pr., 2004. **66**(Supp. 1): p. S27-S32.

Kestilä, K.K., Ekblad, U.U., and Rönnemaa, T., *Continuous glucose monitoring versus self-monitoring of blood glucose in the treatment of gestational diabetes mellitus.* Diabetes Res. Clin. Pr., 2007. **77**(2): p. 174-179.

Khandare, J., and Minko, T., *Polymer-drug conjugates: Progress in polymeric prodrugs.* Prog. Polym. Sci., 2006. **31**(4): p. 359-397.

Khare, A.R., Peppas, N.A., Massimo, G., and Colombo, P., *Measurement of the swelling force in ionic polymeric networks I. Effect of pH and ionic content.* J. Control. Release, 1992. **22**(3): p. 239-244.

Kuzuya, T., Nakagawa, S., Satoh, J., Kanazawa, Y., Iwamoto, Y., Kobayashi, M., Nanjo, K., Sasaki, A., Seino, Y., Ito, C., Shima, K., Nonaka, K., and Kadowaki, T., *Report of the committee on the classification and diagnostic criteria of diabetes mellitus.* Diabetes Res. Clin. Pr., 2002. **55**(1): p. 65-85.

Langer, R., and Peppas, N.A., *Advances in biomaterials, drug delivery, and bionanotechnology.* AIChE J., 2003. **49**(12): p. 2990-3006.

Langguth, P., Bohner, V., Heizmann, J., Merkle, H.P., Wolffram, S., Amidon, G.L., and Yamashita, S., *The challenge of proteolytic enzymes in intestinal peptide delivery.* J. Control. Release, 1997. **46**(1-2): p. 39-57.

Larkin, Marilynn, *Diabetes on the rise worldwide and website.* Lancet, 2001. **357**(9258): p. 815-815.

Lee, K.Y., and Yuk, S.H., *Polymeric protein delivery systems.* Prog. Polym. Sci., 2007. **32**(7): p. 669-697.

Li, C., and Wallace, S., *Polymer-drug conjugates: Recent development in clinical oncology.* Adv. Drug Deliver. Rev., 2008. **60**(8): p. 886-898.

Liang-chang, D., Qi, Y., and Hoffman, A.S., *Controlled release of amylase from a thermal and pH-sensitive, macroporous hydrogel.* J. Control. Release, 1992. **19**(1-3): p. 171-177.

Lim, F., and Sun, A.M., *Microencapsulated islets as bioartificial endocrine pancreas.* Science, 1980. **210**(4472): p. 908-910.

Lindsay, D.G., and Shall, S., *The acetylation of insulin.* Biochem. J., 1971. **121**(5): p. 737-745.

Lowman, A.M., Morishita, M., Kajita, M., Nagai, T., and Peppas, N.A., *Oral delivery of insulin using pH-responsive complexation gels.* J. Pharm. Sci., 1999. **88**(9): p. 933-937.

Lowman, A.M., and Peppas, N.A., *Molecular analysis of interpolymer complexation in graft copolymer networks.* Polymer, 2000. **41**(1): p. 73-80.

Luan, X., Skupin, M., Siepmann, J., and Bodmeier, R., *Key parameters affecting the initial release (burst) and encapsulation efficiency of peptide-containing poly(lactide-co-glycolide) microparticles.* Int. J. Pharm., 2006. **324**(2): p. 168-175.

MacAdam, A., *The effect of gastro-intestinal mucus on drug absorption.* Adv. Drug Deliver. Rev., 1993. **11**(3): p. 201-220.

Mackay, M., Phillips, J., and Hastewell, J., *Peptide drug delivery: Colonic and rectal absorption.* Adv. Drug Deliver. Rev., 1997. **28**(2): p. 253-273.

Madara, J.L., and Trier, J.S., *Functional morphology of the mucosa of the small intestine*. In Physiology of the Gastrointestinal Tract, ed. L.R. Johnson. 1986, New York: Raven Press.

Madsen, F., and Peppas, N.A., *Complexation graft copolymer networks: swelling properties, calcium binding and proteolytic enzyme inhibition.* Biomaterials, 1999. **20**(18): p. 1701-1708.

Mastrandrea, L.D., and Quattrin, T., *Clinical evaluation of inhaled insulin.* Adv. Drug Deliver. Rev., 2006. **58**(9-10): p. 1061-1075.

McKinlay, J., and Marceau, L., *US public health and the 21st century: diabetes mellitus.* Lancet, 2000. **356**(9231): p. 757-761.

Melton, R.G., and Sherwood, R.F., *Antibody-Enzyme Conjugates for Cancer Therapy.* J. Natl. Cancer Inst., 1996. **88**(3-4): p. 153-165.

Mohammed, A., and Dent, A., *Bioconjugation: protein coupling techniques for the biomedical sciences*. Grove's Dictionaries. 1998: New York.

Monnier, L., and Colette, C., *Addition of rapid-acting insulin to basal insulin therapy in type 2 diabetes: indications and modalities.* Diabetes Metab., 2006. **32**(1): p. 7-13.

Morishita, M., Goto, T., Peppas, N.A., Joseph, J.I., Torjman, M.C., Munsick, C., Nakamura, K., Yamagata, T., Takayama, K., and Lowman, A.M., *Mucosal insulin delivery systems based on complexation polymer hydrogels: effect of particle size on insulin enteral absorption.* J. Control. Release, 2004. **97**(1): p. 115-124.

Morishita, M., and Peppas, N.A., *Is the oral route possible for peptide and protein drug delivery?* Drug Discov. Today, 2006. **11**(19-20): p. 905-910.

Moyad, M.A., *Osteoporosis: a rapid review of risk factors and screening methods.* Urol. Oncol.-Semin. O. I., 2003. **21**(5): p. 375-379.

Nakagami, T., Qiao, Q., Tuomilehto, J., Balkau, B., Carstensen, B., Tajima, N., and Iwamoto, Y., *The fasting plasma glucose cut-point predicting a diabetic 2-h OGTT glucose level depends on the phenotype.* Diabetes Res. Clin. Pr., 2002. **55**(1): p. 35-43.

Nakamura, K., Katagai, K., Mori, K., Higo, N., Sato, S., and Yamamoto, K., *Transdermal administration of salmon calcitonin by pulse depolarization-iontophoresis in rats.* Int. J. Pharm., 2001. **218**(1-2): p. 93-102.

Nakamura, K., Morishita, M., Ehara, J., Onuki, Y., Yamagata, T., Kamei, N., Lowman, A.M., Peppas, N.A., and Takayma, K., *Key functions in polymer carriers for intestinal absorption of insulin.* Int. J. Pharm., 2008. **354**(1-2): p. 135-142.

Nakashima, K., Miyagi, M., Goto, K., Matsumoto, Y., and Ueoka, R., *Enzymatic and hyperglycemia stability of chemically modified insulins with hydrophobic acyl groups.* Bioorg. Med. Chem. Lett., 2004. **14**(2): p. 481-483.

Nattrass, M., *Diabetic Ketoacidosis.* Medicine, 2002. **30**(2): p. 51-53.

Niskanen, L., Jensen, L.E., Råstam, J., Nygaard-Pedersen, L., Erichsen, K., and Vora, J.P., *Randomized, multinational, open-label, 2-period, crossover comparison of biphasic insulin aspart 30 and biphasic insulin lispro 25 and pen devices in adult patients with type 2 diabetes mellitus.* Clin. Ther., 2004. **26**(4): p. 531-540.

Nitiyanant, W., Ploybutr, S., Sriussadaporn, S., Yamwong, P., and Vannasaeng, S., *Evaluation of the new fasting plasma glucose cutpoint of 7.0 mmol/l in detection of diabetes mellitus in the Thai population.* Diabetes Res. Clin. Pr., 1998. **41**(3): p. 171-176.

Norris, S.L., Zhang, X., Avenell, A., Gregg, E., Bowman, B., Schmid, C.H., and Lau, J., *Long-term effectiveness of weight-loss interventions in adults with pre-diabetes: A review.* Am. J. Prev. Med., 2005. **28**(1): p. 126-139.

Notoya, M., Arai, R., Katafuchi, T., Minamino, N., and Hagiwara, H., *A novel member of the calcitonin gene-related peptide family, calcitonin receptor-stimulating peptide, inhibits the formation and activity of osteoclasts.* Eur. J. Pharmacol., 2007. **560**(2-3): p. 234-239.

Nystrom, F.H., and Quon, M.J., *Insulin Signalling: Metabolic Pathways and Mechanisms for Specificity.* Cell. Sig., 1999. **11**(8): p. 563-574.

Oliva, A., Farina, J., and Llabres, M., *Development of two high-performance liquid chromatographic methods for the analysis and characterization of insulin and its degradation products in pharmaceutical preparations.* J. Chromatogr. B, 2000. **749**(1): p. 25-34.

Opar, A., *Another blow for inhaled protein therapeutics.* Nat. Rev. Drug. Discov., 2008. **7**(3): p. 189-190.

Owens, D.R., Zinman, B., and Bolli, G., *Insulins today and beyond.* Lancet, 2001. **358**(9283): p. 739-746.

Owens, D.R., Zinman, B., and Bolli, G., *Alternative routes of insulin delivery.* Diabetic Med., 2003. **20**(11): p. 886-898.

Papoz, L., Delcourt, C., Ponton-Sanchez, A., Lokrou, A., Darrack, R., Touré, I.A., and Cuisinier-Raynal, J.C., *Clinical classification of diabetes in tropical West Africa.* Diabetes Res. Clin. Pr., 1998. **39**(3): p. 219-227.

Park, K.S., *Prevention of type 2 diabetes mellitus from the viewpoint of genetics.* Diabetes Res. Clin. Pr., 2004. **66**(Supplement 1): p. S33-S35.

Pasut, G., and Veronese, F.M., *Polymer-drug conjugation, recent achievements and general strategies.* Prog. Polym. Sci., 2007. **32**(8-9): p. 933-961.

Patlak, M., *New weapons to combat an ancient disease: treating diabetes.* FASEB J., 2002. **16**(14): p. 1853e-.

Patton, J.S., Trinchero, P., and Platz, R.M., *Bioavailability of pulmonary delivered peptides and proteins: [alpha]-interferon, calcitonins and parathyroid hormones.* J. Control. Release, 1994. **28**(1-3): p. 79-85.

Patton, J.S., *Pulmonary delivery of drugs for bone disorders.* Adv. Drug Deliver. Rev., 2000. **42**(3): p. 239-248.

Peppas, N.A., and Sahlin, J.J., *Hydrogels as mucoadhesive and bioadhesive materials: a review.* Biomaterials, 1996. **17**(16): p. 1553-1561.

Peppas, N.A., Bures, P., Leobandung, W., and Ichikawa, H., *Hydrogels in pharmaceutical formulations.* Eur. J. Pharm. Biopharm., 2000. **50**(1): p. 27-46.

Peppas, N.A., *Hydrogels*. Biomaterials Science, ed. B.D. Ratner, Hoffman, A., Schoen, F., and Lemons, J. 2004, San Diego, CA: Elsevier Academic Press. pp. 100-106.

Peppas, N.A., and Kavimandan, N.J., *Nanoscale analysis of protein and peptide absorption: Insulin absorption using complexation and pH-sensitive hydrogels as delivery vehicles.* Eur. J. Pharm. Sci., 2006. **29**(3-4): p. 183-197.

Ponchel, G., and Irache, J., *Specific and non-specific bioadhesive particulate systems for oral delivery to the gastrointestinal tract.* Adv. Drug Deliver. Rev., 1998. **34**(2-3): p. 191-219.

Portero, A., Teijeiro-Osorio, D., Alonso, M.J., and Remuñán-López, C., *Development of chitosan sponges for buccal administration of insulin.* Carbohyd. Polym., 2007. **68**(4): p. 617-625.

Puavilai, G., Chanprasertyotin, S., and Sriphrapradaeng, A., *Diagnostic criteria for diabetes mellitus and other categories of glucose intolerance: 1997 criteria by the Expert Committee on the Diagnosis and Classification of Diabetes Mellitus (ADA), 1998 WHO Consultation criteria, and 1985 WHO criteria.* Diabetes Res. Clin. Pr., 1999. **44**(1): p. 21-26.

Qiu, Y., and Park, K., *Environment-sensitive hydrogels for drug delivery.* Adv. Drug Deliver. Rev., 2001. **53**(3): p. 321-339.

Quinn, J.M.W., Morfis, M., Lam, M.H.C., Elliott, J., Kartsogiannis, V., Williams, E.D., Gillespie, M.T., Martin, T.J., and Sexton, P.M., *Calcitonin receptor antibodies in the identification of osteoclasts.* Bone, 1999. **25**(1): p. 1-8.

Rasmussen, S.S., Glümer, C., Sandbaek, A., Lauritzen, T., Carstensen, B., and Borch-Johnsen, K., *Short-term reproducibility of impaired fasting glycaemia, impaired glucose tolerance and diabetes: The ADDITION study, DK.* Diabetes Res. Clin. Pr., 2008. **80**(1): p. 146-152.

Reginster, J., and Burlet, N., *Osteoporosis: A still increasing prevalence.* Bone, 2006. **38**(2, Supplement 1): p. 4-9.

Reginster, J.Y.L., and Lecart, M.P., *Efficacy and safety of drugs for Paget's disease of bone.* Bone, 1995. **17**(5, Supp. 1): p. S485-S488.

Renard, E., *Implantable closed-loop glucose-sensing and insulin delivery: the future for insulin pump therapy.* Curr. Opin. Pharmacol., 2002. **2**(6): p. 708-716.

Rousière, M., Michou, L., Cornélis, F., and Orcel, P., *Paget's disease of bone.* Best Pract. Res. Cl. Rh., 2003. **17**(6): p. 1019-1041.

Russell-Jones, G.J., *Oral delivery of therapeutic proteins and peptides by the vitamin B_{12} uptake system*. Peptide-Based Drug Design: Controlling Transport and Metabolism, ed. M.D. Taylor, and Amidon, G.L. 1995, Washington, DC: ACS. pp. 181-198.

Russell-Jones, G.J., Westwood, S.W., and Habberfield, A.D., *Vitamin B12 Mediated Oral Delivery Systems for Granulocyte-Colony Stimulating Factor and Erythropoietin.* Bioconjugate Chem., 1995. **6**(4): p. 459-465.

Russell-Jones, G.J., *The potential use of receptor-mediated endocytosis for oral drug delivery.* Adv. Drug Deliver. Rev., 2001. **46**(1-3): p. 59-73.

Saito, G., Swanson, J.A., and Lee, K., *Drug delivery strategy utilizing conjugation via reversible disulfide linkages: role and site of cellular reducing activities.* Adv. Drug Deliver. Rev., 2003. **55**(2): p. 199-215.

Salamat-Miller, N., and Johnston, T.P., *Current strategies used to enhance the paracellular transport of therapeutic polypeptides across the intestinal epithelium.* Int. J. Pharm., 2005. **294**(1-2): p. 201-216.

Salamat-Miller, N., Chittchang, M., and Johnston, T.P., *The use of mucoadhesive polymers in buccal drug delivery.* Adv. Drug Deliver. Rev., 2005. **57**(11): p. 1666-1691.

Sanger, F., *Chemistry of insulin: determination of the structure of insulin opens the way to greater understanding of life processes.* Science, 1959. **129**(3359): p. 1340-1344.

Sen, A., Daly, M.E., and Hui, S.W., *Transdermal insulin delivery using lipid enhanced electroporation.* BBA-Biomembranes, 2002. **1564**(1): p. 5-8.

Serra, L., Domenech, J., and Peppas, N.A., *Design of poly(ethylene glycol)-tethered copolymers as novel mucoadhesive drug delivery systems.* Eur. J. Pharm. Biopharm., 2006. **63**(1): p. 11-18.

Shah, D., and Shen, W.C., *Transcellular delivery of an insulin-transferrin conjugate in enterocyte-like Caco-2 cells.* J. Pharm. Sci., 1996. **85**: p. 1306-1311.

Shoyele, S.A., and Slowey, A., *Prospects of formulating proteins/peptides as aerosols for pulmonary drug delivery.* Int. J. Pharm., 2006. **314**(1): p. 1-8.

Siris, E.S., *Epidemiological aspects of Paget's disease: Family history and relationship to other medical conditions.* Semin. Arthritis Rheu., 1994. **23**(4): p. 222-225.

Smith, N.B., Lee, S., Maione, E., Roy, R.B., McElligott, S., and Shung, K.K., *Ultrasound-mediated transdermal transport of insulin in vitro through human skin using novel transducer designs.* Ultrasound Med. Biol., 2003. **29**(2): p. 311-317.

Smith, R., *Paget's disease of bone: past and present.* Bone, 1999. **24**(5, Supplement 1): p. 1S-2S.

Soybel, D.I., *Anatomy and Physiology of the Stomach.* Surg. Clin. N. Am., 2005. **85**(5): p. 875-894.

Stuchbury, T., Shipton, M., Norris, R., Malthouse, J.P., Brocklehurst, K., Herbert, J.A., and Suschitzky, H., *A reporter group delivery system with both absolute and selective specificity for thiol groups and an improved fluorescent probe containing the 7-nitrobenzo-2-oxa-1,3-diazole moiety.* Biochem. J., 1975. **151**: p. 417-432.

Sudhakar, Y., Kuotsu, K., and Bandyopadhyay, A.K., *Buccal bioadhesive drug delivery -- A promising option for orally less efficient drugs.* J. Control. Release, 2006. **114**(1): p. 15-40.

Tamai, I., and Tsuji, A., *Carrier-mediated approaches for oral drug delivery.* Adv. Drug Deliver. Rev., 1996. **20**(1): p. 5-32.

Thomas, B.J., and Finnin, B.C., *The transdermal revolution.* Drug Discov. Today, 2004. **9**(16): p. 697-703.

Thorpe, P.E., Wallace, P.M., Knowles, P.P., Relf, M.G., Brown, A.N.F., Watson, G.J., Knyba, R.E., Wawrzynczak, E.J., and Blakey, D.C., *New Coupling Agents for the Synthesis of Immunotoxins Containing a Hindered Disulfide Bond with Improved Stability in Vivo.* Cancer Res., 1987. **47**(22): p. 5924-5931.

Tobler, P.H., Jöhl, A., Born, W., Maier, R., and Fishcer, J.A., *Identity of calcitonin extracted from normal human thyroid glands with synthetic human calcitonin-(1-32).* BBA-Protein Struct. M., 1982. **707**(1): p. 59-65.

Ugwoke, M.I., Agu, R.U., Verbeke, N., andKinget, R., *Nasal mucoadhesive drug delivery: Background, applications, trends and future perspectives.* Adv. Drug Deliver. Rev., 2005. **57**(11): p. 1640-1665.

Ungell, A.-L.B., *Caco-2 replace or refine?* Drug Discov. Today: Technologies, 2004. **1**(4): p. 423-430.

Väänänen, K., *Mechanism of osteoclast mediated bone resorption--rationale for the design of new therapeutics.* Adv. Drug Deliver. Rev., 2005. **57**(7): p. 959-971.

Veuillez, F., Kalia, Y.N., Jacques, Y., Deshusses, J., and Buri, P., *Factors and strategies for improving buccal absorption of peptides.* Eur. J. Pharm. Biopharm., 2001. **51**(2): p. 93-109.

Visser, E.J., *A review of calcitonin and its use in the treatment of acute pain.* Acute Pain, 2005. **7**(4): p. 185-189.

Walter, E., Blake, S.J., Roessler, J., Hilfinger, J.M., and Amidon, G.L., *HT29-MTX/Caco-2 cocultures as an in vitro model for the intestinal epithelium: In vitro-in vivo correlation with permeability data from rats and humans.* J. Pharm. Sci., 1996. **85**(10): p. 1070-1076.

Whitehead, K., Karr, N., and Mitragotri, S., *Discovery of synergistic permeation enhancers for oral drug delivery.* J. Control. Release, 2008. **128**(2): p. 128-133.

Whitten, C.R., and Saifuddin, A., *MRI of Paget's disease of bone.* Clin. Radiol., 2003. **58**(10): p. 763-769.

Wichterle, O., and Lim, D., *Hydrophilic Gels for Biological Use.* Nature, 1960. **185**(4706): p. 117-118.

Widera, A., Norouziyan, F., and Shen, W.C., *Mechanisms of TfR-mediated transcytosis and sorting in epithelial cells and applications toward drug delivery.* Adv. Drug Deliver. Rev., 2003. **55**(11): p. 1439-1466.

Wikman, A., Karlsson, J., Carlstedt, I., and Artursson, P., *A drug absorption model based on the mucus layer producing human intestinal goblet cell line HT29-H.* Pharm. Res., 1993. **10**: p. 843-852.

Wood, K.M., Stone, G., and Peppas, N.A., *Lectin functionalized complexation hydrogels for oral protein delivery.* J. Control. Release, 2006. **116**(2): p. e66-e68.

Xia, C.Q., Wang, J., and Shen, W.C., *Hypoglycemic Effect of Insulin-Transferrin Conjugate in Streptozotocin-Induced Diabetic Rats.* J. Pharmacol. Exp. Ther., 2000. **295**(2): p. 594-600.

Yamagata, T., Morishita, M., Kavimandan, N.J., Nakamura, K., Fukuoka, Y., Takayama, K., and Peppas, N.A., *Characterization of insulin protection properties of complexation hydrogels in gastric and intestinal enzyme fluids.* J. Control. Release, 2006. **112**(3): p. 343-349.

Yamaoka, T., *Regeneration therapy of pancreatic [beta] cells: towards a cure for diabetes?* Biochem. Bioph. Res. Co., 2002. **296**(5): p. 1039-1043.

Yannas, I.V., Lee, E., Orgill, D.P., Skrabut, E.M., and Murphy, G.F., *Synthesis and Characterization of a Model Extracellular Matrix that Induces Partial Regeneration of Adult Mammalian Skin.* P. Natl. Acad. Sci. U.S.A., 1989. **86**(3): p. 933-937.

Yurgin, N., Secnik, K., and Lage, M.J., *Obesity and the use of insulin: a study of patients with type 2 diabetes in the UK.* J. Diabetes Complicat., 2006. **In Press**.

Zaidi, M., Inzerillo, A.M., Moonga, B.S., Bevis, P.J.R., and Huang, C.L.H., *Forty years of calcitonin--where are we now? A tribute to the work of Iain Macintyre, FRS.* Bone, 2002. **30**(5): p. 655-663.

Zambanini, A., Newson, R.B., Maisey, M., and Feher, M.D., *Injection related anxiety in insulin-treated diabetes.* Diabetes Res. Clin. Pr., 1999. **46**(3): p. 239-246.

Ziv, E., Lior, O., and Kidron, M., *Absorption of protein via the intestinal wall : A quantitative model.* Biochem. Pharmacol., 1987. **36**(7): p. 1035-1039.

VITA

Justin Patrick Shofner was born on August 4, 1983 to Boyce Dean Shofner and Patricia Shofner. He grew up in Pikeville, KY and graduated from Pikeville High School in 2001. After graduating high school, Justin received the Otis A. Singletary Scholarship and attended the University of Kentucky in Lexington, KY for his undergraduate studies. Justin went on to graduate Summa Cum Laude with Honors and received a Bachelor of Science in Chemical Engineering from the University of Kentucky in May 2005.

After finishing his undergraduate studies, Justin Shofner chose the University of Texas at Austin to pursue a Ph.D. in Chemical Engineering. Justin was awarded the National Science Foundation-Integrative Graduate Education and Research Traineeship (NSF-IGERT) and THRUST fellowships before enrolling at the University of Texas at Austin. Justin performed his fellowship research under the guidance of Dr. Nicholas Peppas and Dr. Jennifer Brodbelt. While attending UT, Justin was able to perform international internships in the laboratories of Dr. Hans Merkle at ETH-Zurich in Zurich, Switzerland and Dr. Juergen Siepmann at Faculté des Sciences Pharmaceutiques et Biologiques in Lille, France. Justin married Chelsy Hopperton on September 12, 2008 in Maui, Hawaii.

Permanent Address: 945 Mason Headley Rd., Lexington, KY 40504

This dissertation was typed by the author.